Fall 12-16-2016

Defining the Role of Phosphorylation and Dephosphorylation in the Regulation of Gap Junction Proteins

Hanjun Li
University of Nebraska Medical Center

Tell us how you used this information in this short survey.

Follow this and additional works at: https://digitalcommons.unmc.edu/etd

Part of the Biochemistry Commons, Biophysics Commons, Cell Biology Commons, and the Molecular Biology Commons

DEFINING THE ROLE OF PHOSPHORYLATION AND DEPHOSPHORYLATION IN THE REGULATION OF GAP JUNCTION PROTEINS

by

Hanjun Li

A DISSERTATION

Presented to the Faculty of

The Graduate College in the University of Nebraska

In Partial Fulfillment of the Requirements

For the Degree of Doctor of Philosophy

Cancer Research Doctoral Program

Under the Supervision of Professor Paul L. Sorgen

University of Nebraska Medical Center

Omaha, Nebraska

August, 2016

DEFINING THE ROLE OF PHOSPHORYLATION AND DEPHOSPHORYLATION IN THE

REGULATION OF GAP JUNCTION PROTEINS

Hanjun Li, Ph.D.

University of Nebraska, 2016

Advisor: Paul L. Sorgen, Ph.D.

Gap junctions are intercellular channels that permit the free passage of ions, small metabolites, and signaling molecules between neighboring cells. In the diseased human heart, altered ventricular gap junction organization and connexin expression (i.e., remodeling) are key contributors to rhythm disturbances and contractile dysfunction. Connexin43 (Cx43) is the dominant gap junction protein isoform in the ventricle which is under tight regulation by serine/tyrosine phosphorylation. Phosphorylation and dephosphorylation regulate many aspects of Cx43 function including trafficking, assembly and disassembly, electrical and metabolic coupling at the plaque, as well as to modulate the interaction with other proteins.

Serine phosphorylation has long been reported to regulate Cx43, however, the understanding of tyrosine kinases/phosphatases in the modulation of gap junction intercellular communication and subsequent down-stream effects on cellular processes is limited to Src. Using a combination of biophysical and cellular biology techniques, we identified and characterized a novel tyrosine phosphatase T-Cell Protein Tyrosine Phosphatase (TC-PTP) and a tyrosine kinase Tyrosine Kinase 2 (Tyk2) that directly interact with the Cx43 carboxyl terminal domain (CT). Cx43CT residues Y247 and Y265, which are phosphorylated by c-Src and v-Src, are also directly targeted by both TC-PTP and Tyk2. Additionally, activation of both TC-PTP and Tyk2 also indirectly affect serine

phosphorylation of Cx43. Specifically, TC-PTP leads to dephosphorylation of Cx43 S368 by inactivating PKCα and PKCδ, while Tyk2 increases phosphorylation of S368 and S279/282 through activation of PKC and MAPK, respectively. These effects are independent of Src.

In the cardiovascular system, an increased level of angiotensin II (Ang II) is associated with increased risk of ventricular arrhythmia, hypertrophy, and sudden death. Ang II reduces TC-PTP expression while increasing Tyk2 activity. Our data show that TC-PTP dephosphorylation maintains Cx43 gap junctions at the plaque as well as partially reverses channel closure caused by v-Src phosphorylation. Conversely, Tyk2 inhibits gap junction communication and increases turnover rate by phosphorylating Cx43. These findings suggest that a decrease of TC-PTP and an increase of Tyk2 may mediate Cx43 gap junction remodeling by altering phosphorylation in Ang II induced cardiovascular pathology.

ACKNOWLEDGMENTS

DEDICATION

I dedicate this dissertation to my family especially in memory of my grandfather, Xingguo Li. As a brilliant scientist in geology, he taught me the spirit of science and supported me to pursue my Ph.D. in United States mentally and financially. I wish him happy in heaven.

Thanks to my husband Yan, who is always by my side and helping me when I got difficulties on my projects, when I was feeling stresses of graduate school, when I worked in the lab late at night. He raises me up to more than I can be.

Thanks to my parents. They are always there when I need them. Their unconditional love over the years give me great courage to overcome difficulties in my life.

Thanks to my son, James. He is a little angel who brings me a lot of joy and happiness.

Thanks to all my family members. I cannot have done this without any of you. I love you all!

TABLE OF CONTENTES

LIST OF FIGURES AND TABLES

FIGURES

TABLES

LIST OF ABBREVIATIONS

A	Alanine (single-letter code) or Astrocyte
aa	Amino acids
Abl	Abelson leukemia virus
Ang II	angiotensin II
APC	Antigen presenting cells
Asp	Aspartic acid
ATP	Adenosine triphosphate
AUC	Analytical ultracentrifugation
BCA	Bicinchoninic acid
C	Cysteine (single-letter code) or Celcius or Carboxyl
CaM	Calmodulin
CaMKII	Ca^{2+}/calmodulin-dependent kinase II
CD	Circular dichroism
cDNA	Complimentary deoxyribonucleic acid
CL	Cytoplasmic loop
cm	Centimeter
CMTX	X-linked Charcot-Marie-Tooth Disease
Co-IP	Coimmunoprecipitation
c-Src	Cellular-sarcoma tyrosine kinase
CT	Carboxyl-terminus
Cx	Connexin
DAPI	4',6-Diamidino-2-Phenylindole, Dihydrochloride

DNA	Deoxyribonucleic acid
Drebrin	*D*evelopmentally *r*egulated *br*ain prote*in*
DTSSP	3,3′-dithiobis[sulfosuccinimidylpropionate
DTT	Dithiothreitol
E	Glutamic Acid (single-letter code) or Exracellular loop
E. Coli	Escherichia coli
EDTA	Ethylenediaminetetracetic acid
EGFR	Epidermal growth factor receptor
EGTA	Ethylene glycol tetraacetic acid
Eph	erythropoietin-producing hepatocellular receptor
Ephrin	Eph family receptor interacting protein
ER	Endoplasmic reticulum
ERAD	Endoplasmic-reticulum-associated degradation
ERGIC	ER-Golgi-intermediate compartment
ET-1	Endothelin-1
F	Phenylalanine (single-letter code)
FAT	Focal adhesion targeting domain
FBS	Fetal bovine serum
FERM	Protein 4.1, ezrin, radixin and moesin homological domain
FGF	Fibroblast growth factor
G	Glycine (single-letter code) or Immunoglobulin G
g	Grams or Centrifugation constant (italics)
Glu	Glutamic acid

GST	Glutathione S-transferase
H	Histidine (single-letter code)
HDAC	Histone deacytylase
hr	Hours
HSQC	Heteronuclear single quantum coherance
I	Isoleucine (single-letter code)
IB	Immunoblot
IDP	Intrinsically disordered protein
IP	Immunoprecipitation
IP_3	Inositol 1,4,5-triphosphate
IPTG	Isopropyl β-D-1-thiogalactopyranoside
Itk	interleukin-2-inducible T-cell kinase
Jak	Janus kinase
K	Equilibrium
K	Lysine (single-letter code)
K_D	Dissociation constant
kDa	Kilodaltons
Km	Michaelis constant
L	Leucine (single-letter code)
LB	Luria Broth
Leu	Leucine
M	Methionine (single-letter code) or Molar
MAPK	Mitogen-activated protein kinase

mg	Milligrams
MHC	Major histocompatibility complex
MHz	Megahertz
min	Minutes
ml	Milliliters
mm	Millimeters
mM	Millimolar
mol	Mole
mRNA	Messenger ribonucleic acid
MS	Mass spectrometry
MW	Molecular weight
N	Asparagine (single-letter code) or Node or Amino
n	Number of sites
nM	Nanomolar
nm	Nanometers
NMR	Nuclear magnetic resonance
NRK	Normal rat kidney
NT	Amino-terminus
OD	Optical density
p	Phosphorylated
PAGE	Polyacrylamide gel electrophoresis
PBS	Phosphate buffered saline
PDGFR	Platelet-derived growth factor receptor

PDZ	PSD-95/Dlg/ZO-1
PI3K	Phosphoinositide 3-kinase
PKA	cAMP-dependent protein kinase A
PKC	protein kinase C
PKG	protein kinase G
PMSF	Phenylmethylsulfonyl fluoride
ppm	Parts per million
PPR	Proline rich region
Pyk2	Protein tyrosine kinase 2 beta
R	Arginine (single-letter code)
RAS	Renin–angiotensin system
rpm	Revolutions per minute
RT	Room temperature
S	Serine (single-letter code) or Standard
s	Seconds
S.E.M.	Standard error of mean
SAP	Synapse-associated protein
SD	Standard deviation or Synthetic dropout medium
SDS	Sodium dodecyl sulfate
SH2	Src homology 2 domain
SH3	Src homology 3 domain
siRNA	Small interfering RNA
STAT	Signal transducer and activator of transcription

T	Threonine (single-letter code)
TBST	Tris-buffered saline Tween-20
TC-PTP	T-Cell Protein Tyrosine Phosphatase
TCR	T-cell receptor
TGN	Trans-Golgi network
TK	Tyrosine kinase
TM	Transmembrane
TM4	Transmembrane domain
TM4-Cx43CT	Transmembrane domain four-connexin 43 carboxyl-terminus
Tris	Tris-(hydroxymethyl)aminomethane
TSA	Trichostatin A
TX100	Triton X-100
Tyk2	Tyrosine kinase 2
UTR	Untranslated region
UV	Ultraviolet
VEGFR	Vascular endothelial growth factor receptor
V_j	Transjunctional voltage
W	Tryptophan (single-letter code)
WT	Wild-type
Y	Tyrosine (single-letter code)
ZO-1	Zonula occludens protein 1
α	Alpha
β	Beta

γ	Gamma
δ	Delta or Chemical shift
μg	Micrograms
μl	Microliters
μM	Micromoles

CHAPTER 1

Introduction

1.   Gap Junction Overview

Many mechanisms enable cells to influence the behavior of one another in order to maintain proper tissue and organ function. Cells secrete signal molecules that can influence itself (autocrine signaling), neighboring cells (paracrine signaling), or cells from large distances (endocrine signaling). In addition, cells can directly communicate with adjacent cells by exchanging ions and low molecular weight metabolites (<1 kDa) through gap junction channels.

Gap junctions are integral membrane proteins that provide an intercellular pathway for the propagation and/or amplification of signal transduction cascades triggered by cytokines, growth factors, and other cell signaling molecules involved in growth regulation and development. Gap junctions are formed by the apposition of connexons from adjacent cells, where six connexin proteins make each connexon. Connexins are proteins with four transmembrane domains (TM1-TM4), two extracellular loops (E1 and E2), and intracellular N-terminal (NT), cytoplasmic loop (CL), and C-terminal (CT) domains (Figure 1.1). In mammals, there are 21 human and 20 mouse isoforms, of which 19 can be paired orthologously (Sohl and Willecke, 2004). In invertebrates, gap junctions are assembled from another class of tetra transmembrane proteins named innexins (Phelan et al., 1998). The most frequently used nomenclature of connexin is based on their molecular weight differences. For example, the 43 kDa connexin is named Cx43. Also, connexin genes can be categorized into 3 subgroups (α, β, or γ) based on their overall gene homology and structure motifs (Eiberger et al., 2001), as well as named according to the order of discovery in the subgroup (e.g. Cx43 gene is

also named Gja1).

Connexins are differentially expressed in almost all tissues within the human body, with exceptions in skeletal muscle and mobile cell types such as sperm and erythrocytes (Rackauskas et al., 2010). Commonly, a cell can express several connexin isoforms. The same isoform of connexins oligomerize to form a homomeric connexon, different isoforms oligomerize to form a heteromeric connexon. To date, all heteromeric connexons are composed of two isoforms from the same subgroup (Falk et al., 1997). In addition, a gap junction channel can be formed from two identical connexons (homotypic) or different connexons (heterotypic) (Figure 1.1). Since different types of gap junction channels have different channel properties, including pore size, conductance, and ion selectivity, alterations in both the amount and distribution of connexins in cells are associated with a number of pathological situation such as arrhythmia , atherosclerosis (Morel et al., 2009), deafness (Martinez et al., 2009), and cancers (Naus and Laird, 2010). For example, Cx40, Cx43, and Cx45 expression in a cardiomyocyte can form either homomeric pattern or heterogeneous pattern with each other. The unitary conductance, which reflects single channel current-voltage relationship, is Cx40 (150 ps)>Cx43 (115 ps)>Cx45 (32 ps) (Bukauskas et al., 2002; Rackauskas et al., 2007). Cx40 and Cx45 channels exhibit smaller permeability to anions than cations, whereas Cx43 channels are nonselective to charge (Rackauskas et al., 2007). In failing human hearts, decreased expression of Cx43 correlates with an increase of Cx45. These gap junctions exhibit a decreased conductance which increase the risk of ventricular arrhythmias (Teunissen et al., 2004).
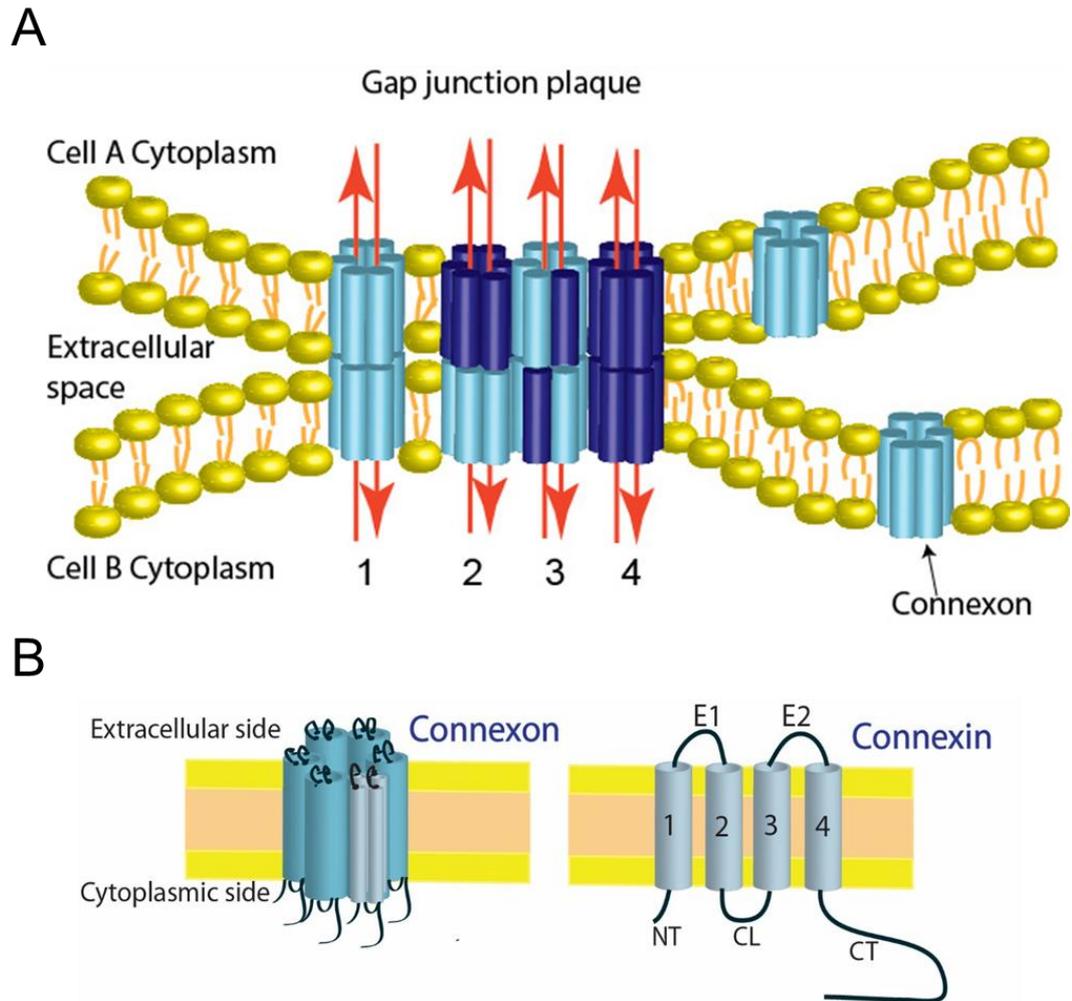
Figure 1.1 Structure and molecular organization of gap junctions. (A) Gap junction channels are composed of hemichannels (connexons) from adjacent cells docking with each other. Three different types of gap junctions have been shown: homomeric/homotypic (1,4), heterotypic (2), and heteromeric (3). (B) A connexon is an assembly of six connexins. A connexin has four transmembrane domains (TM1-TM4), two extracellular loops (E1 and E2), and one cytoplasmic loop (CL), cytoplasmic carboxyl termini (CT) and amino termini (NT).

Gap junction intercellular communication is essential in many physiological processes, including cell growth and sorting, differentiation and synchronization, metabolic coordination, as well as in the immune response. Loss-of-function mutations of connexin genes are often associated with hereditary diseases. Mutations in Cx26 gene are responsible for a large proportion of autosomal recessive hearing impairment in human (Rabionet et al., 2002). Mice with homozygous ablation of Cx26 in the epithelial network of the inner ear leads to deafness and cell death in cochlear epithelial network and sensory hair cells shortly after birth (Cohen-Salmon et al., 2002). More than 240 mutations in Cx32 have been found to be related to Charcot-Marie-Tooth disease (CMTX), one of the most common inherited neurological disorders in the United States (Bergoffen et al., 1993). Cx32 knockout mice also developed CMTX-like phenotype, including a progressive, demyelinating peripheral neuropathy (Rabionet et al., 2002). Both Cx46 and Cx50 are required for lens development in human and mouse eyes (White, 2002). Tissue specific deletion of Cx46 or Cx50 in a mouse model resulted in cataract formation (White, 2002). Knockout of some connexin isoforms are lethal to animals. For example, Cx45-deficient mice died before birth and Cx43-knockout mice died shortly after birth (Kruger et al., 2000; Reaume et al., 1995). These results suggest the importance in development of these isoforms and their function cannot be substituted by other isoforms (Sohl and Willecke, 2004). Mutations in Cx43 lead to oculodentodigital dysplasia (ODDD) in humans, which is characterized by multiple, variable craniofacial, limb, ocular and dental abnormalities. A mouse model harboring the same mutation shows a similar phenotype (Churko et al., 2011).

2.   Gap Junction Regulation

As an important channel that enables communication between adjacent cells, gap junctions are under tight regulation. First, different tissues and cell types express different connexin isoforms and their expression levels vary over time even in the same cell. Multiple mechanisms are involved in tissue and time specific control of connexins at the mRNA level, protein synthesis, trafficking, assembly, and degradation. Additionally, the function of gap junction channels at the plaque is regulated by various factors such as phosphorylation, voltage, Ca^{2+}, pH, and binding partners. In this section, we will discuss the regulation of connexins in details.

2.1   Transcriptional Regulation of Connexins

The gene structure of connexins usually contains two or more exons. Classically, the last exon has the coding region that is preceded by uncoding exons containing a 5′ untranslated region (5′-UTR). These uncoding exons allow alternative splicing to generate different transcripts (Oyamada et al., 2005). This is important for connexin tissue-specific expression. One example is Cx32, which has two transcripts. The first promoter P1 is activated by hepatocyte nuclear factor-1 that leads to the synthesis of one transcript in liver epithelial cells (Koffler et al., 2002). The second promoter P2 is activated by Sox-10 that results in another transcript in Schwann cells (Bondurand et al., 2001). Transcription factors play important role in connexin expression by regulating alternative splicing. For example, nine Cx43 mRNA species have been identified due to three promoter regions in Cx43 and alternative splicing mechanisms

(Pfeifer et al., 2004). These alternatively spliced 5′-UTRs regulate Cx43 at the post-transcriptional level. Since transcription factor profiles are diverse from different cell lines or tissues, the splicing mechanisms of Cx43 vary which generate different Cx43 transcripts, leading to different expression level of Cx43 (Pfeifer et al., 2004). Like most genes, transcription of connexins is regulated by a cooperation of tissue specific and universal transcription factors. For example, universal transcription factor Sp-1 binding sites have been found in connexin genes such as Cx32, Cx40, and Cx43 which regulates the basal transcription of the mentioned connexin isoforms (Echetebu et al., 1999; Linhares et al., 2004; Piechocki et al., 2000). Also, Cx40 can be regulated by cardiac specific transcription factor Nkx2-5, GATA4, and Tbx5 (Linhares et al., 2004). Cx40 is expressed in ventricles up to 14 days postcoitum, and disappears on day 19 (Delorme et al., 1995). This change within a very short period can be explained by transcriptional factor HRT2 repressing the transcription of Tbx5 and GATA4 (Kathiriya et al., 2004). The ubiquitous transcription factors can also be regulated by different physiological conditions, leading to the different expression of connexins at different periods. For example, progesterone inhibits Cx43 transcription by downregulating the universal transcription factor AP-1 which results in the low expression level of Cx43 during pregnancy (Mitchell and Lye, 2002; Ou et al., 1997). At the time of labor, due to the stretch of the myometrium and increase of estrogen, AP-1 expression is upregulated which activates Cx43 transcription (Petrocelli and Lye, 1993; Presley et al., 2005).

Epigenetic regulation also plays an important role in regulating connexin mRNA

levels. This epigenetic regulation includes histone acetylation, DNA methylation, and micro-RNAs. Histone acetylation, which usually associates with loss of chromatin structure and activation of transcription, is mediated by histone acetryltransferases (HATs). The deacetylation is mediated by histone deacytylases (HDAC). In some studies, inhibition of HDAC is associated with increase of connexin expression in some tissues, but this is not always the case (Ogawa et al., 2005) (Hernandez et al., 2006) (Xu et al., 2013). Using a HDAC inhibitor to treat nonmalignant human peritoneal mesothelial cells led to a rise of Cx43 mRNA and protein level in a dose-dependent manner (Ogawa et al., 2005). A similar result was found in prostate cancer cell lines (Hernandez et al., 2006). However, in primary cultured neonatal mouse ventricular myocytes, HDAC inhibitors TSA and vorinostat dose-dependently decreased Cx43 mRNA and protein expression levels as well as the area of Cx43 gap junction plaques (Xu et al., 2013). Interestingly, in primary cultures of adult rat hepatocytes, TSA increased Cx32 protein levels while decreasing Cx26 protein levels (Vinken et al., 2006). These differential regulatory mechanism by histone acetylation on connexins expression may correlate to particular patterns of histone modification and different transcriptional factors that are involved in connexin tissue-specific expression (Hernandez et al., 2006; Vinken et al., 2006).

Methylation of cytosines regulates connexin expression in both normal physiological and pathological situations, especially in cancer cells. In the normal situation, DNA methylation contributes to the differential expression of different isoforms. For example, in liver epithelium which expresses Cx43, the Cx32 promotor

is methylated; whereas in hepatocytes which expresses Cx32, the Cx43 promotor is methylated (Piechocki et al., 1999). In most cancer cells, connexin expression is generally lower than in normal tissue or completely lost which is associated with the uncontrolled growth. A high frequency of connexin promoter methylation is often observed in connexin-silenced patients or cells (Yamasaki et al., 1999). For example, methylation of Cx43 promotor decreasing the level of Cx43 has been found in non-small cell lung cancer (Chen et al., 2003) and nasopharyngeal carcinoma cells (Yi et al., 2007). Cx26 methylation at the promotor region are associated with gene silencing in lung cancer (Shimizu et al., 2006), breast cancer (Tan et al., 2002), and hepatocellular carcinoma (Tsujiuchi et al., 2007). In colorectal carcinomas, hypermethylation was found in Cx37, Cx30, Cx36, and Cx45 at various frequencies, however, only Cx45 methylation status was correlated with gene expression (Sirnes et al., 2011). Treatment with the demethylating drug 5-aza-2'deoxycytidine restored Cx45 expression in cell lines (HCT15, HT29, RKO and SW48) (Sirnes et al., 2011). Demethylation also re-expressed Cx43 and decreased cell growth in HeLa cells (King et al., 2000).

MicroRNA can also regulate connexin mRNA stability and translation. Cx43 is a target for miR1. In coronary artery disease and ischemia, increased miR1 associates with a reduction of Cx43 (Abdellatif, 2012). During skeletal muscle development, the expression of Cx43 is lost in myoblasts, which is associated with the upregulated miR1 and miR-206 (Anderson et al., 2006). In the sciatic nerve of a chronic constriction injury rat model, the downregulation of miR1 corresponds to the increase of Cx43 (Neumann et al., 2015). This high expression of Cx43 contributes to the induction and/or

maintenance of pain (Neumann et al., 2015). Furthermore, a recent study reported that Cx43 is a functional target of miR-1298 in arteriosclerosis obliterans (Hu et al., 2015). To date, Cx43 is the only isoform that has clear linked to the physiological relevance mediated by microRNA. However, on Cx36 and Cx45 genes, multiple binding sites of microRNA have been identifed (Rash et al., 2005).

In most cancers, such as breast cancer (reviewed in (McLachlan et al., 2007)), colorectal cancer (reviewed in (Sirnes et al., 2015)), liver cancer (reviewed in (Vinken et al., 2012)), and ovarian cancer ((Umhauer et al., 2000)), connexin protein expression level decreases or connexins relocalize from the plasma membrane to intracellular compartments. However, mRNA levels do not always correspond to these protein levels. Caltabiano et al. (2010) found 90% of high histological grade astrocyte tumors showed an intracytoplasmic positivity for Cx43 mRNA, although 80% of the high grade astrocyte tumors had a significant reduction or negativity for Cx43 protein (Caltabiano et al., 2010). Likewise, in malignant grade IV glioma samples with minimal Cx43 protein levels, 27.3% of the dataset exhibited a 2-fold decrease of Cx43 mRNA, while 20.3% showed a 2-fold increase of Cx43 mRNA (Gielen et al., 2013). Not only in brain cancers, in lung cancer cell lines, traceable level of Cx43 mRNA and variable level of Cx45 mRNA were detected by RT-PCR, but neither Cx43 nor Cx45 protein could be detected by Western blot (Zhang et al., 2004). These findings suggest that the lack of Cx43 protein in some cancer samples or cell lines are not due to a reduction of transcription. Post-transcriptional and post-translational mechanisms could also play

important roles in the regulation of Cx43's life cycle, such as protein synthesis, trafficking, gap junction assembly, internalization, and degradation.

2.2   Connexin Life Cycle

2.2.1   Synthesis of Connexin

Most connexins co-translationally insert into the ER membrane and fold into a mature form with assistance from chaperones and disulphide-isomerases (John and Revel, 1991) (Figure 1.2). A small portion of Cx26 and Cx43 can also be post-translationally incorporated into ER microsomes (Ahmad et al., 1999; Zhang et al., 1996). These misfolded or superfluous connexins will be removed through ER-associated degradation mechanism (ERAD) which will be discussed later (VanSlyke and Musil, 2002).

Once translated, most connexins have a very short life span. The half-life of connexins usually ranges from 1 to 5 h in both tissue and cultured cells (Beardslee et al., 1998; Fallon and Goodenough, 1981; Laird, 2006). Connexins' very short half-lives contribute to the up- or down-regulation of gap junction coupling in order to meet the quickly changed physiological requirement such as gap junction clear-up after laboring (Laird, 2006). Similar to most proteins that form channels, oligomerization of connexins occurs before delivery to the plasma membrane. Depending on the connexin subtype, oligomerization can occur either in the ER–Golgi intermediate compartment (Cx32) or trans-Golgi network (Cx43) (Koval, 2006).

Key:

Cx43		Open channel	
Closed Connexon		Cadherins	
Channel destined to degrade		Transport Vesicle	
2nd Messengers		Microtubules	
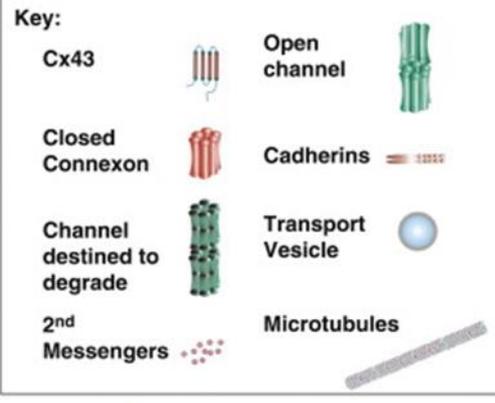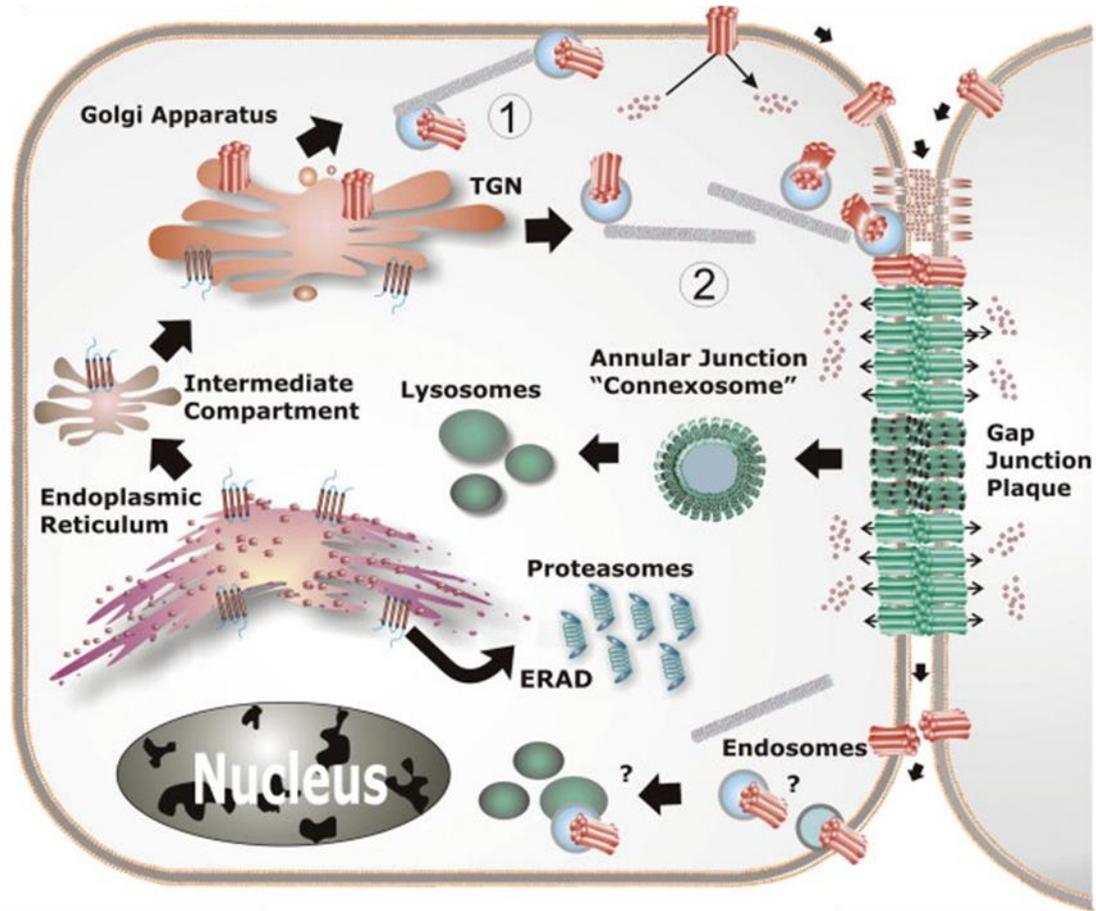
Figure 1.2 Life cycle of connexins. Connexins typically co-translationally insert into the ER. Misfolded connexins are targeted for ERAD. Mature connexins can oligomerize in either trans-Golgi network (TGN, such as Cx43) or in ER-Golgi intermediate compartment (ERGIC, such as Cx32). Connexons are subsequently transported to the plasma membrane, which is facilitated by microtubules. Connexons may be functional as hemichannels or dock with another connexon from neighboring cells to form a gap junction channel. Gap-junction channels assemble into plaques, opening and exchanging secondary messengers. Old channels are found in the center of plaques and new channels are at the boundaries. Gap-junction plaques internalize into one of two adjacent cells as a double-membrane structure named annular junction (connexosome). Also, connexons may internalize via endocytic pathways. Gap junction degradation occurs in lysosomes or proteasome. This figure is adopted from (Laird, 2010).

2.2.2 Connexin Trafficking and Gap Junction Assembly

Trafficking of connexins from Golgi to the cell membrane occurs by successive vesicles budding and fusion from the ER through the Golgi stacks, and then the vesicles are transported to the cell membrane. Some isoforms (e.g. Cx43) require microtubules transport to reach the membrane while some others (e.g. Cx32 and Cx30) trafficking independently from the microtubules (Qu et al., 2009; Thomas et al., 2005). Once inserted into the plasma membranes, connexons diffuse freely within the lipid bilayer (Thomas et al., 2005). A pulse–chase experiment demonstrated that new connexons incorporate at the outer margins of old gap junction plaques (Gaietta et al., 2002). In the Cx43 gap junction plaque, old and new channels can be distinctly separated (Lauf et al., 2002; Thomas et al., 2005), whereas Cx26 plaque has substantially larger mobility (Thomas et al., 2005). Older channels in the middle of a plaque internalize into vesicles with various sizes (Gaietta et al., 2002). Interestingly, the traditional model of how new synthesized Cx43 gap junction incorporate into the plaque was challenged by Shaw et al. (Shaw et al., 2007). They found that Cx43 hemichannels were directly guided to gap junction plaque dependent on EB1 (microtubule plus-end-tracking protein) which tethers microtubules to the adhesion junctions (Shaw et al., 2007). Their model emphasizes the importance of adhesion junction in the gap junction assembly, which could be essential in the gap junction organization.

2.2.3 Gap Junction Internalization and Degradation

The internalization of large double-membrane gap junction vesicles termed

"annular junctions" (also called connexosomes) were identified by electron microscopy (Bjorkman, 1962; Ginzberg and Gilula, 1979). Accumulated evidence confirm that annular junctions exist in cell lines and tissues (Kojima et al., 1996; Mazet et al., 1985; Murray et al., 1997; Naus et al., 1993). When gap junction channels internalize, one cell plays the role of acceptor and the other performs as a donor, as the double-membrane vesicle internalizes into one of two opposing cells (Jordan et al., 2001). The internalization of annular gap junction is clathrin-dependent (Larsen et al., 1979; Piehl et al., 2007), while adaptor proteins such as Dab2, AP-2, and dynamin assist the process (Gumpert et al., 2008). Besides annular junctions, gap junctions also internalize through other mechanisms. In regenerating hepatocytes, the Cx32 gap junction plaque disassembles into smaller aggregates, possibly for internalization (Fujimoto et al., 1997). Caveolin also has been shown to co-immunoprecipitate and colocalize with Cx43 and Cx26, indicating that connexins can be guided to lipid rafts and internalized in a caveolae-dependent mechanism (Schubert et al., 2002).

Connexin degradation depends on both the proteasome and lysosome pathways. The participation of the proteasome has been found for Cx43 and Cx32 degradation in the ER (VanSlyke and Musil, 2002). Although most of the connexin proteins degraded by the proteasome via ERAD are incorrectly folded, VanSlyke et al. (2002) estimated that over 40% of Cx43 and Cx32 undergo ERAD under normal conditions. Inhibition of ERAD increases gap junction channel formation and function (VanSlyke and Musil, 2002). One possible reason is that ERAD may regulate gap junction stability by regulating Cx43's binding partner, like ZO-1 (Girao et al., 2009). Ubiquitination is an

important step for lysosomal degradation. Eps-15 interacts with unbiquitinated Cx43 that leads to degradation of Cx43 via endocytic pathway (Girao et al., 2009). Lysosomal degradation is also important to gap junction. Annular gap junctions were detected in lysosomes by electron microscopy (Ginzberg and Gilula, 1979; Qin et al., 2003). Inhibition of lysosomal function increases the protein level of connexins (Laing et al., 1997; Qin et al., 2003). Blocking lysosomal degradation associates with an increase of Cx43 protein half-life but not preservation of gap junction plaques, while inhibition of proteasomal degradation also increases the level of Cx43 as well as stabilizes Cx43 in gap junction plaques in most cell types (Solan and Lampe, 2016).

Gap junctions are also degraded via autophagy. Cx43 and Cx50 annular gap junctions were detected being enclosed by the autophagy-related protein LC3 via electron microscopy (Lichtenstein et al., 2011). Knockdown of autophagy-related protein Atg5 blocks the starvation induced connexin degradation (Lichtenstein et al., 2011). In the liver, an increased enrichment of Cx26, Cx32, and Cx43 in autophagosomes and lysosomes was identified in starved mice compared with fed wild-type mice (Bejarano et al., 2012).

2.3   Gap Junction Channel Gating

Gap junction channel gating is characterized by conductance. Gap junction conductance Gj is described as $Gj = N \times Po \times \gamma$, where N is the amount of active channels in the plasma membrane, Po is the open probability, and γ is the conductance of a single channel. N is determined by gap junction expression, trafficking, assembly, and

degradation, which was discussed in the last section. γ is dependent on the property of different connexin isoforms. Po is controlled by the voltage, Ca^{2+} pH, phosphorylation, and protein partner interaction which will be discussed in this section (Imanaga et al., 2004).

2.3.1   Voltage Gating

Most gap junction channels are influenced by voltage. Gap junction channel detect voltage changes by a "voltage sensor", which includes charged amino acids. Then, the voltage sensor transfers the electrical energy into mechanical energy, leading to the conformational changes that affect channel gating (Gonzalez et al., 2007).

All vertebrate junctional conductance can be regulated by the transjunctional voltage (V_j) and some gap junctions are sensitive to both V_j and V_m (transmembrane voltage) (Gonzalez et al., 2007). Mutational analyses on Cx32 and Cx26 indicate that charged amino acids on the NT-domain are essential to the V_j dependence (Oh et al., 1999; Purnick et al., 2000; Verselis et al., 1994). The CT-domain is also an important component of fast V_j-gating. Truncation of the CT-domain at $Cx32_{220stop}$ and $Cx43_{257stop}$ lead to the loss of fast conductance and induce novel gating properties mostly dependent on the slow gating (Revilla et al., 1999). A "ball-and-chain" model has helped to describe the mechanism of fast V_j-gating in Cx channels. In this model, the movement of the CT-domain toward the channel pore would cause the physical blockage of the pore (Gonzalez et al., 2007). A similar model (so called "particle-receptor" model) was used in the chemical gating of gap junction channels, such as acidification and

phosphorylation that drive the channels into the closed state (will be discussed later)
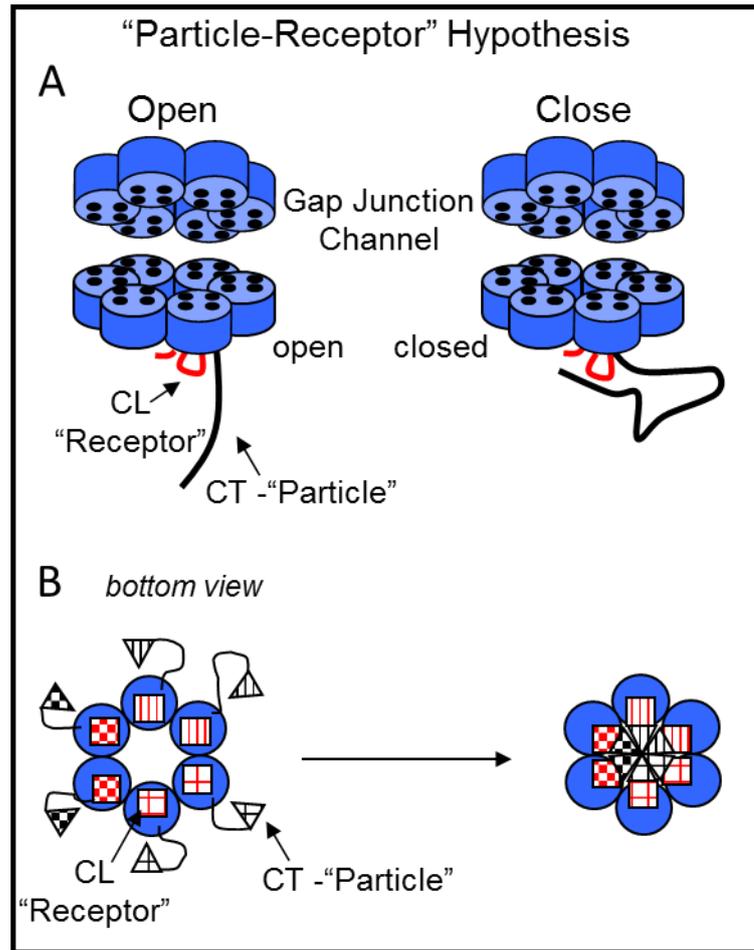
Figure 1.3 "Receptor-and-particle" model (also "ball and chain" model) of connexin regulation. (A) Under normal conditions, the particle (CT) is apart from the pore. Under the particular stimulus (such as pH, Ca^{2+}, phosphorylation), the particle swings toward the channel, interacts with a receptor (CL) and blocks the channel. (B) the bottom view of receptor and particle model.

(Figure 1.3) (Homma et al., 1998; Liu et al., 1993; Zhou et al., 1999).

In some connexin channels, such as the rat Cx43 and the mouse Cx45, junctional conductance is also sensitive to membrane potential, V_m (Barrio et al., 1997). Interestingly, V_m sensitivity of Cx43 was observed in *Xenopus* oocytes but not in HeLa cells (Bukauskas et al., 2001; Revilla et al., 2000). The uncoupling by membrane depolarization may be a protection mechanism to keep neighboring cells from electrotonic effect (passive spread of charge) of damaged cells.

2.3.2   pH-dependent Channel Gating

In the pathological situation, acidification closes most gap junction channels (Bevans and Harris, 1999; Eckert, 2002; Liu et al., 1993; Werner et al., 1991), which may be a mechanism for minimizing injury to normal cells via the bystander effect (Spray et al., 2013). Gap junctions composed of different connexin isoforms have different opening rates at physiological pH. For example, Cx43 channels are mainly open at pH 7.2 (Ek-Vitorin et al., 1996), whereas only 1% of mouse Cx57 channels open at this pH (Palacios-Prado et al., 2009). Under various pH conditions, some connexin CT domains have different secondary structures. For example, circular dichroism (CD) data identified that the soluble Cx43CT domain at pH 5.8 contains 7% α-helical whereas little-to-no α-helical content was observed at pH 7.5 (Bouvier et al., 2009). Besides Cx43, the Cx32 and Cx45 soluble CT domains gain α-helical structure outside the membrane interface under acidic pH conditions (pH 5.8) (Spagnol et al., 2016). Trexler et al. (1999) observed rapid closure with low pH application in Cx46

hemichannels which demonstrates direct action of H^+ on connexins (Trexler et al., 1999). The pH sensor (H^+ binding site) is located on the cytoplasmic side, probably near the entrance of the pore (Trexler et al., 1999). As mentioned previously, pH induced channel gating can also be explained by "particle-receptor" model (Morley et al., 1996). Several studies in *Xenopus* oocytes have suggested the participation of residues located in the CL and the CT in the pH gating (Ek-Vitorin et al., 1996; Ek et al., 1994) (Peracchia and Wang, 1997; Wang and Peracchia, 1996). Truncation of Cx43CT led to pH-insensitivity of the channel (Morley et al., 1996). pH sensitivity was restored when co-expression of Cx43CT domain and the truncated pH-insensitive Cx43 (Morley et al., 1996). Additionally, co-expressing the Cx43CT with Cx32 (a less pH-sensitive connexin isoform) increased the pH sensitivity (Morley et al., 1996). The potential pharmaceutical applications of pH-dependent channel gating include a cyclized heptapeptide, CyRP-71, which binds to Cx43CT and partially inhibits channel closure by acidification (Verma et al., 2009).

2.3.3 Ca^{2+}-dependent Channel Gating

Gap junctional communication can be inhibited by elevated intracellular Ca^{2+} concentration. Ca^{2+} effect on gating is mediated by calmodulin (CaM) via Ca^{2+}-dependent interactions with connexin cytoplasmic domains (Blodow et al., 2003; Peracchia et al., 1983; Sotkis et al., 2001). Channel gating regulated by CaM has been found for Cx32 (Peracchia et al., 2000), Cx36 (Burr et al., 2005), Cx43 (Lurtz and Louis, 2007), Cx44 (Zhou et al., 2009), Cx45 (Peracchia et al., 2003) and Cx50 (Chen et al.,

2011). The interaction of CaM with connexins usually induces a conformational change on the connexin proteins. Zhou et al. (2007) used multiple biophysic methods to identify that CaM directly bound to the Cx43CL (aa 136-158) in a Ca^{2+} dependent manner (Zhou et al., 2007). Upon CaM binding, the α-helical content in this Cx43CL increased (Zhou et al., 2007). Cx32 has two CaM binding sites on the NT and the CT domains respectively (Torok et al., 1997). Cx32CT, which is an intrinsically disordered protein, exhibits an increased α-helical content upon binding CaM (Stauch et al., 2012). Likewise, the induced α-helix by CaM was also found in the other connexin isoforms, such as Cx44 and Cx50 (Chen et al., 2011; Zhou et al., 2009). This induced conformational change in the cytosolic domains may block the pore of the gap junction channel to limit passage of ions (Dodd et al., 2008; Peracchia et al., 2000). Addition of connexin-derived peptides or CaM inhibitor to counteract the Ca^{2+}/CaM-connexin interaction can alter channel gating from the closed to open state (reviewed in (Zou et al., 2014)).

2.4 Importance of the CT Domain for Regulation on Connexins

2.4.1 Intrinsically Disordered Proteins

Many proteins need to adopt a unique and well-ordered structure to be functional. The precise conformation of functional groups is crucial for protein binding or catalysis of a chemical reaction. However, over the last several decades, there has been a growing recognition of functional proteins that do not adopt a defined three-dimensional structure (nearly 40% in eukaryotic proteome). These proteins, which are defined as

having over 30 continuous residues forming unstructured regions or domains, are classified as intrinsically disordered proteins (IDPs). Indeed, the intrinsically disordered portions in a protein are crucial. First, the unstructured regions may provide a large interaction surface area for protein binding. Second, the conformational flexibility of IDPs allows binding motifs to overlap, thus they can interact with numerous other proteins. Third, various post-translational modification may induce a conformation change in order to regulate the function of the protein (Babu et al., 2011).

2.4.2   Connexin Cytoplasmic Domains

The connexin cytoplasmic domains (NT, CL, and CT) play roles in gap junction channel gating and modulating channel formation and function. They contain sites for post-translational modifications and are able to interact with multiple protein partners (Goodenough and Paul, 2009). NT is relatively conserved in length, whereas CL and CT are various among different isoforms. Chimeric and point mutants are used to study different features of cytoplasmic domains; CD, AUC and NMR have allowed for the structural study of these domains. The following sections will provide detailed information regarding the important features and structural aspects of connexin cytoplasmic domains.

The connexin NT domains are composed of 22 (α-group connexins) or 23 (β-group connexins) amino acids except Cx36 (24 residues) and Cx47 (25 residues) (Kyle et al., 2008). NT domain is necessary for proper incorporation into the membrane as several positively charged residues which act as anchors for the insertion are essential (Thomas

et al., 2008). Mutation of a positively charged residue on the NT to a negatively charged amino acid on Cx50 lead to the completely failure of plaque formation (Thomas et al., 2008). Many mutations in the NT domain have been found to associate with different diseases including CMTX (Cx32) (Bergoffen et al., 1993), deafness (Cx30) (Common et al., 2002) and ODDD (Cx43) (Shibayama et al., 2005); most of these mutations cause cytoplasmic retention or non-functional channels. The NT domain also participates in regulating voltage gating and plays a fundamental role in ion permeation since it is close to the channel where it can act as a voltage sensor (Purnick et al., 2000). The 3.5 Å X-ray structure of Cx26 channel showed that the NT domains of six connexins compose the funnel in the pore and could form the plug to close the pore while sensing the Vj change (Maeda et al., 2009). A few post-translational modifications were found in the NT domain of different connexins by MS. These include phosphorylation (Cx26 and Cx32), hydroxylation (Cx26), deamidation (Cx46), and acetylation Cx26 (Locke et al., 2006; Wang and Schey, 2009). However, functional study of these modifications are lacking. Although the length of the NT domain is conserved among different connexin isoforms, the structures are different. Solution NMR was used to determine the NT domain structure from two β-group connexins: while Cx26NT contains a α-helix, Cx32NT is completely disordered (Kalmatsky et al., 2009; Piechocki et al., 2000).

The length of the CL domains varies among the different connexin isoforms. Based on length, they can be divided into three categories: short (30-35 aa), medium (50-55 aa), and large (80-105 aa) (Sohl and Willecke, 2004). The CL is also involved in connexin trafficking and gap junction plaque formation. Studies show that deletion of

the Cx43CL (aa 130-134) forms gap junction plaques but not deletion of aa 130-137, suggesting the amino acids 135-137 could be critical for gap junction assembly (Oyamada et al., 2002; Seki et al., 2004); notably, none of these mutants form functional gap junctions. Similarly, deletion of Cx32CL (aa 111-116) shows less efficiency in the dye transfer assay compare with wild-type (Martin et al., 2000). CL domain is also important for protein interactions, which are involved in channel function. For example, CaM binding sites have been identified in the second half of the CL domain of Cx43, Cx44, and Cx50 (Chen et al., 2011; Zhou et al., 2009; Zhou et al., 2007). As previously mentioned, CaM binding is important for the Ca^{2+}-dependent closure of gap junctions. Cx43CL also has been implicated to interact with the CT domain in a pH-dependent manner; in the "particle-receptor" model, the Cx43CL domain plays the role as receptor (Duffy et al., 2002). Post-translational modification on residues of CL domain includes phosphorylation (Cx49, Cx50, and Cx56) and carboxylation (Cx26 and Cx32) (Locke et al., 2006; Wang and Schey, 2009) (Berthoud et al., 1997). Phosphorylation on Cx56CL S118 leads to down-regulation of intercellular communication and increased degradation (Berthoud et al., 1997). The CL domain is largely unstructured but contains α-helical propensity. The NMR structure of the Cx43CL peptide (D119-K144) shows two α-helices (N122-Q129, K136-G143) in the second half of the loop (Duffy et al., 2002). Cx32 and Cx36 also contain α-helical propensity in the second half of the loop (Fort and Spray, 2009). Acidification or binding with calmodulin induce helical structure in the Cx43CL, which increases the affinity for the Cx43CT (Duffy et al., 2002; Zhou et al., 2007).

In the connexin primary sequence, the most variable domain among connexin isoforms is the CT domain. Different connexin CT domains are diverse in size, which range from 10 amino acids in Cx26 to more than 310 amino acids in Cx62. CD analysis of the soluble CT domain of Cx26, Cx32, Cx37, Cx40, Cx43, Cx45, and Cx50 shows that they are all primarily disordered (Spagnol et al., 2016). However, some of the CT domains have propensity to become α-helical upon post-translational modification or protein-protein interaction (Bouvier et al., 2009). The structure of the Cx43CT domain determined by solution NMR shows that the Cx43CT has two α-helical regions (A315-T326 and D340-A348) (Sorgen et al., 2004). These two helical regions are involved in the Cx43CT dimerization and the pH-dependent interaction with the CL domain, indicating their roles in channel gating and pH sensitivity (Duffy et al., 2002; Sorgen et al., 2004). In the Cx43CT structure when attached to the 4th transmembrane domain (TM4-Cx43CT) reported by our laboratory, seven α-helical regions (H1-7) have been predicted in the CT portion (Grosely et al., 2013). H4 (K303-A322) and H5 (D340-L353), which contain the two helical regions identified in the soluble Cx43CT, span a greater area (Grosely et al., 2013). The disordered regions outside of these helices are responsible for binding with protein partners, and can undergo structural transitions upon binding (Kieken et al., 2009; Saidi Brikci-Nigassa et al., 2012). Cx32CT and Cx36CT also contain two distinctive regions with helical propensity (Fort and Spray, 2009). These α-helical domains may allow the formation of more ordered structure during chemical gating or facilitate the cross-talk between different binding partners (Sorgen et al., 2004). To date, among connexin isoforms, Cx45CT contains the largest

α-helix (33.6%) that is involved in dimer formation (Kopanic and Sorgen, 2013).

Many post-translational modifications occur on the connexin CT domain; these include phosphorylation, ubiquitination, hydroxylation, acetylation, nitrosylation, oxidation, and palmitoylation (reviewed in (Axelsen et al., 2013)). Gap junctions are known to be highly regulated by phosphorylation and ubiquitination (except Cx26, which is the only connexin has not been shown to be phosphorylated to date) (Traub et al., 1989). The frequency of phosphorylation on connexin CT domain is extremely high, because phosphorylation predominantly occurs in the disordered region of a protein (Iakoucheva et al., 2004). Indeed, the disordered structure is crucial for establishing hydrogen bonds between the substrates and its kinase partners, which is less likely if the site is in ordered region (Iakoucheva et al., 2004). Phosphorylation can result in changes of charge (each phosphorylation creates 2 negative charges at pH 7), hydrophobicity, and structural transition (e.g. disorder-to-order) which mediates many of the major functions in channel gating and life cycle (Davis, 2011; Fuxreiter et al., 2004; Nishi et al., 2011). Phosphorylation can also regulate protein-protein interactions by altering the thermodynamic favorability of binding (Boehr et al., 2009). Indeed, many of the phosphorylation sites on the connexin CT domains are included within protein binding regions (Kopanic and Sorgen, 2013; Solan and Lampe, 2005). Details about how phosphorylation regulates gap junction communication will be discussed later.

Many binding partners of the connexin CT domain have been identified, including Zonula Occludens 1 (ZO-1), tubulin, mitogen-activated protein kinase (MAPK), v- and

c-Src, casein kinase 1 (CK1), Drebrin, cAMP-dependent protein kinase, and CaM (Ambrosi et al., 2016; Cooper and Lampe, 2002; Giepmans, 2004; Giepmans et al., 2001; Li et al., 2004; Saez et al., 1990; Zou et al., 2014). A disordered connexin CT domain is an ideal substrate for the regulation of intercellular signaling by facilitating both high specificity and low affinity interaction with many different binding partners to allow the rapid feedback to cytoplasmic signals (Dunker and Obradovic, 2001; Sorgen et al., 2004).

The connexin CT alone has been observed in both of cytoplasm and nucleus to regulate cell growth (de Feijter et al., 1996; Maqbool et al., 2015; Mennecier et al., 2008; Moorby and Patel, 2001). Transfection of the Cx43CT domain in cardiomyocytes and HeLa cells indicate that nuclear localization of the Cx43CT inhibits cell growth (Dang et al., 2003). The 20 kDa fragment which was higher than the expected size of Cx43CT (15 kDa) suggests the presence of post-translational modifications (Dang et al., 2003). Further research discovered that in the Cx43CT down-regulated primary human breast cancer samples, the decrease of Cx43CT is associated with the decrease of p53, suggesting the regulatory role of nuclear localized CT domain on particular genes (Maqbool et al., 2015). Since no DNA-binding motif has been found on the CT domain, it may interact with transcription factors or complexes to regulate cell cycle related gene expression.

3. Phosphorylation of Connexins

3.1 General Introduction of Connexin Phosphorylation

Since connexins were first uncovered as phosphoproteins in the 1980s (Lowenstein, 1985; Saez et al., 1986), numerous phosphorylation sites have been identified (Table 1). Phosphorylation regulates connexin proteins (except Cx26) in all stages of the connexin life cycle (i.e. trafficking, assembly/disassembly, degradation, and channel gating (Solan and Lampe, 2007)), electrical gating, and metabolic coupling (Lampe and Lau, 2004; Solan and Lampe, 2005, 2007; Thevenin et al., 2013). To date, Cx26 is the only connexin not identified to be phosphorylated (Traub et al., 1989). Since Cx26 can form functional channel, together with the fact that truncated Cx43 mutants that lack most of the CT domain (the dominate phosphorylation domain of Cx43) can also form functional channels, phosphorylation is not required for channel formation (Lampe and Lau, 2004).

Most of the phosphorylation events that occur on connexins are serine/threonine residues. Serine/threonine kinases that phosphorylate connexins include PKC, MAPK, p34(cdc2)/cyclin B kinase, PKA, CK1, p34cdc2, PKG, CaMKII, and Akt (Lampe and Lau, 2004; Palatinus et al., 2012). Several connexin isoforms are also phosphorylated on tyrosine residues. To date, tyrosine kinases that have been identified to directly phosphorylate connexin isoforms include Src (Loo et al., 1995), Fps (Kurata and Lau, 1994) and EGFR (Diez et al., 1998). In this section, we will discuss the methods for studying phosphorylation on connexins, serine/threonine phosphorylation, and more emphasis will be on tyrosine phosphorylation. Since Src is the most well studied tyrosine kinase that directly phosphorylates Cx43 on tyrosine residues of the CT domain and Cx43 phosphorylation by Src is fundamental to my dissertation, I will

Table 1.1 Reported phosphorylation sites of connexins, responsible kinases and the effect on gap junctions.

Kinases	Connexins	Phosphorylated residues	Reported effects on GJs
PKA	Cx32	S233	increase GJIC
	Cx35/36	S110, S276	reduce GJIC
			Increase GJIC
	Cx40	n/a	increase GJIC
	Cx43	S364, 365, 368, 369, 373	rapid GJ assembly, increase GJIC
	Cx50	S395	increase GJIC
PKC	Cx43	S373	increase GJ size and GJIC
	Cx50	n/a	increase GJIC
	Cx43	S365, 368, 369, 372, 373	decrease GJ assembly, decrease GJIC, reduce half-life of Cx43, decrease coupling
	Cx32	S233	n/a
	Cx56 chicken homologue of Cx46	S118	decrease GJIC
PKG	Cx35/36	S110, S276, S289	decrease GJIC
CaMKII	Cx43	S244, 255, 257, 296, 297, 306, 314, 325, 328, 330, 364, 365, 369, 372, 373	de-phosphorylation of S306 during ischemia reduces GJIC
	Cx32	n/a	n/a
	Cx36	n/a	increase GJIC
	Cx45	S326, T337, S381, 382, 384, 385, 387, 393	n/a
CK1	Cx43	S 325, 328, 330	increase GJ assembly
	Cx45	S 326, 382, 384, 387, 393	n/a
Cdk5	Cx43	S279, S282	prevents membrane targeting, promotes proteasome dependent degradation
P34cdc2	Cx43	S255, S262	GJ internalization
MAPK	Cx43	S 255, 262, 279, 282	GJ internalization, decrease GJIC
	Cx50	n/a	n/a
Src	Cx43	T247, 265	reduce GJIC
EGFR	Cx32	Y243	n/a

This table is modulated from (Pogoda et al., 2016).

discuss the mechanism and the biological effects of Src phosphorylation on Cx43 in detail.

3.2 Methods of Studying Phosphorylation on Connexins

Traditionally, direct incorporation of ^{32}P was the primary choice to study the phosphorylation on connexins. In this method, tagged-Cx transfected cells were metabolically labelled with [^{32}P] orthophosphate, immunoprecipitated and ran on 2D SDS-PAGE. Serine, tyrosine, and threonine phosphorylation can be separated and analyzed by autoradiography. Although this method does not identify the phosphorylation site(s), it does provide information regarding the type of phosphorylation. To study the function of phosphorylation on connexins, however, identification of the phosphorylation sites is crucial. Before the wide use of MS for this purpose, Edman degradation and site-directed mutagenesis were the main methods employed to identify the specific phosphorylation sites. Cx43 S368 phosphorylated by PKC (Lampe et al., 2000) and S255/279/282 phosphorylated by MAPK (Warn-Cramer et al., 1996) were identified by these methods. In many connexin isoforms, phosphorylation results in slower migration on SDS-PAGE gels, such as Cx40 (Chen et al., 2004), Cx50 (Pelletier et al., 2015), and Cx43 (Solan and Lampe, 2009). Differentially phosphorylated Cx43 results in multiple electrophoretic isoforms: a fast migrating isoform (P0) and multiple slower migrating isoforms (P1 and P2) (Crow et al., 1990; Matesic et al., 1994; Solan and Lampe, 2005). Solan et al. (2009) summarized some of P0, P1, and P2 components in (Solan and Lampe, 2009). Phosphorylation-

dependent shifts may be caused by two reasons: first, phosphorylated residues adjacent to proline could induce structural perturbations of the protein, which change the electrophoretic mobility in SDS-PAGE (Smith et al., 1989). Second, the negative charges on the phosphate group could disturb the charge-to-mass ratio by affecting the protein-SDS interaction (Grosely et al., 2013b).

Within the past decade, a number of Cx43 phospho-specific antibodies were developed and played important roles in study of phosphorylation sites *in cyto* or *in vivo*. For example, by using phospho-specific antibody, Lampe et al. (2006) found phosphorylation of S325/328/330 is involved in the P2 level (Lampe et al., 2006). However, due to the complicated cell-signaling network, phosphorylation by a single kinase on Cx43 is less likely. Thus, using phospho-specific antibody is hard to define the components of the different migration levels of Cx43. For example, Solan et al. (2008) showed pY247 and pY265 exist in all three migration levels in v-Src activated LA-25 cells, suggesting the contribution of other phosphorylation sites (Solan and Lampe, 2008). Therefore, to define the contribution of a single kinase to the migration levels of Cx43, Grosely et al. (2013) used phospho-mimetic of Cx43CT (S/Y-D mutation) and discovered that the nonphosphorylated Cx43CT, Src, PKC, and cdc2 phospho-mimetic isoforms migrate at P0, MAPK at P1, and CK1 at P2 (Grosely et al., 2013b).

Phosphorylation can regulate the conformation of proteins, affecting their subcellular localization. Thus, structure-specific antibodies can help to study the relevance between phosphorylation and connexin localization. Lampe's group in Fred

Hutchinson Cancer Research Center developed two monoclonal antibodies, CT1 and IF1, using the same peptide representing Cx43 360-382. However, two antibodies selectively labelled different subcellular fractions of Cx43. Epitope of Cx43 IF1 developed by mapping to ^{375}PRPDD^{379} requires P^{375} and P^{377} for binding (Sosinsky et al., 2007). This antibody stains only gap junction plaques and recognizes the P0, P1, and P2 forms, suggesting that the tertiary structure of P^{375}–A^{379} is essential in targeting Cx43 at the gap junction plaque (Sosinsky et al., 2007). Whereas, Cx43 CT1 labels mainly perinuclear Golgi-like structures detecting a conformation that is non-phosphorylated on S^{364} and/or S^{365}, suggesting that conformation of pS^{364}/S^{365} may be essential for membrane localization (Sosinsky et al., 2007).

Since the mid-1990s, MS has been consistently used for site-specific phosphorylation analysis due to the development of several technologies. Matrix-associated laser desorption ionization (MALDI)-time-of-flight (TOF)-MS, collision-induced dissociation (CID)-MS/MS, and electron-capture dissociation (ECD)-MS/MS have been successfully used in analyzing phosphorylation sites on connexin isoforms both *in vitro* and *in vivo* (Cooper et al., 2000; Huang et al., 2011; Locke et al., 2006). Compare with traditional methods, MS is highly sensitive which can detect femtomole of phosphopeptides, sensitive enough to detect most of phospho-proteins (Ficarro et al., 2002). Also, it does not require phosphopeptides to be radioactively labeled. Moreover, MS can detect phosphorylation more rapidly and efficiently with relatively low cost. Although MS is the most widely used technique to identify phosphorylation sites, the accuracy can be affected by the following reasons. First, a given phospho-protein is

heterogeneous. Commonly, in sample treated with a kinase, the phosphorylated form of the target protein represents only a small portion of the total protein. Second, due to the limitation of fractionation methods and primary sequence of the given protein, the full coverage of the protein is difficult. Third, when two phosphorylation sites are close to each other, especially next to another, the identification of the exact phosphorylated residue is difficult. Besides, the detection of phosphorylation sites from cell lysate is also affected by the low abundance of phosphorylated proteins and dephosphorylation caused by phosphatases in cells. Thus, although phosphorylation events were studied in most of the known connexin family members, it is possible that more phosphorylation sites will be identified in the future. Some databases based on MS data provide good sources for studying connexin phosphorylation residue, such as http://www.phosphosite.org.

Identification of new kinases that phosphorylate connexins would also be very important for characterizing the function of connexins. One method is combining the computer algorithm with the *in vitro* kinase-screening assay. Many of the online programs can be used to predict connexin's kinase binding partners based on the consensus motifs, such as GPS 3.0 (Xue et al., 2008) and NetPhos 2.0 Server (Blom et al., 1999). Once a list of kinase candidates is identified, purified connexin substrates can be used to conduct *in vitro* kinase screening. More details of this methodology will be discussed in the method section of Chapters 2 and 3.

3.3 Serine Phosphorylation

To date, Cx43 is the most well understood isoform in terms of serine phosphorylation. Since my dissertation focuses on Cx43, a detailed review of serine phosphorylation on this isoform will be emphasized in this section. The Cx43CT is differentially phosphorylated on at least 21 residues including 19 serine and significant progress has been achieved in characterizing these phosphorylation sites (Figure 1.4) (Axelsen et al., 2013; Lampe and Lau, 2004; Solan and Lampe, 2005, 2014).

Phosphorylation on some sites increase gap junctional intercellular communication whereas others decrease gap junctional intercellular communication (Table 1.1). Generally, MAPKs, PKC, and Src associate with channel closure, inhibition of intercellular communication, and enhancement of gap junction internalization (Cottrell et al., 2003; Li et al., 2014; Pogoda et al., 2016; Warn-Cramer et al., 1996). This phenotype has been observed in many different cell models and tissues (Cottrell et al., 2003; Li et al., 2014; Naitoh et al., 2009; Warn-Cramer et al., 1996). To the contrary, phosphorylation of Cx43 by CK1 and PKA promotes gap junction trafficking, assembly, and increase intercellular communication (Cooper and Lampe, 2002; Shah et al., 2002; Solan and Lampe, 2016).

Phosphorylation on Cx43 is spatio-temporally regulated in a "kinase program". Falk et al. (2016) provide a model of consecutive serine phosphorylation events to regulate gap junction assembly and turnover: (1) phosphorylation on S373 (Akt) and S365 (PKA) promote forward trafficking of connexons to the membrane. (2) dephosphorylation on S373 (Akt) allows the binding with ZO-1 which facilitates
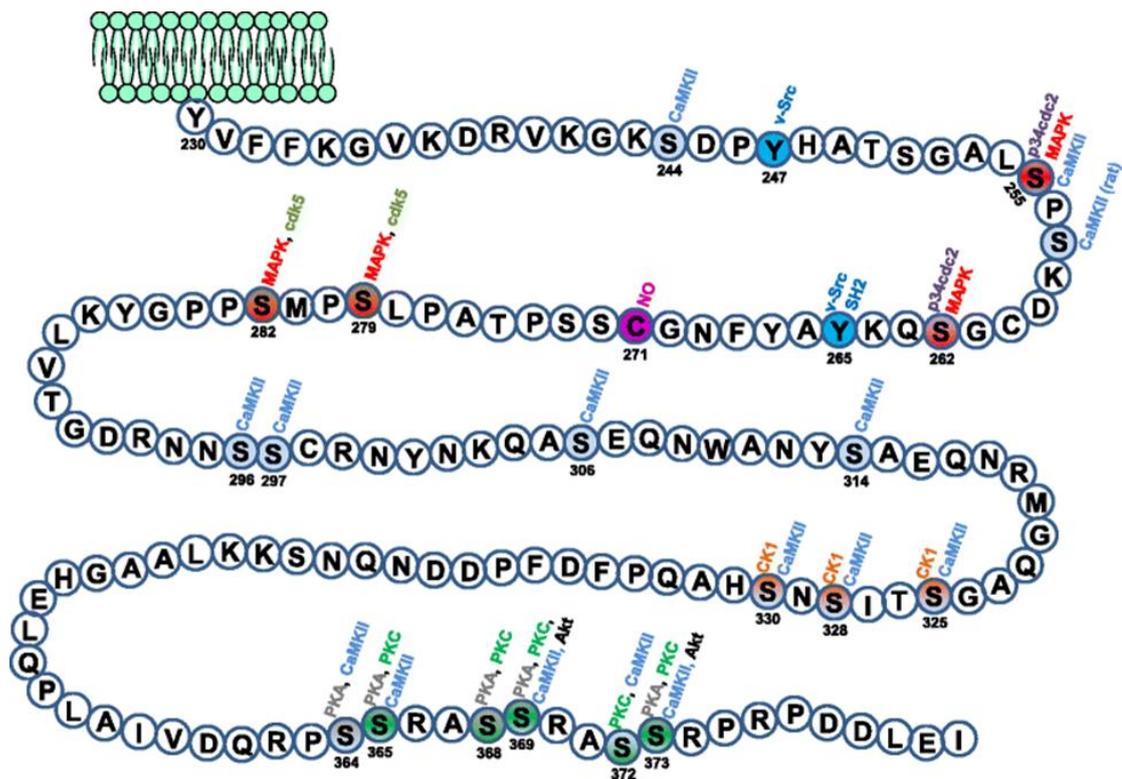
Figure 1.4 Connexin43 phosphorylation sites. 21 residues have been observed to be phosphorylated on the Cx43CT domain.Y247 and Y265 are Src phosphorylation sites, the other 19 residues are serine. Residues phosphorylated by Src (Y247 and Y265), MAPK (S255,262,279,282), CK1 (S325,328,330), PKA (S364,365,369,323), PKC (S368 and S372), Akt (S373 and S369) are firmly confirmed in cells (Cooper and Lampe, 2002; Lampe et al., 2000; Nimlamool et al., 2015; Park et al., 2007; Shah et al., 2002; Solan and Lampe, 2007, 2008; Yogo et al., 2002). Residues phosphorylated by CaMKII are only identified by MS but lack of further evidence in cells (Huang et al., 2011). This figure is reprinted with permission (Pogoda et al., 2016).

connexon docking and channel formation. (3) during the transition from functional to closed gap junction channels, phosphorylation on S365 (PKA) decreases which allows phosphorylation on S368 (PKC). (4) during the prime for internalization, S279/S282 (MAPK) phosphorylation increases. (5) phosphorylation on S279/282 and S368 are linked to clathrin recruitment and endocytosis of annular gap junction (Falk et al., 2016) (Figure 1.5). Early events which include S373 and S365 phosphorylation or de-phosphorylation occur on the far C-terminal portion of the Cx43CT domain, while later events (S279/282 phosphorylation) occur upstream of the around AP-2/clathrin binding sites (Falk et al., 2016). Notably, in their model, S325/328/330 phosphorylated by CK1 which promote gap junction assembly is not mentioned (Cooper and Lampe, 2002; Lampe et al., 2006). Solan and Lampe (2016) proposed a similar model of phosphorylation on Cx43 in response to growth factor (EGF), wounding, or other stimuli (TPA). They measured the time points of these phosphorylation events. According to their study, the involved kinases that phosphorylate Cx43 are Akt at 5–30 min, PKC and MAPK at 15–60 min, and Src at 30 min–24 h (Solan and Lampe, 2016). There are slight differences between these two models. First, in the response to the stimuli, Akt phosphorylation is strong enough to exhaust incoming Cx43 pool to form large gap junction plaques which prepare for annular gap junction formation. This is not the case in normal situation. Second, Src phosphorylation participates in facilitating gap junction internalization in Solan and Lampe's model. The overall effect is the decrease of Cx43 level and gap junction communication, which is necessary for wound

healing because of its role in upregulation of proliferation and migration, or downregulation of the inflammatory response (Solan and Lampe, 2016).

Cx43 phosphorylation does not often occur only at a single site but rather a number of sites that work in concert to coordinate other phosphorylation events and protein partner interactions. For instance, phosphorylation at S365 by PKA serves as a gatekeeper via blocking S368 phosphorylation-induced channel closure by PKC (Solan et al., 2007). Some kinases share common phosphorylation sites. Both PKA and Akt phosphorylate S373. Since they both facilitate Cx43 trafficking to the plasma membrane (Paulson et al., 2000; Solan et al., 2007), their phosphorylation events may be cell-cycle or cell-type dependent.

In some situations, phosphorylation is directly involved in the interaction between Cx43 and other binding partners (Saidi Brikci-Nigassa et al., 2012; Spagnol et al., 2016). Phosphorylation can alter both local structure and long-range structure. At region near the phosphorylation sites, phosphorylation can induce steric or electrostatic effects which impact the secondary structure (Lim et al., 2014). On Cx43CT, serine phosphorylation is usually associated with an increase of α-helical content whereas tyrosine phosphorylation leads to a loss of α-helical structure (Grosely et al., 2013b). Studies from our laboratory compared the secondary structure of Asp-substituted TM4-Cx43CT isoforms (phosphorylation mimetics) with TM4-Cx43CT wild type (Grosely et al., 2013b). CK1, MAPK, PKA and PKC isoforms are more helical than wild type at both pH 7.5 and pH 5.8, while Src isoform is less helical than wild type at acidification situation (Grosely et al., 2013b).

[1]
Secretion

[2]
Docking and Accrual

[3]
Transition

[4]
Prime for Internalization

[5]
Internalization

Cell 1

S373 Ⓟ

ZO-1   ZO-1

S373

S373

GJ plaque edge

GJ plaque center

Hemichannels

Ⓟ

S373   S373

ZO-1   ZO-1

S365 Ⓟ

S368 Ⓟ

S279/Ⓟ
S282 Ⓟ

Cell 2

S373 Ⓟ

S365

PKC
S368

Ub

Dunn & Lampe, 2014

S373 Ⓟ
S365 Ⓟ

MAPK

S279/
S282

AP-2   AP-2

connexon

clathrin

Park et al., 2006/'07

ZO-1

Nimlamool et al., 2015

Eps15

clathrin

Transport vesicle

Rhett et al., 2011

Fong et al., 2014

Piehl et al., 2007
Gumpert et al., '08
Falk et al., 2009
Fong et al., 2013

Akt   PKA

Solan et al., 2007

AGJ

ER/Golgi

Cone et al., 2014

Early:

Late:

Figure 1.5 Schematic of the post-translational modifications that regulate gap junction assembly and internalization. Steps [1 − 5] promote and coordinate the process from functional (green) to close, internalization-prone gap junction channels (yellow, orange) that then are primed to interact with clathrin components which mediate their internalization (red). This figure is reprinted with permission (Falk et al., 2016).

Phosphorylation on some serine residues promote Cx43CT interacting with its binding partners. S373 phosphorylated by Akt is required for 14-3-3 binding, which facilitates Cx43 trafficking to the plasma membrane and incorporation into gap junction plaques (Park et al., 2007). MAPK phosphorylation on serine residues (pS282 and pS279) increases the binding affinity by two-fold for the Nedd4 WW domains which explains why MAPK phosphorylation is involved in Cx43 degradation (Spagnol et al., 2016).

Although many studies have provided a wealth of information on Cx43 serine phosphorylation, there are still a number of questions to be addressed. For example, S365 phosphorylated by PKA and S368 phosphorylated by PKC are in close proximity and both induce an increase in α-helical content compare to the WT TM4-Cx43CT at pH 7.5 (Grosely et al., 2013b), however, their effect on gap junctional intercellular communication is opposite. What mechanism mediates the differential response in gap junctional intercellular communication to S365 and S368 phosphorylation? Another example is that both phosphorylation and dephosphorylation on S368 have been reported in ischemia (Axelsen et al., 2006; Solan et al., 2007). The controversial results suggest a complexity of phosphorylation events arise from a large number of phosphorylation sites, differential phosphorylation level or different time frame. What are the particular cellular conditions that result in differential phosphorylation to regulate gap junction communication?

3.4   Tyrosine Phosphorylation

3.4.1 Mechanism of Src Interaction with Cx43

In the 1980s, pp60^{v-src} was shown to decrease gap junctional communication in NIH3T3 cells (Azarnia et al., 1988; Lowenstein, 1985). However, understanding about tyrosine kinases directly phosphorylating Cx43CT is still limited to v-Src and v-Fps. Since v-Fps induces phosphorylation of Cx43 in a similar manner to v-Src and is far less studied, here we will only focus on the mechanism of Src interaction with Cx43.

The Src kinase is composed of a conserved membrane-associated region on its NT that is myristoylated, followed with SH3, SH2, and kinase domains (Boggon and Eck, 2004). Phosphorylation on the Y416 in the kinase domain is required for Src activation and the autoinhibitory phosphorylation site is Y527 at the CT domain (Boggon and Eck, 2004). v-Src, the oncogene which lacks the Y527, is therefore constitutively active as opposed to normal Src (c-Src) (Smart et al., 1981). Two identified tyrosine sites on Cx43, Y265 and Y247, are sequentially phosphorylated by v-Src. The interaction of v-Src and Cx43 is dependent on the SH3 and SH2 domains of v-Src (Kanemitsu et al., 1997). The proline-rich sequence of Cx43 P274–P284 (contains a PXXP motif) is required for the interaction with the v-Src SH3 domain which adopts a left-handed type II helix upon binding (Kieken et al., 2009); this interaction leads to the phosphorylation of Cx43 Y265 site occurring first, which creates a docking site for the v-Src SH2 domain (Lin et al., 2001). Consequently, the Cx43 Y247 is phosphorylated (Lin et al., 2001). Additionally, in Cx43 Y265F and v-Src co-transfected HEK293 cells, co-immunoprecipitation between Cx43 Y265F and v-Src was lost, and phosphorylation on Cx43 was significantly decreased. These data indicate

that Y265 is the prime site of phosphorylation (Kanemitsu et al., 1997). This potential mechanism would explain why pY265 appears in this and other studies to label a larger population of plaques than pY247 (Solan and Lampe, 2008).

Early study indicates that v-Src phosphorylated Cx43 on tyrosine residues and expression of v-Src completely blocked the communication induced by Cx43 in paired *Xenopus oocytes* (Swenson et al., 1990). Later, investigations showed that Src also increasesd phosphorylation level of MAPK (S279/282 and S262) and PKC (S368) sites, and decreased PKA phosphorylation at S364/365 (Li et al., 2014; Solan and Lampe, 2008). Results of biological effects caused by Src on gap junctional communication are controversial from different groups. In Cx43 knock-out mouse cell line, expression of Y247F, Y265F, or Y247F/Y265F Cx43 mutants was resistant to disruption of gap junctional intercellular communication by v-Src (Lin et al., 2001). However, in another study using *Xenopus* oocyte system, junctional conductance established by Y247F, Y265F, or Y247F/Y265F mutants were disrupted by v-Src (3-6 hrs after v-Src injection), which suggested that phosphorylation sites other than the two tyrosines are involved in the disruption of gap junctional intercellular communication induced by the v-Src (Zhou et al., 1999). Why are results different between using stable cell lines and *Xenopus* oocyte? First, the different cell system could have different activation of signaling pathways by Src, thus, the effects caused by Src may be different. Considering half-life of Cx43 in Xenopus oocyte is around 22 hours (Lin et al., 2006), Solan and Lampe (2014) hypothesized that tyrosine phosphorylation by v-Src is necessary for decreasing gap junction communication

chronically but not acutely; Src induced phosphorylation by MAPK and PKC are responsible for the rapid gap junction closure (Solan and Lampe, 2014).

Src kinase can also directly affect the interaction between the Cx43CT and other molecular partners by inducing favorable/unfavorable conformations or blocking the binding site. ZO-1 is a PDZ domain containing scaffolding protein and the interaction between Cx43 and ZO-1 is essential in regulating gap junction size, stability, localization, and turnover in cardiomyocyte (Hunter et al., 2005; Toyofuku et al., 1998). The binding of ZO-1 to Cx43 can be disrupted by Src (Toyofuku et al., 2001). NMR results indicate that the interaction between SH3 and Cx43CT induces indirect long range changes in the Cx43CT structure, which disrupts binding of the PDZ-2 domain of ZO-1 to the last residues of Cx43CT (S372-I382) (Kieken et al., 2009; Sorgen et al., 2004).

3.4.2   Regulation of Receptor Tyrosine Kinases on Cx43 Phosphorylation

Tyrosine kinases increasing the level of Cx43 serine phosphorylation indirectly is commonly observed since tyrosine kinases activate serine kinases in cell signaling networks. Activation of EGFR, PDGFR, and VEGFR are associated with a decrease in gap junctional intercellular communication (reviewed in (Warn-Cramer and Lau, 2004)). These receptor tyrosine kinases do not directly phosphorylate Cx43, but indirectly induce Cx43 serine phosphorylation via downstream activation of MAPK and/or c-Src (Warn-Cramer and Lau, 2004). The activation of insulin receptor tyrosine kinase also increases serine phosphorylation of Cx43 via activation of PKCγ, and induces a decrease of gap junctional

intercellular communication in rabbit lens epithelial cells (Lin et al., 2003). Tropomyosin receptor kinase A (TrkA) activated by nerve growth factor also rapidly increases Cx43 serine phosphorylation in bovine thecal (Mayerhofer et al., 1996).

Some tyrosine kinases can regulate Cx43 expression at the transcription level. Long-term activation of basic fibroblast growth factor receptor (bFGR) (>6 h) up-regulates Cx43 mRNA and protein levels in cardiac fibroblasts (Doble and Kardami, 1995). Since fibroblast growth factor is important in wound healing, this would be consequential in injured myocardium.

3.4.3   The Significance of Tyrosine Residues on Cx43CT in Binding Motifs

The Cx43CT domain has 6 tyrosine residues (Y247, Y265, Y267, Y286, Y301, Y313). Some of them are involved in binding motifs of Cx43 protein partners, thus, phosphorylation or de-phosphorylation on these residues could affect the protein-protein interaction. An NMR study using a nonphosphorylated and phosphorylated Cx43CT peptide (K234–D259) found that phosphorylated Y247 negatively regulated the interaction between Cx43 peptide and tubulin by destabilizing the hydrophobic face necessary for the interaction (Saidi Brikci-Nigassa et al., 2012). The disorder nonphosphorylated-peptide adopts an α-helix upon interaction with tubulin where Y247 is on the hydrophobic face (Saidi Brikci-Nigassa et al., 2012). Because microtubules play important roles in rapid connexin delivery to gap junction plaques (Shaw et al., 2007), phosphorylation on Y247 would be detrimental to Cx43 trafficking and intercellular communication.

Y265 is located in the domain essential for many binding partners that regulate gap junction endocytosis. As mentioned above, phosphorylation on Y265 establishes a docking site for the SH2 domain of Src, increasing binding affinity (Lin et al., 2001). Moreover, Ambrosi et al. (2016) reported that the point mutation Y265D (phosphorylation mimetic) abolished the interaction with drebrin, an F-actin-binding protein that is required for stabilizing gap junctions at the plasma membrane (Ambrosi et al., 2016; Butkevich et al., 2004) (del Valle et al., 2012). Another function of Y265 is to form part of a tyrosine-based sorting motif (YXXΦ, where Y is tyrosine, X is any amino acid, and Φ is a bulky hydrophobic amino acid) which enables an interaction with the μ subunit of the heterotetrameric adaptor protein complex AP-2 to mediate clathrin-dependent internalization of Cx43 (Fong et al., 2013) (Gumpert et al., 2008; Piehl et al., 2007). However, the ability of this tyrosine residue to bind AP-2 is negatively influenced by tyrosine phosphorylation. For example, phosphorylation of GluN2B residue Y1472 within the YEKL tyrosine-based sorting signal motif by Fyn inhibits AP2 binding and internalization of GluN2B-containing NMDA-type glutamate receptors (Nakazawa et al., 2001). Similarly, phosphorylation of GluN2A by Src inhibits endocytosis of GluN2A-containing NMDA-type glutamate receptors (Hayashi et al., 2009; Yang et al., 2012). These results suggest that Y265 phosphorylation may not be directly involved in clathrin-dependent internalization, but indirectly increase internalization by destabilizing gap junctions at the plaque. To date, there is no published data regarding phosphorylation of Y267. However, we can not exclude it as a potential target of phosphorylation. Since Y267

is very close to Y265 and it is also involved in the AP-2 binding motif, the phosphorylation of Y267 could interfere with the phosphorylation of both Y265 and Y247, as well as decrease AP-2 binding capability.

Y286 is located in the other YXXΦ AP-2-binding motif (^{286}YKLV^{289}); additionally, this residue is involved in the binding site PPXY motif (^{283}PPGY^{286}) of a ubiquitin ligase, NEDD4 (Leykauf et al., 2006; Spagnol et al., 2016). All three WW domains of NEDD4 interact with the ^{283}PPGY^{286} motif (Spagnol et al., 2016). Of note, the WW domains, named after the presence of two conserved tryptophan residues, regulate substrate selection. Our NMR study shows that any modification of Y286 (mutation, Y286A; phosphorylation, pY286) significantly decreased the binding affinity with all three WW domains, suggesting that Y286 is crucial for the NEDD4 binding (Spagnol et al., 2016). Also, Y286 is required for targeting Cx43-eYFP to the basolateral membrane domain of MDCK cells since mutagenesis of Y286 to A or substitution of ^{284}PGYKLV^{289} by a sequence containing the transferrin receptor internalization signal disrupted basolateral targeting (Chtchetinin et al., 2009). Although phosphorylation on Y286 and the kinase that phosphorylates Y286 site are unknown, the potential important role of phosphorylation on Y286 in Cx43 degradation and cell polarity is expected.

Y313 phosphorylation was observed in FGF-2 stimulated human embryonic stem cells (phosphoproteomics data) (Li et al., 2016; Lundby et al., 2013). Located in one of the helical regions identified in the TM4-Cx43CT (K303-A322) (Grosely et al., 2013), Y313 phosphorylation may induce a conformational change since the negative charge of

phosphate would disrupt or form electrostatic interactions. FGF has been reported to increase serine phosphorylation (Sakurai et al., 2013; Srisakuldee et al., 2009). However, no study show which tyrosine kinase directly targets to Y313. In Chapter 3 and Chapter 4, we will discuss our study which identify that Src and Pyk2 that phosphorylate Y313.

3.4.4 Cx43 Tyrosine Phosphorylation and Diseases

A. Cx43 Tyrosine Phosphorylation in Cancer

As a proto-oncogene, c-Src is found to be over-expressed and/or highly activated in a wide variety of human cancers (Irby and Yeatman, 2000). Phosphorylation on Cx43 by Src affects cancer initiation, development, and treatments. One of the problem in cancer chemotherapy is the resistance of cancer cells to chemotherapeutic drugs like cisplatin. Previous research suggested that the cytotoxic signal triggered by cisplatin could transmit to a neighboring cell via gap junctional intercellular communication to cause cell death (Jensen and Glazer, 2004). Active Src phosphorylating Cx43 could increase cell survival of the neighboring cells in response to cisplatin while using Src inhibitor Dasatinib (sprycel) could be a strategy to enhance the efficacy of cisplatin (Peterson-Roth et al., 2009). In radiotherapy, irradiated cells can pass signals through the gap junctional intercellular communication to neighboring non-irradiated cells or release signals through connexin hemichannels causing bystander effect (Edwards et al., 2004; Ohshima et al., 2012). Closure of Cx43 gap junctions which is associated with hyperphosphorylation of Cx43 is proportional to the dose of ultrasoft X-rays received (Edwards et al., 2004). Thus, radiation

type and dose need to be carefully considered in order to get best anti-tumor effect by allowing the spread of cytotoxic metabolites (Edwards et al., 2004).

B.   Cx43 Tyrosine Phosphorylation in Cardiovascular Diseases

Gap junctions are essential for normal electrical propagation in heart. Many cardiac diseases are associated with remodeling of gap junction organization and connexin expression, including ischemic cardiomyopathy, heart failure, and sudden cardiac death (Severs et al., 2006). In the normal situation, gap junctions preferentially locate at intercalated discs, which is the region between two adjacent cardiomyocytes in longitude (Severs, 1985). In this way, gap junctions mediate myocyte-to-myocyte electrical coupling and communication. In the pathological situation, Cx43 redistributes and localizes at the cardiomyocyte lateral membranes, which would result in a reduction of ventricular conduction velocity (Severs, 2001). Evidence show that Src is crucial for Cx43 expression and distribution in some cardiac pathologies. In epicardial border zone myocytes after myocardial infarction, active c-Src is significantly increased and colocalized with Cx43 at the intercalated disk 1 hr after postcoronary occlusion while the colocalization of ZO-1 and Cx43 decreases (Kieken et al., 2009). These alternations are associated with the loss of Cx43 from the intercalated disk (Kieken et al., 2009). Another group used the similar myocardial infarction mice model (12-week-old mice by coronary artery occlusion) and found that inhibition of Src by PP1 treatment increased Cx43 level in both scar border (69%) and distal ventricle (73%) (Rutledge et al., 2014). Chronically, c-Src activation is

associated with the decrease of Cx43 level in different animal models. In an angiotensin II (Ang II) over-activation mice model (ACE8/8), c-Src was increased and Cx43 was decreased in ventricular myocytes (Sovari et al., 2011). Further study indicated that the decreased Cx43 level and impaired Cx43 gap junction is caused by caveolin-1 (Cav-1) dissociation from c-Src which resulted in the c-Src activation (Yang et al., 2014). Although the tyrosine phosphorylation level of Cx43 in these animal model was not studied, c-Src and ZO-1 competitively interact with Cx43 which results in the destabilization of Cx43 at the gap junction plaque. In hereditary cardiomyopathic model Syrian BIO 14.6 hamsters, c-Src activation in the late stage of congestive heart failure is associated with increased Cx43 tyrosine phosphorylation level (Toyofuku et al., 1999). These are directly evidence that tyrosine phosphorylation by Src plays a role in cardiac pathology.

C.   Cx43 Tyrosine Phosphorylation in Other Diseases

A variety of extracellular pathological and inflammatory stimuli regulating changes in gap junction communication includes lipopolysaccharide (LPS) and tumor necrosis factor α (TNFα). LPS not only induces Cx43 tyrosine phosphorylation and decreases gap junction coupling in cultured rat microvascular endothelial cells (Lidington et al., 2002), but also leads to the degradation of Cx43 in rat astrocytes (Liao et al., 2013). Airway epithelial cells initiate immune signaling caused by inhaled bacteria, which play a surveillance role in the respiratory tract. TNFα rapidly closes Cx43 gap junction channels in the airway epithelial cells (Huang et al., 2003; Huang et al., 2003). TNFα induces the activation of c-Src in

airway epithelial cell but not in cystic fibrosis airway epithelial cells (Huang et al., 2003).

Expression of a dominant negative version of c-Src or transfection of Cx43 mutants on

Y247 and Y265 prevented the effect of TNFα on gap junction closure, which suggests that

c-Src mediates the closure of gap junction channel caused by TNFα (Huang et al., 2003).

In diabetes, c-Src participates in down-regulation of Cx43 protein level. In high glucose

stimulated glomerular mesangial cells, Cx43 downregulation by NF-κB activates c-Src

which in turn activates NF-κB, resulting in renal inflammation (Xie et al., 2013). In this

situation, activated NF-κB regulates the further decrease of Cx43 in kidneys of diabetic

animals (Xie et al., 2013).

3.4.5 Tyrosine Phosphorylation on Isoforms Other Than Cx43

Despite Cx43 phosphorylation being well studied, our understanding of the complex

symphony of tyrosine phosphorylation events and their outcomes is lacking. Furthermore,

tyrosine phosphorylation of other Cx family members has not been studied as extensively

as Cx43 and thus poorly characterized. Diez et al. (1998) found that the only two tyrosine

residues on Cx32, Y243 on the CT and/or Y7 on the NT, were phosphorylated directly by

the EGFR *in vitro* (Diez et al., 1998). However, they did not test if the phosphorylation

occurs in cells. Locke et al. (2006) used MALDI–TOF-MS to detect post-translational

modification in Cx32 transfected HeLa cells and found tyrosine phosphorylation on the

Cx32 NT domain (Locke et al., 2006). Traub et al. (1998) studied the different types of

phosphorylation in the mouse Cx37 transfected HeLa cells by autoradiography and found

phosphorylation mainly on serine, less on tyrosine and little on threonine residues (Traub et al., 1998). Hertlein et al. (1998) used autoradiography and found that in the mouse Cx45 stable transfected HeLa cells, serine, tyrosine, threonine phosphorylation are detectable (Hertlein et al., 1998). Of note, most of the phosphorylated residues are found on the CT domain (Hertlein et al., 1998). Using a tyrosine phosphatase inhibitor pervanadate increases phosphorylated form of Cx45 suggesting the exist of tyrosine phosphorylation on Cx45 (van Veen et al., 2000). Although there is no direct evidence that Cx40 has tyrosine phosphorylation, Bolon et al. (2007) found that lipopolysaccharide treatment decreased the electrical coupling in cultured mouse microvascular endothelial cells by targeting Cx40 via tyrosine-, ERK1/2-, PKA-, and PKC-dependent signaling (Bolon et al., 2007). Evidence has been found that tyrosine phosphorylation can occur on connexin isoforms other than Cx43, nevertheless, new phosphorylation sites and additional kinases that target connexins need to be identified and characterized.

4.   Regulation of Connexins by Phosphatases

Phosphorylation is a highly regulated dynamic interplay between protein kinases and phosphatases. Phosphatase counterbalance the effects of kinases, thus plays important roles in regulating connexins life cycle, channel gating as well as interaction with other cellular proteins (Herve and Sarrouilhe, 2002). Although kinases play established roles in the life cycle of connexin, less information exists about the involvement of phosphatases. In this

section, regulation of connexins by phosphoserine/phosphothreonine protein phosphatases (PS/PTPP) and protein-tyrosine phosphatases (PTP) will be discussed.

4.1   PS/PTPP and Connexins

PS/PTPP are divided by function into two classes, protein phosphatase 1 (PP1) and protein phosphatase 2 (PP2). The latter includes PP2A, PP2B, and PP2C (Ingebritsen and Cohen, 1983). In ventricular myocytes of newborn rats, inhibition of PP1 and PP2A, but not PP2B and PP2C, preserved the channel activity (Duthe et al., 2001). In MDCK, WB-F344 and cultured astrocytes, PP1/PP2A inhibitors also increased Cx43 phosphorylation (Berthoud et al., 1992; Guan et al., 1996; Li and Nagy, 2000). In another study, serine phosphatases PP1, PP2A, PP2B, and PP2C were used to test the dephosphorylation of immunoprecipitated Cx43, and PP2A was the most efficient (Cruciani et al., 1999). However, the same study also found PP2B participated in the maintenance of intercellular communication in TPA-treated V79 fibroblasts, although did not dephosphorylate immunoprecipitated Cx43 (Cruciani et al., 1999). This could associate with dephosphorylation of Cx43 binding partners by PP2B, since PP2B has been shown to regulate PKC(Lum et al., 2001). In arrhythmogenic rabbit model of non-ischemic heart failure and heart failure patients, Cx43 colocalized and coimmunoprecipitated with both PP1 and PP2A (Ai and Pogwizd, 2005). An increased colocalization of PP2A and Cx43 (but not PP1 and Cx43), which is responsible for a decrease of phosphorylated Cx43, contributed to uncoupling (Ai and Pogwizd, 2005). In TNF-α acutely treated FS TtT/GF cell

line, there was a transient dephosphorylation of S368 caused by recruitment of PP2A at the

plasma membrane; this led to a transient cell uncoupling (Meilleur et al., 2007). Although

phosphorylation of S368 is accepted as a factor of cell uncoupling, the author emphasized

that the length of the treatment is the key point (Meilleur et al., 2007). Specifically, PMA

treated cells exhibit transient (within 5min and only last for 5 min) increase of gap junction

coupling, and followed up with fast decrease of gap junction coupling (Meilleur et al.,

2007). Similarly, during the acquirment of the epidermal barrier function in embryonic

development, there is a transient interaction between Cx43 and ZO-1. PP2A is necessary

both for the initial interaction between ZO-1 and Cx43 and the consequential

dephosphorylation of Cx43 on S368 (Gerner et al., 2013).

4.2 PTPs and Connexins

Traditionally, PTPs have been categorized into two types, the receptor-like and the

intracellular PTPs (Zhang, 1998). The receptor-like PTP generally contains an extracellular

domain, a single transmembrane region, and a cytoplasmic PTP domains (Zhang, 1998).

The intracellular PTP is composed of a single catalytic domain and various amino or

carboxyl terminal domains usually determining substrate binding or regulating

phosphatase functions (Zhang, 1998). The importance of PTP on gap junction regulation

was initially evidenced from studies using pervanadate, a PTP inhibitor, which was found

to decrease gap junctional intercellular communication and enhance Cx43 tyrosine

phosphorylation in syrian hamster embryo cells, and in V79 Chinese hamster lung

fibroblasts (Husoy et al., 1993). In Cx45 transfected HeLa cells, pervanadate reduced the junctional conductance and relatively increased the 48 kD signal, suggesting PTP is involved in the regulation of Cx45 phosphorylation (van Veen et al., 2000).

In 2003, two potential Cx43 tyrosine phosphatases were identified – vascular protein tyrosine phosphatase 1 (identified by mass spectroscopy) and receptor protein tyrosine phosphatase μ (RPTPμ) (identified by immunoprecipitation) (Giepmans et al., 2003; Singh and Lampe, 2003); however, direct interactions were not verified, and direct roles in cell-to-cell communication were not established. Lezcano et al. (2014) showed that Cx43 and RPTPμ colocalized throughout the entire ROS 17/2.8 cells, although RPTPμ is a transmembrane protein and the interaction was expected to occur at the plasma membrane (Lezcano et al., 2014).

5. Objective

Phosphorylation is one of the most important post-translational modifications of connexins. Although significant strides have been made in understanding connexin regulation by serine phosphorylation, few tyrosine kinases and phosphatases that interact with connexins have been identified.

The objective of this dissertation is to identify novel tyrosine phosphatase and kinases that directly interact with Cx43 to affect the function and to characterize the biological function of the interactions, *in vitro* and *in cyto*. Chapter 2 includes the mechanistic study of Cx43 dephosphorylation by a novel protein-tyrosine phosphatase, TC-PTP. In Chapter

3, we will discuss a novel kinase, Tyk2, that phosphorylates Cx43 in a manner similar to Src but independent from Src activation. Chapter 4 contains additional studies on connexin phosphorylation and dephosphorylation extending from my dissertation. In Chapter 5, I will summarize my projects and propose future directions.

The important roles of gap junction in growth control, electronic coupling, cell differentiation, cell sorting and immune response indicate the possibility of using gap junction as therapeutic target in particular diseases. Understanding phosphorylation and dephosphorylation might lead to methods that modulate the regulation of gap junction channels, with potential benefits for human health.

CHAPTER 2

Tyrosine Phosphatase TC-PTP Directly Interacts with Connexin43 to Regulate Gap Junction Intercellular Communication

6. Introduction

In Chapter 1, we discussed that kinases have well-established roles in the regulation of a connexin's function. However, phosphorylation are highly regulated and dynamic due to the action of phosphatase, and to date, very little is known about the regulation of Cx43 by phosphatase. In this Chapter, we will discuss our findings that a tyrosine phosphatase, TC-PTP (also known as PTPN2), is a novel bind partner for Cx43.

TC-PTP was cloned from a peripheral human T-cell cDNA library and despite its name, is ubiquitously expressed in all tissues and at all stages of mammalian development (Cool et al., 1989). Alternative splicing in the C-terminus gives rise to a 48-kDa form (PTP1B, minor) localized to the ER and a 45-kDa form (TC-PTP, major) that is targeted to the nucleus (Cool et al., 1989). Mice lacking the TC-PTP gene die within five weeks of birth from defects in hematopoiesis and immune function (You-Ten et al., 1997). Heterozygous TC-PTP$^{+/-}$ mice implicated TC-PTP as an important regulator of inflammatory cytokine signaling and in the pathophysiology associated with inflammatory bowel disease (Hassan et al., 2010). Several substrates, such as the insulin receptor and EGFR (Galic et al., 2003; Tiganis et al., 1998), as well as cytoplasmic JAK and STAT proteins (Lu et al., 2007; Simoncic et al., 2002; ten Hoeve et al., 2002), have implicated broad roles of TC-PTP in regulation of celling pathways. Additionally, a high level of Ang II (10^{-7} M) decreases TC-PTP in vascular smooth muscle cells, suggesting that TC-PTP is improtant in pathogenesis of Ang II induced cardiovascular diseases (Tsiropoulou S, 2014). We provide evidence of a relationship between Cx43 tyrosine phosphorylation by v-Src and de-phosphorylation by

TC-PTP. TC-PTP increased gap junction stability at the plasma membrane and partially reversed closure of Cx43 gap junction channels caused by v-Src phosphorylation.

7. Materials and Methods

7.1 Expression and Purification of Recombinant GST-tagged Proteins

Rat $Cx43CT_{236-382}$ was expressed and purified as described previously (Duffy et al., 2002). $TC-PTP_{1-314}$ was cloned into the pGEX-6p-2 vector and overexpressed in the BL21 (DE3)-derived Rosetta strain (Novagen). A 20 ml overnight culture was diluted 1:50 and grown at 37°C to $A_{600} = 0.6$, then induced with 0.5 mM isopropyl β-D-thiogalactoside for 20 h at 19°C. 1 L of cultured cells was lysed by an EmulsiFlex-C3 in 25 ml of the following buffer: 25 mM Tris-HCl (pH 7.5), 5 mM DTT, 0.1% Brij 35, and one protease inhibitor cocktail tablet (Roche). The cell lysate was incubated with glutathione-Sepharose beads (Genescript) for 2 h at 4°C, then the beads were incubate with Tris-HCl buffer (50 mM Tris-HCl, 2 mM ATP, 10 mM $MgSO_4$) for 10 min at 37°C to remove a contaminating chaperone protein. The beads were washed in Tris-HCl buffers containing high salt (300 mM NaCl) or detergent (1% Brij 35) and then washed 4x with 25 mM Tris-HCl (pH 7.5) and 5 mM DTT. Turbo 3C protease (Accelagen) was used to cleave $TC-PTP_{1-314}$ from glutathione S-transferase tag at 4°C for two days.

7.2 NMR

All NMR data were acquired using a 600 MHz Varian INOVA NMR Spectrometer

outfitted with a cryo-probe at the NMR Facility of the University of Nebraska Medical Center. Gradient-enhanced two-dimensional ^{15}N-HSQC experiments were acquired to detect backbone amide bond resonances from the ^{15}N-Cx43CT (30 μM) in the absence and presence of different concentration of unlabeled TC-PTP$_{1-314}$. NMR spectra were processed using NMRPipe (Delaglio et al., 1995) and analyzed with NMRView (Johnson and Blevins, 1994). Binding affinity from the ^{15}N-HSQC titration experiments were calculated by Graphpad Prism 5 (GraphPad Software, Inc.).

7.3 Cell Culture and transfection

NRK and LA-25 cells (NRK cells containing temperature sensitive v-Src) were generous gifts from Dr. Paul Lampe (Fred Hutchinson Cancer Research Center). Both cell lines were grown in Dulbecco's modified Eagle's medium (DMEM) (Hyclone, Thermo Fisher Scientific Inc.) supplemented with 10% fetal bovine serum (FBS) (Hyclone, Thermo Fisher Scientific Inc.) and antibiotics in an atmosphere of humidified 5% CO_2. NRK cells were serum staved for 4 hrs in DMEM with 0.1% FBS before EGF treatment. TC-PTP $_{1-314}$ was cloned in pcDNA 3.1 vector and transfected in to NRK or LA-25 cells following lipofectmine 2000 protocol (Thermo Fisher Scientific).

7.4 Antibodies and Immunostaining

The following antibodies were used in this study: Cx43 monoclonal antibodies against amino acids 360-382 (Cx43CT1 and Cx43IF1, described in (Cooper and Lampe, 2002;

Lampe et al., 2006)), rabbit anti-phosphorylated Y247, rabbit anti-phosphorylated Y265, and rabbit anti-phosphorylated S279/282 (described in (Solan and Lampe, 2008)) (all generous gifts from Dr. Paul Lampe, Fred Hutchinson Cancer Research Center); Cx43 monoclonal antibody against residues 1-20 (Cx43NT1, Fred Hutchinson Cancer Research Center Hybridoma Development Facility); rabbit anti-phosphorylated S368 (Millipore); TC-PTP antibodies against the N-terminus and C-terminus (SAB4200495 and SAB4200249, Sigma-Aldrich); non-specific phospho-tyrosine antibody (Abcam); and antibodies against total and active Src (phosphorylated Y416, Millipore).

Cells were immunostained as described previously (Mehta et al., 1991). Briefly, cells grown on cover slips to ~60% confluence were fixed with 2% para-formaldehyde for 15 min. Cells were blocked for 30 min at room temperature (RT) by MPS buffer (1x PBS, 1% Goat Serum) containing 0.2% TX100 for permeabilization. Then, cells were immunostained with appropriate primary antibodies at RT for 1 h, followed by several PBS-0.5% Tween washes. Secondary antibodies (Alexa 594-conjugated goat anti-rabbit antibody and/or Alexa 488-conjugated goat anti-mouse antibody) were applied for 1 h at RT. Images of immunostained cells were acquired with a Zeiss 510 Meta Confocal Laser Scanning Microscope using a 63×1.4 numerical aperture objective with appropriate filters. Colocalization was quantified using the Manders method in Image J plugin JACoP, by which the Cx43 signal (green) coincident with a signal in the red channel over the total intensity of Cx43 was measured (Bolte and Cordelieres, 2006).

7.5 Co-IP and Western blot

NRK cells were lysed in complete lysis buffer (50 mM Tris-HCl [pH 7.4], 150 mM NaCl, 0.5% Na-deoxycholate, 1% TX 100, 5 mM NaF, and one-half tablet of complete protease inhibitor [Roche] in 20 ml buffer), maintained on ice for 30 min, precleared with protein G beads for 30 min at 4°C, and then spun at 12,000 rpm for 15 min. Total protein was assessed using the BCA protein assay kit (Pierce). 2 mg lysate was incubated with 2 μg of anti-TC-PTP-NT or anti-TC-PTP-CT or rabbit IgG (4 h at 4°C) and then incubated with 100 μl of protein G sepharose (GE Healthcare) (overnight at 4°C). The sepharose was washed 4x with cold lysis buffer and the co-IP was analyzed by SDS-PAGE and Western blot. Anti-Cx43 antibody Cx43NT1 was used to detect Cx43 co-IP with TC-PTP.

Protein levels were detected by SDS-PAGE and Western blot. One exception for detecting tyrosine phosphorylation was that 5 mM Na_3VO_4 was added in the blocking buffer and primer antibody buffer in order to minimize the loss of phosphorylation. Western blot data were scanned and quantified using Image J as described in (Schneider et al., 2012).

7.6 GST Pull Downs

The GST pull down assay was modified from (Leykauf et al., 2006). Briefly, purified GST-fusion TC-PTP$_{1-314}$ and GST control protein were bound to glutathione-Sepharose beads in buffer 1 containing 25 mM Tris-HCl (pH=7.4),150 mM NaCl, 0.1% TX100, 1 mM DTT, 0.1 mM EDTA and one-half tablet of complete protease inhibitor in 20 ml buffer. 5 mg of purified Cx43CT were incubated with GST-fusion TC-PTP$_{1-314}$ or the GST control

overnight at 4°C on a rotating wheel. Beads were washed for 5 times with buffer 1 and bound protein were eluted with SDS-PAGE sample buffer and were used for SDS-PAGE. Western blot was used to analyze GST pull down results.

7.7 *In vitro* Phosphatase Assay

Cx43 phospho-peptides pY247 (KGKSDPpYHATSGA) and pY265 (GSQKpYAYFNG) were used in the malachite green assay (Millipore) to detect if they are substrates of TC-PTP *in vitro*. Positive and negative controls were DADEpYL (described in (Peters et al., 2000)) and ARKRIpYPP (described in (Ren et al., 2011)), respectively. Peptides and enzyme were dissolved and diluted in reaction buffer (60 mM Hepes [pH 7.2], 150 mM NaCl, 1 mM EDTA, 0.17 mM DTT, 0.83% glycerol, 0.017% BSA, and 0.002% Brij-35) and temperature-equilibrated for 15 min at 25°C. 500 μM of each peptide was added into a 96-well plate, and then TC-PTP$_{1-314}$ was added to each peptide at different time points. The final concentration of TC-PTP$_{1-314}$ was 0.6 nM. All reactions were terminated by adding 100 μl malachite green solution and incubated for 15 min at RT to allow color development. Absorbance at 650 nm was read using a SpectraMax 190 spectrometer (Molecular devices).

The Malachite green assay was also used to measure the kinetic parameters of de-phosphorylation (Peters et al., 2000). The reaction was performed in 96-well plates with a final volume of 25 μl. A standard curve of KH$_2$PO$_4$, used for calculating the release of inorganic phosphate, was determined on the same plate as the reaction samples. Different

concentrations of peptides [substrate] were combined with 1.2 nM TC-PTP$_{1-314}$. Time

points of the reaction were sampled from 0-15 min to calculate the initial velocity (v) versus

[substrate]. Lineweaver-Burk double-reciprocal plot (rearranged from the Michaelis-

Menten equation) was created based on 1/v and 1/[substrate]. The kinetic parameters were

determined by the linear equation from the lineweaver-Burk double-reciprocal plot. All the

reactions were conducted at pH 7.5, 25°C. The reported results were calculated from three

independent experiments.

The *in vitro* phosphatase screening assay was conducted by SignalChem (Richmond,

Canada). The CDC25A, CDC25B, CDC25C, PP1A, PP1B, PP2Aalpha, PP2Calpha and

PP2Cgamma phosphatase activity to pS279/282 phospho-peptide (Cx43CT 276-289) was

determined by performing assays at 37°C for 15 min in a final volume of 25μl according to

the following assay reaction recipe:

Component 1	5 μl of diluted active protein phosphatase
Component 2	10 μl of substrate assay solution OMFP for CDC25 family, Thr-phosphopeptide T69-58 for PP1 and PP2 family
Component 3	5 μl Phosphatase assay Buffer
Component 4	5 μl of compound (50 μM) or assay buffer.

The assay was started by incubating the reaction mixture at 37°C for 15 minutes. After

the 15 minutes incubation period, the assay was terminated by the addition of 100 μl of

Malachite Green reagent. The absorbance of the reaction solution was measured in a

63

spectrophotometer at 650 nm. Blank control was set up that included all the assay components except the addition of the substrate (replace with equal volume of phosphatase assay buffer). The corrected activity for CDC25A, CDC25B, CDC25C, PP1A, PP1B, PP2Aalpha, PP2Calpha and PP2Cgamma targets was determined by removing the blank control value.

7.8   Scrape-loading Assay

Cells were scrape-loaded as described in (Stauch et al., 2012). Briefly, LA-25 cells seeded on cover slips were transfected with TC-PTP$_{1-314}$ or pcDNA3.1 vector (mock group) for 24 h at 37°C and then incubated at 40°C for 1 hr before addition of the MAPK inhibitor (U0126, 50 µM) or PKC inhibitor (BIM, 0.1 µM) at 40°C for another 30 min. Then, cells were incubated at 35°C for 12 hrs. The medium with the inhibitor was changed every 3 hrs to ensure a consistent effect during the treatment. The confluence of cells was 100% on the cover slips. Cell culture medium from 100% confluent cells was removed and replaced with 1 ml of PBS containing 0.25% Lucifer Yellow and Texas Red-conjugated fluorescent dextran (10 kDa, 1.5 mg/ml: fixable). Cells were scrape-loaded with a sterile scalpel by two longitudinal scratches and then incubate at RT for 1 min. Cells were washed quickly 3x with warm PBS (contain MgCl$_2$ and CaCl$_2$) or cell culture medium followed by incubating at 37°C for 5 min. After incubation, cells were washed 2x with warm PBS, and fixed with 3.7% buffered paraformaldehyde for 15 min. 0.1 M glycine was used to quench autofluorescence for 15 min. Cover slips were mounted on glass slides in a droplet of SlowFade (invitrogen). The result was confirmed by repeating the experiment 3x and for

each trial, capturing 4 side-by-side images. The method to quantify dye transfer was described previously (Stauch et al., 2012). Briefly, cells with Lucifer yellow were counted while the cells with dextran which indicated the initially loaded cells were excluded.

7.9   TX 100 (TX100) Solubility

The TX100 solubility assay was modified from the method described in (Mitra et al., 2006). LA-25 cells grown in 10 cm petri dishes were rinsed 3x with PBS and scraped into 1 ml lysis buffer (50 mM Tris-HCl [pH 7.4], 1 mM EGTA, 1 mM EDTA, 1 mM PMSF, 100 mM NaCl, one-half tablet of complete protease inhibitor for 25 ml of buffer [Roche], 5 mM NaF, 5 mM Na_3VO_4). Then, cells were sonicated for 10 s on ice. Protein estimation was determined using the BCA method. 450 μl cell lysate samples were added to 50 μl of 10% SDS, which was saved as total protein, or to 10% TX100 (final concentration of 1%) and incubated at 4°C for 30 min. Lysates were then separated into cytosolic (supernatant, soluble) and membrane (pellet, insoluble) fractions by centrifugation at 100,000 g for 1 h at 4°C. The pellets were dissolved in 500 μl dissolving buffer (70 mM Tris-HCl [pH 6.8], 8 M urea, 2.5% SDS, 0.1 M DTT, 5 mM NaF, 5 mM Na_3VO_4, and one-half tablet of complete protease inhibitor for 25 ml of buffer). Equal volume of total lysate, TX100 soluble and insoluble portions, were loaded on a 12% SDS-PAGE and immunoblotted with the Cx43NT1 antibody.

For the detergent extraction *in situ*, LA-25 cells on cover slips were extracted *in situ* with 1% TX100 buffer (1% TX100, PBS pH 7.4, 1mM $CaCl_2$, 1 mM $MgCl_2$, and protease

inhibitor cocktail) for 30 min at 4°C, gently shacked every 10 min. The control cells were treated in the same way without 1% TX100. The cover slips were fixed and immunostained as described in (Johnson et al., 2013).

7.10 TC-PTP siRNA Treatment

Oligonucleotides siRNA1 (5'AACAGATACAGAGATGTAAGC3') and siRNA 2m (5'AAGATTGACAGACACCTAAAT3') used to knockdown TC-PTP in LA-25 cells according to (Galic et al., 2005). Oligonucleotide from the non-target pool (Dharmacon, Lafayette, CO) was used as negative control. Lipofectmine RNAi MAX (Invitrogen) was used to carry the oligonucleotide according to manufacture protocol. Cells were incublated at 35°C for another 12 hrs after 36 hrs of siRNA treatment. Protein levels were detected by Western blot.

7.11 Subcellular Fractionation

Analysis of subcellular colocalization of the PKC isoforms was performed according to (Saxon et al., 1994; Zang et al., 1995). Briefly, cells with different treatments from 60-mm petri dishes were washed with ice-cold PBS and then suspended in 0.4 ml digitonin buffer (0.5 mg/ml digitonin in 20 mM Tris-HCl pH 7.5, 140 mM NaCl, 25 mM KCl, 5 mM $MgCl_2$, 2 mM EDTA, 2 mM EGTA, 1/4 protease inhibitor tablet, and 1 phosphatase inhibitor tablet for 10 ml buffer). Cells were dispersed by pipetted up and down, incubated on ice for 5 min, and the cell lysate was centrifuged at 100,000g for 1 h. The supernatant

was collected as cytosolic fraction. The pellet was re-suspended in the same volume of triton buffer (1% TX100 to substitute for the digitonin in the digitonin buffer) and incubated on a rotating wheel for 30 min at 4°C. The suspension was centrifuged as described above and the supernatant was collected as the membrane fraction.

7.12 Statistical Analysis

All data were analyzed by GraphPad Prism 5.0 and presented as the standard error of the mean ($\pm$S.E.M). Paired t-test was used to compare differences between the experimental group and control or the two parallel experimental groups. $P<0.05$ was considered to be statistically significant.

8. Results

8.1 TC-PTP Directly Interacts and Dephosphorylates the Cx43CT Domain

Identification of proteins that interact with connexins has been invaluable towards understanding the regulation of gap junctional communication. Based upon the well-characterized role of Src phosphorylation to inhibit gap junctional communication, we sought to identify if a tyrosine phosphatase could reverse this effect. Interestingly, a correlation exists between the activation of Src by stress conditions (e.g. oxidation stress) (Zhuang and Schnellmann, 2004) or mitogens (e.g. insulin and EGF) (Goi et al., 2000; Li et al., 2010; Rosenzweig et al., 2004) and redistribution of the tyrosine phosphatase TC-PTP (diffusion from the nucleus and/or prevented from (re)entry into the nucleus) to the

plasma membrane (Fukushima et al., 2010; Lam et al., 2001; Tiganis et al., 1998). To identify if a direct interaction exists between TC-PTP and the Cx43 carboxyl terminal (CT) domain, nuclear magnetic resonance (NMR) titration experiments were performed with purified TC-PTP catalytic domain (TC-PTP$_{1-314}$) and Cx43CT. NMR is an ideal method to detect protein-protein interactions because chemical shifts are sensitive to the environment and even small changes in structure and/or dynamics can influence the chemical shift of an amino acid. Different concentrations of unlabeled TC-PTP$_{1-314}$ were titrated into ^{15}N-labeled Cx43CT (residues 236-382) and ^{15}N-HSQC spectra were acquired. The ^{15}N-HSQC is a 2D experiment in which each residue (expect proline) gives one chemical shift that corresponds to the amide group. Therefore, the Cx43CT resonance assignment is necessary to determine which residues are affected by the interaction. Our lab has published the Cx43CT ^{15}N-HSQC assignment (Grosely et al., 2013c), however the spectrum was collected in Phosphate Buffered Saline (PBS), a buffer that caused TC-PTP$_{1-314}$ to precipitate at elevated concentrations, unlike Tris-NaCl buffer. To assign the Cx43CT domain in Tris-NaCl buffer at pH 7.5, Cx43CT in PBS was initially titrated from pH 5.8 to pH 7.5 and then PBS was titrated to Tris-NaCl buffer at pH 7.5. The optimal buffer to visualize the peaks and maintain solubility of TC-PTP$_{1-314}$ was 25% PBS/75% Tris-NaCl buffer at pH 7.5 (a sampling of the reassignments is shown in Figure 2.1A). Titration of TC-PTP$_{1-314}$ caused a subset of Cx43CT residues to broaden beyond detection. These are highlighted on the Cx43CT sequence (Figure 2.1B). Strongly affected Cx43CT residues G261-T275 include Y265 and Y267. Also affected were areas which include Y247, Y286,

Y301, and Y313. The decrease in signal intensity caused by increasing TC-PTP$_{1-314}$ concentrations was fit according to the nonlinear least square method. The binding affinity (K_D) was determined to be 350±80 μM. A glutathione S-*transferase* (*GST*) pull down experiment was performed to validate the NMR results. Purified GST or GST-TC-PTP$_{1-314}$ bound to glutathione agarose were incubated with purified Cx43CT and immunoblotting using an anti-Cx43CT antibody identified that GST-TC-PTP$_{1-314}$, but not GST, directly interacted with the Cx43CT (Figure 2.1C).

Of the 6 Cx43CT tyrosine residues affected by TC-PTP$_{1-314}$, Y265 and Y247 are known sites phosphorylated by c- and v-Src, leading to closure of Cx43 gap junction channels (Kanemitsu et al., 1997; Lin et al., 2001). To identify if TC-PTP dephosphorylates these residues, an *in vitro* phosphatase assay was conducted using peptides containing phospho-Y247 (pY247) or phospho-Y265 (pY265) incubated with TC-PTP$_{1-314}$. Following the protocol for the Malachite green assay (Millipore), we observed an increase in the amount of inorganic phosphate production indicating TC-PTP dephosphorylates Cx43 on pY247 and pY265 (Figure. 2.2). The rate of de-phosphorylation was different between the two sites, with pY265 being a more efficient substrate for TC-PTP than pY247. This observation is consistent with the kinetic rate constant data (K_m and k_{cat}) which indicate that TC-PTP is more efficient in dephosphorylating pY265 than pY247 (Table 1.1).
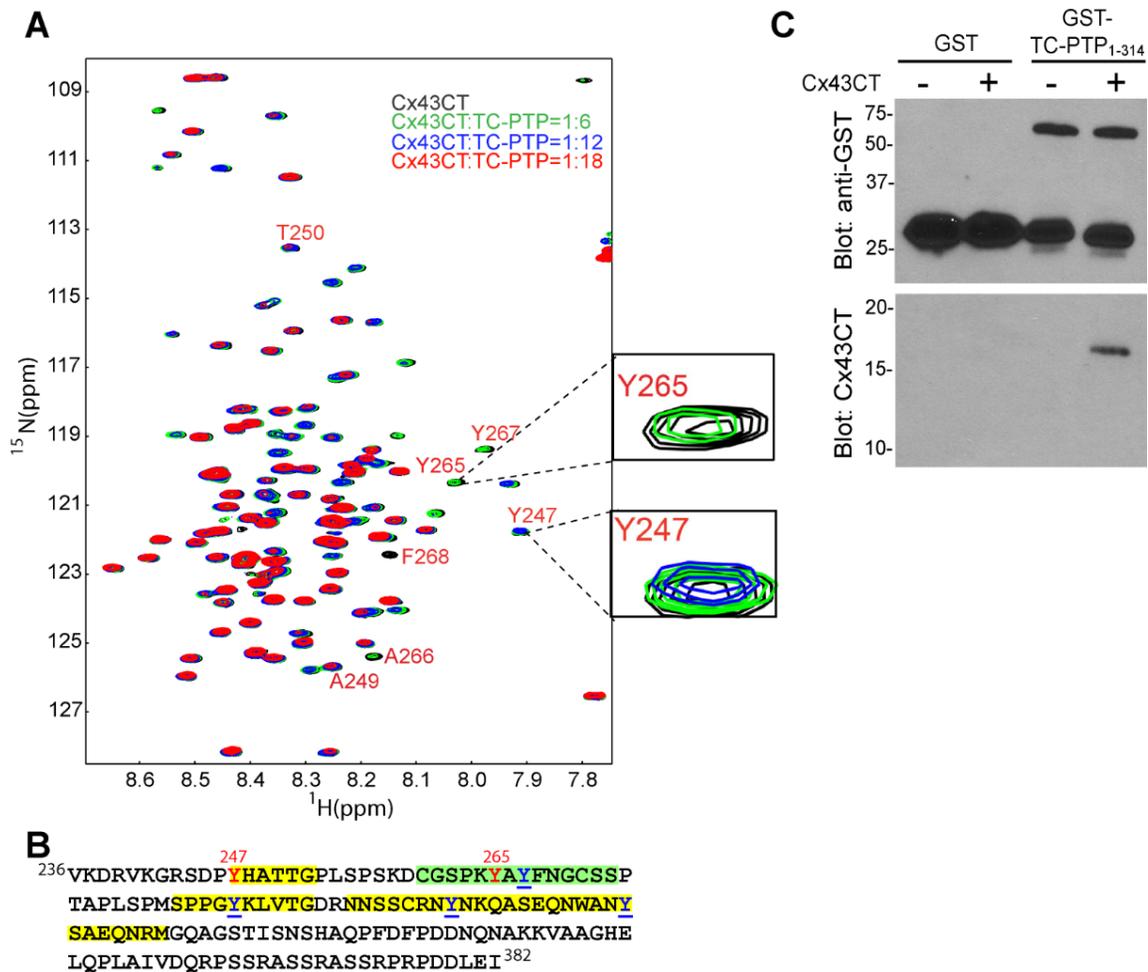
Figure 2.1 Cx43CT residues affected by the direct interaction with TC-PTP. (A) Overlaid ^{15}N-HSQC spectra of the ^{15}N-Cx43CT (residues 236-382; 30 μM) in the presence of different concentrations (60 μM - 540 μM) of unlabeled TC-PTP$_{1-314}$. The cross-peak color changes according to the concentration ratio. A sample of the affected peaks is labeled. (B) Amino acid sequence of Cx43CT. Residues strongly affected by addition of TC-PTP$_{1-314}$ are highlighted in green (residues broadened beyond detection at 1:12 molar ratio) and those less affected in yellow (residues broadened beyond detection at 1:18 molar ratio). In red are the Cx43 residues Y247 and Y265 phosphorylated by Src. The remaining four tyrosine residues have been underlined. (C) Purified GST or GST-TC-PTP$_{1-314}$ on glutathione agarose beads were incubated with (+) and without (-) purified Cx43CT$_{236-382}$. After washes, the anti-GST antibody (top) detected both GST alone (26 kDa) and GST-TC-PTP$_{1-314}$ (58 kDa), however the anti-Cx43CT antibody (bottom) only detected Cx43CT when incubated with GST-TC-PTP$_{1-314}$.
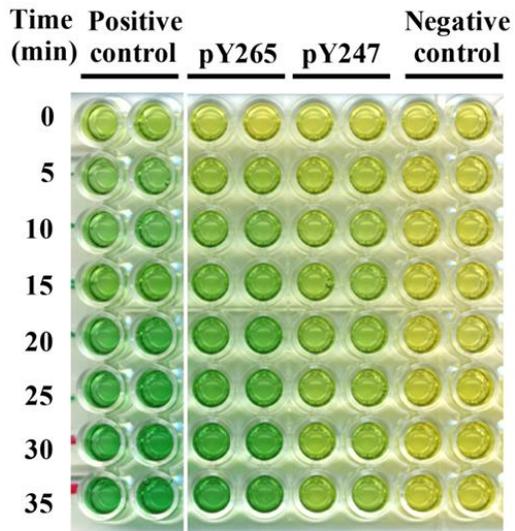
Malachite Green Assay
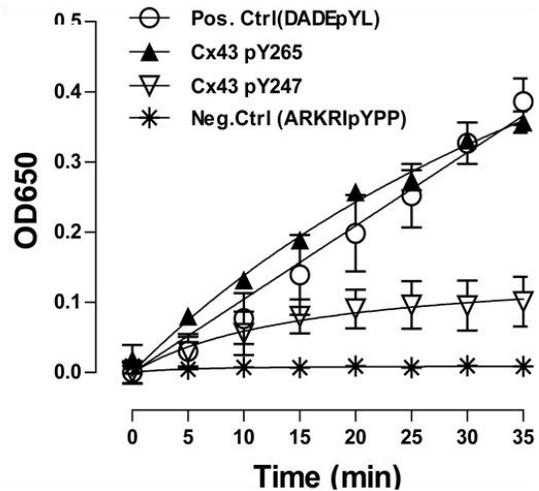
Figure 2.2 TC-PTP dephosphorylated Cx43 residues pY247 and pY265 *in vitro***.** Plot

of the Malachite green assay showed the time course of Cx43 phospho-peptides (600 nM)

containing pY247 or pY265 dephosphorylated by the TC-PTP catalytic domain (0.6 nM).

Statistic data were recorded based on readings at OD_{650}. Each experiment was repeated

three times.

Table 2.1. Kinetic constants for de-phosphorylation of pY265 and pY247 by TC-PTP $_{1\text{-}314}$

	K_m (mM)	k_{cat} (s^{-1})	$k_{cat}/K_m \cdot 10^{-6}$ ($M^{-1}s^{-1}$)
Positive control*[#]	0.022±0.001	52.820±10.622	2.418±0.473
pY265*	0.075±0.003	56.588±3.320	0.751±0.197
pY247*	0.224±0.035	14.164±1.295	0.064±0.012

*All data were collected at pH 7.5, 25°C

[#]Notably, the kinetic constants determined for the positive control (DADEpYL) by TC-PTP$_{1\text{-}314}$ are consistent with a previous report of the same peptide with the PTP1B catalytic domain, whose sequence is very similar with TC-PTP$_{1\text{-}314}$ (Peters et al., 2000).

8.2 TC-PTP Dephosphorylates Cx43 in Normal Rat Kidney (NRK) Epithelial Cells

To determine if de-phosphorylation of pY265 and pY247 by TC-PTP occurs in cells, we initially tested whether endogenous Cx43 and TC-PTP colocalize in NRK cells. Immunostaining in the absence of EGF shows TC-PTP in the nucleus and Cx43 at the plasma membrane (Figure. 2.3A, -EGF). Within one hour after EGF treatment, TC-PTP is recruited to the plasma membrane and partially colocalizes with Cx43 (Figure. 2.3A, +EGF). Co-immunoprecipitation (IP) using an anti-TC-PTP antibody that interacts with the CT domain (anti-TC-CT) followed by Western blot analysis demonstrated TC-PTP and Cx43 are in the same complex (Figure. 2.3B). Numerous studies have shown that differentially phosphorylated Cx43 results in multiple electrophoretic isoforms: a fast migrating isoform (P0), and multiple slower migrating isoforms (P1 and P2) (Crow et al., 1990; Matesic et al., 1994; Solan and Lampe, 2005). TC-PTP has a preference for the P2 isoform in NRK cells.
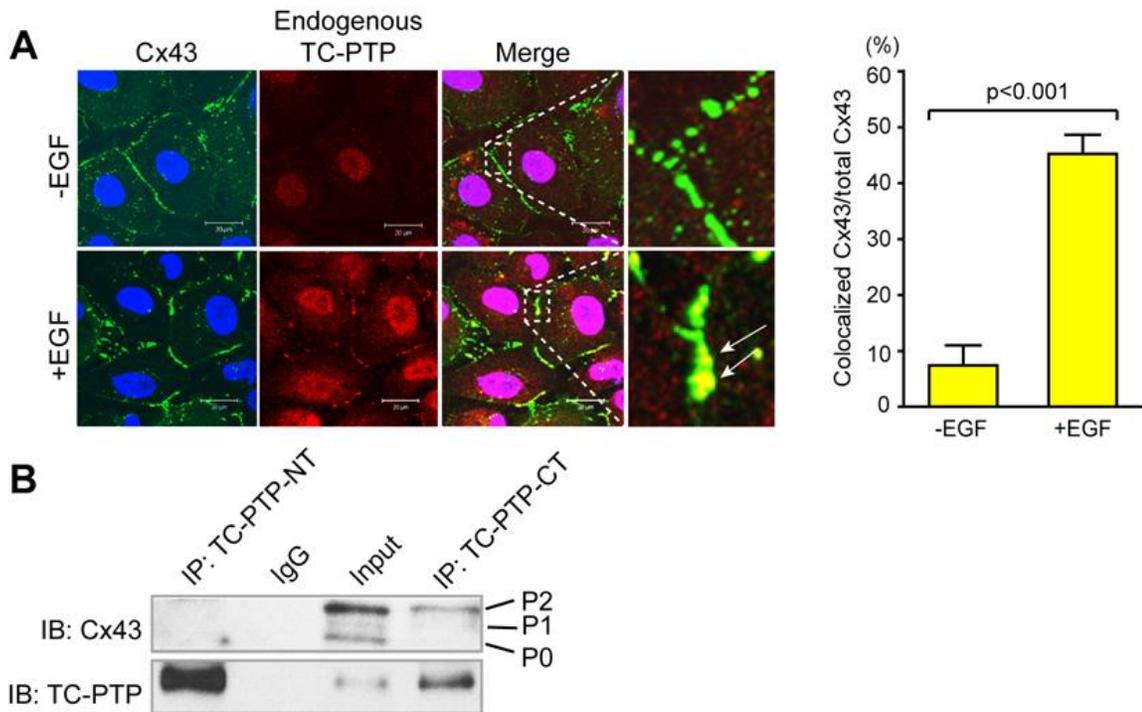
Figure 2.3 EGF induced TC-PTP to colocalize with Cx43 in NRK cells. (A) Cellular localization of endogenous Cx43 and TC-PTP in NRK cells with or without human recombinant EGF (50 ng/ml; 1 hr, Peprotech, Rocky Hill, NJ) using immunofluorescence (green, Cx43; blue, DAPI; red, TC-PTP). Colocalization of Cx43 and TC-PTP (yellow) is highlighted by white arrows. Scale bar is 20 μm. Colocalization of Cx43 and TC-PTP was analyzed based on 10 images from 3 independent experiments. Manders method was used to measure green signal (Cx43) coincident with red signal (TC-PTP) over the total intensity of green signal. Error bars indicate S.E.M. (B) Lysates of NRK cells were IP with anti-TC-NT, anti-TC-CT, or IgG and then blotted for Cx43 and TC-PTP. Input was lysates of NRK cells. The Cx43 mobility shift P0, P1, and P2 have been labeled.

TC-PTP can interact with protein partners through both the N-terminal (NT) catalytic domain and the CT inhibitory and nuclear targeting domain (Iversen et al., 2002). De-phosphorylation of Cx43 would therefore depend on the interaction with the TC-PTP catalytic domain. Co-IP using an anti-TC-PTP-CT antibody pulled down Cx43 (Figure. 2.3B). However, an anti-TC-PTP-NT antibody was unable to pull down Cx43, suggesting that the epitope was blocked due to the interaction of the catalytic domain with Cx43; results consistent with the *in vitro* binding experiments. Based on these observations, the catalytic domain alone (TC-PTP$_{1-314}$; missing nuclear localization domain and localized in the cytoplasm) was transfected into NRK cells to test for TC-PTP de-phosphorylation of Cx43. Immunostaining demonstrates that TC-PTP$_{1-314}$ colocalizes with Cx43 on the plasma membrane with or without EGF treatment (Figure. 2.4A). Next, Cx43 phospho-specific antibodies were used to test if TC-PTP can decrease Cx43 tyrosine phosphorylation levels in cells (Figure. 2.4B). The amount of pY265 and pY247 was decreased in the TC-PTP$_{1-314}$ transfected group compared with the pcDNA 3.1 vector transfection group. Of note, the basal level of Cx43 tyrosine phosphorylation observed in the NRK cells (Figure. 2.4B, -TC-PTP$_{1-314}$) is significantly greater than what has been observed in other cell lines (Kanemitsu et al., 1997; Lampe et al., 1998; Lau et al., 1992; Lidington et al., 2002). While to the best of our knowledge the basel level of tyrosine phosphorylation in NRK cells has not been previously reported, a basel level of tyrosine phosphorylation has been observed in a derivative of the NRK cell line (called LA-25 (Solan and Lampe, 2014), discussed further below). The differences may be the result of higher sensitivity by the specific
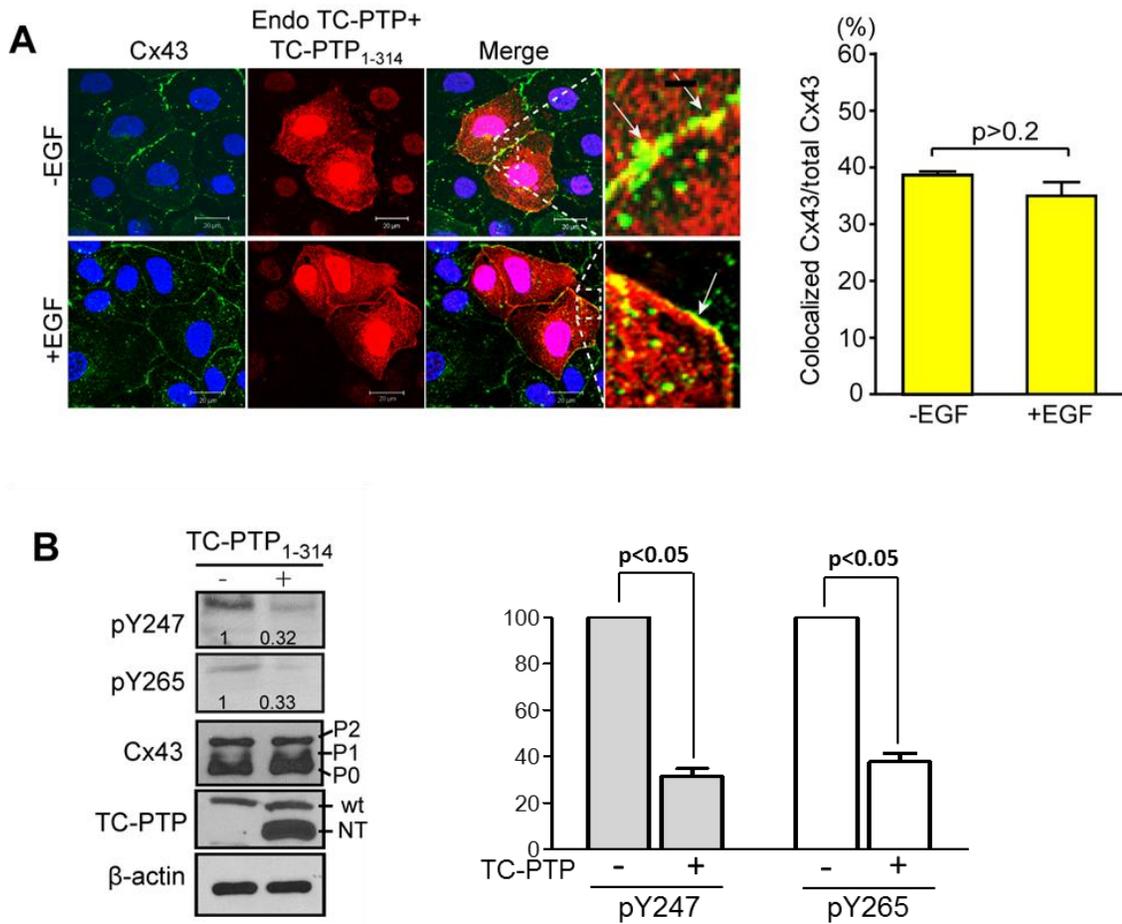
Figure 2.4 TC-PTP causes Cx43 de-phosphorylation in NRK cells. (A) Immunofluorescence of NRK cells transfected with the catalytically active, cytoplasmic TC-PTP domain (TC-PTP$_{1-314}$) with or without EGF (50 ng/ml; 1 hr). Colocalization of Cx43 and TC-PTP (yellow) is highlighted by white arrows. Scale bar is 20 μm. Colocalization of Cx43 and TC-PTP was analyzed based on 8 images from three independent experiments. (B) Western blot using Cx43 Y247 and Y265 phospho-specific, as well as Cx43 and TC-PTP antibodies in NRK cells. Relative protein levels were quantified by analyzing scanned blots by Image J software. The data are representative of three independent experiments.

tyrosine antibodies (used in this study and in (Solan and Lampe, 2014)) and/or TC-PTP might be somewhat less active in NRK (and LA-25) cells under the given conditions. Altogether, these studies indicate that TC-PTP and Cx43 exist in the same complex in cells and that TC-PTP can cause a decrease in the levels of Cx43 tyrosine phosphorylation.

8.3 TC-PTP Dephosphorylates Cx43 Residues pY247 and pY265 in LA-25 cells

NRK cells containing a temperature sensitive v-Src, called LA-25, are commonly used in the gap junction field to characterize Cx43 regulation by v-Src (Solan and Lampe, 2008; Zhou et al., 1999). v-Src is active in this cell line at the permissive temperature (35°C) and not at the non-permissive temperature (40°C). Worth mentioning, temperature alone does not affect gap junction communication in NRK cells (Atkinson et al., 1981). Here, the LA-25 cells were used to characterize the interplay between TC-PTP and v-Src on Cx43 tyrosine phosphorylation levels. To begin with, immunostaining data indicate that active v-Src at 35°C resulted in v-Src colocalization with Cx43 at the plasma membrane (Figure. 2.5A). Immunostaining data then confirmed that after activation of v-Src, endogenous TC-PTP colocalizes with Cx43 at the plasma membrane (Figure. 2.5B). These data suggest TC-PTP could mitigate the effect caused by v-Src in order to maintain cell-to-cell communication.
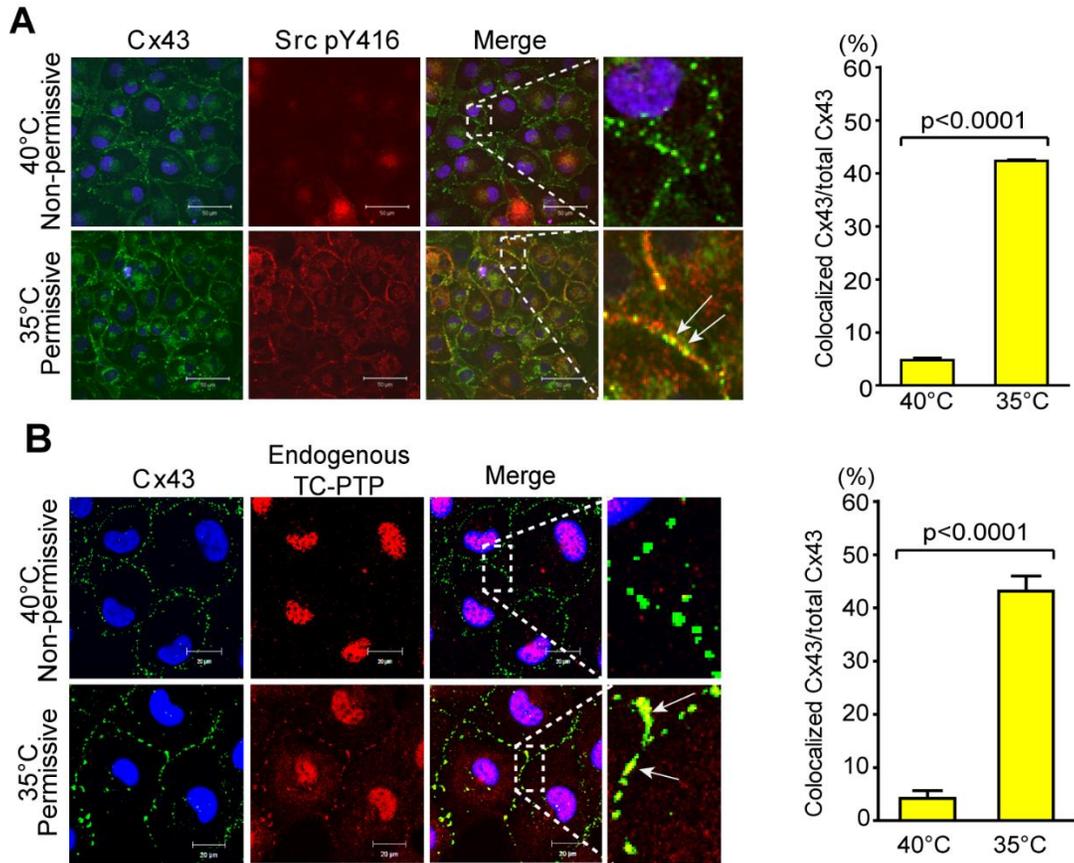
Figure 2.5 v-Src induces TC-PTP to colocalize with Cx43 in LA-25 cells. Immunostaining studies show (A) active Src (Src pY416, red) and (B) TC-PTP (red) co-localized with Cx43 at the permissive temperature (35°C) in LA-25 cells. For each panel, green and blue represent Cx43 and DAPI, respectively. Colocalization of Cx43 and active v-Src or TC-PTP (yellow) is highlighted by white arrows. Scale bar is 50 μm for (A) and 20 μm for (B). Colocalization of Cx43 and active v-Src or TC-PTP was analyzed based on 12 images from three independent experiments.

To test this possibility, tyrosine phosphorylation levels were evaluated in the LA-25 cells using the Cx43 pY265 and pY247 phospho-specific antibodies (Figure. 2.6). Active v-Src at 35°C increased both Y265 and Y247 phosphorylation levels as compared to 40°C. However, if transfected with TC-PTP$_{1-314}$ prior to v-Src activation, Y265 and Y247 phosphorylation levels decreased significantly. Additionally, at 35°C, TC-PTP$_{1-314}$ did not dephosphorylate v-Src (Src pY416), which supports that the decrease of pY247 and pY265 in the TC-PTP$_{1-314}$ transfected group is caused by TC-PTP and not by decreased kinase activity of v-Src. Since MAPK and PKC were reported to phosphorylate Cx43 to down regulate Cx43 gap junction intercellular communication in response to active v-Src in the LA-25 cells (as well as other cell lines (Mitra et al., 2012; Solan and Lampe, 2008)), we investigated if TC-PTP indirectly affected serine phosphorylation. Cx43 serine phosphorylation levels were evaluated using phospho-serine specific antibodies to pS279/282 (MAPK target) and pS368 (PKC target). pS279/282 and pS368 levels were up-regulated at 35°C as expected; interestingly, expression of TC-PTP$_{1-314}$ indirectly led to decreased pS368 levels but not pS279/282 at 35°C. S368 is a known phosphorylation site by different PKC isoforms (α, δ, and ε) (Cone et al., 2014; Mitra et al., 2012) as well as PKCα and PKCδ, in particular, can be up-regulated by v-Src expression (Zang et al., 1995). To address if TC-PTP is affecting activation of PKC, we initially identified that LA-25 cells express PKCα and PKCδ (Figure. 2.6B) but not PKCε (data not shown). Next, a well-established method of measuring membrane-associated PKC isoforms was used since PKC isoforms translocate from cytosolic to membrane distribution when activated. (Borner et

al., 1992; Ha and Exton, 1993; Saxon et al., 1994). The level of activated PKCα and PKCδ increased at 35°C compared to 40°C (16.3±2% to 25.7±3% for PKCα; 13.0±2% to 36.7±0.3% for PKCδ). Transfection of TC-PTP$_{1-314}$ caused a decrease in the level of both membrane-associated PKCα (14.3±4%) and PKCδ (16.7±5%) indicating that TC-PTP can inhibit the activation of PKCα and PKCδ by v-Src (Figure. 2.6B).

To determine the specificity of TC-PTP to decrease the level of Cx43 tyrosine phosphorylation, TC-PTP siRNA was used to knockdown endogenous TC-PTP in the LA-25 cells. Colocalization between TC-PTP and Cx43 was investigated at 35°C, where endogenous TC-PTP colocalizes with Cx43 at cell membrane (Figure 2.5B). In the TC-PTP siRNA group, both pY265 and pY247 increased approximately 2-fold in the TC-PTP siRNA group (even with a decrease in the total levels of Cx43), compared to the scramble siRNA group. The decrease of Cx43 correlates with the decrease observed for pS279/282, indicating that down-regulation of TC-PTP does not affect MAPK phosphorylation. On the other hand, the relative decrease of Cx43 was greater than that of pS368, indicating up-regulation of PKC activity in the absence of TC-PTP. This result is consistent with the down-regulation of PKCα and PKCδ with the transfection of TC-PTP $_{1-314}$ (Figure 2.6B). Next, we addressed the functional significance of Cx43 de-phosphorylation by TC-PTP.

A

	40°C		35°C	
+TC-PTP₁₋₃₁₄	–	+	–	+

TC-PTP — wt / NT

total Src	0.28	0.34	1	1.1
Src pY416	0	0	1	0.95
Cx43 pY265 (Src target)	0.1	0.02	1	0.5
Cx43 pY247 (Src target)	0.05	0.05	1	0.29
Cx43 pS279/282 (MAPK target)	0.2	0.18	1	1.04
Cx43 pS368 (PKC target)	0.21	0.03	1	0.08
Cx43	0.91	0.52	1	0.84
β-actin	1.04	0.97	1	0.93

Cx43: P2 / P1 / P0

B

	40°C		35°C Ctrl		35°C +TC-PTP	
	C	M	C	M	C	M
PKCα						
PKCδ						
Na⁺/K⁺ATPase						
GAPDH						

PKCα

PKCδ

□ cytosolic
▨ membrane associated

C

	scramble	TC-PTP siRNA
TC-PTP	1	0.15
total Src	1	1.02
Src pY416	1	1.15
Cx43 pY265 (Src target)	1	2.2
Cx43 pY247 (Src target)	1	2.3
Cx43 pS279/282 (MAPK target)	1	0.65
Cx43 pS368 (PKC target)	1	0.84
Cx43	1	0.6
β-actin	1	0.94

Figure 2.6 TC-PTP dephosphorylated Cx43 residues pY247 and pY265 in LA-25 cells. (A) Western blot of TC-PTP (wild type-WT and transfected TC-PTP$_{1\text{-}314}$-NT), active v-Src (Src pY416), total v-Src, pY265, pY247, pS279/282, pS368, and total Cx43 (blot with Cx43NT1) levels from LA-25 cells at 40°C and 35°C (12 hr) with or without TC-PTP$_{1\text{-}314}$ transfection. Relative protein levels were quantified by analyzing scanned blots by Image J software with normalization of protein expression to the - TC-PTP$_{1\text{-}314}$ lane at 35°C lane (value = 1). The data is representative of three independent experiments. (B) Activation of PKC isoforms α and δ in LA-25 cells at 40°C and 35°C with or without TC-PTP$_{1\text{-}314}$ transfection. PKC isoforms α and δ in cytosolic (C) and membrane (M) fractions were analyzed by Western blot. Na$^+$/K$^+$ ATPase was blotted as membrane fraction marker, GAPDH was blotted as cytosolic fraction marker. Relative protein levels were quantified by analyzing scanned blots from 3 independent experiment by Image J software. (C) Scramble RNA or TC-PTP siRNA treated LA-25 cells were incubated at 35°C for 12 hrs. Cx43 phosphorylation level were analyzed by Western blot.

8.4 TC-PTP Increases Gap Junction Intercellular Communication and Stability of the Gap Junction Plaque

To determine if TC-PTP de-phosphorylation of Cx43 affects cell-to-cell communication, the junctional transfer of the fluorescent tracer Lucifer yellow (MW 443) was measured in a scrape-loading using the LA-25 cells (Figure 2.7A). Gap junctions were functional at 40°C and the number of fluorescent cells was significantly reduced at 35°C from 115.2±5 to 8.6±3 (Figure 2.7B). Conversely, transfection of TC-PTP$_{1-314}$ increased the number of fluorescent cells at 35°C, albeit not to levels observed without active v-Src (from 8.6±3 to 56.4±3 vs. 115.2±5). These findings indicate that the inhibition of Cx43 gap junction intercellular communication caused by v-Src can be partially rescued by TC-PTP. A plausible explanation for the "partial" rescue of gap junction intercellular communication is that Cx43 MAPK phosphorylation levels were unaffected (Figure 2.6). Using the MAPK specific inhibitor U0126, the number of fluorescent (non-TC-PTP$_{1-314}$ transfected) cells at 35°C increased greater than what was observed with TC-PTP$_{1-314}$ transfection alone (88±5), but still reduced from 40°C. Finally, we used the PKC specific inhibitor BIM to test the contribution of PKC phosphorylation on channel closure. BIM treatment also resulted in increased fluorescent cells (43±5) from control (DMSO), but not to the levels of TC-PTP$_{1-314}$ transfection or the presence of the MAPK specific inhibitor U0126.

A

	DAPI	Dextran	LY	Merge

40°C Non-permissive

35°C Permissive
- DMSO
- +TC-PTP1-314
- U0126 MAPK Inhibitor
- BIM PKC Inhibitor
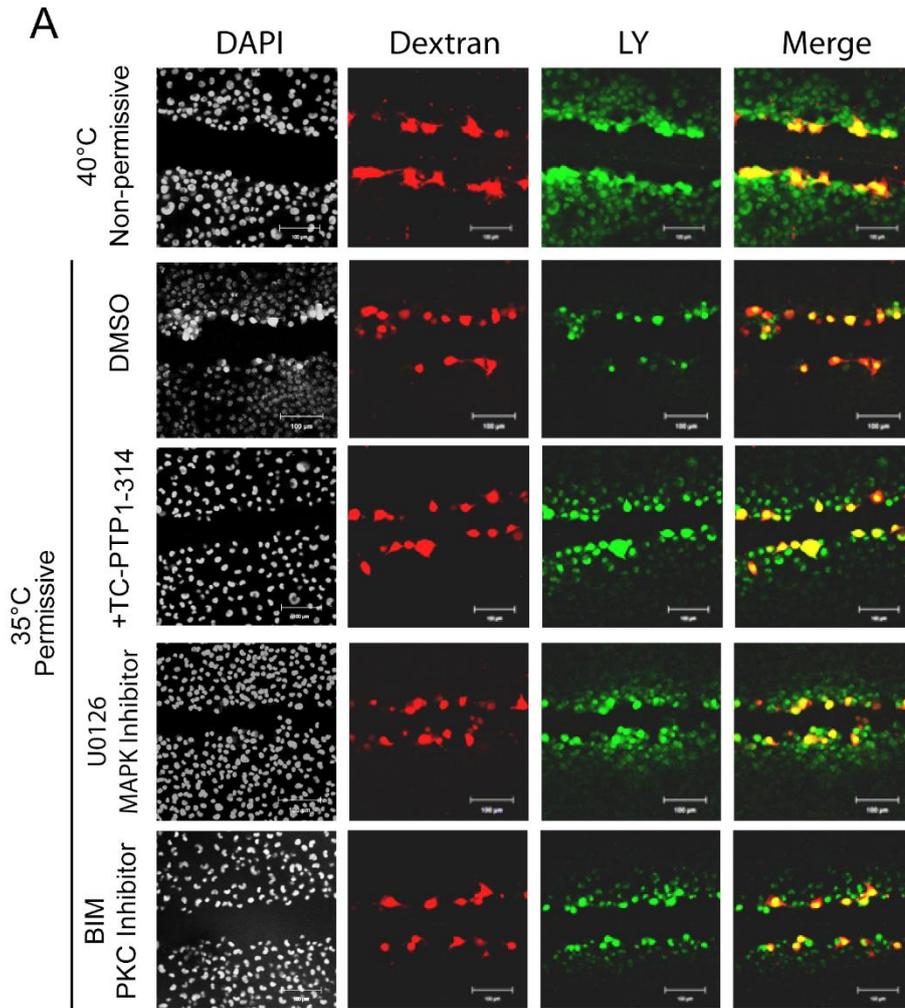
B

Transfer of Lucifer Yellow following Scrape-Loading

Numbers of cells that are negative for dextran but positive for LY

p<0.005
p<0.0001
p<0.0001

40°C | DMSO | TC-PTP | U0126 | BIM

35°C
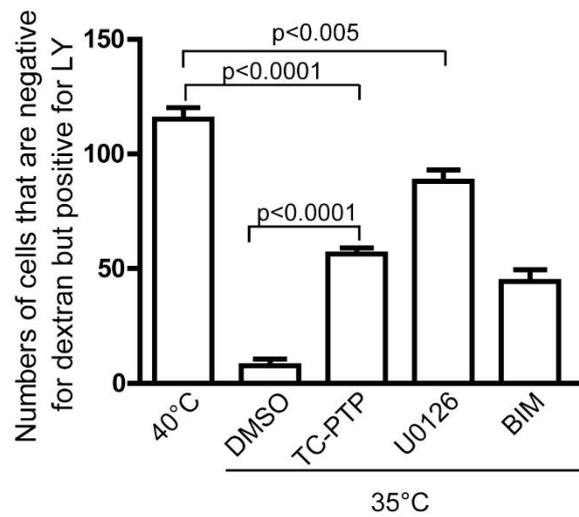
Figure 2.7 Scrape loading assay shows TC-PTP increased gap junction intercellular communication in LA-25 cells. (A) Cells grown on glass cover slips were scrape-loaded with Lucifer Yellow (LY, green) and Texas Red-conjugated dextran (red). Cell nucleus was stained by DAPI to show the confluence of cells. Scale bar is 100 μm. (B) Quantification of fluorescent cells shows the effect of TC-PTP$_{1-314}$ and serine kinase inhibitors on gap junctional permeability. Number of fluorescent cells at 40°C is significantly more than at 35°C ($p<0.0001$). At 35°C, transfection of TC-PTP$_{1-314}$ or addition of the MAPK inhibitor U0126 (50 μM) or PKC inhibitor BIM (0.1 μM) significantly increased the number of fluorescent cells compared with control (DMSO) at 35°C ($p<0.0001$). Each experiment was repeated for three times.

Both MAPK and PKC phosphorylation contribute to gap junction channel closure. TC-PTP can prevent the phosphorylation and channel closure caused by PKC but not MAPK. S279/282 phosphorylated by MAPK could increase binding with Nadd 4, that is associated with Cx43 internalization (Spagnol et al., 2016). Thus, the dephosphorylation on Cx43 MAPK sites is important for indirectly increasing gap junction intercellular communication. Previous studies showed that PP2A dephosphorylated TPA-treated immunoprecipitated Cx43, however they did not test phosphorylation sites that PP2A affects (Cruciani et al., 1999). To further study which phosphatase targets MAPK sites, the MAPK phospho-peptide was used as the substrate in *in vitro* phosphatase screening assay, several phosphatases were used in the assay (Table 2.2). The results show that the PP2A was the most specific phosphatase to dephosphorylate S279/282 compare to the other tested phosphatases, with 39% of control activity. PP2A could also dephosphorylate the PKC site (pS368) with high efficiency, which is 122% activity of control (Figure 2.8).

Cx43 gap junction channels are localized in detergent-insoluble junctional plaques (Musil and Goodenough, 1991; Sirnes et al., 2008). To test the possibility that rescue of gap junctional coupling by TC-PTP was caused by an increase in the amount of Cx43 at junctional plaques, we assessed levels of TX100 detergent solubility. The detergent extraction *in situ* fluorescence and Western blot data show that active v-Src in LA-25 cells at 35°C decreased the detergent-insoluble fraction of Cx43 (Figure. 2.9A, B). Quantification of the data revealed that the insoluble to insoluble+soluble ratio (I/(S+I)) was 79.6±8% at 40°C (Figure. 2.9C). However, the number of assembled gap junctions

Table 2.2 PP2Aalpha dephosphorylated pS279/282 peptide

phosphatase	% Activity
PP1A	6
PP1B	3
PP2A alpha	39
PP2C alpha	-1
PP2C gamma	0
CDC25A	5
CDC25B	6
CDC25C	18

In vitro phosphatase screening assay using pS279/282 peptide as substrate. The profiling data for the peptide substrate pS279/282 against various protein phosphatase targets using the melachite green assay method showed weak to moderate de-phosphorylation of the peptide substrate pS279/282 by 2 phosphatase targets PP2A alpha and CDC25C. The protein phosphatase target PP2A alpha showed the highest activity against the peptide substrate pS279/282. The rest of the phosphatase targets did not show any significant activity against the peptide substrate pS279/282 (values of >10% to be significant).
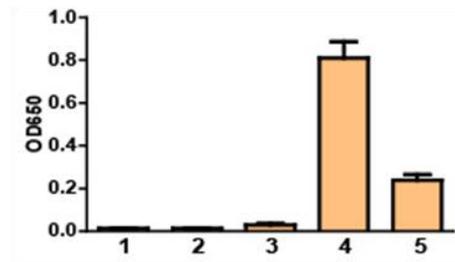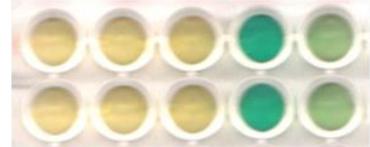
Figure 2.8 *In vitro* phosphatase assay using Cx43CT pS279/282 or Cx43CT pS368 phospho-peptides as substrates. (A) Using PP2B to dephosphorylate the Cx43CT pS279/282 peptide. (B) Using PP2A to dephosphorylate the Cx43CT pS279/282 peptide. (C) Using PP2B to dephosphorylate the Cx43CT pS368 peptide. (D) Using PP2A to dephosphorylate the Cx43CT pS368 peptide. Lanes 1, 2, and 3 are different negative controls. Lane 4 is a positive control. In Lane 5, Cx43CT phospho-peptides were used as substrates.

significantly decreased at 35°C to 45.1±10%. The effect of v-Src was substantially blocked by transfection of TC-PTP$_{1-314}$. TC-PTP$_{1-314}$ increased the Cx43 resistant to TX100 (I/(S+I) = 72.9±8%) at 35°C, suggesting that TC-PTP contributed to the stability of Cx43 at the junctional plaque.

9. Discussion

Here we identified that TC-PTP is the first tyrosine phosphatase, to the best of our knowledge, which directly interacts with Cx43 to modulate gap junction intercellular communication. TC-PTP-mediated de-phosphorylation of Cx43 tyrosine residues Y265 and Y247, as well as indirect serine de-phosphorylation at S368, increased gap junction intercellular communication, and stability of gap junction channels at the plaque. Our studies are consistent with prior observations that TC-PTP is a negative regulator of cytokine signaling as EGF stimulation of NRK cells caused TC-PTP to co-localize with Cx43 at the plasma membrane. In addition, v-Src expression alone was able to mimic the effects of cytokine stimulation. How cytokines and/or v-Src induce TC-PTP redistribution is not clear. TC-PTP has been reported to exit from the nucleus via passive diffusion after cellular stress, while another possibility is that cytoplasmic accumulation occurs by inhibiting nuclear import (Lam et al., 2001).

Closure of Cx43 gap junction channels by v-Src was first observed over 30 years ago (Atkinson et al., 1981); however, the specific sites of Cx43 phosphorylation required for this process are still a matter of debate. Several studies implicate the activation of v-Src in both the direct phosphorylation of Cx43 tyrosines (Y247 and Y265) and the indirect phosphorylation of serines by MAPK (S279/S282) and PKC
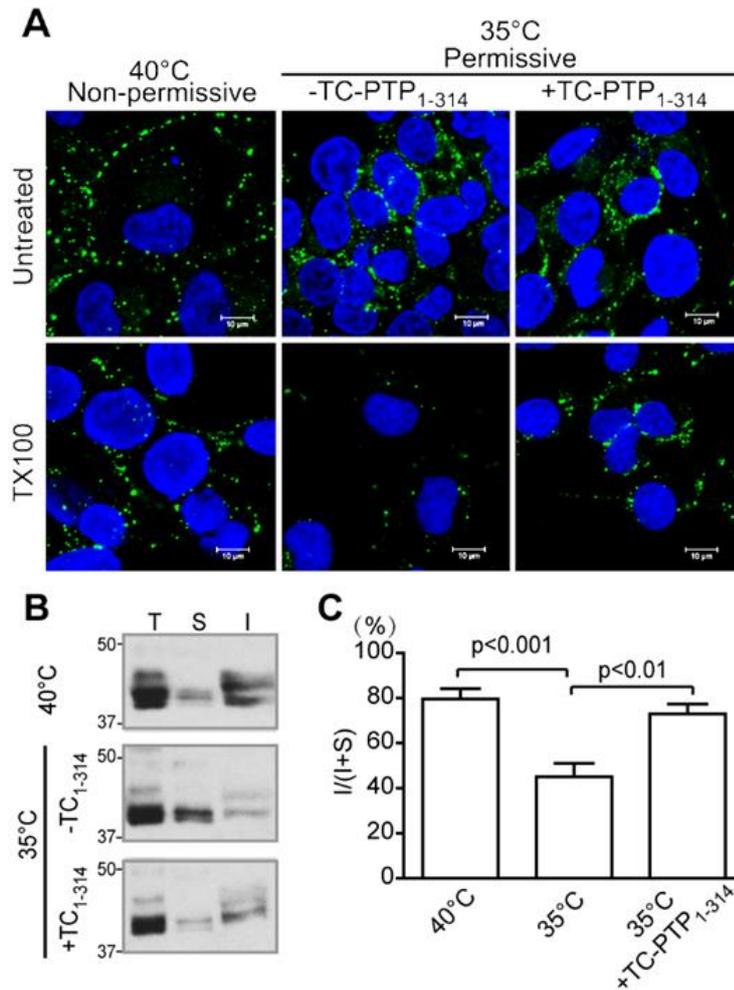
Figure 2.9 TX100 solubility assay shows TC-PTP stabilized Cx43 at the gap junction plaque in LA-25 cells. (A) Cx43 was extracted *in situ* with 1% TX100 and immunostained for Cx43 (green). Scale bar is 10 μm. (B) Equal amounts of total protein fraction (T), TX100 soluble fraction (S), and insoluble fraction (I) were run on SDS-PAGE and blotted with anti-Cx43 antibody. (C) Protein levels were quantified to determine the insoluble to insoluble+soluble ratio I/(I+S). I/(I+S) at 40°C is significantly higher than at 35°C (p<0.001). At 35°C, I/(I+S) in the TC-PTP$_{1-314}$ transfected group is significantly different from the empty vector transfected control (p<0.01).

(S368) (Mitra et al.,2012; Solan and Lampe, 2008). We also show that v-Src increased the level of Y265, Y247, S279/282 and S368 phosphorylation. Conversely, TC-PTP decreased the phosphorylation level of Y265 (direct), Y247 (direct), and S368 (indirect), but not S279/282. The indirect decrease of pS368 was caused by inactivation of PKCα PKCδ. No change in pS279/282 levels is consistent with a previous study in which TC-PTP had no effect on MAPK signaling after EGF-induced activation (van Vliet et al., 2005). Of note, one mechanism by which EGF up regulates MAPK signaling is through c-Src activation (Faivre and Lange, 2007; Zhang et al., 2012). The use of kinase inhibitors identified that v-Src, MAPK, and PKC are all involved in gap junction closure, although they decreased the level of communication differently. MAPK phosphorylation had the greatest effect on channel closure and the observation that TC-PTP did not affect the phosphorylation level of S279/282 explains why TC-PTP only partially reversed gap junction closure caused by v-Src.

To detect the phosphatase(s) that dephosphorylate Cx43CT residues S279/282, we performed *in vitro* phosphatase screening assays. We found that only PP2A could dephosphorylate the pS279/282 sites, however, only 39% of control. Future studies to validate this finding would include cell studies. Western blot using Cx43 phospho-specific antibodies could be applied on PP2A transfected cells with TPA stimulation. In fact, some of MAPK substrates can be dephosphorylated by PP2A, such as Caspase 3 (Alvarado-Kristensson and Andersson, 2005) and pro-apoptotic protein Bad (Grethe and Porn-Ares, 2006). These evidence suggest the possibility of dephosphorylation on Cx43 S279/282 by PP2A. Other strategies targeting MAPK phosphorylation sites, such

as peptide or small molecule drugs to block S279/282 on Cx43, could be applied to maintain functional gap junction.

Several hypotheses, which are not mutually exclusive, could describe the mechanism(s) by which phosphorylation regulates gap junction intercellular communication. First, the negative charge of the phosphate could affect the permeability of ions through the pore via electrostatic attraction or repulsion. In this study, the negatively charged Lucifer yellow was used as probe for gap junction intercellular communication. The placement of at least 60 negative charges (5 phosphorylation sites: 2 Src, 2 MAPK, and 1 PKC; phosphate charge of -2) within a connexon (6 connexins) caused by v-Src could contribute to the reduction of Lucifer yellow transport. Second, phosphorylation can directly (and possibly indirectly, see (Grosely et al., 2013c)) alter the binding affinities of proteins involved in Cx43 regulation. As mentioned in the introduction section, Y247 is directly involved in microtubule binding and pY247 would be detrimental to Cx43 intercellular communication.(Saidi Brikci-Nigassa et al., 2012). This is consistent with our results that dephosphorylation of pY247 by TC-PTP correlates with an increase in the number of Cx43 gap junctions at the plaque. Phosphorylation on Y265 also facilitates gap junction endocytosis by disrupting the interaction with drebrin, an F-actin-binding protein that is required for stabilizing gap junctions at the plasma membrane (Ambrosi et al., 2016; Butkevich et al., 2004) (del Valle et al., 2012). These results are in agreement with our finding that TC-PTP dephosphorylation of Y265 also correlates with an increase in Cx43 gap junction channels at the plaque. Finally, Cx43CT

phosphorylation could alter the structure of the transmembrane α-helices to influence pore size and/or drive gating by a "ball and chain" mechanism, similar to what had been shown for pH gating of Cx43 (ek-vitorin 1996 and Morley 1996).

Phosphorylation is a primary means of mediating signal transduction events that control cellular processes via a highly regulated dynamic interplay between protein kinases and phosphatases. Many kinases are known to phosphorylate Cx43 with the predominant effect being a decrease in gap junction intercellular communication. While kinases have established roles in the life cycle of a connexin, unfortunately, a significantly less amount of information is known about the involvement of phosphatases. Identification of a new tyrosine phosphatase TC-PTP, which dephosphorylates Src-mediated phosphorylation of Cx43, presents an opportunity to contribute beyond what other studies have focused upon, which is channel closure, by characterizing the timeline of gap junction channel opening. Understanding both phosphorylation and de-phosphorylation will help build a better foundation to target gap junction channels to benefit human health. For example, inhibitor treatment of c-Src in a myocardial infarction mouse model significantly increased Cx43 expression in scar border and distal ventricle, leading to improved conduction velocity and lower arrhythmic inducibility (Rutledge et al., 2014). Our data demonstrating that TC-PTP dephosphorylates Cx43 and increases the level of Cx43 level on the cell membrane supports their conclusion, from a cellular perspective. Future research using an animal model to study the relevance of Cx43 de-phosphorylation by TC-PTP may provide new avenues for disease therapy.

CHAPTER 3

Regulation of Connexin43 Function and Expression by Tyrosine Kinase 2

10. Introduction

The Cx43CT is differentially phosphorylated on at least 20 residues and significant progress has been achieved in characterizing the kinases involved (Axelsen et al., 2013; Lampe and Lau, 2004; Solan and Lampe, 2005, 2014). Unfortunately, an understanding of the mechanism(s) by which Cx43 phosphorylation alters channel function is lacking. Several problems contributing to this difficulty include the transient nature of a particular CT phosphorylation state, the ability of many kinases to phosphorylate more than one CT residue, the ability of various kinases to phosphorylate the CT at the same time, and the inability to precisely control which residue(s) are phosphorylated. Strategies employed to overcome these difficulties include the use of phospho-specific CT antibodies (Sosinsky et al., 2007) and short CT phosphopeptides (Chen et al., 2008; Saidi Brikci-Nigassa et al., 2012). Also well appreciated is the use of Asp (or Glu) substitutions as a mimetic for phosphorylation (Grosely et al., 2013b; Solan et al., 2007). Numerous serine protein kinases have been identified to directly phosphorylate Cx43 (for review see (Axelsen et al., 2013)), however tyrosine protein kinases have been limited to the well-studied cases involving c- and v-Src-induced phosphorylation (Azarnia et al., 1988; Filson et al., 1990; Kanemitsu et al., 1997; Kurata and Lau, 1994; Loo et al., 1995). In this study, we identified Cx43 as a novel substrate of Tyrosine kinase 2 (Tyk2).

Tyk2, a JAK family member, is a ubiquitously expressed non-receptor tyrosine kinase. Tyk2 associates with the intracellular domains from a wide range of cytokine and growth factor receptors via its N-terminal FERM and SH2-like (Firmbach-Kraft et

al., 1990; Strobl et al., 2011; Wallweber et al., 2014). This leads to recruitment and phosphorylation of STATs (Ghoreschi et al., 2009), which translocate to the nucleus where they induce transcription of genes involved in diverse biological processes (e.g. cellular proliferation and differentiation, inflammation, and defense against infection (Leonard, 2001; Stark and Darnell, 2012)). Patients with non-functional Tyk2 display a number of immunodeficiency conditions and increased susceptibility to infections caused by defects in IFNα/β, IL-6, IL-10, IL-12 and IL-23 signaling (Minegishi et al., 2006). Tyk2 deficient mice display reduced responses to IFNα/β and IL-12 and a deficiency in STAT3 activation (Karaghiosoff et al., 2000). The Tyk2/STAT3 axis has also been implicated in the induction of neuronal death in Alzheimer disease (Wan et al., 2010), as a biomarker for Crohn's disease (Sato et al., 2009), and in controlling allergic asthma (Ubel et al., 2014). Marrero et al. (Marrero et al., 1995) first showed that Ang II induces Tyk2 activation in rat aortic smooth muscle cells; a finding verified in other studies (Kodama et al., 1998; Pan et al., 1997; Pan et al., 1999; Yoon et al., 2013). The renin-angiotensin system (RAS) is a key signaling pathway associated with the pathogenesis of cardiovascular disease (Lonn et al., 1994; Pagliaro and Penna, 2005). Increased Ang II levels are linked with an increased risk of ventricular arrhythmia, and treatment with angiotensin-converting enzyme (ACE) inhibitors has demonstrated survival benefits in congestive heart failure and myocardial infarction (1991; Akar et al., 2004; Pfeffer et al., 1992). A transgenic mouse model of RAS activation by overexpression of ACE restricted to the heart (ACE8/8) has normal ventricular structure; however, it exhibits cardiac oxidative stress, a high incidence of

ventricular tachycardia and subsequent sudden cardiac death. With no significant change in Na^+ current, these observations were associated with downregulation of Cx43 gap junction intercellular communication (Kasi et al., 2007). Altered cardiac Cx43 protein level and change in cellular localization were also observed in other models of RAS activation (hypertension, hypertrophy, mechanical stress; (Emdad et al., 2001; Hussain et al., 2010; Tan et al., 2013; Wang et al., 2014)). We provide evidence of a relationship between Tyk2 activation by Ang II and Tyk2 phosphorylation of Cx43. Tyk2 decreased gap junction stability at the plasma membrane, and through STAT3 activation increased the intracellular protein level of Cx43.

11. Materials and Methods

11.1 Cell Culture

Normal rat kidney (NRK) and LA-25 cells (NRK cells containing temperature sensitive v-Src) were generous gifts from Dr. Paul Lampe (Fred Hutchinson Cancer Research Center). The MDA-MB-231 cell line was from Dr. Melissa Teoh-Fitzgerald (University of Nebraska Medical Center). All cells were grown in Dulbecco's modified Eagle's medium (DMEM) (Hyclone, Thermo Fisher Scientific Inc.) supplemented with 10% fetal bovine serum (FBS) (Hyclone, Thermo Fisher Scientific Inc.) and antibiotics in an atmosphere of humidified 5% CO_2.

11.2 Antibody and Immunostaining

The following antibodies were used in this study: Cx43 monoclonal antibodies

against amino acids 360-382 (Cx43CT1 and Cx43IF1, described in (Cooper and Lampe, 2002; Lampe et al., 2006)); Cx43 polyclonal antibody (C6219, Sigma-aldrich); rabbit anti-Cx43 phosphorylated Y247, rabbit anti-phosphorylated Y265, and rabbit anti-phosphorylated S279/282 (described in (Solan and Lampe, 2008)) (all generous gifts from Dr. Paul Lampe, Fred Hutchinson Cancer Research Center); rabbit anti-Cx43 phosphorylated S368 (Millipore); non-specific phospho-tyrosine antibody (P-Tyr-100, Cell Signaling); anti-Tyk2 (Santa Cruz), anti-active Tyk2 (phosphorylated 1054/1055); anti-tubulin β (Sigma); and antibodies against total and active Src (phosphorylated Y416, Millipore), STAT antibodies sampler kit (9939, Cell Signalling).

Cells were immunostained as described previously (Mehta et al., 1991). Briefly, cells grown on cover slips to ~60% confluence were fixed with 3.7 % para-formaldehyde for 10 min. Cells were blocked for 30 min at room temperature (RT) by MPS buffer (1x Phosphate-buffered saline (PBS), 1% Goat Serum) containing 0.2% TX-100 for permeabilization. Then, cells were immunostained with appropriate primary antibodies at RT for 1 h, followed by several PBS-0.5% Tween washes. Secondary antibodies (Alexa 594-conjugated goat anti-rabbit antibody and/or Alexa 488-conjugated goat anti-mouse antibody) were applied for 1 hr at RT. Images of immunostained cells were acquired with a Zeiss 510 Meta Confocal Laser Scanning Microscope using a 63×1.4 numerical aperture objective with appropriate filters. Colocalization was quantified using the Manders method in Image J (Bolte and Cordelieres, 2006).

11.3 *In vitro* Kinase Assay

Rat Cx43CT$_{236-382}$ was expressed and purified as described previously (Duffy et al., 2002). An *in vitro* kinase screen was performed by Eurofins Scientific using the purified protein. The catalytic domain of JAK1 (866-1154), JAK2 (808-1132), and Tyk2 (875-1187) were used to phosphorylate the Cx43CT. A positive control was used for each kinase (JAK1, GEEPLYWSFPAKKK; JAK2, KTFCGTPEYLAPEVRREPRILSEEEQEMFRDFDYIADWC; Tyk2, GGMEDIYFEFMGGKKK). Controls and Cx43CT were incubated with the tyrosine kinase and ATP [γ-^{33}P] for 40 min at 30°C and then transferred to P30 Filtermat for substrate capture. Assays were performed in duplicate and acid blanks were used as a negative control. The level of phosphorylation for each sample was determined according to Merck Millipore's radiometric assay.

11.4 Mass Spectrometry

Purified rat Cx43CT$_{236-382}$ (12.5 nmol) was incubated with 1.5 µg Tyk2 (amino acids 833-1187, ThermoFisher Scientific) and 500 µM ATP at 30°C for 15 hrs. In the control group, the volume of Tyk2 was substituted by reaction buffer (25 mM HEPES [pH 7.5], 10 mM MgCl$_2$, 0.5 mM EGTA, and 0.005% Brij-35). The reaction was stopped on ice, and 1 nmol of protein was ran on a SDS-PAGE gel and Western blotted using a phospho-tyrosine antibody. 10 nmol of protein was run on a SDS-PAGE gel and stained with Coomassie. The Cx43CT band was cut and sent to the Beth Israel Deaconess Medical Center Mass Spectrometry Facility for analysis (Breitkopf and Asara, 2012).

11.5　Glutathione S-transferase (GST) Pull-down Assay

The GST pull-down assay was modified from (Leykauf et al., 2006). Briefly, purified GST-fusion Cx43CT and GST control proteins were bound to glutathione-Sepharose beads in buffer containing 25 mM Tris-HCl [pH=7.4], 150 mM NaCl, 1 mM DTT, 0.5% TX-100 and Complete protease inhibitor (Roche). 4 mg of MDA-MB-231 or LA-25 cell lysate protein (in cell lysis buffer containing 25 mM Tris-HCl (pH 7.4), 150 mM NaCl, 0.5% TX-100, 0.5% sodium deoxycholate, 2 mM EDTA, PhosSTOP (Roche), and Complete protease inhibitor) were incubated with GST-fusion Cx43CT or the GST control for 6 hrs at 4°C on a rotating wheel. Beads were washed 5x with cell lysis buffer and bound proteins were eluted with SDS-PAGE sample buffer, and analyzed by Western blot.

11.6　Co-immunoprecipitation (IP)

NRK or LA-25 cells were lysed in complete lysis buffer (50 mM Tris-HCl [pH 7.4], 150 mM NaCl, 0.5% Na-deoxycholate, 0.5 % TX 100, 5 mM NaF, and Complete protease inhibitor), maintained on ice for 30 min, precleared with protein G beads for 30 min at 4°C, and then spun at 12,000 rpm for 15 min. Total protein was assessed using the bicinchoninic acid (BCA) protein assay kit (Pierce). 2 mg lysate was incubated with 2 μg of Cx43 polyclonal or rabbit IgG (4 h at 4°C) and then incubated with 100 μl of protein G sepharose (GE Healthcare) (overnight at 4°C). The sepharose was washed 4x with cold lysis buffer and the co-IP product was analyzed by SDS-PAGE and Western blot.

When detecting tyrosine phosphorylation levels, 5 mM Na_3VO_4 was added in the blocking and primary antibody buffer in order to minimize the loss of phosphorylation. Western blot data were scanned and quantified using ImageJ software as described in (Schneider et al., 2012).

11.7 Tyk2 siRNA Treatment

Tyk2 siRNA (Invitrogen) was used to knockdown Tyk2 expression in LA-25 cells. Oligonucleotide from the non-target pool (Dharmacon) was used as negative control. Lipofectmine RNAi MAX (Invitrogen) was used to carry the oligonucleotide according to manufacturer's protocol. Cells were treated with Tyk2 siRNA for 36 hrs and then incubated at 35°C for another 12 hrs. Protein levels were detected by Western blot.

11.8 Cycloheximide Treatment and Cx43 Degradation

Cells equally seeded on 60-mm dishes were grown for 24 hrs to 70-80% confluency before transfection. 24 hrs post-tranfection, cells were treated with 100 μg/ml cycloheximide (Cell Signaling) for 1, 1.5, 2, 2.5, 3, 4 hrs to inhibit protein synthesis. Cells were then scraped off and lysed for Cx43 immunoblotting. β-actin was also blotted for quantification.

11.9 TX 100 Solubility

The T100 solubility assay was modified from the method described in (Mitra et al., 2006). NRK cells grown in 10-cm dishes were rinsed 3x with PBS and scraped into 1

ml lysis buffer (50 mM Tris-HCl [pH 7.4], 1 mM EGTA, 1 mM EDTA, 1 mM PMSF, 100 mM NaCl, PhosSTOP, and Complete protease inhibitor). Then, cells were sonicated for 10 s on ice. Protein estimation was determined using the BCA method. 450 μl cell lysate samples were added to 50 μl of 10% SDS, which was saved as total protein, or to 10% TX-100 (final concentration of 1%) and incubated at 4°C for 30 min. Lysates were then separated into cytosolic (supernatant, soluble) and membrane (pellet, insoluble) fractions by centrifugation at 100,000 g for 1 h at 4°C. The pellets were dissolved in 500 μl dissolving buffer (70 mM Tris-HCl [pH 6.8], 8 M urea, 2.5% SDS, 0.1 M DTT, 5 mM NaF, 5 mM Na_3VO_4, and Complete protease inhibitor). Equal volume of total lysate, TX-100 soluble and insoluble portions, were loaded on a 10% SDS-PAGE and immunoblotted with the Cx43 polyclonal antibody.

11.10 Surface Biotinylation Assay

Surface biotinylation assay followed the method described in (Johnson et al., 2013). Briefly, cells were seeded in 60-mm dishes in replicate and grown to 70-80% confluence. 24 hrs after transfection, cells were washed once with PBS and then 5 ml of ice cold DMEM plus HEPES buffer (pH = 7.4, final concentration 30 mM) was added for 10 min at 4°C. Cells were washed twice with cold PBS-plus (PBS with 1 mM $CaCl_2$ and 1 mM $MgCl_2$). The biotinylation reaction was performed at 4°C using freshly prepared EZ-LinkSulfo-NHS-SS Biotin reagent (Pierce) at 0.5 mg/ml in PBS-plus for 30 min. The reaction was terminated by adding PBS-plus containing 20 mM glycine. Cells were lysed in lysis buffer (25 mM Tris-HCl pH 7.5, 0.05% SDS, 20 mM Glycine,

and Complete protease inhibitor) with homogenization by passing through a 25G needle. 500 μg of total protein were incubated with 100 μl of streptavidin-agarose beads (Pierce) on a rotator overnight at 4°C. Beads were then washed 6x and the streptavidin-bound biotinylated proteins were eluted and resolved by SDS–PAGE followed by Western blotting.

11.11 Biotin Peptide Pull Down Assay

Biotin-tagged phosphorylated (Y247) and non-phosphorylated $Cx43CT_{234-255}$ peptides (LifeTein) were bound to streptavidin-agarose resin (GenScript) in PBS. NRK cells were lysed in HEPES lysis buffer (50 mM HEPES, 150 mM NaCl, 0.25% TX-100, 2 mM PMSF, 10 mM EDTA, 50 mM NaF, 5 mM Na_3VO_4, and PhosSTOP and Complete tablets, pH 7.4) and total protein concentration was assessed using the BCA protein assay. A total of 2.5 mg of protein lysate was incubated with each of the resin-bound peptide, overnight at 4°C. Beads were washed 3x with PBS before analyzing the pull-down products by SDS-PAGE and Western blot.

11.12 Semi-Quantitative Reverse Transcription (RT) PCR

Semiquantitative RT-PCR was modified from the method described in (Marone et al., 2001). Briefly, NRK cells grown in 35-mm dishes were transfected with $Tyk2_{V678F}$ and pretreated with the inhibitor Nifuroxazide (50 μM, Millipore) or SH-4-54 (5 μM, Millipore). RNA extractions were carried out with the RNeasy mini kit (Quiagen), according to the manufacturer's protocol. RT was performed with ProtoScript cDNA

synthesis kit (New England Biolab). The following primers were used: Cx43 5'-AGCCTCCAAGGAGTTCCA-3' and 5'-AGAGCACTGACAGCCACA-3', β-actin 5'-CACCCGCGAGTACAACCTTC-3' and 5'-CCCATACCCACCATCACACC-3'. Cx43 yielded an amplification product of 160 bp and β-actin of 207 bp. DreamTaq green PCR master mix (Thermo Fisher Scientific) was used for PCR amplification. To find out the exponential phase of amplification, different PCR cycles from 16 to 30 were tested. Each set of reaction included a no-sample negative control.

11.13 Statistical Analysis

All data were analyzed by GraphPad Prism 5.0 and presented as the standard error of the mean (±S.E.M). Paired t-test was used to compare differences between the experimental group and control or the two parallel experimental groups. $P<0.05$ was considered to be statistically significant.

12. Results

12.1 Tyk2 Directly Interacts and Phosphorylates the Cx43CT Domain

Src (c-/v-Src) is the only known tyrosine kinase to both directly phosphorylate the Cx43CT domain (pY247 and pY265) and affect gap junction intercellular communication (Kieken et al., 2009; Sorgen et al., 2004). However, proteomic discovery-mode mass spectrometry (MS) data identified other tyrosine residues (Y267, Y286, Y301, and Y313) as potential phosphorylation targets (PhosphoSitePlus web site). Unfortunately, the kinases involved were not identified nor was the functional significance of phosphorylation at these sites. In this study, we focused on the JAK

family of tyrosine kinases because of the potential direct link between Cx43 and RAS in the pathogenesis of cardiovascular disease (Delmar and Makita, 2012; Lonn et al., 1994; Pagliaro and Penna, 2005; Palatinus et al., 2012). An *in vitro* tyrosine phosphorylation screen performed by Eurofins Scientific (KinaseProfiler) found that Tyk2 phosphorylated purified Cx43CT (236-382; Figure 3.1A). JAK1 and JAK2, also JAK family members, had significantly less ability to phosphorylate the Cx43CT domain (JAK3 was not tested because it is not expressed in the heart). To confirm the interaction between Cx43 and Tyk2, purified GST-tagged Cx43CT$_{236-382}$ was immobilized on glutathione-Sepharose beads and lysate from MDA-MB-231 cells that express Tyk2 (but not Cx43) was used in a pull-down assay (Figure 3.1B). Tyk2 can be pulled-down by GST-Cx43CT but not GST in MDA-MB-231 cells. v-Src was used as a positive control.

12.2 Identifying the Cx43CT Tyrosine Residue(s) Phosphorylated by Tyk2

Purified Cx43CT$_{236-382}$ was incubated *in vitro* with active Tyk2 (Life Technologies) as described in (Cooper et al., 2000; Huang et al., 2012) and phosphorylation was confirmed using an anti-phospho-tyrosine antibody (Figure 3.2B). After trypsin digestion, Tandem MS/MS identified phosphorylation at Y247, Y265, Y267, and Y313 (Figure 3.2A and Table 3.1). To confirm tyrosine phosphorylation can occur at residues other than Y247 and Y265, the *in vitro* kinase assay was performed using the Cx43CT$_{236-382}$(Y247,265F) (2YF) construct and phosphorylation detected with an anti-phospho-tyrosine antibody (Figure 3.2B). The data indicate that while a majority of
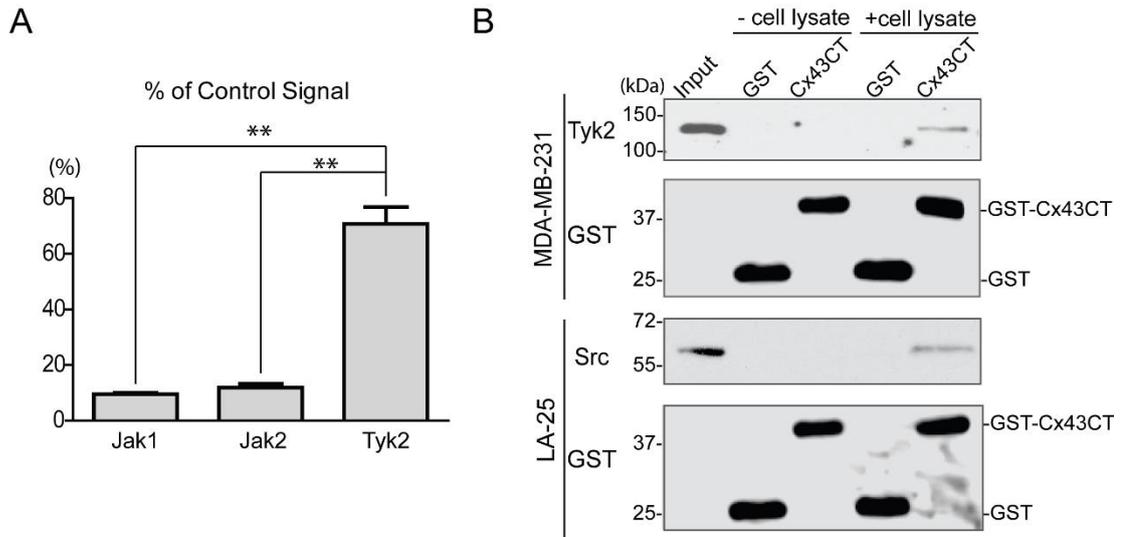
Figure 3.1 Phosphorylation of the Cx43CT domain by JAK tyrosine kinases. (A) An *in vitro* kinase assay was performed using the catalytic domain of Jak1, Jak2, and Tyk2 to phosphorylate purified Cx43CT. The amount of Cx43CT phosphorylation was compared with a positive control peptide for each kinase (100% signal) (**P<0.01*). (B) Purified GST (26 kDa) or GST-Cx43CT (42 kDa) bound on glutathione-agarose beads were incubated with or without MDA-MB-231 cell lysate (top) and the pull-downed product was analyzed by Western blot using an anti-Tyk2 antibody. GST-Cx43CT pull down of v-Src from LA-25 cell lysate was used as positive control (bottom).

A

^{236}VKDRVKGRSDP**Y**^{247}HATTGPLSPSKDCGSPK**Y**^{265}A**Y**^{267}FNGCSSPTAPLSPMS
PPGY^{286}KLVTGDRNNSSCRNY^{301}NKQASEQNWAN**Y**^{313}SAEQNRMGQAGSTISNSHA
QPFDFPDDNQNAKKVAAGHELQPLAIVDQRPSSRASSRASSRPRPDDLEI^{382}

B
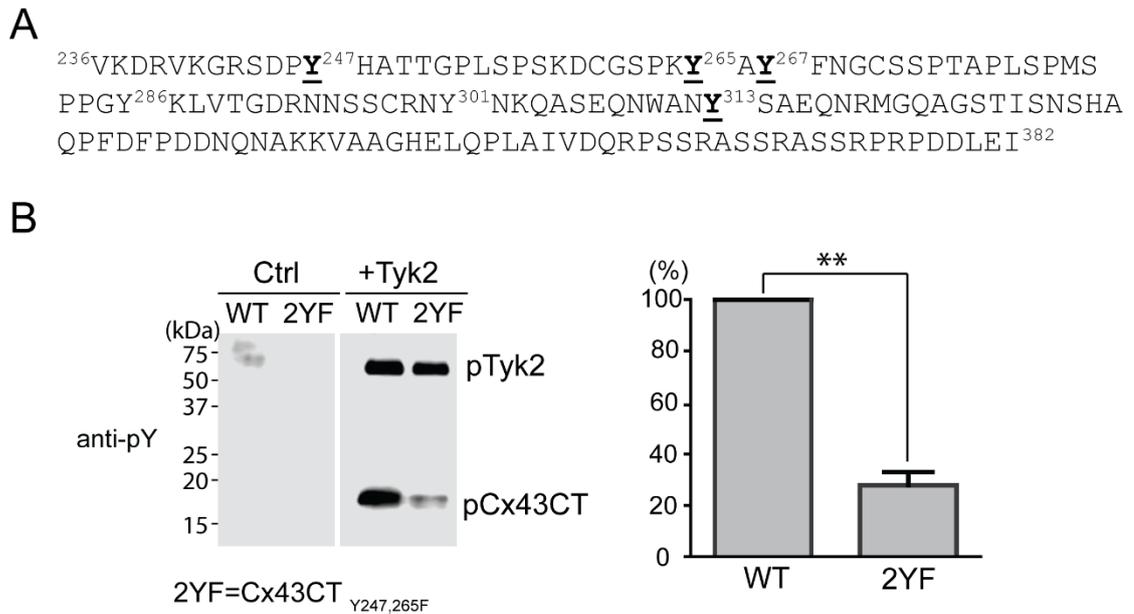
Figure 3.2 Identification of the Cx43CT tyrosine residues phosphorylated by Tyk2.
(A) Sequence of the Cx43CT domain. Highlighted (bold and underlined) are the tyrosine residues identified from mass spectrometry to be phosphorylated from an *in vitro* kinase assay using the Tyk2 catalytic domain to phosphorylate the Cx43CT. (B) The same *in vitro* kinase assay in (A) was performed using wild type Cx43CT$_{236-382}$ or a Y247,265F (2YF) mutant as substrate and phosphorylation was detected by Western blot using a general anti-phospho-tyrosine antibody. The control (Ctrl) group did not contain Tyk2. The phospho-tyrosine level was quantified using ImageJ software (n=3, **P<0.01*)

Table 3.1 Phospho-tyrosine containing peptides identified from mass spectrometry of the Cx43CT domain phosphorylated in vitro by Tyk2

Peptide sequence	Start-end	Average Mascot Delta Ion Score	*Number of phospho-peptides	Actual peptide mass	Calculated +1H peptide mass	Phosphorylation site localization
GRSDPyHATTGPLSPSK	242-258	15.35	4	1849.84	1850.84	Y247
SDPyHATTGPLSPSK	244-258	18.5	6	1636.72	1637.72	Y247
GRSDPyHATTGPLSPSKDc(Carbamidomethyl)GSPK	242-264	9.37	2	2667.04	2668.05	Y247
QASEQNWANySAEQNR	304-319	13.7	2	1974.79	1975.79	Y313
yAYFNGc(Carbamidomethyl)SSPTAPLSPm(Oxidation)SPPGYK	265-287	7.14	1	2588.07	2588.09	Y265
yAyFNGc(Carbamidomethyl)SSPTAPLSPm(Oxidation)SPPGYK	265-287	13.8	1	2667.05	2668.05	Y265, Y267

* Peptides with Mascot Delta Ion Score >7 were used to obtain the average Mascot Delta Ion Score according to (Savitski et al., 2011).

Tyk2 phosphorylation occurs on Y247 and Y265 (of note, Y247 and Y265 phospho-specific antibodies will be used in the next sections to further characterize these sites), other tyrosine sites (i.e., Y267 and Y313) can be phosphorylated by Tyk2 *in vitro*.

12.3   Tyk2 Phosphorylates Cx43 Residues Y247 and Y265 Leading to Decreased Stability of the Gap Junction Plaque in Normal Rat Kidney Epithelial (NRK) cells.

To determine if Tyk2 phosphorylation of Cx43 occurs in cells, we initially tested in NRK cells if Cx43 (endogenously expressed) and Tyk2 (not expressed; transiently transfected with a constitutively active construct, Tyk2$_{V678F}$) colocalize (Figure 3.3). The images suggest little-to-no colocalization in NRK cells that are over-expressing active Tyk2. However, in those same NRK cells, Cx43 is significantly decreased at the plasma membrane. The data suggests over-expressing active Tyk2 is leading to internalization of Cx43 from the plasma membrane.

Next, tyrosine phosphorylation levels were evaluated in the NRK cells using the only available Cx43 tyrosine phospho-specific antibodies pY247 and pY265 (Figure 3.4). Constitutively active Tyk2 increased both Y247 and Y265 phosphorylation levels as compared to control (non-transfected cells). Importantly, the presence of active Tyk2 did not cause activation of c-Src. Since MAPK and PKC were reported to phosphorylate Cx43 to down regulate Cx43 gap junction intercellular communication in response to active Src in different cell lines (Mitra et al., 2012; Solan and Lampe, 2008), we investigated if Tyk2 also indirectly affects serine phosphorylation. Cx43 serine phosphorylation levels were evaluated using phospho-serine specific antibodies to

pS279/282 (MAPK target) and pS368 (PKC target). pS279/282 and pS368 levels were up-regulated in the presence of active Tyk2. Finally, while the amount of Cx43 at the plasma membrane decreased (Figure 3.3A), active Tyk2 directly or indirectly caused an overall increase in the total amount of Cx43. Numerous studies have shown that differentially phosphorylated Cx43 results in multiple electrophoretic isoforms: a fast migrating isoform (P0), and multiple slower migrating isoforms (P1 and P2) (Crow et al., 1990; Matesic et al., 1994; Solan and Lampe, 2005). In particular, the P2 isoform has been found at the stage of gap junctional plaques. Consistently, Western blots (here and next sections) show an increase in the lower migrating P0 and P1 isoforms of Cx43 in the presence of active Tyk2.

Cx43 gap junction channels are localized in detergent-insoluble junctional plaques (Musil and Goodenough, 1991; Sirnes et al., 2008). To confirm the increased amount of Cx43 is not leading to an increase in the amount of Cx43 at junctional plaques, we assessed the level of TX-100 detergent solubility. The detergent extraction Western blot data show that active Tyk2 in NRK cells decreased the detergent-insoluble fraction of Cx43 (Figure 3.5A). Quantification of the data revealed that the control insoluble to insoluble + soluble ratio (I/(S+I)) was 67.1±6.0%. However, the number of assembled gap junctions significantly decreased to 19.5±0.9% in the presence of active Tyk2. The decreased amount of Cx43 in junctional plaques was corroborated by a biotinylation assay which detected a significant decrease in the amount of Cx43 at the plasma membrane (Figure 3.5B).
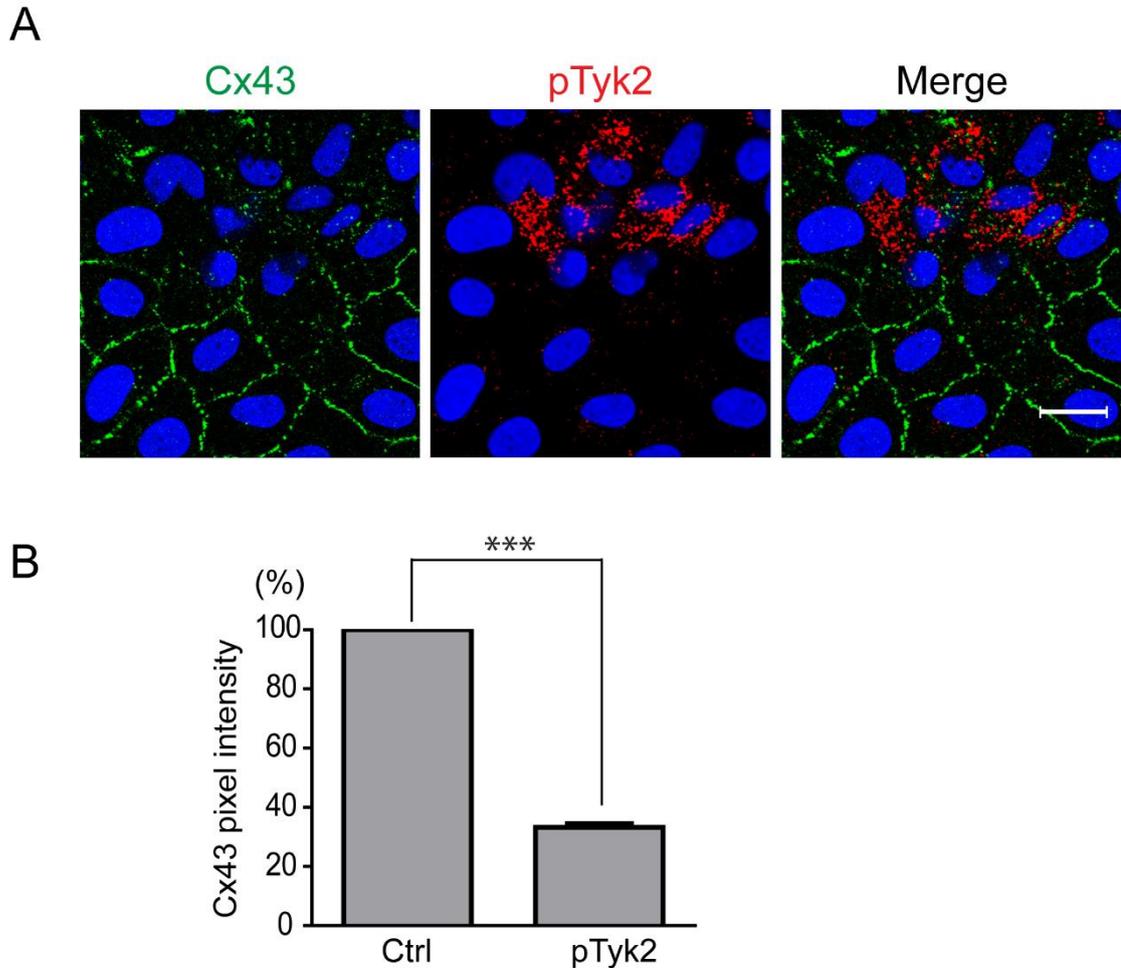
Figure 3.3 Effect of Tyk2 on the cellular localization of Cx43. (A) Cellular localization of endogenous Cx43 and constitutively active Tyk2 (Tyk2$_{V678F}$) in NRK cells detected by immunofluorescence (green, Cx43; blue, DAPI-stained DNA; red, active Tyk2). Scale bar is 20 μm. (B) Quantification of Cx43 expression level at the plasma membrane. Cx43 pixel intensity of 204 cell pairs containing p-Tyk2 was normalized to the Cx43 pixel intensity of 204 cell pairs without p-Tyk2 (Ctrl) by ImageJ software. Cell pairs with p-Tyk2 or without p-Tyk2 were from the same images. The data are representative of three independent experiments (***$P<0.001$).

Figure 3.4 Phosphorylation of Cx43 by Tyk2 in NRK cells. Western blot of active

Tyk2 (p-Tyk2), total Tyk2, active c-Src (p-Src), total c-Src, Cx43 pY247, pY265,

pS279/282, pS368 and total Cx43 from NRK cells without (Ctrl) or with transfection

of Tyk2$_{V678F}$. The Cx43 mobility shifts (P0, P1 and P2) are labeled. Relative protein

levels were quantified by analyzing scanned blots using ImageJ software, with

normalization of protein expression to the control lane (value set arbitrarily as 100%).

The data are representative of three independent experiments (*$P<0.05$, ***$P<0.001$).
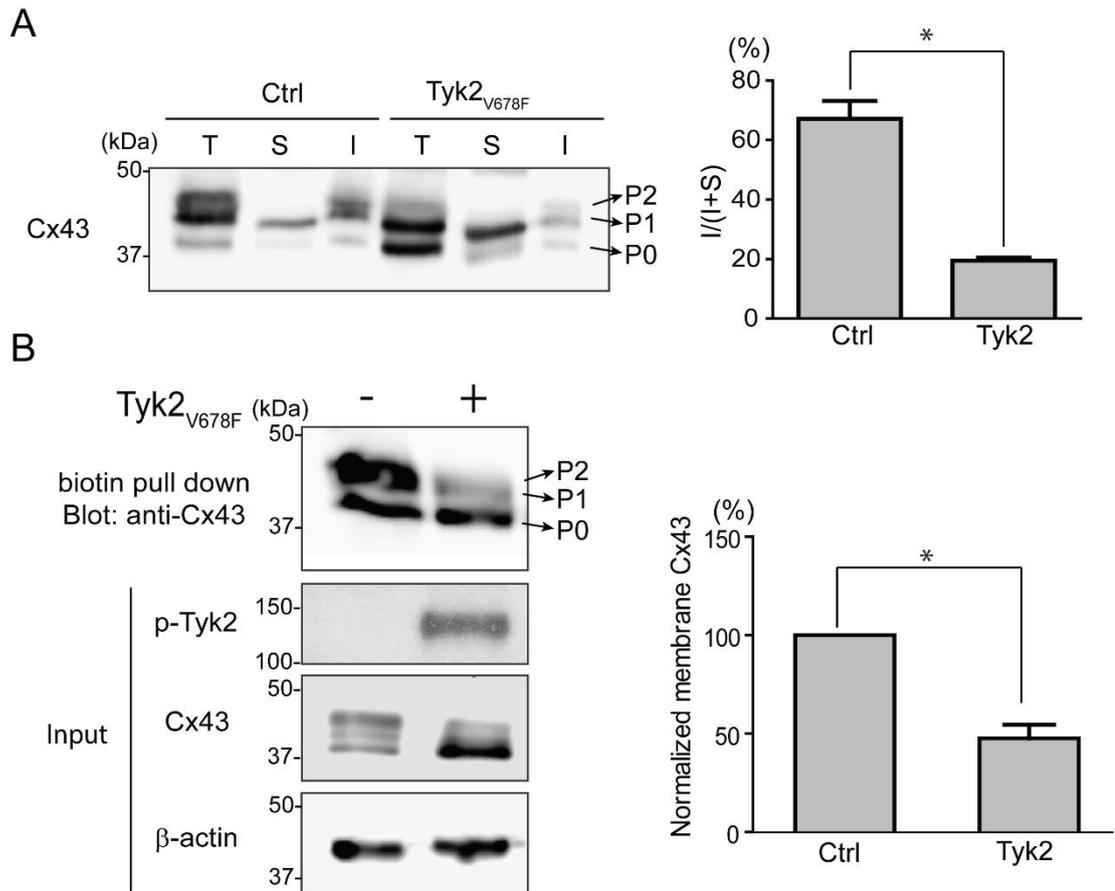
Figure 3.5 Effect of Tyk2 on the plasma membrane localization of Cx43 in NRK cells. (A) TX-100 solubility assay: Equal amounts of total protein fraction (T), TX-100 soluble fraction (S) and the insoluble fraction (I) were run on SDS-PAGE and blotted with anti-Cx43 antibody. Protein levels were quantified to determine the insoluble to insoluble + soluble ratio [I/(I+S)] (*$P<0.05$). (B) Biotinylation assay: NRK cells with or without Tyk2$_{V678F}$ transfection were cell-surface biotinylated. Biotinylated proteins were pulled down by immobilization on streptavidin agarose beads, and immunoblotted for Cx43. Protein levels of biotinylated Cx43 were quantified (*$P<0.05$). Input shows active Tyk2 and Cx43 protein in the cell lysate.

12.4 Interplay between Src and Tyk2 in the Regulation of Cx43

Murakami et al. (1998) observed that v-Src transfected cells indirectly caused constitutive activation of Tyk2 and STAT3. Therefore, a modified NRK cell line containing a temperature sensitive v-Src (called LA-25), commonly used in the gap junction field to characterize Cx43 regulation by v-Src (Solan and Lampe, 2008; Zhou et al., 1999), was used to study the effect of Tyk2 on Cx43 tyrosine phosphorylation levels upon Src activation. v-Src is active in this cell line at the permissive temperature (35°C) and not at the non-permissive temperature (40°C). Of note, temperature alone does not affect gap junction communication in NRK or LA-25 cells (Atkinson et al., 1981) and Tyk2 is endogenously expressed in LA-25 cells. To begin with, Western blot data confirmed that active v-Src at 35°C resulted in activation of endogenous Tyk2 (Figure 3.6A). Immunostaining data then indicated that after 4 hrs of v-Src activation, endogenous Tyk2 colocalizes with Cx43 at the plasma membrane (Figure3.6B). After 12 hrs, there was a decrease in the level of Cx43 and Tyk2 colocalization as well as the amount of Cx43 at the plasma membrane. These results are similar to the overexpression of active Tyk2 in the NRK cells (Figure 3.3). Next, Tyk2 siRNA was transfected into the LA-25 cells (35°C) to differentiate the effect of v-Src and Tyk2 on direct and indirect phosphorylation of Cx43 (Figure 3.7). Tyk2 siRNA significantly reduced the level of active Tyk2 (>75%). As important, the Tyk2 siRNA does not affect the level of active v-Src. Knock-down of Tyk2 in the presence of active v-Src significantly decreases the level of Y247 and Y265 phosphorylation as compared to control (scramble siRNA). Indirect serine phosphorylation was also affected by the

knock-down of Tyk2. While pS279/282 phosphorylation was reduced by ~50%, phosphorylation of pS368 was reduced by almost ~75% in the absence of Tyk2. Finally, the knock down of Tyk2 led to a decrease in the total level of Cx43. Altogether, the data indicate that similarities exist in the residues affected by Src or Tyk2, but differences exist in the level of phosphorylation at each site and the overall amount of protein.

12.5   Tyk2 Increases Total Cx43 Protein Level through the STAT3 Pathway

In both the NRK and LA-25 cells, active Tyk2 caused an increase in the total protein level of Cx43. To determine the mechanism for this effect, cycloheximide was used to compare the turnover rate of Cx43 with or without Tyk2 (Figure 3.8). Western blot analysis of Cx43 from NRK cells revealed that active Tyk2 increased the Cx43 turnover. The data suggest the increased protein level of Cx43 is not a result of direct tyrosine or indirect serine phosphorylation. Next, RT-PCR from cell lysate of NRK cells transfected with active Tyk2 was used to determine if active Tyk2 indirectly affects the level of Cx43 mRNA. Using different numbers of RT-PCR cycles, the data revealed that active Tyk2 caused an increase in the level of Cx43 mRNA (Figure 3.9A). Actin was used as a loading control. Because Tyk2 activates the STAT signaling pathway, we tested if this is the mechanism leading to the increased mRNA and protein levels. Experiments performed using NRK cells incubated with the STAT1/3/5 inhibitor Nifuroxazide or the STAT3/5 inhibitor SH-4-54 eliminated the effect of active Tyk2 increasing Cx43 mRNA (Figure 3.9B) and protein levels (Figure 3.10A). Based upon NRK cells expressing a very small amount of STAT1 and no STAT5 (Figure 3.10B),
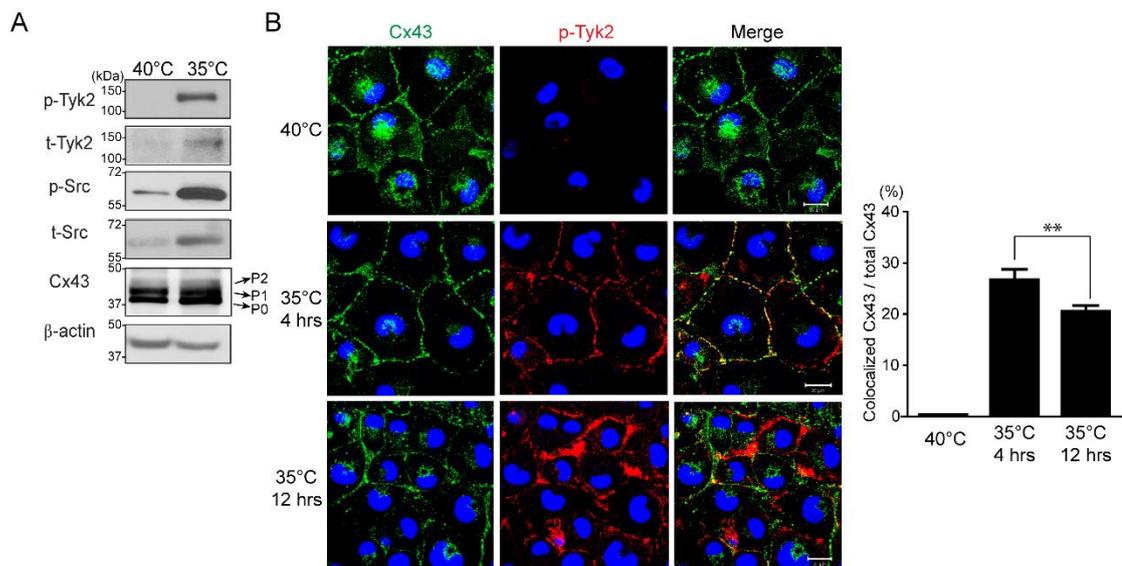
Figure 3.6 Colocalization of endogenous Tyk2 and Cx43 in LA-25 cells. (A) Western blot of active v-Src (p-Src), total v-Src, active Tyk2 (p-Tyk2), total Tyk2, and Cx43 in LA-25 cells at 40°C and 35°C. (B) Cellular localization of endogenous Cx43 and active Tyk2 in LA-25 cells at 40°C or 35°C was visualized by using immunofluorescence (green, Cx43; blue, DAPI-stained DNA; red, Tyk2). Scale bars is 20 μm. Colocalization of Cx43 and p-Tyk2 was analyzed based on 12 images from three independent experiments. Manders method was used to measure green signal (Cx43) coincident with red signal (active Tyk2) over the total intensity of green signal (***P<0.01*).
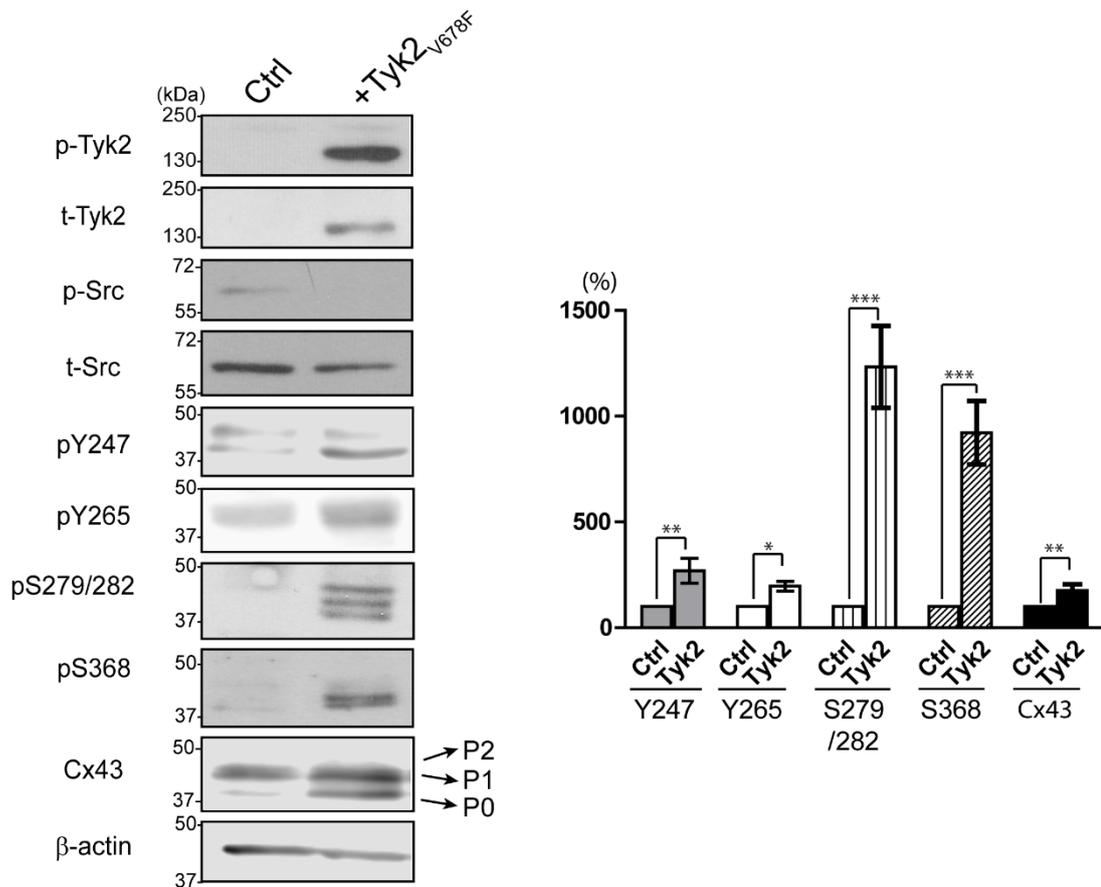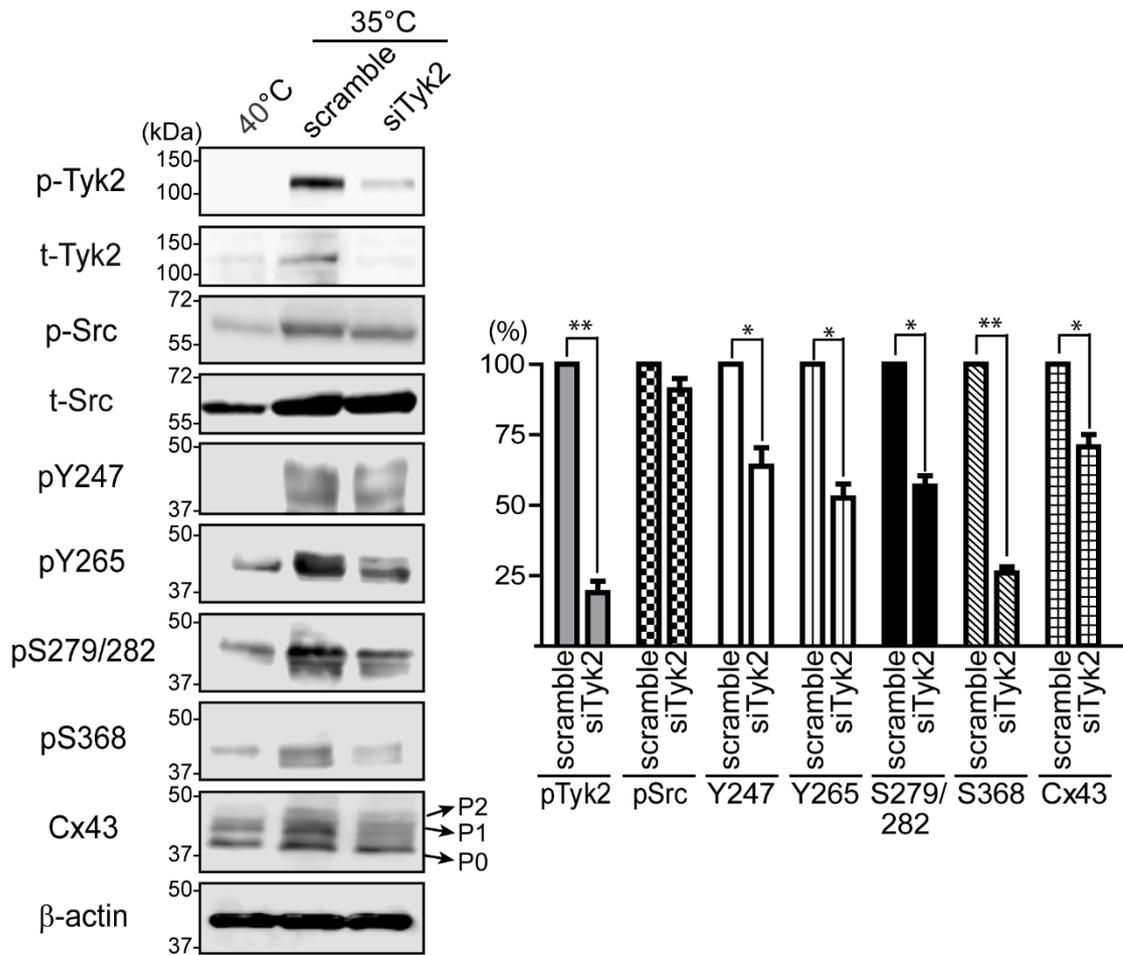
Figure 3.7 Effect of Tyk2 knockdown on the phosphorylation level of Cx43 in LA-25 cells. Western blot of active Tyk2 (p-Tyk2), total Tyk2, active v-Src (p-Src), total v-Src, Cx43 pY247, pY265, pS279/282, pS368 and total Cx43 from LA-25 cells at 40°C or 35°C treated with scrambled or Tyk2 siRNA for 12 h. Relative protein levels were quantified using ImageJ software, and normalized to the expression level in the scramble-RNA-treated sample at 35 ˚C (*P<0.05, **P<0.01).
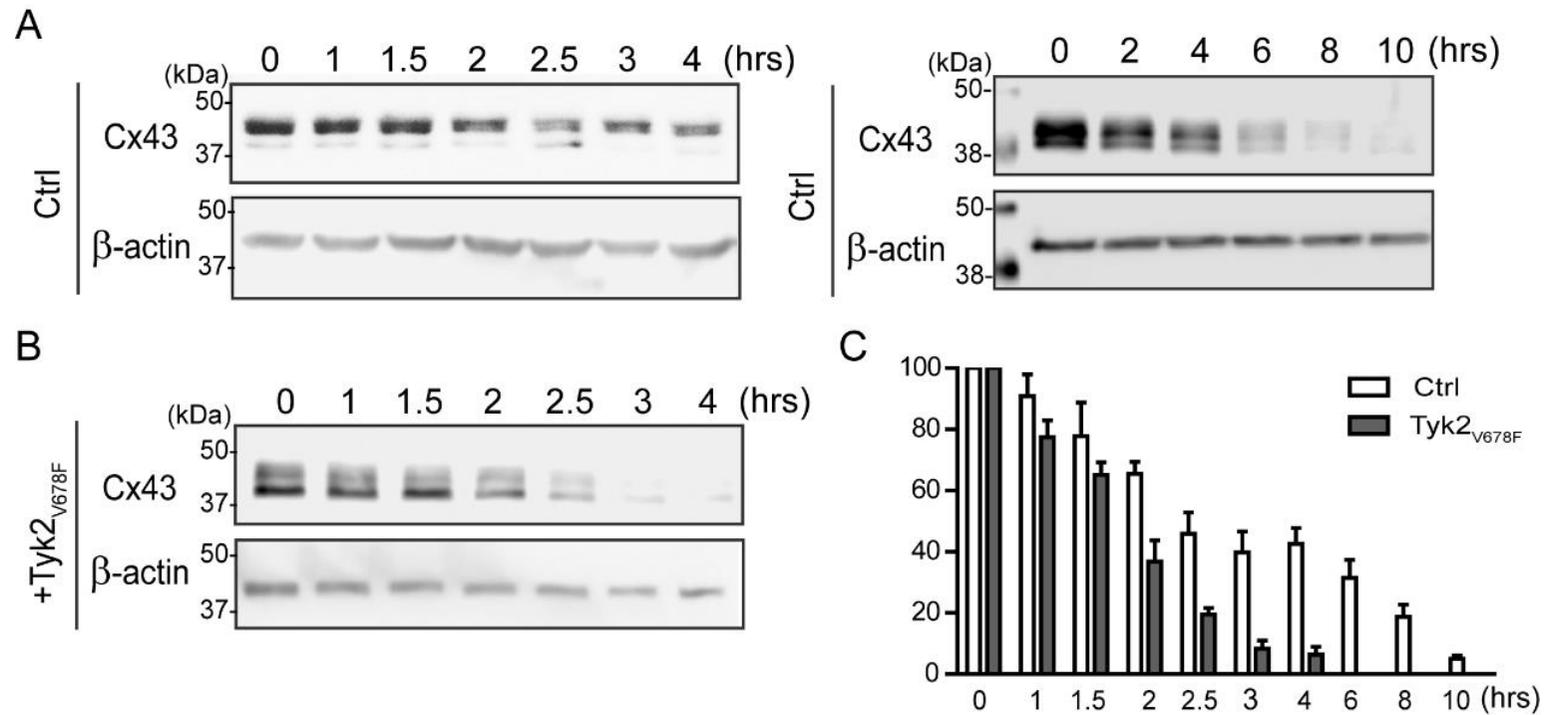
Figure 3.8 Effect of Tyk2 on the turnover rate of Cx43 in NRK cells. Control (A) or transfected (B) NRK cells with the constitutively active

Tyk2 (Tyk2$_{V678F}$) construct were treated with 100 µg/ml cycloheximide for different durations prior to lysis. Total Cx43 protein was immunoblotted.

(C) Protein level of three independent experiments quantified using ImageJ software and normalized to protein level at 0 hr.
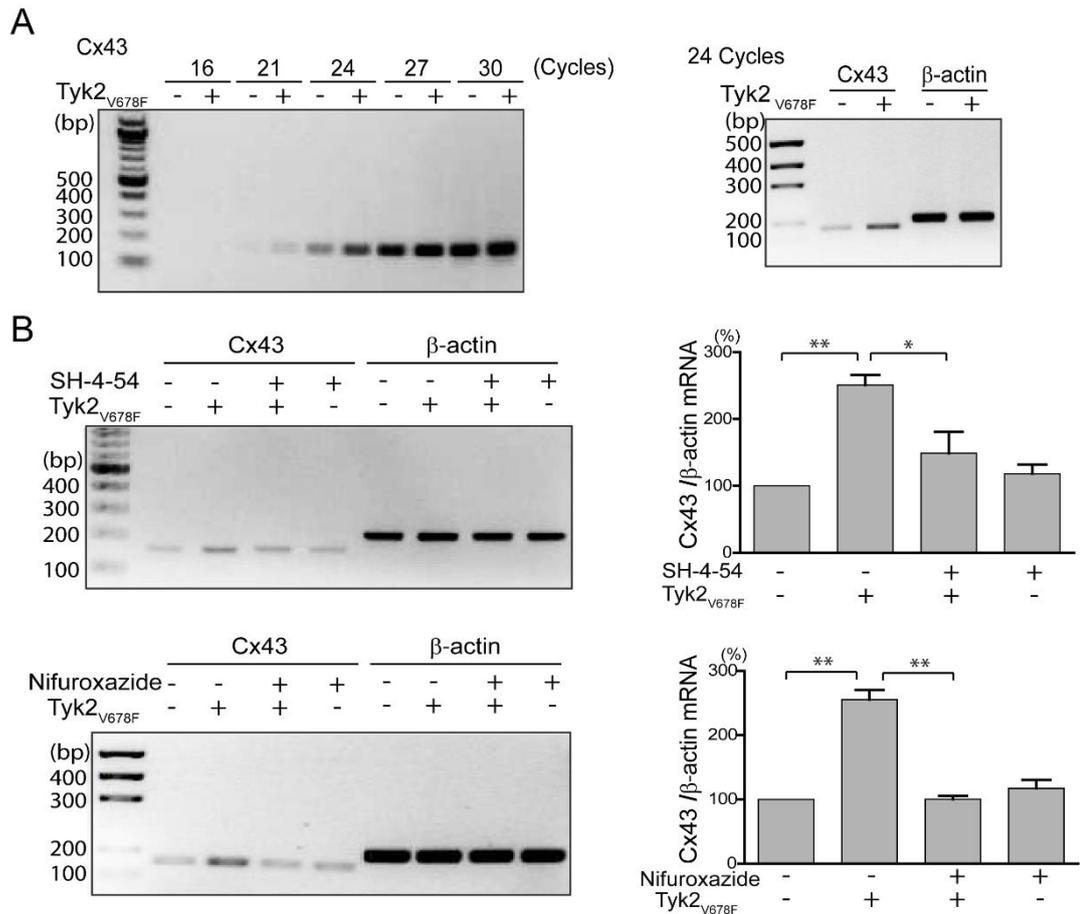
Figure 3.9 Effect of STAT3 activation by Tyk2 on Cx43 mRNA level. (A) RT-PCR shows Cx43 mRNA level with or without transfection of active Tyk2 (Tyk2$_{V678F}$). An appropriate number of cycles was determined by testing different number of cycles (16, 21, 24, 27, 30) for Cx43 amplification (top panel). Cx43 intensity increased up to 24 cycles where a plateau was reached, thus 24 cycles was used to run semi-quantification RT-PCR. Cx43 and β-actin were amplified for 24 cycles and ran on 2% agarose gel (right panel). (B) NRK cells with or without active Tyk2 (Tyk2$_{V678F}$) transfection for 8 hrs were treated with the STAT3/5 inhibitor SH-4-54 (5 μM) or STAT1/3/5 inhibitor Nifuroxazide (50 μM) for another 16 hrs. Cx43 and β-actin were amplified for 24 cycles and ran on 2% agarose gel. Cx43 and β-actin mRNA levels were quantified by densitometry from three independent experiments (*P<0.05, **P<0.01).
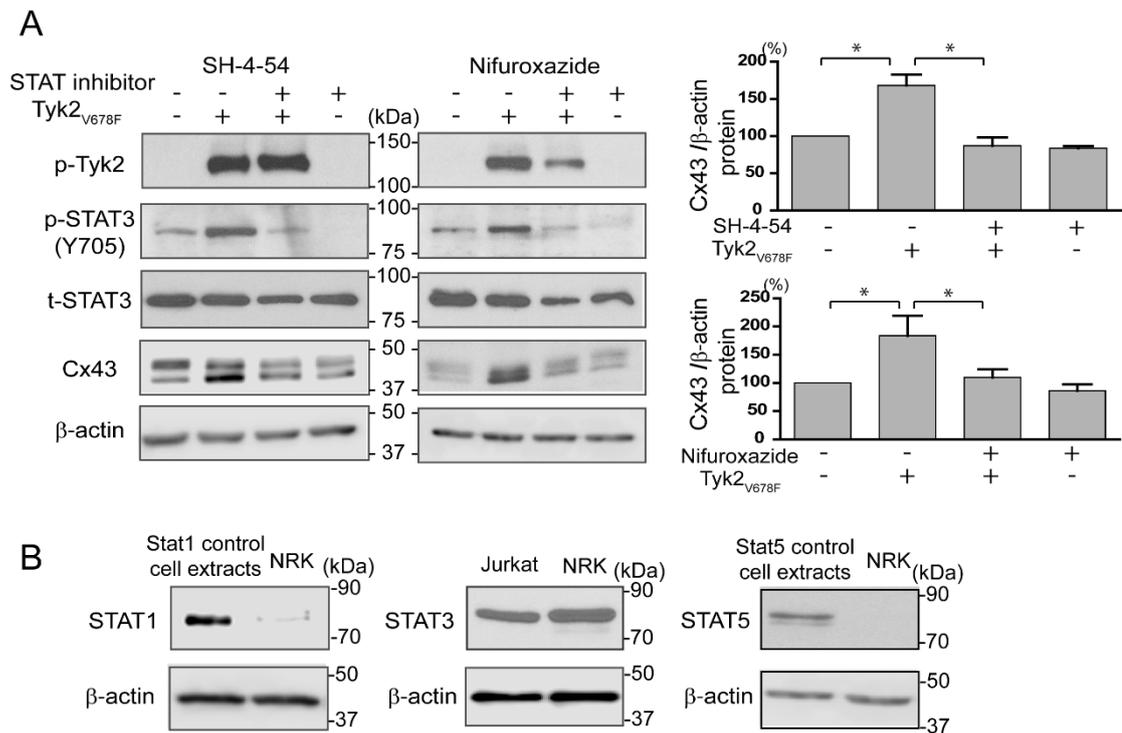
Figure 3.10 Effect of STAT3 activation by Tyk2 on Cx43 protein level. (A) Western

blot of active Tyk2 (p-Tyk2), active STAT3 (p-STAT3), total STAT3, and Cx43 in NRK

cells transfected with or without active Tyk2 (Tyk2$_{V678F}$) and treated with and without

SH-4-54 or Nifuroxazide. Cx43 protein level was quantified using ImageJ software

(*P<0.05, **P<0.01). (B) Western blot of STAT1, STAT3, and STAT5 from NRK cell

lysate. Cell extracts from HeLa cells treated with IFN-α (100ng/ml) for 5 min (9173,

Cell Signalling) were used as positive control for blotting STAT1 and STAT5. Jurkat

cell lysate was used as positive control for blotting STAT3.

the data strongly indicates Tyk2 activation of STAT3 is responsible for the increased

Cx43 mRNA and subsequent protein levels.

12.6 Tyk2 Mediates Ang II Regulation of Cx43

Dysregulation of the RAS affects many aspects of the cardiovascular system

(Delmar and Makita, 2012; Lonn et al., 1994; Pagliaro and Penna, 2005; Palatinus et

al., 2012). RAS activation also decreases Cx43 gap junction intercellular

communication and changes cellular localization (Emdad et al., 2001; Hussain et al.,

2010). Based upon the involvement of Tyk2 in RAS signaling via the Angiotensin II

receptor 1 (AT1R), we tested if the changes observed for Cx43 are caused by Tyk2.

Western blot analysis was used to investigate wild type (WT) Tyk2 transfected NRK

cells treated with Ang II (Figure 3.11). The transfection of WT Tyk2 alone caused a

basal level of activation, however the presence of Ang II significantly increased the

amount of active Tyk2. The presence of Tyk2 or Ang II alone caused a significant

increase in the level of Y247, Y265, S279/282 and S368 phosphorylation. While the

phosphorylation level of Y247, S279/S282, and S368 was the greatest in the presence

of both Tyk2 and Ang II, only S279/282 phosphorylation was statistically significant

compared to Tyk2 alone. Interestingly, while the presence of Tyk2 or Ang II alone

caused an increase in the level of total Cx43 that was further increased in the company

of both, the presence of Tyk2 but not Ang II caused an increase in the lower migrating

P0 and P1 isoforms of Cx43.
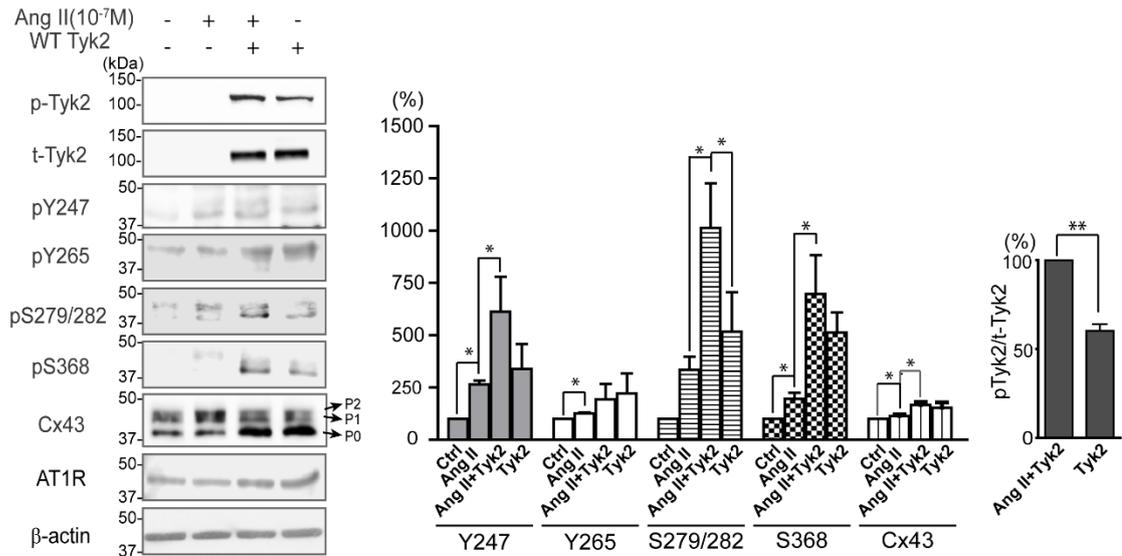
Figure 3.11 Effect of angiotensin II (Ang II) activation of Tyk2 on the phosphorylation level of Cx43. Western blot of active Tyk2 (p-Tyk2), total Tyk2, Cx43 pY265, pY247, pS279/282, pS368, total Cx43 and the Angiotensin II type 1 receptor (AT1R) from NRK cells with or without transfected wild-type (WT) Tyk2 and treated with or without Ang II (10^{-7} M). Protein phosphorylation level were quantified using ImageJ software (*P<0.05).
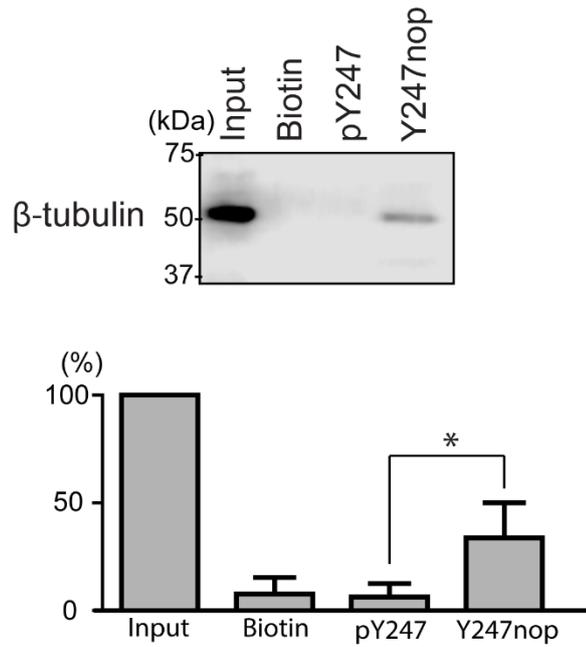
Figure 3.12 Effect of Cx43 Y247 phosphorylation on the interaction with β-tubulin.

Western blot of β-tubulin from a biotin pull-down assay using a biotinylated-phospho-peptide Cx43CT$_{234\text{-}255}$ (pY247) or non-phospho-peptide (Y247nop) bound to streptavidin beads and incubated with NRK cell lysate. Biotin bound to streptavidin agarose beads was used as negative control. Protein level were quantified using ImageJ and normalized by input (1:20 loaded compared to pull-down groups) from three independent experiments.

12.7 Phosphorylation of Cx43 residue Y247 Prevents the Binding of Tubulin

Previous studies have identified that Cx43 phosphorylation can inhibit the interaction with the ZO-1 PDZ-2 domain (pS373; (Chen et al., 2008)) or enhance the interaction with the Nedd4 WW2 domain (pS279/282; (Spagnol et al., 2016)). Additionally, a Cx43 phospho-peptide (pY247) was not able to interact with purified tubulin *in vitro* (Saidi Brikci-Nigassa et al., 2012). Since pY247 level was significantly increased by Tyk2 in cells (Figures 3.4 and 3.11), a biotin-tagged Cx43 pY247 phosphorylated peptide or non-phosphorylated (K234-S255) version was used in a pull down assay to assess the interaction with β-tubulin in NRK cell lysate (Figure 3.12). The data indicate that Tyk2 phosphorylation of Y247 would inhibit the interaction with β-tubulin.

13. Discussion

Up until now, Src has been the only non-receptor tyrosine kinase to directly phosphorylate Cx43 leading to an inhibition of gap junctional intercellular communication and subsequent gap junction disassembly (Lin et al., 2001; Swenson et al., 1990). In this study, we identified another tyrosine kinase, Tyk2, which can directly phosphorylate Cx43 on residues Y247 and Y265, and lead to indirect phosphorylation on residues S368 and S279/282. While this phosphorylation pattern is similar to what has been observed after Src activation (Solan and Lampe, 2008), importantly, the response caused by Tyk2 (e.g. overexpression of the constitutively active version) occurred when c-Src was inactive in NRK cells. This indicates that different signaling

pathways can lead to the same cellular response to regulate Cx43 gap junctions. Unexpectedly, when v-Src was activated in the LA-25 cells at the permissive temperature, Tyk2 was activated as well. This observation is not unique to the LA-25 cells as constitutive activation of Tyk-2 was observed in a human gallbladder adenocarcinoma cell line transfected with v-Src (Murakami et al., 1998). A significant decrease in the phosphorylation of Cx43 residues Y247, Y265, S279/282, and especially S368 (75% decrease) was observed in the LA-25 cells at the permissive temperature when the expression of Tyk2 was knocked down. The data suggest that although activation of Tyk2 and v-Src lead to phosphorylation of the same Cx43CT residues they are not identical in level at each site. Additionally, the data would suggest that activation of both Tyk2 and v-Src would work together to amplify the phosphorylation response on Cx43. Differences in the level of phosphorylation between Tyk2 and Src can be explained from the knowledge that the Tyk2 SH2 domain does not need a phosphate to interact with its substrate, combined with the absence of the SH3 domain (Smyth et al., 2010).

A consistent observation from the immunofluorescence experiments was that prolonged activation of Tyk2 led to a near complete removal of Cx43 from the plasma membrane. Brikci-Nigassa et al. (Saidi Brikci-Nigassa et al., 2012) showed that a Cx43CT phosphopeptide (pY247) does not interact with purified tubulin. We used a biotinylated Cx43CT control (K234-S255) and phosphopeptide (pY247) in a pull down assay using NRK cell lysate to show that phosphorylation inhibits the Cx43CT/β-tubulin interaction. Increased levels of pY247 by Tyk2 (or Src) would block the Cx43

interaction with tubulin (Saidi Brikci-Nigassa et al., 2012). At the gap junction plaque, this may be a mechanism in the disassembly process; at the trans-Golgi network, this may re-route trafficking to the plasma membrane (e.g., lateral membrane vs. intercalated disc) or inhibit trafficking to the plasma membrane, leading to increased intracellular proteasomal and/or lysosomal degradation (Alberts et al., 2002). Other mechanisms that would contribute to the lack of Cx43 at the plasma membrane include phosphorylation of residues S279/282 (MAPK) and S368 (PKC). Phosphorylation of S279/282 increases the binding affinity by two-fold for the WW2 domain from the ubiquitin ligase Nedd4 leading to Cx43 gap junction degradation (Girao et al., 2009; Leykauf et al., 2006; Spagnol et al., 2016). Activation of PKC can halt the assembly of new gap junctions and phosphorylation on S368 has been implicated in affecting gating and/or disassembly (Lampe, 1994; Lampe et al., 2000; Saez et al., 1997). Of note, although not investigated in this study, Src activation also leads to phosphorylation of Cx43 on S373 by Akt (Park et al., 2007). The importance of phosphorylation on this site is that the interaction with ZO-1 is inhibited, transitioning Cx43 from the non-junctional plasma membrane into the gap junction plaque, and then through the degradation pathway(s).

One difference observed in our (and others) studies performed *in vitro* as compared to *in vivo* is the effect of Ang II on Cx43 protein level. We identified that activation of Tyk2 by Ang II *in vitro* causes an increase in Cx43 protein level via the STAT3 pathway. Other *in vitro* examples of an increase in Cx43 protein level include exposing freshly isolated aortas of wild-type mice to Ang II for 4 hrs and the aorta smooth muscle cell

line A7r5 to Ang II from 2 hrs to 48 hrs (maximum expression was observed at 4 hrs and was maintained to the last time point of 48 hrs) (Alonso et al., 2010; Stein et al., 2009). Conversely, chronic exposure of Ang II in animal models shows a decrease in the protein level of Cx43. This was seen in the atria and ventricles of the transgenic mouse model of cardiac-restricted overexpression of ACE (ACE8/8) described above (Kasi et al., 2007) and in the double transgenic rat which harbors the human renin and angiotensinogen genes (dTGR) (Fischer et al., 2007). While the length of Ang II exposure (acute vs. chronic) and experimental conditions (*in vitro* and *in vivo*) are important factors when interpreting the protein level of Cx43, the combined data can be explained from the study of Kostin et al. (Kostin et al., 2004). Cx43 expression was increased in the compensated hypertrophic stage from the left ventricles of pressure-overloaded human hearts with valvular aortic stenosis, but decreased and heterogeneously distributed throughout the ventricles in the decompensated stage.

We identified that the effect Tyk2 elicited on the Cx43 protein level in NRK cells was mediated through activation of STAT3. However, this increase did not correlate with increased gap junction intercellular communication as Cx43 was not localized to the plasma membrane. Evidence that STAT3 directly increases the transcriptional activity of Cx43 was provided by Ozog et al. (Ozog et al., 2004). Three putative ciliary neurotrophic factor-response elements (binding sites for STAT3 dimers that contain base sequences TTCCN3-5AA) were identified in the promoter region of the mouse Cx43 gene (located at regions -1510, -1179, and -893) as essential for enhanced Cx43 expression. Interestingly, STAT3 activation also leads to down-regulation of E-cadherin

(Xiong et al., 2012). One mechanism for the decreased gap junction assembly may be explained by the observation that expression of E-cadherin is necessary to enable the assembly of Cx43 into gap junctions (Govindarajan et al., 2010).

CHAPTER 4

Additional Studies

In the following chapter, we will discuss additional studies that are still on going in the lab at various stages as extension from my main projects. The first section contains the identification of a kinase and a phosphatase that interact with Cx32. Tyrosine phosphorylation has been found to modify Cx32 by different groups (Diez et al., 1998; Locke et al., 2006; Stauch et al., 2012), Thus, understanding the regulatory mechanism of tyrosine phosphorylation of Cx32 is crucial. Using i*n vitro* kinase and immunoprecipitation assays, we identified direct phosphorylation on Cx32 by EphB1. We also showed evidence that TC-PTP directly dephosphorylates Cx32.

In the second section, we will discuss a novel phosphorylation site on Cx43CT, Y313. Although phosphorylated Y313 was detected in multiple phosphoproteomic data, for the first time, we identified that Y313 is phosphorylated by Src, Tyk2 and Pyk2 *in vitro*.

When we identified that Tyk2 kinase phosphorylates Cx43 by the *in vitro* kinase assay, we found that Pyk2 and Itk can also phosphorylate the Cx43CT. Cx43 gap junction remodeling has been found in heart failure where Pyk2 is activated (Ai et al., 2011; Glukhov et al., 2012); additionally, increase of Cx43 phosphorylation occurs at the immunological synapse which is coincident with the activation of Itk (Andreotti et al., 2010; Mendoza-Naranjo et al., 2011). These pieces of evidence implicate the potential interplay between Cx43 and Pyk2 or Itk. In the third section, I will show data regarding the phosphorylation of Cx43CT by Pyk2 and Itk. Future research will be conducted to characterize the biological function of phosphorylated Cx43 in particular situations.

14. EhpB1 and TC-PTP Regulate Tyrosine Phosphorylation of Cx32

14.1   Introduction

Cx32 is the major gap junction protein in liver (Gingalewski et al., 1996). Cx32 is also found in other tissues such as nervous tissue (myelinating cells), lung, placenta, and kidney (Grazul-Bilska et al., 2011; King and Lampe, 2004; Wilgenbus et al., 1992). Cx32 deficient mice have an increased chance of getting spontaneous liver tumors and are more vulnerable to chemical-induced liver tumorigenesis (King and Lampe, 2004; Temme et al., 1997). These mice exhibit other pathological phenotypes such as decrease of nerve-dependent bile secretion, enhanced pancreatic amylase secretion, and peripheral nerve demyelination (Chanson et al., 1998; Scherer et al., 1998; Temme et al., 2001).

Cx32 is phosphorylated on its tyrosine residues in cytoplasm domains (Diez et al., 1998; Locke et al., 2006; Stauch et al., 2012). So far, the only identified tyrosine kinase that directly phosphorylates Cx32 is EGFR (Diez et al., 1998). Cx32 has three tyrosine residues on its intracellular domains: one is on the NT domain (Y7) and two are on the CT domain (Y211 and Y243). Since Y211 is at the juxtamembrane region, we speculate that only Y7 and Y243 are accessible to tyrosine kinases. In Cx32 transfected HeLa cells, phosphorylated Y7 has been observed by MS (Locke et al., 2006). However, to date, no direct evidence of Y243 phosphorylation has been reported.

Using an *in vitro* kinase screening assay, we identified EphB1 as a novel tyrosine kinase that phosphorylates Cx32. EphB1 is a erythropoietin-producing hepatocellular

(Eph) receptor family member which has a wide expression in human organs including liver, colon, brain, kidney, and in the cardiovascular system (Adams et al., 1999; Davy et al., 2006; Ivanov et al., 2005; Kosinski et al., 2007; Zhou et al., 2014). Eph family is the largest known subfamily of receptor tyrosine kinases (Lisabeth et al., 2013). This family is divided into two groups, EphA and EphB, both of which need to interact with their ligands, the Eph family receptor interacting proteins (Ephrins), for activation. Ephrins are also divided into EphrinA and EphrinB groups due to structural and functional differences. Membrane-bound or Fc-clustered Ephrins are capable of activating Eph receptors. Eph-Ephrin complexes induce bidirectional signals that influence cells that express both Eph receptor and Ephrin (Lisabeth et al., 2013). Eph-ephrins signaling is important for proper cell sorting during development, cell-cell adhesion, migration, repair after nervous system injury, and maintenance of intercellular junctions (Pasquale, 2008; Poliakov et al., 2004). A recently study showed that the EphB4 receptor co-immunoprecipitated with Cx43 and its activation in primary cultures of rodent cardiomyocytes inhibited gap junctional intercellular communication (Ishii et al., 2011). Another study indicated that junctional Cx43 was decreased at ectopic Eph/ephrin boundaries in mice (Davy et al., 2006). These studies suggest a possibility of EphB interacting with gap junction proteins. However, whether Cx32 also interacts with an EphB member is not known.

In this study, we used multiple approaches and identified that EphB1 phosphorylates the Cx32CT but not the NT in HeLa cells expressing Cx32 and EphB1. We also tested TC-PTP, a tyrosine phosphatase that dephosphorylates Cx43, and

discovered that TC-PTP directly dephosphorylates the Cx32CT *in vitro* and in HeLa cells.

14.2 Results

14.2.1 EphB1 Directly Interacts and Phosphorylates the Cx32CT Domain

Softwares GPS 2.0, NetPhos 2.0 Server, and KinasePhos 2.0 were used to predict novel kinases that phosphorylate Cx32. Five tyrosine kinases were selected for an *in vitro* tyrosine phosphorylation screening assay performed by Eurofins Scientific (KinaseProfiler) using the Cx32NT (1-21) or the Cx32CT (217-283) as substrates (Figure 4.1A). Only the Cx32CT phosphorylated by EphB1 gave over 50% of control signal. None of kinases efficiently phosphorylated the Cx32NT. Then, we repeated the kinase assay using EphB1, Ron, and EGFR in our laboratory. Consistant with data from Eurofins Scientific, EphB1 and Ron phosphorylated the Cx32CT but not EGFR (Figure 4.1B). Of note, EGFR was reported to phosphorylate immunoprecipitated Cx32 *in vitro* (Diez et al., 1998). To confirm the Cx32 interaction with EphB1 and Ron kinases, the purified GST, GST-tagged Cx32NT or CT were immobilized on glutathione-Sepharose beads and lysates from HeLa cells that express EphB1 and Ron (but not Cx32) were used in a pull-down assay (Figure 4.2A). EphB1 was pulled down by GST-Cx32CT but not GST nor GST-Cx32NT in cells, whereas Ron could not be pulled down by any of the three GST-tagged purified proteins. The crosslinker DTSSP (3,3′-dithiobis[sulfosuccinimidylpropionate]) was used to capture weak and/or transient interactions (Liu et al., 2011). Co-immunoprecipitate also showed EphB1 and Cx32

were in the same complex in cells (Figure 4.2B). Ron could phosphorylate the Cx32CT

domain but was not pulled down by Cx32CT or NT, indicating the interaction between

Cx32 and Ron may be too weak to be detected in cells. Thus, Ron was excluded from

the following studies.

14.2.2 TC-PTP Interacts with and Dephosphorylates Cx32CT

Our previous study showed that TC-PTP directly interacts and dephosphorylates

Cx43CT (Li et al., 2014). Whether TC-PTP can dephosphorylate other connexin

isoforms is unknown. To identify if a direct interaction exists between TC-PTP and the

Cx32CT domain, NMR titration experiments were performed with purified TC-PTP

catalytic domain (TC-PTP$_{1-314}$) and Cx32CT. Different concentrations of unlabeled TC-

PTP$_{1-314}$ were titrated into ^{15}N-labeled Cx32CT (residues 217-283) and ^{15}N-HSQC

spectra were acquired (Figure 4.3A). Titration of TC-PTP$_{1-314}$ caused a subset of

Cx32CT residues to broaden beyond detection. These are highlighted on the Cx32CT

sequence (Figure 4.3C). Strongly affected Cx32CT residues S240-G272 include Y243,

which is the only accessible tyrosine residue in CT domain. The decrease in signal

intensity caused by increasing TC-PTP$_{1-314}$ concentrations was fit according to the

nonlinear least square method. The binding affinity (K_D) was determined to be 19.9 ±

4.5µM (Figure 4.3B). A GST pull down experiment was performed to validate the NMR

results. Purified GST alone, GST-Cx32CT, or GST-Cx32NT bound to glutathione

agarose were incubated with purified TC-PTP$_{1-314}$. Immunoblotting using an anti-TC-

PTP NT antibody identified that GST-Cx32CT, but not NT, directly interacted with the
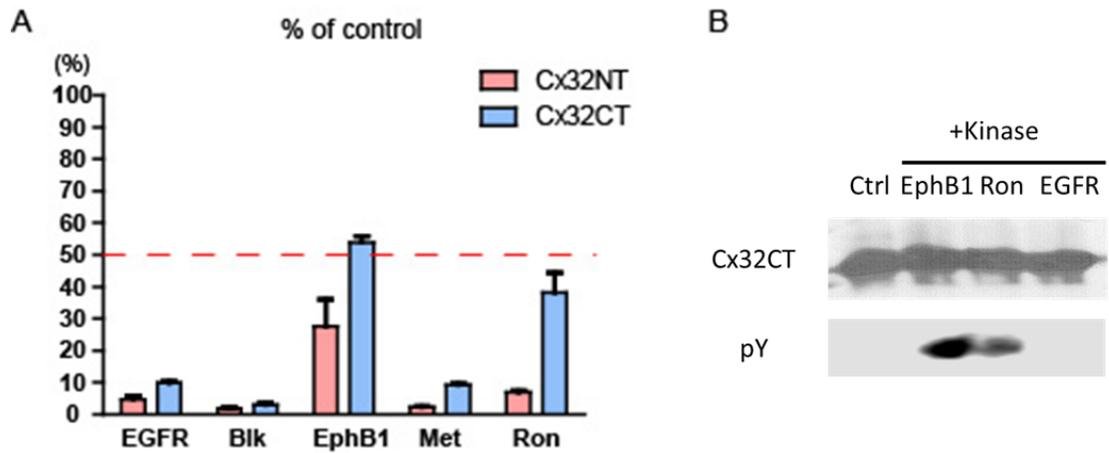
Figure 4.1 EphB1 and Ron phosphorylate the Cx32CT domain *in vitro*. (A) Cx32NT and Cx32CT were used as substrates to be phosphorylated by EGFR, Blk, EphB1, Met, and Ron kinases. The amount of Cx32CT phosphorylation was compared with a positive control peptide for each kinase (% of control signal). Dash line highlights the 50% of the control signal. (B) *in vitro* kinase assay was performed to repeat the kinase screening assay done by Eurofin Scientific (EphB1, Ron, and EGFR). A general anti-phospho-tyrosine antibody was used to detect the phosphorylation level on Cx32CT by Western blot. Control group used buffer to substitute the kinases in the reactions.
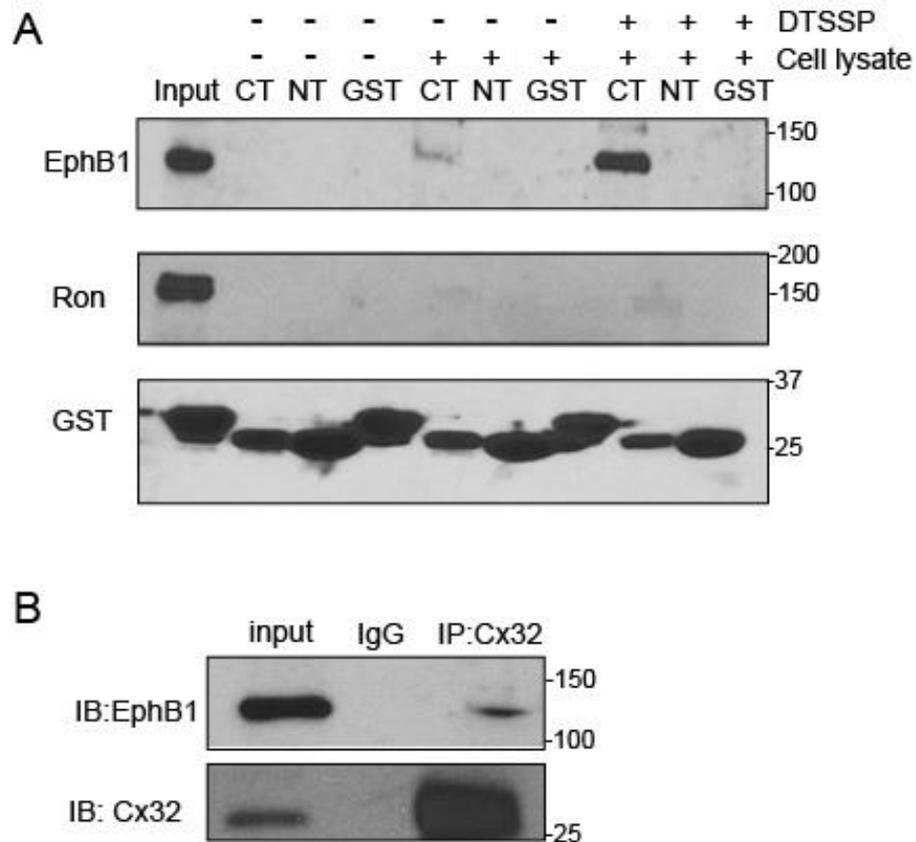
Figure 4.2 Cx32 interacts with EphB1. (A) Purified GST alone, GST-Cx32CT (CT), or GST-Cx32NT (NT) bound on glutathione-agarose beads were incubated with or without HeLa cell lysate and the pull-downed product was analyzed by Western blot using an anti-EphB1 or anti-Ron antibodies. The chemical crosslinker DTSSP was used to capture the weak and/or transient interaction. (B) Co-IP experiment was performed in HeLa cells stably expressing Cx32. Lysates were immunoprecipitated with anti-Cx32 or IgG and then blotted for Cx32 and EphB1.

TC-PTP catalytic domain (Figure. 4.4A, B). GST-Cx32CT also pulled down wild-type TC-PTP from HeLa cell lysate (Figure. 4.4C).

To identify if TC-PTP dephosphorylates the Cx32 on residue Y243, an *in vitro* phosphatase assay was conducted using a peptide (H237-N249) containing pY243 incubated with TC-PTP$_{1-314}$. Following the protocol for the Malachite green assay (Millipore), we observed an increase in the amount of inorganic phosphate production indicating TC-PTP dephosphorylated Cx43 on pY243 (Figure. 4.5). The rate of dephosphorylation shows TC-PTP is efficient in dephosphorylating pY243 (table 4.1).

14.3 EphB1 Phosphorylates and TC-PTP De-phosphorylates Cx32 in HeLa Cells

We show that EphB1 phosphorylates Cx32 and TC-PTP dephosphorylates Cx32 *in vitro*. To determine if EphB1 and TC-PTP affect pY243 level in cells, HeLa cells stably expressing Cx32 wild-type were transfected with EphB1 or the TC-PTP catalytic domain, and tyrosine phosphorylation level were detected on immunoprecipitated Cx32. Results show that EphB1 increased Cx32 tyrosine phosphorylation and TC-PTP$_{1-314}$ decreased tyrosine phosphorylation. Cx32 Y7 on the Cx32 NT has been reported to be phosphorylated (Locke et al., 2006). To study if EphB1 phosphorylate Y7 as well, we immunoprecipitated Cx32 from HeLa cells stably expressing Cx32 wild-type or Cx32 Y243F with or without EphB1 transfection, and Cx32 tyrosine phosphorylation level was measured. EphB1 increased Cx32 wild-type phosphorylation, and using EphB2-Fc to activate EphB1 further increased Cx32 phosphorylation. However, this effect was not observed in the Cx32 Y243F mutant, suggesting EphB1 only phosphorylates

A

^{15}N-Cx32CT / TC-PTP

Black, 1:0
Green, 1:0.1
Purple, 1:0.2
Blue, 1:0.5
Red, 1:1

G linker

S linker

S229

S225

H237

Q222

N226   C217

R223   L239   R220

R230   R224, K231

A221

A218

^{15}N (ppm)

^{1}H (ppm)

B

K_D **Determination**

K_D = 19.9 +/- 4.5 μM

Peak Volume

[TC-PTP] (uM)

● S229
▲ S253
◆ E247
○ K250
□ L263

C

217

243

GPLGSCARRAQRRSNPPSRKGSGFGHRLSPEYKQN

EINKLLSEQDGSLKDILRRSPGTGAGLAEKSDRCSAC   283

141
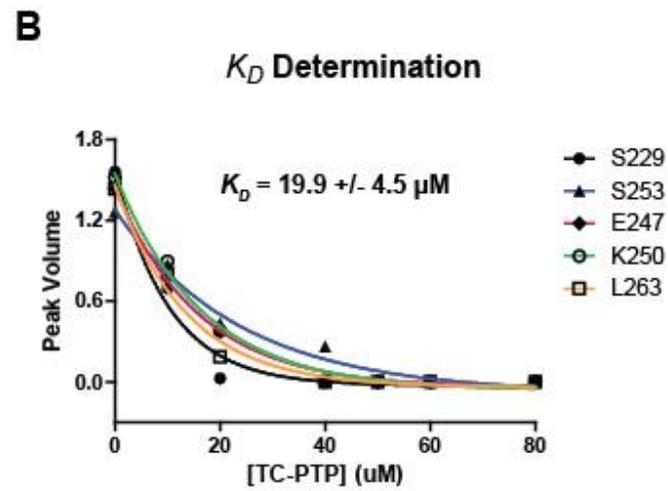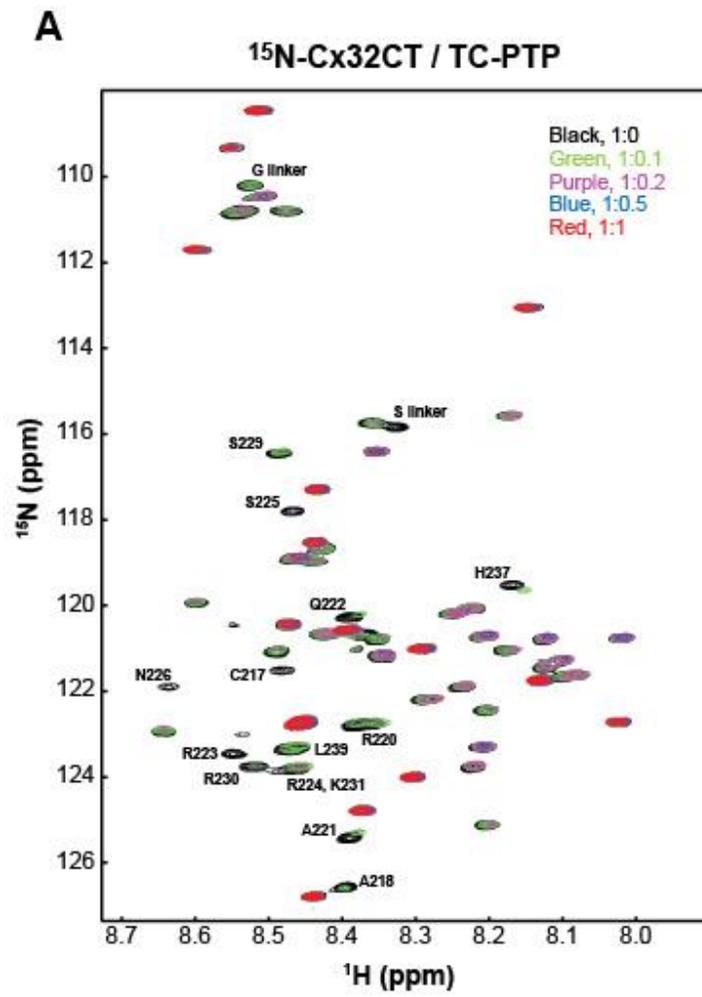
Figure 4.3 Cx32CT residues affected by the direct interaction with TC-PTP. A) Overlaid ^{15}N-HSQC spectra of the ^{15}N-Cx32CT (residues 217-283; 30 µM) in the presence of different concentrations of unlabeled TC-PTP$_{1-314}$. The cross-peak color changes according to the concentration ratio. The strongly affected peaks are labeled. B) The K_D for the Cx32CT/TC-PTP$_{1-314}$ interaction was estimated by fitting the decrease in signal intensity for the Cx32CT residues S229, S253, E247, K250, L263 as a function of TC-PTP$_{1-314}$ concentration. C) Amino acid sequence of Cx32CT. Residues strongly affected by the addition of TC-PTP$_{1-314}$ are highlighted in yellow (residues broadened beyond detection at 1:0.1 molar ratio) and those less affected in green (residues broadened beyond detection at 1:1 molar ratio). In red is the Cx32 residues Y243.
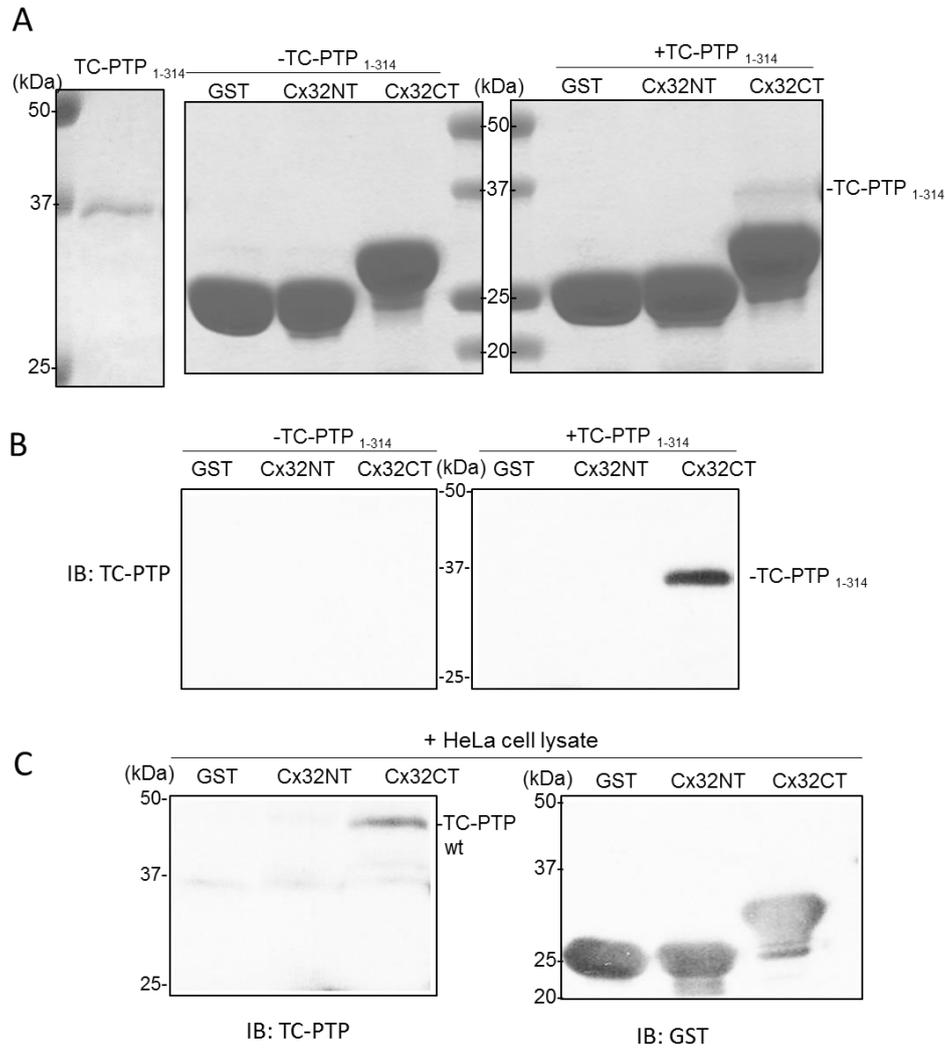
Figure 4.4 Cx32CT pulls down purified TC-PTP wild-type and catalytic domain.

(A) Purified GST or GST-Cx32CT or GST-Cx32NT on glutathione agarose beads were incubated with (+) and without (-) purified TC-PTP$_{217-283}$. After washes, samples were ran on SDS-PAGE gel and stained with Coomassie Blue. (B) GST pull-down samples were blotted with the anti-TC-PTP NT antibody. The TC-PTP catalytic domain is 36 kDa. (C) Purified GST, GST-Cx32CT, or GST-Cx32NT bound on glutathione agarose beads were incubated with HeLa cell lysate containing endogenous TC-PTP. Pull-downed products were analyzed by Western blot using an anti-TC-PTP NT or anti-GST antibodies.
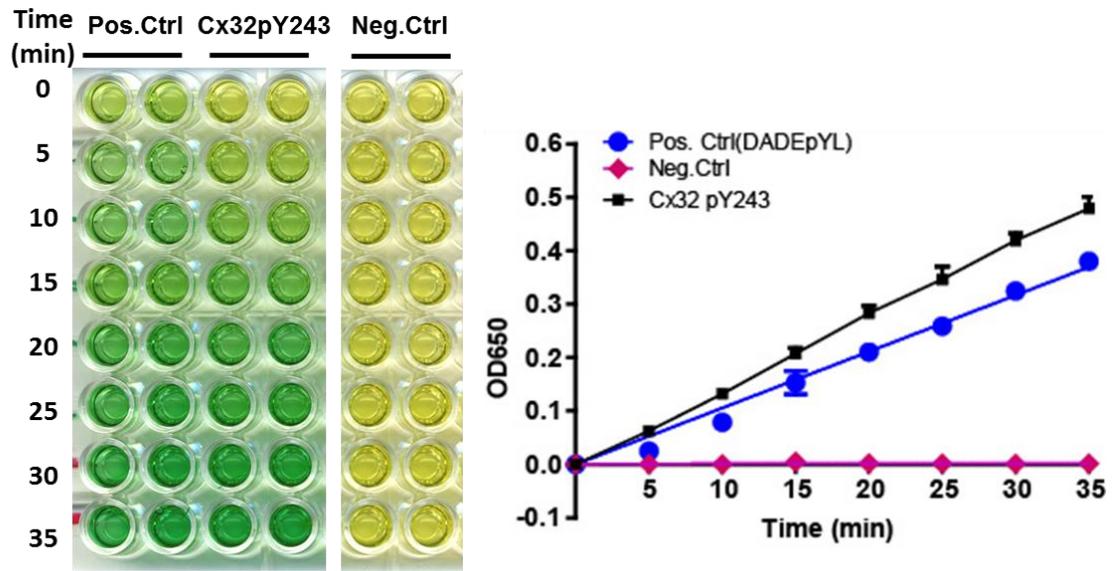
Figure 4.5 TC-PTP dephosphorylates Cx32 residues pY243 *in vitro*. Plot of the Malachite green assay shows the time course of Cx32 phospho-peptides (600 nM) containing pY243 dephosphorylated by the TC-PTP catalytic domain (0.6 nM). Statistic data were recorded based on readings at OD_{650}. Each experiment was repeated three times.

Table 4.1. Kinetic constants for de-phosphorylation of Cx32 pY243 by TC-PTP$_{1-314}$

	K_m	k_{cat}	$k_{cat}/K_m \cdot 10^{-6}$
	(mM)	*(s^{-1})*	*($M^{-1}s^{-1}$)*
Positive control*#	0.022±0.001	52.820±10.622	2.418±0.473
pY243*	0.034±0.004	63.337±13.720	1.833±0.164

*All data were collected at pH 7.5, 25°C

#Notably, the kinetic constants determined for the positive control (DADEpYL) by TC-PTP$_{1-314}$ are consistent with a previous report of the same peptide with the PTP1B catalytic domain, whose sequence is very similar with TC-PTP$_{1-314}$ (Peters et al., 2000).
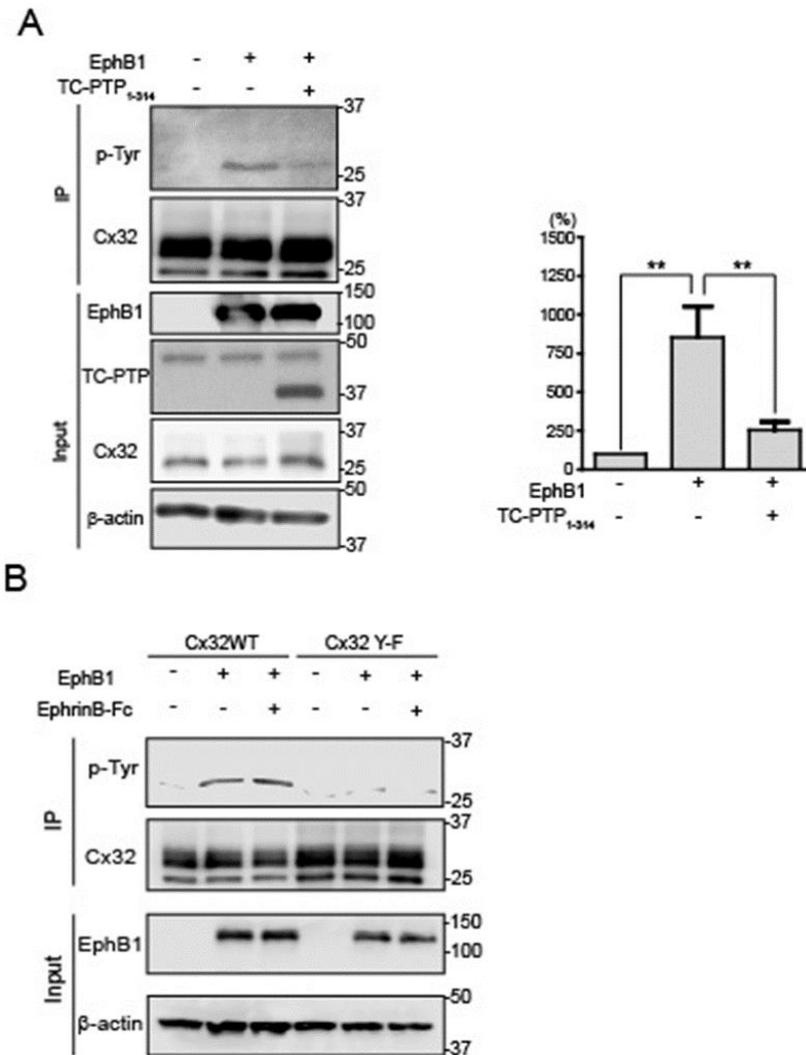
Figure 4.6 EphB1 increases tyrosine phosphorylation level on Cx32 whereas TC-PTP decreases tyrosine phosphorylation on Cx32. (A) HeLa cells stably expressing Cx32 were transfected with EphB1 or TC-PTP catalytic domain. Cx32 was pulled down and phospho-tyrosine antibody was used to detect tyrosine phosphorylation level. Tyrosine phosphorylation level were quantified by densitometry from three independent experiments (**$P<0.01$). (B) HeLa cells stably expressing Cx32 wild-type and Cx32 Y-F mutant were transfected with EphB1. EphrinB1-Fc was used to activate EphB1 receptor. Cx32 was pulled down and tyrosine phosphorylation level was detected.

Cx32CT on Y243 residue.

14.4 Discussion and Future Direction

In this study, we identified a tyrosine kinase EphB1, which phosphorylates Cx32 on the Y243 residue in the CT domain but not Y7 on NT domain. Addtionally, we showed that TC-PTP, a tyrosine phosphatase, can dephosphorylate pY243. To the best of our knowledge, our work is the first demonstration of the direct interaction between a phosphatase and Cx32.

The first reported tyrosine kinase that phosphorylates immunoprecipitated Cx32 is EGFR (Diez et al., 1998). However, in our *in vitro* kinase assay, EGFR did not directly phosphorylate purified Cx32CT. A possible explanation is that a complex, but not pure Cx32, could be pulled down in the immunoprecipitation assay. Thus, unknown Cx32 binding partner(s) in the complex may mediate the phosphorylation on Cx32 by EGFR. We also found that Cx32 co-immunoprecipitated with EGFR which indicated that Cx32 and EGFR were in the same complex (data not shown). Thus, we suspect that EGFR may indirectly increase tyrosine phosphorylation of Cx32.

Cx32 is considered as a tumor suppressor in many different cancers (Fujimoto et al., 2005; King and Lampe, 2004; Temme et al., 1997). Cx32-deficient mice exhibit a higher incidence compare with wild-type mice in lung tumor and liver cancer (King and Lampe, 2004; Temme et al., 1997). Expression of Cx32 in renal cell carcinoma cell line (Caki-1 cell) reduces invasion capacity (Fujimoto et al., 2005). Besides, Cx32 can suppress human prostate cancer cell growth (Mehta et al., 1999). EphBs also play roles

as cancer suppressors. During metastatic progression, EphB expression is lost which leads to tight junction instability and allows cancer cells to become invasive (Park and Lee, 2015). Evidence shows that loss of EphB1 is associated with invasion and metastasis in gastric cancer and ovarian cancer (Wang et al., 2014; Wang et al., 2007); decreased expression of EphB1 has also been found in renal cell carcinoma patients (Zhou et al., 2014). Additionally, the tight junction protein E-cadherin interacts with both EphB and Cx32 (Lee and Daar, 2009). Activation of EphB enhances E-cadherin-dependent adhesion in colorectal cancer cell lines (Lee and Daar, 2009). Also, positive correlation between the expression of E-cadherin and Cx32 has been found in colorectal cancers (Kanczuga-Koda et al., 2014), and colocalization of Cx32 and E-cadherin has been found in Schwann cells (Balice-Gordon et al., 1998). These pieces of evidence indicate a link between EphB and Cx32. Our data identify the direct interaction between Cx32 and EphB1, which could help to understand the mechanism of Cx32 gap junction decrease in cancer.

One question that has not been answered in this study is the biological effects of phosphorylation on Cx32CT. The only well-defined phosphorylation site on Cx32 is S233 which increases gap junctional communication when phosphorylated (Saez et al., 1990). Based on the fact that both EphB1 and Cx32 decrease in cancer, we hypothesize that phosphorylation on Y243 also increases gap junction intercellular communication. To further study the function of Y243, Y243F mutant and wild-type Cx32 stably expressed in HeLa cells will be transfected with or without EphB1. Dye transfer, TX100 solubility, and cycloheximide assays will be used to test the gap junction coupling,

measure gap junction plaque, and study the gap junction turnover rate, respectively.

15. Identification and Functional Study of a Novel Phosphorylation Site on Cx43CT

15.1 Introduction

We identified four tyrosine residues phosphorylated by Tyk2 (Y247, Y265, Y267, Y313) by MS. Y313, which is located in one helix (K303-A322) in the Cx43CT (predicted by our laboratory, (Grosely et al., 2013)), triggered our greatest interest. First, tyrosine phosphorylation associates with decrease of helical propensity in the Cx43CT (Grosely et al., 2013b). Therefore, Y313 phosphorylation may affect the secondary structure of Cx43. Moreover, MS data obtained from the PhosphoSitePlus database shows that Y313 is frequently detected as a phosphorylation site (Table 4.2). Of note, Src phosphorylation sites Y247 and Y265 are also detected to be phosphorylated in high frequency. Interestingly, when we studied Src in the *in vitro* kinase assay, we found that Y313 was also phosphorylated by Src in addition to Y247 and Y265. Our hypothesis is that Y313 phosphorylation induces a structure change in the Cx43CT and participates in Cx43 degradation.

15.2 Results

Purified Cx43CT$_{236-382}$ was incubated *in vitro* with active Src (Life Technologies) as described in (Cooper et al., 2000; Huang et al., 2012) and phosphorylation was confirmed using an anti-phospho-tyrosine antibody (Figure 4.7B). After trypsin

digestion, Tandem MS/MS identified phosphorylation at Y247, Y265, Y267, and Y313 (Figure 4.7A and Table 4.3). To confirm tyrosine phosphorylation occurs at residues other than Y247 and Y265, the *in vitro* kinase assay was performed using five Cx43CT$_{236-382}$ mutants and phosphorylation was detected with an anti-phospho-tyrosine antibody (Figure 4.7B). The data indicate that Src phosphorylated Cx43 wild-type, which showed a slower migration on SDS-PAGE gel (Figure 4.7B). Y267 and Y313 can be phosphorylated by Src *in vitro*. The Cx43CT mutant with all tyrosine residues except Y313 mutated to F also showed a slower migration on the SDS-PAGE gel suggesting a possible alteration of structure.

15.3 Discussion and Future Direction

Y247 and Y265 are well established as phosphorylation sites for Src (for review see (Lampe and Lau, 2004; Solan and Lampe, 2007)). Interestingly, for the first time, we found that Src can also phosphorylate the Y313 site *in vitro*. Since Y313 is contained within one of the CT α-helical domains, the negatively charged phosphate could induce a conformational change of the Cx43CT and further affect the function of Cx43 gap junctions. In fact, phosphorylated Y313 has been observed in proteomics data multiple times which strongly suggests its existent in cells. However, no study has identified a kinase that directly phosphorylates Y313.

We hypothesize that Y313 phosphorylation by Src induces gap junction closure and Cx43 degradation. We recently acquired a custom phospho-specific antibody to pY313. This antibody will be used to test if Y313 is phosphorylated in cells after v-Src

Table 4.2 Tyrosine phosphorylation sites on the Cx43CT domain summarized by PhosphoSitePlus.

Modification site	SS	MS	Species
Y247-p	9	253	H, M, R
Y265-p	14	12	H, M, R
Y267-p	1	10	H, M, R
Y286-p	1	12	H, M
Y301-p	0	8	H
Y313-p	1	312	H, M, R

SS: the number of record in which this modification site was determined using site-specific methods, including amino acid sequencing, site direct mutagenesis, modification site specific antibodies, etc. MS: The number of record in which this modification site was assigned using ONLY proteomic discovery mode. Species: H: human, M: mouse, R: rat

A

^{236}VKDRVKGRSDP**pY^{247}**HATTGPLSPSKDCGSPK**p Y^{265}**A**pY^{267}**FNGCSSPTAPLSPMSPPG**Y^{286}**KLVTGD RNNSSCRN**Y^{301}**NKQASEQNWAN**pY^{313}**SAEQNRMGQ AGSTISNSHAQPFDFPDDNQNAKKVAAGHELQPLA IVDQRPSSRASSRASSRPRPDDLEI^{382}

B
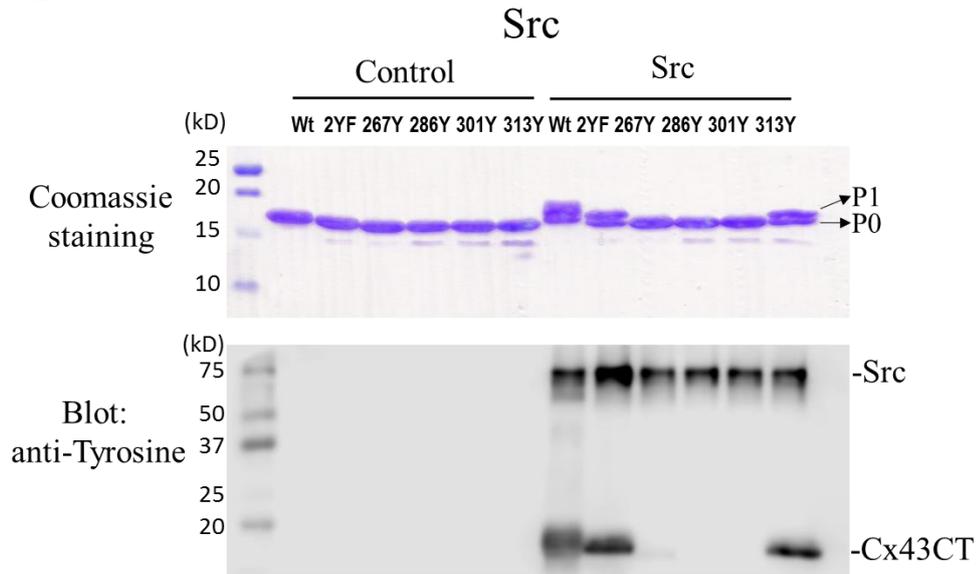
Figure 4.7 *In vitro* kinase assay using active Src to phosphorylate Cx43CT wild-type and mutants. Purified Cx43CT wild-type and mutants were incubated with or without (Control) Src for 16 hrs at 30°C. 2YF=Y247/265F, 267Y=Y247/265/286/301/313F, 286Y=Y247/265/267/301/313F, 301Y=Y247/265/267/286/313F, 313Y=Y247/265/267/286/301F (A) Sequence of the Cx43CT domain. Highlighted in red are phospho-tyrosine residues identified by MS in an *in vitro* kinase assay using Src to phosphorylate the Cx43CT. show The two tyrosines which are not phosphorylated by Src are highlighted in blue. (B) Products from kinase assay were ran on SDS-PAGE gel, stained with Coomassie blue and Western blotted with anti-tyrosine antibody.

Table 4.3 Phospho-tyrosine containing peptides identified from mass spectrometry of the Cx43CT domain phosphorylated *in vitro* by Src.

Peptide sequence	Start-end	Average Mascot Delta Ion Score	*Number of phospho-peptides	Actual peptide mass	Calculated +1H peptide mass	Phosphorylation site localization
SDPyHATTGPLSPSK	244-258	17.1	9	1636.72	1,637.72	Y247
GRSDPyHATTGPLSPSK	242-258	16.9	5	1849.84	1850.84	Y247
GRSDPyHATTGPLSPSKDc(Carbamidomethyl)GSPK	242-264	17	1	2667.04	2668.05	Y247
QASEQNWANySAEQNR	304-319	14.1	11	1974.79	1975.79	Y313
yAYFNGc(Carbamidomethyl)SSPTAPLSPm(Oxidation)SPPGYK	265-287	9.8	13	2588.07	2588.09	Y265
yAyFNGc(Carbamidomethyl)SSPTAPLSPm(Oxidation)SPPGYK	265-287	26.9	10	2667.05	2668.05	Y265, Y267

*Peptides with Mascot Delta Ion Score >7 were used to obtain the average Mascot Delta Ion according to (Savitski et al., 2011).

activation. Seven Cx43 mutants (Y247F, Y265F, Y313F, Y247/313F, Y256/313F, Y247/265F, Y247/265/313F) have been successfully cloned in pcDNA3.1 and pEGFP vectors. With these constructs, we will test the cellular localization of Cx43 wild-type and mutants after Src activation in HeLa cells (gap junction negative cell line) and Cx43 knock-out NRK cells. Also, the localization of Cx43 phosphorylated at Y313 will be observed by immunofluorescence assay using the pY313 phospho-antibody. Gap junction closure and Cx43 degradation will be studied by dye transfer assay and surface biotinylation assay, respectively.

Additionally, we briefly studied the Y267 phosphorylation site, however, our results are inconsistent with previous study. Giepmans et al. (2001) used COS-7 cells co-transfected with Myc-tagged Cx43 (wild-type, Y265F, and Y267F) and c-Src, and they showed that wild-type Cx43 and Y267F mutants were phosphorylated on tyrosine but not Y265F mutant (Giepmans et al., 2001). They concluded that Y267 is not a phosphorylation site for Src (Giepmans et al., 2001). However, our MS study shows that Y267 was phosphorylated by Src *in vitro*. To test if Y267 is phosphorylated *in cyto*, a phospho-specific antibody will be necessary.

16. Characterize the Mechanism and Biological Function of the other Tyrosine Kinases that Phosphorylate Cx43.

16.1 Introduction

One goal of my dissertation is to identify novel tyrosine kinases that phosphorylate

Cx43. By using the *in vitro* phosphorylation screen (Merck Millipore), we identified eight

tyrosine kinases which have high likelihood of phosphorylating Cx43. Among these

tyrosine kinases, Pyk2 and Itk showed the best affinity for the Cx43CT domain in a GST

pull down assay, and will be the focus of this study.

Pyk2 is a Ca^{2+}-dependent non-receptor tyrosine kinase of the FAK family (Figure 4.8).

Many factors can induce Pyk2 activation, including activation of Src and PKC, as well as

an increase in intracellular Ca^{2+} level (Avraham et al., 2000). In normal adult heart, Pyk2

is expressed in ventricular tissue and cardiomyocytes, but much less than in neonatal

(Bayer et al., 2001). In animal models of heart failure (pressure-overload-induced or

overexpression of tropomodulin), an increase in Pyk2 expression, activation, and

phosphorylation has been reported (Bayer et al., 2002; Melendez et al., 2002). Since

changes in the level and pattern of Cx43 phosphorylation are commonly observed in both

ischemic and nonischemic forms of human heart failure (Ai et al., 2011; Glukhov et al.,

2012), our hypothesis is that in the failing heart, phosphorylation of Cx43 by Pyk2 leads to

gap junction channel closure and relocation of Cx43 from the intercalated disc.

Itk is a Tec kinase family member which is predominantly expressed in T-cell. The

most important function that Itk is involved in is the antigen-dependent T cell activation.

Interaction of the T-cell receptor with peptide-MHC complexes on antigen presenting cells

promotes Itk recruitment to the membrane and its activation, leading to the phosphorylation

of its downstream targets (Andreotti et al., 2010). Similar with Src, Itk also contains an

SH3-SH2-kinase cassette (Figure 4.8). This structure similarity supports the possibility for

Itk to phosphorylate Cx43.

Antigen-dependent T cell activation relies on cell-cell contact, therefore intercellular communication is necessary. Indeed, the increase of Cx43 expression and phosphorylation are observed to be associated with T cell activation (Oviedo-Orta et al., 2010). During T cell priming, Cx43 is recruited at the immunological synapse (Mendoza-Naranjo et al., 2011). This accumulation is antigen-specific and time-dependent (Mendoza-Naranjo et al., 2011). As both Itk activation and Cx43 relocation occur during the antigen-dependent T cell activation, we hypothesize that Itk phosphorylates Cx43 resulting in Cx43 redistribution at the immunological synapse.

16.2   Results

To identify novel kinases that can phosphorylate Cx43CT, an *in vitro* phosphorylation screening assay was conducted using purified Cx43CT as substrate (by Eurofins Scientific, KinaseProfiler). 27 tyrosine kinases were selected for the kinase assay as they were predicted to phosphorylate the Cx43CT by GPS 2.0 software, and NetPhos 2.0 and KinasePhos 2.0 servers. Eight tyrosine kinases which gave over 50% of positive control signal were considered to be capable to phosphorylate Cx43CT (Figure 4.9).

Then, we tested if these kinases that phosphorylated Cx43 can bind with Cx43 in cells by performing a GST pull down assay. Purified GST and GST-Cx43CT were immobilized on glutathione-sepharose beads, and cell lysates from cell lines that express each of kinase
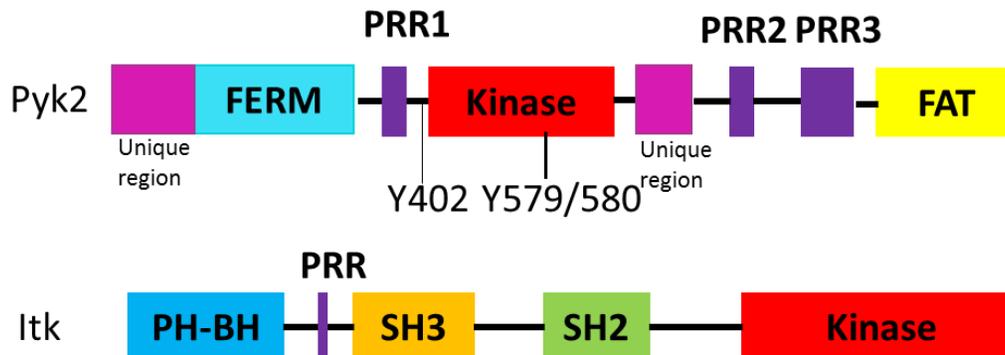
Figure 4.8 Pyk2 and Itk Schematic. Pyk2 is composed of a N-terminal FERM (protein 4.1, ezrin, radixin and moesin homology) domain, a CT focal adhesion targeting (FAT) domain, a kinase domain, and several proline rich regions (PRR). Phosphorylation of Pyk2 at Y402 creates a SH2 binding site for Src. Association of Pyk2 with c-Src leads to further phosphorylation of Pyk2 at Y579 and 580 in the kinase domain. Itk contains an NT region that includes a pleckstrin homology (PH) domain, followed by a Zn^{++} binding region termed the Btk homology (BH) motif, a PRR that conforms to the consensus sequence of an SH3 ligand, SH3 and SH2 domains, and kinase domain at the C-terminus.

of interest were added. Out of the eight candidates, six kinases were in the same complex with the Cx43CT. In particular, Pyk2 and Itk were pulled down by Cx43CT without crosslinker (Figure 4.10). Of note, the crosslinker DTSSP captures weak and transient interactions (Liu et al., 2011). These data suggest that Pyk2 and Itk have a greater binding affinity for the Cx43CT than the other tested kinases.

To study which tyrosine residues are phosphorylated by Pyk2, we conducted an *in vitro* kinase assay followed by MS (Figure 4.11). In the *in vitro* kinase assay, Cx43CT wild type and Cx43 mutants were incubated with Pyk2 and products were ran on SDS-PAGE gel. Similar to Src phosphorylation on Cx43, MS data show that Pyk2 induced phosphorylation on Y247, Y265, Y267, and Y313. Western blot using a general phospho-tyrosine antibody conformed that Y313 is one of the sites phosphorylated by Pyk2. However, the Y267 mutant did not show any signal suggesting little to no phosphorylation at Y267 by Pyk2.

16.3 Discussion and Future Directions

We showed that Pyk2 directly phosphorylates Cx43CT on Y247, Y265, Y267, and Y313, while Itk also phosphorylates Cx43CT *in vitro*. These residues have not been identified in a cell system yet. From our studies and others, we know that at least 3 tyrosine kinases target Cx43CT on Y247/265/313, suggesting a possible competition between these kinases. They may also coordinate with each other (for example, one kinase creating docking site to amplify the binding affinity for another kinase) to increase Cx43
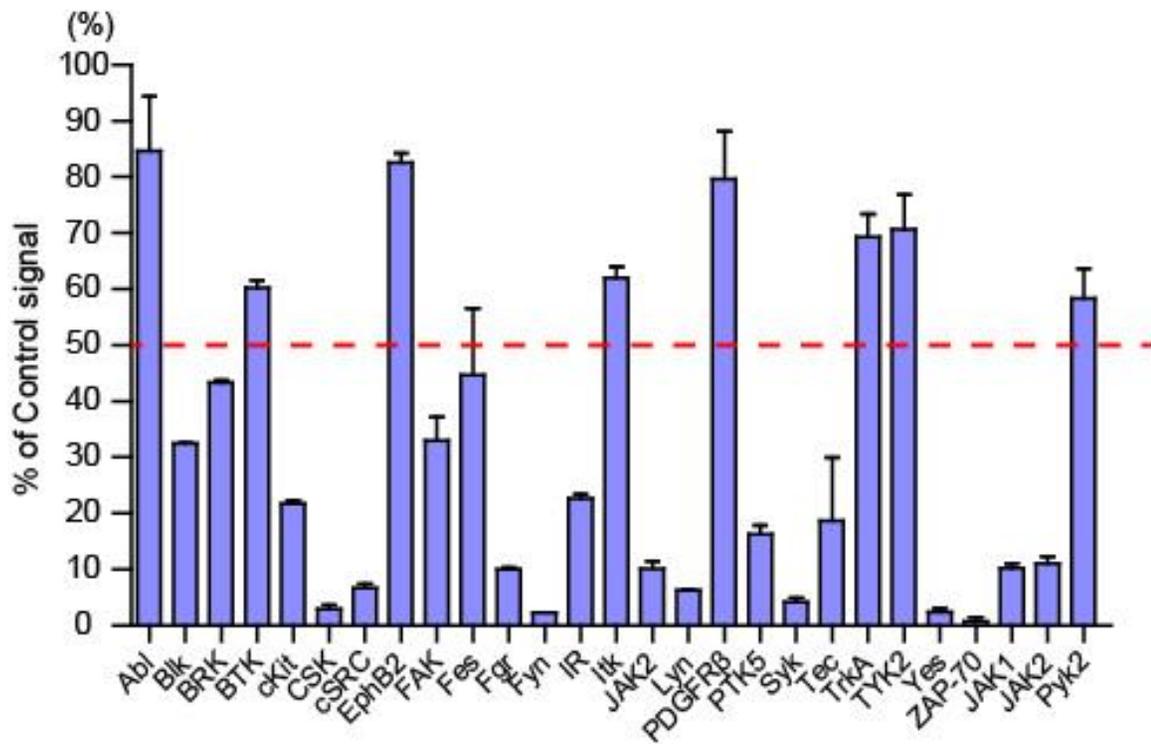
Figure 4.9 Identification of tyrosine kinases phosphorylating Cx43. *In vitro* kinase

assays were conducted using *E. coli* expressed Cx43CT as substrate. Peptides which can

be phosphorylated by each kinase were used as positive control. The phosphorylated

substrates were detected by radiometric assay. Quantification of phosphorylated Cx43CT

was normalized to the control phospho-peptide for each kinase (% of control signal). Dash

line highlights 50% of the control signal.
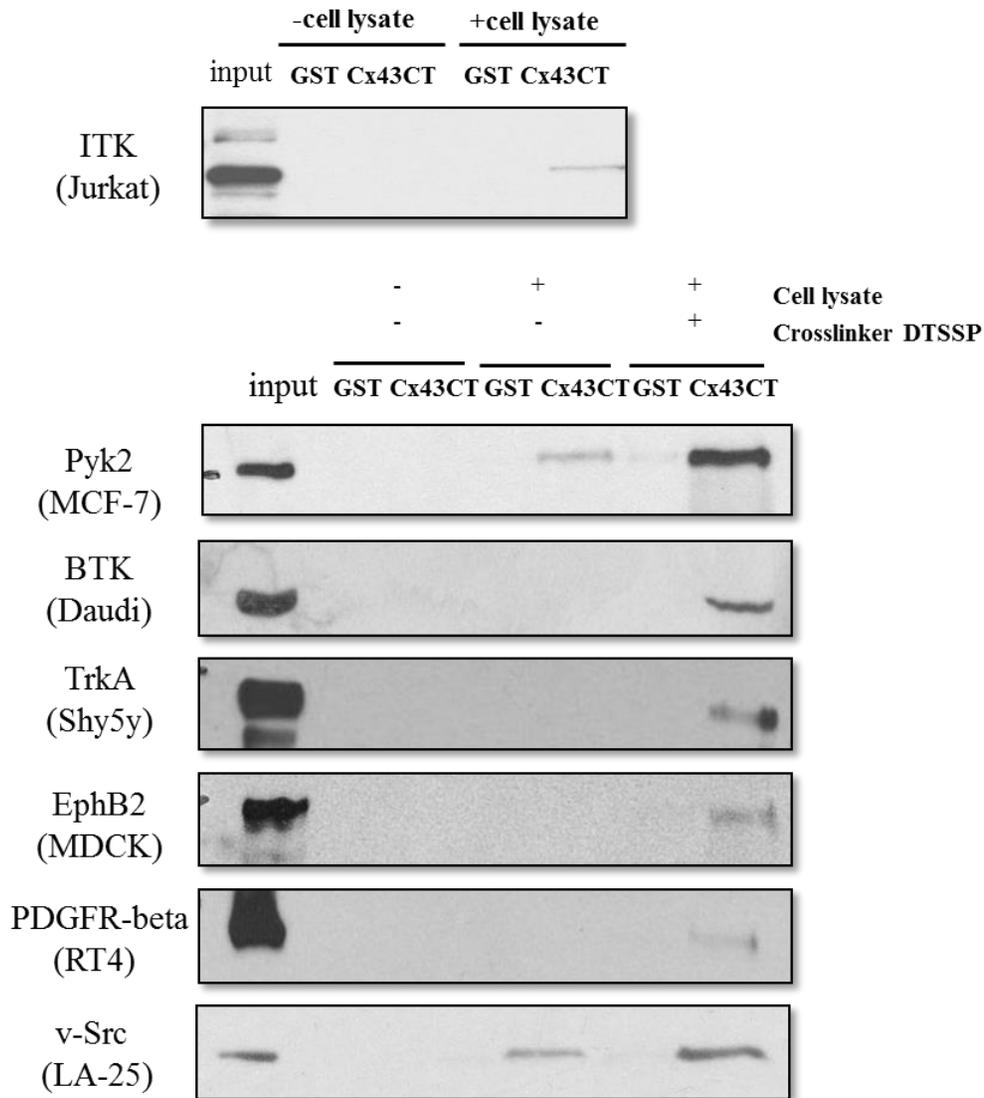
Figure 4.10 Itk and Pyk2 interact with Cx43CT. GST pull down assays using GST (negative control) and GST-Cx43CT immobilized on glutathione beads as baits were conducted in different cell lines. Eight kinases (giving >50% of control signal in the *in vitro* kinase assay) were blotted. Pyk2 and Itk were pulled down by GST-Cx43CT but not GST without crosslinker DTSSP. BTK, TrkA, EphB2 and PDGFRβ were pulled down by GST-Cx43CT only in present of the crosslinker DTSSP. V-Src which is known to bind with Cx43CT was pulled down by GST-Cx43CT both with and without crosslinker DTSSP.

A

²³⁶VKDRVKGRSDP**pY**²⁴⁷HATTGPLSPSKDCGSPK**p**
Y²⁶⁵A**pY**²⁶⁷FNGCSSPTAPLSPMSPPG**Y**²⁸⁶KLVTGD
RNNSSCRN**Y**³⁰¹NKQASEQNWAN**pY**³¹³SAEQNRMGQ
AGSTISNSHAQPFDFPDDNQNAKKVAAGHELQPLA
IVDQRPSSRASSRASSRPRPDDLEI³⁸²

B
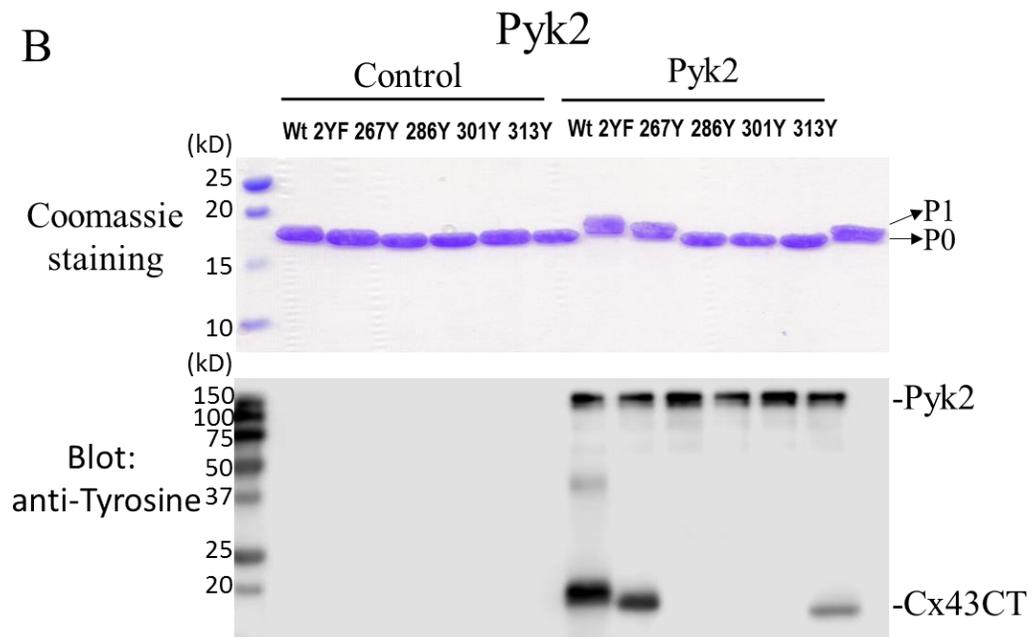
Figure 4.11 Identification of the phosphorylation sites on Cx43CT by Pyk2. Active

Pyk2 was used to phosphorylate Cx43CT wild-type and mutants in an *in vitro* kinase assay.

Purified Cx43CT wild-type and mutants (2YF=Y247/265F,

267Y=Y247/265/286/301/313F, 286Y=Y247/265/267/301/313F,

301Y=Y247/265/267/286/313F, 313Y=Y247/265/267/286/301F) were incubated with or

without (Control) Pyk2 for 16 hrs at 30°C. (A) Sequence of the Cx43CT domain.

Highlighted in red are the phospho-tyrosine residues identified by MS in an *in vitro* kinase

assay using Pyk2 to phosphorylate Cx43CT. Highlighted in blue show two tyrosines which

are not phosphorylated by Pyk2. (B) Products from the kinase assays were ran on SDS-

PAGE gel followed with Coomassie staining, and western blotted with an anti-tyrosine

antibody were performed.

phosphorylation level. Moreover, although these kinases phosphorylate on the same tyrosine residues, the phosphorylation levels could be different, suggesting that these kinases may regulate Cx43 gap junction in slightly different ways. To sum up, different kinases may permit a fine-tuning of Cx43 function to meet the specific needs of a certain tissue or developmental stage.

Future direction will focus on the functional study in cells and particular disease model. To characterize the phosphorylation events caused by Pyk2 *in cyto*, the LA-25 cell line stably expressing Pyk2 will be used to study Cx43 phosphorylation levels (Western blot) and cellular localization (immunostaining) with or without v-Src activation. Structured illumination microscopy could be used to determine the relationship between Pyk2 and Cx43 at the gap junction plaque. Heart failure rat model could be used to study the effect of Pyk2 on Cx43 regulation in pathological situations. To find out the biological relevance between Pyk2 and Cx43 in heart failure, we will quantify mRNA and phospho-protein levels of Cx43 and Pyk2, and define the cellular distribution of Cx43 and Pyk2.

The biological function of Cx43 phosphorylation by Itk in T cells activation will be characterized in co-cultured spleen dendritic and T cells with or without antigen presentation. We will test the relevance between phosphorylation of Cx43 and activation of Itk, observe the cellular localization of Itk and Cx43, and study the gap junctional communication. Itk inhibitors (BMS 509744 and CTA 056) will be used to test if the effects are caused by Itk specifically. These innovative studies will help to demonstrate how phosphorylation affects Cx43 channel gating and degradation, and provide a foundation

163

for understanding cardiac pathophysiology and T-cell activation.

CHAPTER 5

Summary and Future Directions

17. Summary

Gap junctions mediate vitally important processes such as electrical impulse propagation and cell-to-cell metabolic coupling. A better understanding of the functional and structural basis of connexin regulation will lead to improved strategies to modulate and/or reestablish junctional communication that has been altered in different pathological situation such as heart failure and cancer. Our laboratory's major focus has been to comprehensively address the regulatory mechanism of gap junction channel gating and a connexin's life cycle. As one important post-translational modification, phosphorylation has been involved in all these regulatory mechansims. Falk et al. (2016) provide a model of continuous phosphorylation event to regulate Cx43 life cycle, in which Akt, PKA, PKC, MARK phosphorylation occur sequentially (Falk et al., 2016). In some particular situations including wounding and EGF stimulation, Src is responsible for chronic gap junction degradation (Solan and Lampe, 2016; Spagnol et al., 2016). The regulatory mechanism of phosphorylation on gap junctions is complicated. The negative charge of the phosphate could affect the permeability of ions to the pore, alter the structure of the transmembrane α-helices to influence pore size, or modify the binding affinities of protein binding partners involved in regulating gap junction (Grosely et al., 2013b). Notably, if phosphorylation modifies protein interactions to affect the kinetics of channel assembly/disassembly or degradation, cell-to-cell communication will also be altered. Evidence have been emerged that a phosphate can directly block the Cx43CT interaction with ZO-1 (Chen et al., 2008), tubulin (Saidi Brikci-Nigassa et al., 2012) and drebrin (Ambrosi et al., 2016) or enhance

the interaction with Nedd4 (Leykauf et al., 2006; Spagnol et al., 2016). This information is critical because a particular cellular condition can be correlated with a specific Cx43 phosphorylation status to understand which proteins will and will not interact to affect regulation of Cx43.

Numerous serine phosphorylation sites have been identified on the Cx43CT. Compare with serine phosphorylation, studies on tyrosine phosphorylation are relatively lacking. The objective of this project was to use a multidisciplinary approach to investigate the role of tyrosine phosphorylation in altering the structure and function of Cx43 gap junctions. By using a kinase screening assay, we identified eight tyrosine kinases that phosphorylate Cx43CT *in vitro*. One of them is a JAK family member, Tyk2. We focused on Tyk2 because of its role in Ang II induced cardiovascular diseases. Tyk2 can be activated by a high level of Ang II (Kodama et al., 1998; Marrero et al., 1995; Pan et al., 1997; Pan et al., 1999; Yoon et al., 2013). Over-activation of RAS signaling is associated with increased risk of ventricular arrhythmia, hypertrophy, and sudden death (Luft, 2011; Sadoshima and Izumo, 1993). Besides, we found that among three JAK family members expressed in heart (JAK1, JAK2 and Tyk2), only Tyk2 phosphorylates Cx43CT. Our data described in Chapter 3 identified that Tyk2 phosphorylates Cx43 on Y247 and Y265 both *in vitro* and *in cyto*. Similar to Src, Tyk2 leads to an indirect phosphorylation on residues S279/282 (MAPK) and S368 (PKC), and, this response occurred when Src was inactive in NRK cells. Y313 phosphorylation was also detected by MS in the *in vitro* kinase assay and functional study will be conducted with phospho-specific antibody. Different kinases phosphorylating the

same sites is commonly occurring on Cx43, suggesting a fine-tuning mechanism on gap junction function.

Tyrosine phosphorylation is regulated by the coordination of protein tyrosine kinases and protein tyrosine phosphatases. To date, only two potential Cx43 tyrosine phosphatases have been reported, however, the directly interaction was not demonstrated. We identified a ubiquitously expressed phosphatase TC-PTP which directly interacts and dephosphorylates Cx43 on Y247 and Y265 by NMR and *in vitro* phosphatase assay, respectively. By co-immunoprecipitation and immunofluorescence assay, we were able to observe that Cx43 and TC-PTP were in the same complex in NRK cells. In LA-25 cells which express a temperature sensitive v-Src, TC-PTP indirectly led to dephosphorylation of Cx43 S368 by inactivating PKCα and PKCδ, suggesting a cross-talk between tyrosine phosphatase and PKC pathways. However, TC-PTP does not affect S279 and S282 phosphorylation levels.

Since Cx43 is a highly phosphorylated protein, understanding the effect of phosphorylation would be fundamental for deciphering the regulatory mechanism of gap junction function. We know that Y247 phosphorylation disrupts tubulin binding; Y265 phosphorylation is involved in the chronical decrease of gap junctional communication; while S368 and S279/282 phosphorylation lead to acute gap junction closure. By using dye transfer and TX100 assay, we observed that the activation of v-Src significantly decreased gap junctional communication, while dephosphorylation by TC-PTP partially reversed channel closure caused by v-Src as well as stabilized gap junctions at the plaque. Similar

as Src, Tyk2 phosphorylation decreases gap junction plaque stability and increase turnover rate. These observations are in agreement with reported effects of phosphorylation on these involved individual residues. Since TC-PTP does not decrease S279/282 phosphorylation level, we tried to identify if any serine phosphatase could dephosphorylate these sites. An *in vitro* phosphatase screening assay was conducted using phospho-peptides with pS279/282 or pS368 as substrate. Unfortunately, only PP2A present a moderate efficiency on dephosphorylating pS279/282, although PP2A targeted pS368 with a high efficiency. These results from *in vitro* experiment need to be validated in cell system.

Our data implicate that Tyk2 not only regulates Cx43 translationally, but also increases Cx43 expression transcriptionally. Evidence show that the Cx43 protein level increased acutely (in cell lines) but decreased chronically (in animal model) with high level of Ang II stimulation (Iravanian et al., 2011; Jia et al., 2008; Sovari et al., 2011). Ang II increased Src while decreasing TC-PTP expression in vascular smooth muscle cells (Touyz et al., 2002; Tsiropoulou S, 2014). Therefore, we propose a hypothetic model of Ang II induced pathogenesis in cardiovascular system: over-activation of Ang II increases Src and Tyk2 activation and decreases TC-PTP expression, thus Cx43 phosphorylation level is increased resulting in Cx43 internalization. To compensate, Tyk2 may increase Cx43 level through STAT3 in the early stage; however, the Cx43 level eventually drops due to the increased degradation. Since our studies are based on Cx43 model cell lines (NRK and LA-25), not cardiovascular cells, further studies in a mouse model or cardiomyocytes may be needed to test our hypothetic model. Our findings provide a molecular mechanism of Cx43

remodeling in cardiac pathological situation. Understanding phosphorylation/dephosphorylation of Cx43 will help build a better foundation to modulate the regulation of gap junction channels and benefit human health.

18. Future Directions

18.1 The Potential Role of PTP1B in the Regulation of Cx43 ERAD

PTP1B and TC-PTP exhibit high identity in their catalytic domain (Iversen et al., 2002). PTP1B mainly locates in the ER while TC-PTP mainly locates in the nucleus and can translocate to the cytoplasmic membrane (Bourdeau et al., 2005). PTP1B and TC-PTP share some membrane protein substrates such as EGFR and PDGFR (Dube and Tremblay, 2005). Inspired by our discovery of the interaction between TC-PTP and Cx43, we hypothesize that PTP1B interacts with Cx43 in ER and regulates Cx43 ERAD. The other rationale include the facts that 1) Cx43 is phosphorylated as early as in the ER or Golgi apparatus (Laird et al., 1995); 2) PTP1B is a mediator of ERAD (Nezvitsky et al., 2014); 3) PTP1B dephosphorylates Tyk2 (Myers et al., 2001). These studies will provide a new perspective of the regulatory role of phosphorylation on Cx43 gap junction.

18.2 The Mechanism for a Decreased Level of Cx43 in Cardiovascular Diseases

Our Tyk2 study shows that Cx43 level increases in response to high level of Ang II stimulation in cells. However, in the ACS8/8 mouse model, Cx43 gap junctions decrease significantly compare with normal mice. We hypothesize that Ang II stimulation induces

the increase of Cx43 synthesis as a compensation mechanism of reduced gap junction channel at the plaque caused by increased internalization. In the long term, Cx43 level decreases due to degradation. Further studies are necessary to prove this hypothesis. Also, the mechanism of transition from the increase to the decrease of the Cx43 protein level could be essential to the progression of cardiovascular pathology. Moreover, we are interested in the cellular destiny of these redundant Cx43. Do they work as signaling molecules in the cytoplasm and trigger the feedback mechanism to decrease Cx43 expression? And what degradation pathway do they undergo?

19. References

1991. Effect of enalapril on survival in patients with reduced left ventricular ejection fractions and congestive heart failure. The SOLVD Investigators. N Engl J Med 325, 293-302.

Abdellatif, M., 2012. Differential expression of microRNAs in different disease states. Circulation research 110, 638-650.

Adams, R.H., Wilkinson, G.A., Weiss, C., Diella, F., Gale, N.W., Deutsch, U., Risau, W., Klein, R., 1999. Roles of ephrinB ligands and EphB receptors in cardiovascular development: demarcation of arterial/venous domains, vascular morphogenesis, and sprouting angiogenesis. Genes & development 13, 295-306.

Ahmad, S., Diez, J.A., George, C.H., Evans, W.H., 1999. Synthesis and assembly of connexins in vitro into homomeric and heteromeric functional gap junction hemichannels. The Biochemical journal 339 (Pt 2), 247-253.

Ai, X., Jiang, A., Ke, Y., Solaro, R.J., Pogwizd, S.M., 2011. Enhanced activation of p21-activated kinase 1 in heart failure contributes to dephosphorylation of connexin 43. Cardiovasc Res 92, 106-114.

Ai, X., Pogwizd, S.M., 2005. Connexin 43 downregulation and dephosphorylation in nonischemic heart failure is associated with enhanced colocalized protein phosphatase type 2A. Circulation research 96, 54-63.

Akar, F.G., Spragg, D.D., Tunin, R.S., Kass, D.A., Tomaselli, G.F., 2004. Mechanisms underlying conduction slowing and arrhythmogenesis in nonischemic dilated cardiomyopathy. Circ Res 95, 717-725.

Alberts, Lewis, Lewis, Raff, Roberts, Walter, 2002. Transport from the Trans Golgi Network to Lysosomes, Molecular Biology of the Cell. Garland Science, New York.

Alonso, F., Krattinger, N., Mazzolai, L., Simon, A., Waeber, G., Meda, P., Haefliger, J.A., 2010. An angiotensin II- and NF-{kappa}B-dependent mechanism increases connexin 43 in murine arteries targeted by renin-dependent hypertension. Cardiovasc Res.

Alvarado-Kristensson, M., Andersson, T., 2005. Protein phosphatase 2A regulates apoptosis in neutrophils by dephosphorylating both p38 MAPK and its substrate caspase 3. The Journal of biological chemistry 280, 6238-6244.

Ambrosi, C., Ren, C., Spagnol, G., Cavin, G., Cone, A., Grintsevich, E.E., Sosinsky, G.E., Sorgen, P.L., 2016. Connexin43 Forms Supramolecular Complexes through Non-Overlapping Binding Sites for Drebrin, Tubulin, and ZO-1. PloS one 11, e0157073.

Anderson, C., Catoe, H., Werner, R., 2006. MIR-206 regulates connexin43 expression during skeletal muscle development. Nucleic acids research 34, 5863-5871.

Andreotti, A.H., Schwartzberg, P.L., Joseph, R.E., Berg, L.J., 2010. T-cell signaling regulated by the Tec family kinase, Itk. Cold Spring Harbor perspectives in biology 2, a002287.

Atkinson, M.M., Menko, A.S., Johnson, R.G., Sheppard, J.R., Sheridan, J.D., 1981. Rapid and reversible reduction of junctional permeability in cells infected with a temperature-sensitive mutant of avian sarcoma virus. J Cell Biol 91, 573-578.

Avraham, H., Park, S.Y., Schinkmann, K., Avraham, S., 2000. RAFTK/Pyk2-mediated cellular signalling. Cellular signalling 12, 123-133.

Axelsen, L.N., Calloe, K., Holstein-Rathlou, N.H., Nielsen, M.S., 2013. Managing the complexity of communication: regulation of gap junctions by post-translational modification. Frontiers in pharmacology 4, 130.

Axelsen, L.N., Stahlhut, M., Mohammed, S., Larsen, B.D., Nielsen, M.S., Holstein-Rathlou, N.H., Andersen, S., Jensen, O.N., Hennan, J.K., Kjolbye, A.L., 2006. Identification of ischemia-regulated phosphorylation sites in connexin43: A possible target for the antiarrhythmic peptide analogue rotigaptide (ZP123). Journal of molecular and cellular cardiology 40, 790-798.

Azarnia, R., Reddy, S., Kmiecik, T.E., Shalloway, D., Loewenstein, W.R., 1988. The cellular src gene product regulates junctional cell-to-cell communication. Science 239, 398-401.

Babu, M.M., van der Lee, R., de Groot, N.S., Gsponer, J., 2011. Intrinsically disordered proteins: regulation and disease. Current opinion in structural biology 21, 432-440.

Balice-Gordon, R.J., Bone, L.J., Scherer, S.S., 1998. Functional gap junctions in the schwann cell myelin sheath. The Journal of cell biology 142, 1095-1104.

Barrio, L.C., Capel, J., Jarillo, J.A., Castro, C., Revilla, A., 1997. Species-specific voltage-gating properties of connexin-45 junctions expressed in Xenopus oocytes. Biophysical journal 73, 757-769.

Bayer, A.L., Ferguson, A.G., Lucchesi, P.A., Samarel, A.M., 2001. Pyk2 expression and phosphorylation in neonatal and adult cardiomyocytes. J Mol Cell Cardiol 33, 1017-1030.

Bayer, A.L., Heidkamp, M.C., Patel, N., Porter, M.J., Engman, S.J., Samarel, A.M., 2002. PYK2 expression and phosphorylation increases in pressure overload-induced left ventricular hypertrophy. Am J Physiol Heart Circ Physiol 283, H695-706.

Beardslee, M.A., Laing, J.G., Beyer, E.C., Saffitz, J.E., 1998. Rapid turnover of connexin43 in the adult rat heart. Circulation research 83, 629-635.

Bejarano, E., Girao, H., Yuste, A., Patel, B., Marques, C., Spray, D.C., Pereira, P., Cuervo, A.M., 2012. Autophagy modulates dynamics of connexins at the plasma membrane in a ubiquitin-dependent manner. Molecular biology of the cell 23, 2156-2169.

Bergoffen, J., Scherer, S.S., Wang, S., Scott, M.O., Bone, L.J., Paul, D.L., Chen, K., Lensch, M.W., Chance, P.F., Fischbeck, K.H., 1993. Connexin mutations in X-linked Charcot-Marie-Tooth disease. Science 262, 2039-2042.

Berthoud, V.M., Beyer, E.C., Kurata, W.E., Lau, A.F., Lampe, P.D., 1997. The gap-junction protein connexin 56 is phosphorylated in the intracellular loop and the carboxy-terminal region. European journal of biochemistry / FEBS 244, 89-97.

Berthoud, V.M., Ledbetter, M.L., Hertzberg, E.L., Saez, J.C., 1992. Connexin43 in MDCK cells: regulation by a tumor-promoting phorbol ester and Ca2+. European journal of cell biology 57, 40-50.

Bevans, C.G., Harris, A.L., 1999. Regulation of connexin channels by pH. Direct action of the protonated form of taurine and other aminosulfonates. The Journal of biological chemistry 274, 3711-3719.

Bjorkman, N., 1962. A study of the ultrastructure of the granulosa cells of the rat ovary. Acta anatomica 51, 125-147.

Blodow, A., Ngezahayo, A., Ernst, A., Kolb, H.A., 2003. Calmodulin antagonists suppress gap junction coupling in isolated Hensen cells of the guinea pig cochlea. Pflugers Archiv : European journal of physiology 446, 36-41.

Blom, N., Gammeltoft, S., Brunak, S., 1999. Sequence and structure-based prediction of eukaryotic protein phosphorylation sites. Journal of molecular biology 294, 1351-1362.

Boehr, D.D., Nussinov, R., Wright, P.E., 2009. The role of dynamic conformational ensembles in biomolecular recognition. Nature chemical biology 5, 789-796.

Boggon, T.J., Eck, M.J., 2004. Structure and regulation of Src family kinases. Oncogene 23, 7918-7927.

Bolon, M.L., Kidder, G.M., Simon, A.M., Tyml, K., 2007. Lipopolysaccharide reduces electrical coupling in microvascular endothelial cells by targeting connexin40 in a tyrosine-, ERK1/2-, PKA-, and PKC-dependent manner. Journal of cellular physiology 211, 159-166.

Bolte, S., Cordelieres, F.P., 2006. A guided tour into subcellular colocalization analysis in light microscopy. Journal of microscopy 224, 213-232.

Bondurand, N., Girard, M., Pingault, V., Lemort, N., Dubourg, O., Goossens, M., 2001. Human Connexin 32, a gap junction protein altered in the X-linked form of Charcot-Marie-Tooth disease, is directly regulated by the transcription factor SOX10. Human molecular genetics 10, 2783-2795.

Borner, C., Guadagno, S.N., Fabbro, D., Weinstein, I.B., 1992. Expression of four protein kinase C isoforms in rat fibroblasts. Distinct subcellular distribution and regulation by calcium and phorbol esters. The Journal of biological chemistry 267, 12892-12899.

Bourdeau, A., Dube, N., Tremblay, M.L., 2005. Cytoplasmic protein tyrosine phosphatases, regulation and function: the roles of PTP1B and TC-PTP. Current opinion in cell biology 17, 203-209.

Bouvier, D., Spagnol, G., Chenavas, S., Kieken, F., Vitrac, H., Brownell, S., Kellezi, A., Forge, V., Sorgen, P.L., 2009. Characterization of the structure and intermolecular interactions between the connexin40 and connexin43 carboxyl-terminal and cytoplasmic loop domains. The Journal of biological chemistry 284, 34257-34271.

Breitkopf, S.B., Asara, J.M., 2012. Determining in vivo phosphorylation sites using mass spectrometry. Current protocols in molecular biology / edited by Frederick M. Ausubel Chapter 18, Unit18 19 11-27.

Bukauskas, F.F., Angele, A.B., Verselis, V.K., Bennett, M.V., 2002. Coupling asymmetry of heterotypic connexin 45/ connexin 43-EGFP gap junctions: properties of fast and slow gating mechanisms. Proceedings of the National Academy of Sciences of the United States of America 99, 7113-7118.

Bukauskas, F.F., Bukauskiene, A., Bennett, M.V., Verselis, V.K., 2001. Gating properties of gap junction channels assembled from connexin43 and connexin43 fused with green fluorescent protein. Biophysical journal 81, 137-152.

Burr, G.S., Mitchell, C.K., Keflemariam, Y.J., Heidelberger, R., O'Brien, J., 2005. Calcium-dependent binding of calmodulin to neuronal gap junction proteins. Biochemical and biophysical research communications 335, 1191-1198.

Butkevich, E., Hulsmann, S., Wenzel, D., Shirao, T., Duden, R., Majoul, I., 2004. Drebrin is a novel connexin-43 binding partner that links gap junctions to the submembrane cytoskeleton. Current biology : CB 14, 650-658.

Caltabiano, R., Torrisi, A., Condorelli, D., Albanese, V., Lanzafame, S., 2010. High levels of connexin 43 mRNA in high grade astrocytomas. Study of 32 cases with in situ hybridization. Acta histochemica 112, 529-535.

Chanson, M., Fanjul, M., Bosco, D., Nelles, E., Suter, S., Willecke, K., Meda, P., 1998. Enhanced secretion of amylase from exocrine pancreas of connexin32-deficient mice. The Journal of cell biology 141, 1267-1275.

Chen, H.H., Baty, C.J., Maeda, T., Brooks, S., Baker, L.C., Ueyama, T., Gursoy, E., Saba, S., Salama, G., London, B., Stewart, A.F., 2004. Transcription enhancer factor-1-related factor-transgenic mice develop cardiac conduction defects associated with altered connexin phosphorylation. Circulation 110, 2980-2987.

Chen, J., Pan, L., Wei, Z., Zhao, Y., Zhang, M., 2008. Domain-swapped dimerization of ZO-1 PDZ2 generates specific and regulatory connexin43-binding sites. EMBO J 27, 2113-2123.

Chen, J.T., Cheng, Y.W., Chou, M.C., Sen-Lin, T., Lai, W.W., Ho, W.L., Lee, H., 2003. The correlation between

aberrant connexin 43 mRNA expression induced by promoter methylation and nodal micrometastasis in non-small cell lung cancer. Clinical cancer research : an official journal of the American Association for Cancer Research 9, 4200-4204.

Chen, Y., Zhou, Y., Lin, X., Wong, H.C., Xu, Q., Jiang, J., Wang, S., Lurtz, M.M., Louis, C.F., Veenstra, R.D., Yang, J.J., 2011. Molecular interaction and functional regulation of connexin50 gap junctions by calmodulin. The Biochemical journal 435, 711-722.

Chtchetinin, J., Gifford, W.D., Li, S., Paznekas, W.A., Jabs, E.W., Lai, A., 2009. Tyrosine-dependent basolateral targeting of human connexin43-eYFP in Madin-Darby canine kidney cells can be disrupted by the oculodentodigital dysplasia mutation L90V. The FEBS journal 276, 6992-7005.

Churko, J.M., Chan, J., Shao, Q., Laird, D.W., 2011. The G60S connexin43 mutant regulates hair growth and hair fiber morphology in a mouse model of human oculodentodigital dysplasia. The Journal of investigative dermatology 131, 2197-2204.

Cohen-Salmon, M., Ott, T., Michel, V., Hardelin, J.P., Perfettini, I., Eybalin, M., Wu, T., Marcus, D.C., Wangemann, P., Willecke, K., Petit, C., 2002. Targeted ablation of connexin26 in the inner ear epithelial gap junction network causes hearing impairment and cell death. Current biology : CB 12, 1106-1111.

Common, J.E., Becker, D., Di, W.L., Leigh, I.M., O'Toole, E.A., Kelsell, D.P., 2002. Functional studies of human skin disease- and deafness-associated connexin 30 mutations. Biochemical and biophysical research communications 298, 651-656.

Cone, A.C., Cavin, G., Ambrosi, C., Hakozaki, H., Wu-Zhang, A.X., Kunkel, M.T., Newton, A.C., Sosinsky, G.E., 2014. Protein Kinase Cdelta-mediated Phosphorylation of Connexin43 Gap Junction Channels Causes Movement within Gap Junctions followed by Vesicle Internalization and Protein Degradation. The Journal of biological chemistry 289, 8781-8798.

Cool, D.E., Tonks, N.K., Charbonneau, H., Walsh, K.A., Fischer, E.H., Krebs, E.G., 1989. cDNA isolated from a human T-cell library encodes a member of the protein-tyrosine-phosphatase family. Proceedings of the National Academy of Sciences of the United States of America 86, 5257-5261.

Cooper, C.D., Lampe, P.D., 2002. Casein kinase 1 regulates connexin-43 gap junction assembly. The Journal of biological chemistry 277, 44962-44968.

Cooper, C.D., Solan, J.L., Dolejsi, M.K., Lampe, P.D., 2000. Analysis of connexin phosphorylation sites. Methods 20, 196-204.

Cottrell, G.T., Lin, R., Warn-Cramer, B.J., Lau, A.F., Burt, J.M., 2003. Mechanism of v-Src- and mitogen-activated protein kinase-induced reduction of gap junction communication. American journal of physiology. Cell physiology 284, C511-520.

Crow, D.S., Beyer, E.C., Paul, D.L., Kobe, S.S., Lau, A.F., 1990. Phosphorylation of connexin43 gap junction protein in uninfected and Rous sarcoma virus-transformed mammalian fibroblasts. Mol Cell Biol 10, 1754-1763.

Cruciani, V., Kaalhus, O., Mikalsen, S.O., 1999. Phosphatases involved in modulation of gap junctional intercellular communication and dephosphorylation of connexin43 in hamster fibroblasts: 2B or not 2B? Experimental cell research 252, 449-463.

Dang, X., Doble, B.W., Kardami, E., 2003. The carboxy-tail of connexin-43 localizes to the nucleus and inhibits cell growth. Molecular and cellular biochemistry 242, 35-38.

Davis, F.P., 2011. Phosphorylation at the interface. Structure 19, 1726-1727.

Davy, A., Bush, J.O., Soriano, P., 2006. Inhibition of gap junction communication at ectopic Eph/ephrin boundaries underlies craniofrontonasal syndrome. PLoS biology 4, e315.

de Feijter, A.W., Matesic, D.F., Ruch, R.J., Guan, X., Chang, C.C., Trosko, J.E., 1996. Localization and function of the connexin 43 gap-junction protein in normal and various oncogene-expressing rat liver epithelial cells. Molecular carcinogenesis 16, 203-212.

del Valle, J., Bayod, S., Camins, A., Beas-Zarate, C., Velazquez-Zamora, D.A., Gonzalez-Burgos, I., Pallas, M., 2012. Dendritic spine abnormalities in hippocampal CA1 pyramidal neurons underlying memory deficits in the SAMP8 mouse model of Alzheimer's disease. Journal of Alzheimer's disease : JAD 32, 233-240.

Delaglio, F., Grzesiek, S., Vuister, G.W., Zhu, G., Pfeifer, J., Bax, A., 1995. NMRPipe: a multidimensional spectral processing system based on UNIX pipes. Journal of biomolecular NMR 6, 277-293.

Delmar, M., Makita, N., 2012. Cardiac connexins, mutations and arrhythmias. Curr Opin Cardiol 27, 236-241.

Delorme, B., Dahl, E., Jarry-Guichard, T., Marics, I., Briand, J.P., Willecke, K., Gros, D., Theveniau-Ruissy, M., 1995. Developmental regulation of connexin 40 gene expression in mouse heart correlates with the differentiation of the conduction system. Developmental dynamics : an official publication of the American Association of Anatomists 204, 358-371.

Diez, J.A., Elvira, M., Villalobo, A., 1998. The epidermal growth factor receptor tyrosine kinase phosphorylates connexin32. Molecular and cellular biochemistry 187, 201-210.

Doble, B.W., Kardami, E., 1995. Basic fibroblast growth factor stimulates connexin-43 expression and intercellular communication of cardiac fibroblasts. Molecular and cellular biochemistry 143, 81-87.

Dodd, R., Peracchia, C., Stolady, D., Torok, K., 2008. Calmodulin association with connexin32-derived peptides suggests trans-domain interaction in chemical gating of gap junction channels. The Journal of biological chemistry 283, 26911-26920.

Dube, N., Tremblay, M.L., 2005. Involvement of the small protein tyrosine phosphatases TC-PTP and PTP1B in signal transduction and diseases: from diabetes, obesity to cell cycle, and cancer. Biochimica et biophysica acta 1754, 108-117.

Duffy, H.S., Sorgen, P.L., Girvin, M.E., O'Donnell, P., Coombs, W., Taffet, S.M., Delmar, M., Spray, D.C., 2002. pH-dependent intramolecular binding and structure involving Cx43 cytoplasmic domains. The Journal of biological chemistry 277, 36706-36714.

Dunker, A.K., Obradovic, Z., 2001. The protein trinity--linking function and disorder. Nature biotechnology 19, 805-806.

Duthe, F., Plaisance, I., Sarrouilhe, D., Herve, J.C., 2001. Endogenous protein phosphatase 1 runs down gap junctional communication of rat ventricular myocytes. American journal of physiology. Cell physiology 281, C1648-1656.

Echetebu, C.O., Ali, M., Izban, M.G., MacKay, L., Garfield, R.E., 1999. Localization of regulatory protein binding sites in the proximal region of human myometrial connexin 43 gene. Molecular human reproduction 5, 757-766.

Eckert, R., 2002. pH gating of lens fibre connexins. Pflugers Archiv : European journal of physiology 443, 843-851.

Edwards, G.O., Botchway, S.W., Hirst, G., Wharton, C.W., Chipman, J.K., Meldrum, R.A., 2004. Gap junction communication dynamics and bystander effects from ultrasoft X-rays. British journal of cancer 90, 1450-1456.

Eiberger, J., Degen, J., Romualdi, A., Deutsch, U., Willecke, K., Sohl, G., 2001. Connexin genes in the mouse and human genome. Cell communication & adhesion 8, 163-165.

Ek-Vitorin, J.F., Calero, G., Morley, G.E., Coombs, W., Taffet, S.M., Delmar, M., 1996. PH regulation of connexin43: molecular analysis of the gating particle. Biophysical journal 71, 1273-1284.

Ek, J.F., Delmar, M., Perzova, R., Taffet, S.M., 1994. Role of histidine 95 on pH gating of the cardiac gap junction protein connexin43. Circulation research 74, 1058-1064.

Emdad, L., Uzzaman, M., Takagishi, Y., Honjo, H., Uchida, T., Severs, N.J., Kodama, I., Murata, Y., 2001. Gap junction remodeling in hypertrophied left ventricles of aortic-banded rats: prevention by angiotensin II type 1 receptor blockade. J Mol Cell Cardiol 33, 219-231.

Faivre, E.J., Lange, C.A., 2007. Progesterone receptors upregulate Wnt-1 to induce epidermal growth factor receptor transactivation and c-Src-dependent sustained activation of Erk1/2 mitogen-activated protein kinase in breast cancer cells. Molecular and cellular biology 27, 466-480.

Falk, M.M., Bell, C.L., Kells Andrews, R.M., Murray, S.A., 2016. Molecular mechanisms regulating formation, trafficking and processing of annular gap junctions. BMC cell biology 17 Suppl 1, 22.

Falk, M.M., Buehler, L.K., Kumar, N.M., Gilula, N.B., 1997. Cell-free synthesis and assembly of connexins into functional gap junction membrane channels. The EMBO journal 16, 2703-2716.

Fallon, R.F., Goodenough, D.A., 1981. Five-hour half-life of mouse liver gap-junction protein. The Journal of cell biology 90, 521-526.

Ficarro, S.B., McCleland, M.L., Stukenberg, P.T., Burke, D.J., Ross, M.M., Shabanowitz, J., Hunt, D.F., White, F.M., 2002. Phosphoproteome analysis by mass spectrometry and its application to Saccharomyces cerevisiae. Nature biotechnology 20, 301-305.

Filson, A.J., Azarnia, R., Beyer, E.C., Loewenstein, W.R., Brugge, J.S., 1990. Tyrosine phosphorylation of a gap junction protein correlates with inhibition of cell-to-cell communication. Cell growth & differentiation : the molecular biology journal of the American Association for Cancer Research 1, 661-668.

Firmbach-Kraft, I., Byers, M., Shows, T., Dalla-Favera, R., Krolewski, J.J., 1990. tyk2, prototype of a novel class of non-receptor tyrosine kinase genes. Oncogene 5, 1329-1336.

Fischer, R., Dechend, R., Gapelyuk, A., Shagdarsuren, E., Gruner, K., Gruner, A., Gratze, P., Qadri, F., Wellner, M., Fiebeler, A., Dietz, R., Luft, F.C., Muller, D.N., Schirdewan, A., 2007. Angiotensin II-induced sudden arrhythmic death and electrical remodeling. American journal of physiology. Heart and circulatory physiology 293, H1242-1253.

Fong, J.T., Kells, R.M., Falk, M.M., 2013. Two tyrosine-based sorting signals in the Cx43 C-terminus cooperate to mediate gap junction endocytosis. Molecular biology of the cell 24, 2834-2848.

Fort, A.G., Spray, D.C., 2009. Trifluoroethanol reveals helical propensity at analogous positions in cytoplasmic domains of three connexins. Biopolymers 92, 173-182.

Fujimoto, E., Sato, H., Shirai, S., Nagashima, Y., Fukumoto, K., Hagiwara, H., Negishi, E., Ueno, K., Omori, Y., Yamasaki, H., Hagiwara, K., Yano, T., 2005. Connexin32 as a tumor suppressor gene in a metastatic renal cell carcinoma cell line. Oncogene 24, 3684-3690.

Fujimoto, K., Nagafuchi, A., Tsukita, S., Kuraoka, A., Ohokuma, A., Shibata, Y., 1997. Dynamics of connexins, E-cadherin and alpha-catenin on cell membranes during gap junction formation. Journal of cell science 110 (Pt 3), 311-322.

Fukushima, A., Loh, K., Galic, S., Fam, B., Shields, B., Wiede, F., Tremblay, M.L., Watt, M.J., Andrikopoulos, S.,

Tiganis, T., 2010. T-cell protein tyrosine phosphatase attenuates STAT3 and insulin signaling in the liver to regulate gluconeogenesis. Diabetes 59, 1906-1914.

Fuxreiter, M., Simon, I., Friedrich, P., Tompa, P., 2004. Preformed structural elements feature in partner recognition by intrinsically unstructured proteins. Journal of molecular biology 338, 1015-1026.

Gaietta, G., Deerinck, T.J., Adams, S.R., Bouwer, J., Tour, O., Laird, D.W., Sosinsky, G.E., Tsien, R.Y., Ellisman, M.H., 2002. Multicolor and electron microscopic imaging of connexin trafficking. Science 296, 503-507.

Galic, S., Hauser, C., Kahn, B.B., Haj, F.G., Neel, B.G., Tonks, N.K., Tiganis, T., 2005. Coordinated regulation of insulin signaling by the protein tyrosine phosphatases PTP1B and TCPTP. Molecular and cellular biology 25, 819-829.

Galic, S., Klingler-Hoffmann, M., Fodero-Tavoletti, M.T., Puryer, M.A., Meng, T.C., Tonks, N.K., Tiganis, T., 2003. Regulation of insulin receptor signaling by the protein tyrosine phosphatase TCPTP. Molecular and cellular biology 23, 2096-2108.

Gerner, L., Youssef, G., O'Shaughnessy, R.F., 2013. The protein phosphatase 2A regulatory subunit Ppp2r2a is required for Connexin-43 dephosphorlyation during epidermal barrier acquisition. Experimental dermatology 22, 754-756.

Ghoreschi, K., Laurence, A., O'Shea, J.J., 2009. Janus kinases in immune cell signaling. Immunol Rev 228, 273-287.

Gielen, P.R., Aftab, Q., Ma, N., Chen, V.C., Hong, X., Lozinsky, S., Naus, C.C., Sin, W.C., 2013. Connexin43 confers Temozolomide resistance in human glioma cells by modulating the mitochondrial apoptosis pathway. Neuropharmacology 75, 539-548.

Giepmans, B.N., 2004. Gap junctions and connexin-interacting proteins. Cardiovascular research 62, 233-245.

Giepmans, B.N., Feiken, E., Gebbink, M.F., Moolenaar, W.H., 2003. Association of connexin43 with a receptor protein tyrosine phosphatase. Cell communication & adhesion 10, 201-205.

Giepmans, B.N., Hengeveld, T., Postma, F.R., Moolenaar, W.H., 2001. Interaction of c-Src with gap junction protein connexin-43. Role in the regulation of cell-cell communication. The Journal of biological chemistry 276, 8544-8549.

Giepmans, B.N., Verlaan, I., Moolenaar, W.H., 2001. Connexin-43 interactions with ZO-1 and alpha- and beta-tubulin. Cell communication & adhesion 8, 219-223.

Gingalewski, C., Wang, K., Clemens, M.G., De Maio, A., 1996. Posttranscriptional regulation of connexin 32 expression in liver during acute inflammation. Journal of cellular physiology 166, 461-467.

Ginzberg, R.D., Gilula, N.B., 1979. Modulation of cell junctions during differentiation of the chicken otocyst sensory epithelium. Developmental biology 68, 110-129.

Girao, H., Catarino, S., Pereira, P., 2009. Eps15 interacts with ubiquitinated Cx43 and mediates its internalization. Experimental cell research 315, 3587-3597.

Glukhov, A.V., Fedorov, V.V., Kalish, P.W., Ravikumar, V.K., Lou, Q., Janks, D., Schuessler, R.B., Moazami, N., Efimov, I.R., 2012. Conduction remodeling in human end-stage nonischemic left ventricular cardiomyopathy. Circulation 125, 1835-1847.

Goi, T., Shipitsin, M., Lu, Z., Foster, D.A., Klinz, S.G., Feig, L.A., 2000. An EGF receptor/Ral-GTPase signaling cascade regulates c-Src activity and substrate specificity. The EMBO journal 19, 623-630.

Gonzalez, D., Gomez-Hernandez, J.M., Barrio, L.C., 2007. Molecular basis of voltage dependence of connexin

channels: an integrative appraisal. Progress in biophysics and molecular biology 94, 66-106.

Goodenough, D.A., Paul, D.L., 2009. Gap junctions. Cold Spring Harbor perspectives in biology 1, a002576.

Govindarajan, R., Chakraborty, S., Johnson, K.E., Falk, M.M., Wheelock, M.J., Johnson, K.R., Mehta, P.P., 2010. Assembly of connexin43 into gap junctions is regulated differentially by E-cadherin and N-cadherin in rat liver epithelial cells. Molecular biology of the cell 21, 4089-4107.

Grazul-Bilska, A.T., Vonnahme, K.A., Bilski, J.J., Borowczyk, E., Soni, D., Mikkelson, B., Johnson, M.L., Reynolds, L.P., Redmer, D.A., Caton, J.S., 2011. Expression of gap junctional connexin proteins in ovine fetal ovaries: effects of maternal diet. Domestic animal endocrinology 41, 185-194.

Grethe, S., Porn-Ares, M.I., 2006. p38 MAPK regulates phosphorylation of Bad via PP2A-dependent suppression of the MEK1/2-ERK1/2 survival pathway in TNF-alpha induced endothelial apoptosis. Cellular signalling 18, 531-540.

Grosely, R., Kieken, F., Sorgen, P.L., 2013. (1)H, (1)(3)C, and (1)(5)N backbone resonance assignments of the connexin43 carboxyl terminal domain attached to the 4th transmembrane domain in detergent micelles. Biomolecular NMR assignments 7, 299-303.

Grosely, R., Kopanic, J.L., Nabors, S., Kieken, F., Spagnol, G., Al-Mugotir, M., Zach, S., Sorgen, P.L., 2013b. Effects of phosphorylation on the structure and backbone dynamics of the intrinsically disordered connexin43 C-terminal domain. The Journal of biological chemistry 288, 24857-24870.

Grosely, R., Kopanic, J.L., Nabors, S., Kieken, F., Spagnol, G., Al-Mugotir, M., Zach, S., Sorgen, P.L., 2013c. Effects of phosphorylation on the structure and backbone dynamics of the intrinsically disordered Connexin43 carboxyl-terminal domain. The Journal of biological chemistry.

Guan, X., Wilson, S., Schlender, K.K., Ruch, R.J., 1996. Gap-junction disassembly and connexin 43 dephosphorylation induced by 18 beta-glycyrrhetinic acid. Molecular carcinogenesis 16, 157-164.

Gumpert, A.M., Varco, J.S., Baker, S.M., Piehl, M., Falk, M.M., 2008. Double-membrane gap junction internalization requires the clathrin-mediated endocytic machinery. FEBS letters 582, 2887-2892.

Ha, K.S., Exton, J.H., 1993. Differential translocation of protein kinase C isozymes by thrombin and platelet-derived growth factor. A possible function for phosphatidylcholine-derived diacylglycerol. The Journal of biological chemistry 268, 10534-10539.

Hassan, S.W., Doody, K.M., Hardy, S., Uetani, N., Cournoyer, D., Tremblay, M.L., 2010. Increased susceptibility to dextran sulfate sodium induced colitis in the T cell protein tyrosine phosphatase heterozygous mouse. PLoS One 5, e8868.

Hayashi, T., Thomas, G.M., Huganir, R.L., 2009. Dual palmitoylation of NR2 subunits regulates NMDA receptor trafficking. Neuron 64, 213-226.

Hernandez, M., Shao, Q., Yang, X.J., Luh, S.P., Kandouz, M., Batist, G., Laird, D.W., Alaoui-Jamali, M.A., 2006. A histone deacetylation-dependent mechanism for transcriptional repression of the gap junction gene cx43 in prostate cancer cells. The Prostate 66, 1151-1161.

Hertlein, B., Butterweck, A., Haubrich, S., Willecke, K., Traub, O., 1998. Phosphorylated carboxy terminal serine residues stabilize the mouse gap junction protein connexin45 against degradation. The Journal of membrane biology 162, 247-257.

Herve, J.C., Sarrouilhe, D., 2002. Modulation of junctional communication by phosphorylation: protein phosphatases, the missing link in the chain. Biology of the cell / under the auspices of the European Cell Biology Organization 94, 423-432.

Homma, N., Alvarado, J.L., Coombs, W., Stergiopoulos, K., Taffet, S.M., Lau, A.F., Delmar, M., 1998. A particle-receptor model for the insulin-induced closure of connexin43 channels. Circulation research 83, 27-32.

Hu, W., Wang, M., Yin, H., Yao, C., He, Q., Yin, L., Zhang, C., Li, W., Chang, G., Wang, S., 2015. MicroRNA-1298 is regulated by DNA methylation and affects vascular smooth muscle cell function by targeting connexin 43. Cardiovascular research 107, 534-545.

Huang, Q.Y., Chen, Y.C., Liu, S.P., 2012. Connexin 43, angiotensin II, endothelin 1, and type III collagen alterations in heart of rats having undergone fatal electrocution. The American journal of forensic medicine and pathology 33, 215-221.

Huang, R.Y., Laing, J.G., Kanter, E.M., Berthoud, V.M., Bao, M., Rohrs, H.W., Townsend, R.R., Yamada, K.A., 2011. Identification of CaMKII phosphorylation sites in Connexin43 by high-resolution mass spectrometry. Journal of proteome research 10, 1098-1109.

Huang, S., Dudez, T., Scerri, I., Thomas, M.A., Giepmans, B.N., Suter, S., Chanson, M., 2003. Defective activation of c-Src in cystic fibrosis airway epithelial cells results in loss of tumor necrosis factor-alpha-induced gap junction regulation. The Journal of biological chemistry 278, 8326-8332.

Huang, S., Jornot, L., Wiszniewski, L., Rochat, T., Suter, S., Lacroix, J.S., Chanson, M., 2003. Src signaling links mediators of inflammation to Cx43 gap junction channels in primary and transformed CFTR-expressing airway cells. Cell communication & adhesion 10, 279-285.

Hunter, A.W., Barker, R.J., Zhu, C., Gourdie, R.G., 2005. Zonula occludens-1 alters connexin43 gap junction size and organization by influencing channel accretion. Molecular biology of the cell 16, 5686-5698.

Husoy, T., Mikalsen, S.O., Sanner, T., 1993. Phosphatase inhibitors, gap junctional intercellular communication and [125I]-EGF binding in hamster fibroblasts. Carcinogenesis 14, 2257-2265.

Hussain, W., Patel, P.M., Chowdhury, R.A., Cabo, C., Ciaccio, E.J., Lab, M.J., Duffy, H.S., Wit, A.L., Peters, N.S., 2010. The Renin-Angiotensin system mediates the effects of stretch on conduction velocity, connexin43 expression, and redistribution in intact ventricle. Journal of cardiovascular electrophysiology 21, 1276-1283.

Iakoucheva, L.M., Radivojac, P., Brown, C.J., O'Connor, T.R., Sikes, J.G., Obradovic, Z., Dunker, A.K., 2004. The importance of intrinsic disorder for protein phosphorylation. Nucleic acids research 32, 1037-1049.

Imanaga, I., Hai, L., Ogawa, K., Matsumura, K., Mayama, T., 2004. Phosphorylation of connexin in functional regulation of the cardiac gap junction. Experimental and clinical cardiology 9, 161-164.

Ingebritsen, T.S., Cohen, P., 1983. The protein phosphatases involved in cellular regulation. 1. Classification and substrate specificities. European journal of biochemistry / FEBS 132, 255-261.

Iravanian, S., Sovari, A.A., Lardin, H.A., Liu, H., Xiao, H.D., Dolmatova, E., Jiao, Z., Harris, B.S., Witham, E.A., Gourdie, R.G., Duffy, H.S., Bernstein, K.E., Dudley, S.C., Jr., 2011. Inhibition of renin-angiotensin system (RAS) reduces ventricular tachycardia risk by altering connexin43. Journal of molecular medicine 89, 677-687.

Irby, R.B., Yeatman, T.J., 2000. Role of Src expression and activation in human cancer. Oncogene 19, 5636-5642.

Ishii, M., Mueller, I., Nakajima, T., Pasquale, E.B., Ogawa, K., 2011. EphB signaling inhibits gap junctional intercellular communication and synchronized contraction in cultured cardiomyocytes. Basic research in cardiology 106, 1057-1068.

Ivanov, A.I., Steiner, A.A., Scheck, A.C., Romanovsky, A.A., 2005. Expression of Eph receptors and their ligands, ephrins, during lipopolysaccharide fever in rats. Physiological genomics 21, 152-160.

Iversen, L.F., Moller, K.B., Pedersen, A.K., Peters, G.H., Petersen, A.S., Andersen, H.S., Branner, S., Mortensen,

S.B., Moller, N.P., 2002. Structure determination of T cell protein-tyrosine phosphatase. The Journal of biological chemistry 277, 19982-19990.

Jensen, R., Glazer, P.M., 2004. Cell-interdependent cisplatin killing by Ku/DNA-dependent protein kinase signaling transduced through gap junctions. Proceedings of the National Academy of Sciences of the United States of America 101, 6134-6139.

Jia, G., Cheng, G., Gangahar, D.M., Agrawal, D.K., 2008. Involvement of connexin 43 in angiotensin II-induced migration and proliferation of saphenous vein smooth muscle cells via the MAPK-AP-1 signaling pathway. Journal of molecular and cellular cardiology 44, 882-890.

John, S.A., Revel, J.P., 1991. Connexon integrity is maintained by non-covalent bonds: intramolecular disulfide bonds link the extracellular domains in rat connexin-43. Biochemical and biophysical research communications 178, 1312-1318.

Johnson, B.A., Blevins, R.A., 1994. NMR View: A computer program for the visualization and analysis of NMR data. Journal of biomolecular NMR 4, 603-614.

Johnson, K.E., Mitra, S., Katoch, P., Kelsey, L.S., Johnson, K.R., Mehta, P.P., 2013. Phosphorylation on Ser-279 and Ser-282 of connexin43 regulates endocytosis and gap junction assembly in pancreatic cancer cells. Molecular biology of the cell 24, 715-733.

Jordan, K., Chodock, R., Hand, A.R., Laird, D.W., 2001. The origin of annular junctions: a mechanism of gap junction internalization. Journal of cell science 114, 763-773.

Kalmatsky, B.D., Bhagan, S., Tang, Q., Bargiello, T.A., Dowd, T.L., 2009. Structural studies of the N-terminus of Connexin 32 using 1H NMR spectroscopy. Archives of biochemistry and biophysics 490, 9-16.

Kanczuga-Koda, L., Wincewicz, A., Fudala, A., Abrycki, T., Famulski, W., Baltaziak, M., Sulkowski, S., Koda, M., 2014. E-cadherin and beta-catenin adhesion proteins correlate positively with connexins in colorectal cancer. Oncology letters 7, 1863-1870.

Kanemitsu, M.Y., Loo, L.W., Simon, S., Lau, A.F., Eckhart, W., 1997. Tyrosine phosphorylation of connexin 43 by v-Src is mediated by SH2 and SH3 domain interactions. J Biol Chem 272, 22824-22831.

Karaghiosoff, M., Neubauer, H., Lassnig, C., Kovarik, P., Schindler, H., Pircher, H., McCoy, B., Bogdan, C., Decker, T., Brem, G., Pfeffer, K., Muller, M., 2000. Partial impairment of cytokine responses in Tyk2-deficient mice. Immunity 13, 549-560.

Kasi, V.S., Xiao, H.D., Shang, L.L., Iravanian, S., Langberg, J., Witham, E.A., Jiao, Z., Gallego, C.J., Bernstein, K.E., Dudley, S.C., Jr., 2007. Cardiac-restricted angiotensin-converting enzyme overexpression causes conduction defects and connexin dysregulation. American journal of physiology. Heart and circulatory physiology 293, H182-192.

Kathiriya, I.S., King, I.N., Murakami, M., Nakagawa, M., Astle, J.M., Gardner, K.A., Gerard, R.D., Olson, E.N., Srivastava, D., Nakagawa, O., 2004. Hairy-related transcription factors inhibit GATA-dependent cardiac gene expression through a signal-responsive mechanism. The Journal of biological chemistry 279, 54937-54943.

Kieken, F., Mutsaers, N., Dolmatova, E., Virgil, K., Wit, A.L., Kellezi, A., Hirst-Jensen, B.J., Duffy, H.S., Sorgen, P.L., 2009. Structural and molecular mechanisms of gap junction remodeling in epicardial border zone myocytes following myocardial infarction. Circulation research 104, 1103-1112.

King, T.J., Fukushima, L.H., Donlon, T.A., Hieber, A.D., Shimabukuro, K.A., Bertram, J.S., 2000. Correlation between growth control, neoplastic potential and endogenous connexin43 expression in HeLa cell lines: implications for tumor progression. Carcinogenesis 21, 311-315.

King, T.J., Lampe, P.D., 200a. The gap junction protein connexin32 is a mouse lung tumor suppressor. Cancer research 64, 7191-7196.

King, T.J., Lampe, P.D., 2004. Mice deficient for the gap junction protein Connexin32 exhibit increased radiation-induced tumorigenesis associated with elevated mitogen-activated protein kinase (p44/Erk1, p42/Erk2) activation. Carcinogenesis 25, 669-680.

Kodama, H., Fukuda, K., Pan, J., Makino, S., Sano, M., Takahashi, T., Hori, S., Ogawa, S., 1998. Biphasic activation of the JAK/STAT pathway by angiotensin II in rat cardiomyocytes. Circulation research 82, 244-250.

Koffler, L.D., Fernstrom, M.J., Akiyama, T.E., Gonzalez, F.J., Ruch, R.J., 2002. Positive regulation of connexin32 transcription by hepatocyte nuclear factor-1alpha. Archives of biochemistry and biophysics 407, 160-167.

Kojima, T., Yamamoto, M., Tobioka, H., Mizuguchi, T., Mitaka, T., Mochizuki, Y., 1996. Changes in cellular distribution of connexins 32 and 26 during formation of gap junctions in primary cultures of rat hepatocytes. Experimental cell research 223, 314-326.

Kopanic, J.L., Sorgen, P.L., 2013. Chemical shift assignments of the connexin45 carboxyl terminal domain: monomer and dimer conformations. Biomolecular NMR assignments 7, 293-297.

Kosinski, C., Li, V.S., Chan, A.S., Zhang, J., Ho, C., Tsui, W.Y., Chan, T.L., Mifflin, R.C., Powell, D.W., Yuen, S.T., Leung, S.Y., Chen, X., 2007. Gene expression patterns of human colon tops and basal crypts and BMP antagonists as intestinal stem cell niche factors. Proceedings of the National Academy of Sciences of the United States of America 104, 15418-15423.

Kostin, S., Dammer, S., Hein, S., Klovekorn, W.P., Bauer, E.P., Schaper, J., 2004. Connexin 43 expression and distribution in compensated and decompensated cardiac hypertrophy in patients with aortic stenosis. Cardiovasc Res 62, 426-436.

Koval, M., 2006. Pathways and control of connexin oligomerization. Trends in cell biology 16, 159-166.

Kruger, O., Plum, A., Kim, J.S., Winterhager, E., Maxeiner, S., Hallas, G., Kirchhoff, S., Traub, O., Lamers, W.H., Willecke, K., 2000. Defective vascular development in connexin 45-deficient mice. Development 127, 4179-4193.

Kurata, W.E., Lau, A.F., 1994. p130gag-fps disrupts gap junctional communication and induces phosphorylation of connexin43 in a manner similar to that of pp60v-src. Oncogene 9, 329-335.

Kyle, J.W., Minogue, P.J., Thomas, B.C., Domowicz, D.A., Berthoud, V.M., Hanck, D.A., Beyer, E.C., 2008. An intact connexin N-terminus is required for function but not gap junction formation. Journal of cell science 121, 2744-2750.

Laing, J.G., Tadros, P.N., Westphale, E.M., Beyer, E.C., 1997. Degradation of connexin43 gap junctions involves both the proteasome and the lysosome. Experimental cell research 236, 482-492.

Laird, D.W., 2006. Life cycle of connexins in health and disease. The Biochemical journal 394, 527-543.

Laird, D.W., 2010. The gap junction proteome and its relationship to disease. Trends in cell biology 20, 92-101.

Laird, D.W., Castillo, M., Kasprzak, L., 1995. Gap junction turnover, intracellular trafficking, and phosphorylation of connexin43 in brefeldin A-treated rat mammary tumor cells. The Journal of cell biology 131, 1193-1203.

Lam, M.H., Michell, B.J., Fodero-Tavoletti, M.T., Kemp, B.E., Tonks, N.K., Tiganis, T., 2001. Cellular stress regulates the nucleocytoplasmic distribution of the protein-tyrosine phosphatase TCPTP. The Journal of biological chemistry 276, 37700-37707.

Lampe, P.D., 1994. Analyzing phorbol ester effects on gap junctional communication: a dramatic inhibition of assembly. J Cell Biol 127, 1895-1905.

Lampe, P.D., Cooper, C.D., King, T.J., Burt, J.M., 2006. Analysis of Connexin43 phosphorylated at S325, S328 and S330 in normoxic and ischemic heart. Journal of cell science 119, 3435-3442.

Lampe, P.D., Kurata, W.E., Warn-Cramer, B.J., Lau, A.F., 1998. Formation of a distinct connexin43 phosphoisoform in mitotic cells is dependent upon p34cdc2 kinase. Journal of cell science 111 (Pt 6), 833-841.

Lampe, P.D., Lau, A.F., 2004. The effects of connexin phosphorylation on gap junctional communication. The international journal of biochemistry & cell biology 36, 1171-1186.

Lampe, P.D., TenBroek, E.M., Burt, J.M., Kurata, W.E., Johnson, R.G., Lau, A.F., 2000. Phosphorylation of connexin43 on serine368 by protein kinase C regulates gap junctional communication. The Journal of cell biology 149, 1503-1512.

Larsen, W.J., Tung, H.N., Murray, S.A., Swenson, C.A., 1979. Evidence for the participation of actin microfilaments and bristle coats in the internalization of gap junction membrane. The Journal of cell biology 83, 576-587.

Lau, A.F., Kanemitsu, M.Y., Kurata, W.E., Danesh, S., Boynton, A.L., 1992. Epidermal growth factor disrupts gap-junctional communication and induces phosphorylation of connexin43 on serine. Molecular biology of the cell 3, 865-874.

Lauf, U., Giepmans, B.N., Lopez, P., Braconnot, S., Chen, S.C., Falk, M.M., 2002. Dynamic trafficking and delivery of connexons to the plasma membrane and accretion to gap junctions in living cells. Proceedings of the National Academy of Sciences of the United States of America 99, 10446-10451.

Lee, H.S., Daar, I.O., 2009. EphrinB reverse signaling in cell-cell adhesion: is it just par for the course? Cell adhesion & migration 3, 250-255.

Leonard, W.J., 2001. Role of Jak kinases and STATs in cytokine signal transduction. Int J Hematol 73, 271-277.

Leykauf, K., Salek, M., Bomke, J., Frech, M., Lehmann, W.D., Durst, M., Alonso, A., 2006. Ubiquitin protein ligase Nedd4 binds to connexin43 by a phosphorylation-modulated process. Journal of cell science 119, 3634-3642.

Lezcano, V., Bellido, T., Plotkin, L.I., Boland, R., Morelli, S., 2014. Osteoblastic protein tyrosine phosphatases inhibition and connexin 43 phosphorylation by alendronate. Experimental cell research 324, 30-39.

Li, B., Antonyak, M.A., Druso, J.E., Cheng, L., Nikitin, A.Y., Cerione, R.A., 2010. EGF potentiated oncogenesis requires a tissue transglutaminase-dependent signaling pathway leading to Src activation. Proceedings of the National Academy of Sciences of the United States of America 107, 1408-1413.

Li, H., Spagnol, G., Naslavsky, N., Caplan, S., Sorgen, P.L., 2014. TC-PTP directly interacts with connexin43 to regulate gap junction intercellular communication. Journal of cell science 127, 3269-3279.

Li, H., Spagnol, G., Zheng, L., Stauch, K.L., Sorgen, P.L., 2016. Regulation of Connexin43 function and expression by Tyrosine kinase 2. The Journal of biological chemistry.

Li, W.E., Nagy, J.I., 2000. Connexin43 phosphorylation state and intercellular communication in cultured astrocytes following hypoxia and protein phosphatase inhibition. The European journal of neuroscience 12, 2644-2650.

Li, X., Olson, C., Lu, S., Kamasawa, N., Yasumura, T., Rash, J.E., Nagy, J.I., 2004. Neuronal connexin36 association with zonula occludens-1 protein (ZO-1) in mouse brain and interaction with the first PDZ domain

of ZO-1. The European journal of neuroscience 19, 2132-2146.

Liao, C.K., Jeng, C.J., Wang, H.S., Wang, S.H., Wu, J.C., 2013. Lipopolysaccharide induces degradation of connexin43 in rat astrocytes via the ubiquitin-proteasome proteolytic pathway. PloS one 8, e79350.

Lichtenstein, A., Minogue, P.J., Beyer, E.C., Berthoud, V.M., 2011. Autophagy: a pathway that contributes to connexin degradation. Journal of cell science 124, 910-920.

Lidington, D., Tyml, K., Ouellette, Y., 2002. Lipopolysaccharide-induced reductions in cellular coupling correlate with tyrosine phosphorylation of connexin 43. Journal of cellular physiology 193, 373-379.

Lim, W., Mayer, B., Pawson, T., 2014. Cell signaling : principles and mechanisms.

Lin, D., Boyle, D.L., Takemoto, D.J., 2003. IGF-I-induced phosphorylation of connexin 43 by PKCgamma: regulation of gap junctions in rabbit lens epithelial cells. Investigative ophthalmology & visual science 44, 1160-1168.

Lin, R., Warn-Cramer, B.J., Kurata, W.E., Lau, A.F., 2001. v-Src-mediated phosphorylation of connexin43 on tyrosine disrupts gap junctional communication in mammalian cells. Cell Commun Adhes 8, 265-269.

Lin, R., Warn-Cramer, B.J., Kurata, W.E., Lau, A.F., 2001. v-Src phosphorylation of connexin 43 on Tyr247 and Tyr265 disrupts gap junctional communication. The Journal of cell biology 154, 815-827.

Linhares, V.L., Almeida, N.A., Menezes, D.C., Elliott, D.A., Lai, D., Beyer, E.C., Campos de Carvalho, A.C., Costa, M.W., 2004. Transcriptional regulation of the murine Connexin40 promoter by cardiac factors Nkx2-5, GATA4 and Tbx5. Cardiovascular research 64, 402-411.

Lisabeth, E.M., Falivelli, G., Pasquale, E.B., 2013. Eph receptor signaling and ephrins. Cold Spring Harbor perspectives in biology 5.

Liu, H., Huang, R.Y., Chen, J., Gross, M.L., Pakrasi, H.B., 2011. Psb27, a transiently associated protein, binds to the chlorophyll binding protein CP43 in photosystem II assembly intermediates. Proceedings of the National Academy of Sciences of the United States of America 108, 18536-18541.

Liu, S., Taffet, S., Stoner, L., Delmar, M., Vallano, M.L., Jalife, J., 1993. A structural basis for the unequal sensitivity of the major cardiac and liver gap junctions to intracellular acidification: the carboxyl tail length. Biophysical journal 64, 1422-1433.

Locke, D., Koreen, I.V., Harris, A.L., 2006. Isoelectric points and post-translational modifications of connexin26 and connexin32. FASEB journal : official publication of the Federation of American Societies for Experimental Biology 20, 1221-1223.

Lonn, E.M., Yusuf, S., Jha, P., Montague, T.J., Teo, K.K., Benedict, C.R., Pitt, B., 1994. Emerging role of angiotensin-converting enzyme inhibitors in cardiac and vascular protection. Circulation 90, 2056-2069.

Loo, L.W., Berestecky, J.M., Kanemitsu, M.Y., Lau, A.F., 1995. pp60src-mediated phosphorylation of connexin 43, a gap junction protein. The Journal of biological chemistry 270, 12751-12761.

Lowenstein, W.R., 1985. Regulation of cell-to-cell communication by phosphorylation. Biochemical Society symposium 50, 43-58.

Lu, X., Chen, J., Sasmono, R.T., Hsi, E.D., Sarosiek, K.A., Tiganis, T., Lossos, I.S., 2007. T-cell protein tyrosine phosphatase, distinctively expressed in activated-B-cell-like diffuse large B-cell lymphomas, is the nuclear phosphatase of STAT6. Molecular and cellular biology 27, 2166-2179.

Luft, F.C., 2011. Connecting the renin-angiotensin-aldosterone system with sudden death. Journal of molecular medicine 89, 631-633.

Lundby, A., Andersen, M.N., Steffensen, A.B., Horn, H., Kelstrup, C.D., Francavilla, C., Jensen, L.J., Schmitt,

N., Thomsen, M.B., Olsen, J.V., 2013. In vivo phosphoproteomics analysis reveals the cardiac targets of beta-adrenergic receptor signaling. Science signaling 6, rs11.

Lurtz, M.M., Louis, C.F., 2007. Intracellular calcium regulation of connexin43. American journal of physiology. Cell physiology 293, C1806-1813.

Maeda, S., Nakagawa, S., Suga, M., Yamashita, E., Oshima, A., Fujiyoshi, Y., Tsukihara, T., 2009. Structure of the connexin 26 gap junction channel at 3.5 A resolution. Nature 458, 597-602.

Maqbool, R., Rashid, R., Ismail, R., Niaz, S., Chowdri, N.A., Hussain, M.U., 2015. The carboxy-terminal domain of connexin 43 (CT-Cx43) modulates the expression of p53 by altering miR-125b expression in low-grade human breast cancers. Cellular oncology 38, 443-451.

Marone, M., Mozzetti, S., De Ritis, D., Pierelli, L., Scambia, G., 2001. Semiquantitative RT-PCR analysis to assess the expression levels of multiple transcripts from the same sample. Biological procedures online 3, 19-25.

Marrero, M.B., Schieffer, B., Paxton, W.G., Duff, J.L., Berk, B.C., Bernstein, K.E., 1995. The role of tyrosine phosphorylation in angiotensin II-mediated intracellular signalling. Cardiovasc Res 30, 530-536.

Martin, P.E., Mambetisaeva, E.T., Archer, D.A., George, C.H., Evans, W.H., 2000. Analysis of gap junction assembly using mutated connexins detected in Charcot-Marie-Tooth X-linked disease. Journal of neurochemistry 74, 711-720.

Martinez, A.D., Acuna, R., Figueroa, V., Maripillan, J., Nicholson, B., 2009. Gap-junction channels dysfunction in deafness and hearing loss. Antioxidants & redox signaling 11, 309-322.

Matesic, D.F., Rupp, H.L., Bonney, W.J., Ruch, R.J., Trosko, J.E., 1994. Changes in gap-junction permeability, phosphorylation, and number mediated by phorbol ester and non-phorbol-ester tumor promoters in rat liver epithelial cells. Molecular carcinogenesis 10, 226-236.

Mayerhofer, A., Dissen, G.A., Parrott, J.A., Hill, D.F., Mayerhofer, D., Garfield, R.E., Costa, M.E., Skinner, M.K., Ojeda, S.R., 1996. Involvement of nerve growth factor in the ovulatory cascade: trkA receptor activation inhibits gap junctional communication between thecal cells. Endocrinology 137, 5662-5670.

Mazet, F., Wittenberg, B.A., Spray, D.C., 1985. Fate of intercellular junctions in isolated adult rat cardiac cells. Circulation research 56, 195-204.

McLachlan, E., Shao, Q., Laird, D.W., 2007. Connexins and gap junctions in mammary gland development and breast cancer progression. The Journal of membrane biology 218, 107-121.

Mehta, P.P., Hotz-Wagenblatt, A., Rose, B., Shalloway, D., Loewenstein, W.R., 1991. Incorporation of the gene for a cell-cell channel protein into transformed cells leads to normalization of growth. The Journal of membrane biology 124, 207-225.

Mehta, P.P., Perez-Stable, C., Nadji, M., Mian, M., Asotra, K., Roos, B.A., 1999. Suppression of human prostate cancer cell growth by forced expression of connexin genes. Developmental genetics 24, 91-110.

Meilleur, M.A., Akpovi, C.D., Pelletier, R.M., Vitale, M.L., 2007. Tumor necrosis factor-alpha-induced anterior pituitary folliculostellate TtT/GF cell uncoupling is mediated by connexin 43 dephosphorylation. Endocrinology 148, 5913-5924.

Melendez, J., Welch, S., Schaefer, E., Moravec, C.S., Avraham, S., Avraham, H., Sussman, M.A., 2002. Activation of pyk2/related focal adhesion tyrosine kinase and focal adhesion kinase in cardiac remodeling. J Biol Chem 277, 45203-45210.

Mendoza-Naranjo, A., Bouma, G., Pereda, C., Ramirez, M., Webb, K.F., Tittarelli, A., Lopez, M.N., Kalergis,

A.M., Thrasher, A.J., Becker, D.L., Salazar-Onfray, F., 2011. Functional gap junctions accumulate at the immunological synapse and contribute to T cell activation. Journal of immunology 187, 3121-3132.

Mennecier, G., Derangeon, M., Coronas, V., Herve, J.C., Mesnil, M., 2008. Aberrant expression and localization of connexin43 and connexin30 in a rat glioma cell line. Molecular carcinogenesis 47, 391-401.

Minegishi, Y., Saito, M., Morio, T., Watanabe, K., Agematsu, K., Tsuchiya, S., Takada, H., Hara, T., Kawamura, N., Ariga, T., Kaneko, H., Kondo, N., Tsuge, I., Yachie, A., Sakiyama, Y., Iwata, T., Bessho, F., Ohishi, T., Joh, K., Imai, K., Kogawa, K., Shinohara, M., Fujieda, M., Wakiguchi, H., Pasic, S., Abinun, M., Ochs, H.D., Renner, E.D., Jansson, A., Belohradsky, B.H., Metin, A., Shimizu, N., Mizutani, S., Miyawaki, T., Nonoyama, S., Karasuyama, H., 2006. Human tyrosine kinase 2 deficiency reveals its requisite roles in multiple cytokine signals involved in innate and acquired immunity. Immunity 25, 745-755.

Mitchell, J.A., Lye, S.J., 2002. Differential expression of activator protein-1 transcription factors in pregnant rat myometrium. Biology of reproduction 67, 240-246.

Mitra, S., Annamalai, L., Chakraborty, S., Johnson, K., Song, X.H., Batra, S.K., Mehta, P.P., 2006. Androgen-regulated formation and degradation of gap junctions in androgen-responsive human prostate cancer cells. Molecular biology of the cell 17, 5400-5416.

Mitra, S.S., Xu, J., Nicholson, B.J., 2012. Coregulation of multiple signaling mechanisms in pp60v-Src-induced closure of Cx43 gap junction channels. The Journal of membrane biology 245, 495-506.

Moorby, C., Patel, M., 2001. Dual functions for connexins: Cx43 regulates growth independently of gap junction formation. Experimental cell research 271, 238-248.

Morel, S., Burnier, L., Kwak, B.R., 2009. Connexins participate in the initiation and progression of atherosclerosis. Seminars in immunopathology 31, 49-61.

Morley, G.E., Taffet, S.M., Delmar, M., 1996. Intramolecular interactions mediate pH regulation of connexin43 channels. Biophysical journal 70, 1294-1302.

Murakami, Y., Nakano, S., Niho, Y., Hamasaki, N., Izuhara, K., 1998. Constitutive activation of Jak-2 and Tyk-2 in a v-Src-transformed human gallbladder adenocarcinoma cell line. J Cell Physiol 175, 220-228.

Murray, S.A., Williams, S.Y., Dillard, C.Y., Narayanan, S.K., McCauley, J., 1997. Relationship of cytoskeletal filaments to annular gap junction expression in human adrenal cortical tumor cells in culture. Experimental cell research 234, 398-404.

Musil, L.S., Goodenough, D.A., 1991. Biochemical analysis of connexin43 intracellular transport, phosphorylation, and assembly into gap junctional plaques. The Journal of cell biology 115, 1357-1374.

Myers, M.P., Andersen, J.N., Cheng, A., Tremblay, M.L., Horvath, C.M., Parisien, J.P., Salmeen, A., Barford, D., Tonks, N.K., 2001. TYK2 and JAK2 are substrates of protein-tyrosine phosphatase 1B. The Journal of biological chemistry 276, 47771-47774.

Naitoh, K., Yano, T., Miura, T., Itoh, T., Miki, T., Tanno, M., Sato, T., Hotta, H., Terashima, Y., Shimamoto, K., 2009. Roles of Cx43-associated protein kinases in suppression of gap junction-mediated chemical coupling by ischemic preconditioning. American journal of physiology. Heart and circulatory physiology 296, H396-403.

Nakazawa, T., Komai, S., Tezuka, T., Hisatsune, C., Umemori, H., Semba, K., Mishina, M., Manabe, T., Yamamoto, T., 2001. Characterization of Fyn-mediated tyrosine phosphorylation sites on GluR epsilon 2 (NR2B) subunit of the N-methyl-D-aspartate receptor. J Biol Chem 276, 693-699.

Naus, C.C., Hearn, S., Zhu, D., Nicholson, B.J., Shivers, R.R., 1993. Ultrastructural analysis of gap junctions in

C6 glioma cells transfected with connexin43 cDNA. Experimental cell research 206, 72-84.

Naus, C.C., Laird, D.W., 2010. Implications and challenges of connexin connections to cancer. Nature reviews. Cancer 10, 435-441.

Neumann, E., Hermanns, H., Barthel, F., Werdehausen, R., Brandenburger, T., 2015. Expression changes of microRNA-1 and its targets Connexin 43 and brain-derived neurotrophic factor in the peripheral nervous system of chronic neuropathic rats. Molecular pain 11, 39.

Nezvitsky, L., Tremblay, M.L., Takano, T., Papillon, J., Cybulsky, A.V., 2014. Complement-mediated glomerular injury is reduced by inhibition of protein-tyrosine phosphatase 1B. American journal of physiology. Renal physiology 307, F634-647.

Nimlamool, W., Andrews, R.M., Falk, M.M., 2015. Connexin43 phosphorylation by PKC and MAPK signals VEGF-mediated gap junction internalization. Molecular biology of the cell 26, 2755-2768.

Nishi, H., Hashimoto, K., Panchenko, A.R., 2011. Phosphorylation in protein-protein binding: effect on stability and function. Structure 19, 1807-1815.

Ogawa, T., Hayashi, T., Tokunou, M., Nakachi, K., Trosko, J.E., Chang, C.C., Yorioka, N., 2005. Suberoylanilide hydroxamic acid enhances gap junctional intercellular communication via acetylation of histone containing connexin 43 gene locus. Cancer research 65, 9771-9778.

Oh, S., Rubin, J.B., Bennett, M.V., Verselis, V.K., Bargiello, T.A., 1999. Molecular determinants of electrical rectification of single channel conductance in gap junctions formed by connexins 26 and 32. The Journal of general physiology 114, 339-364.

Ohshima, Y., Tsukimoto, M., Harada, H., Kojima, S., 2012. Involvement of connexin43 hemichannel in ATP release after gamma-irradiation. Journal of radiation research 53, 551-557.

Ou, C.W., Orsino, A., Lye, S.J., 1997. Expression of connexin-43 and connexin-26 in the rat myometrium during pregnancy and labor is differentially regulated by mechanical and hormonal signals. Endocrinology 138, 5398-5407.

Oviedo-Orta, E., Perreau, M., Evans, W.H., Potolicchio, I., 2010. Control of the proliferation of activated CD4+ T cells by connexins. Journal of leukocyte biology 88, 79-86.

Oyamada, M., Oyamada, Y., Takamatsu, T., 2005. Regulation of connexin expression. Biochimica et biophysica acta 1719, 6-23.

Oyamada, Y., Zhou, W., Oyamada, H., Takamatsu, T., Oyamada, M., 2002. Dominant-negative connexin43-EGFP inhibits calcium-transient synchronization of primary neonatal rat cardiomyocytes. Experimental cell research 273, 85-94.

Ozog, M.A., Bernier, S.M., Bates, D.C., Chatterjee, B., Lo, C.W., Naus, C.C., 2004. The complex of ciliary neurotrophic factor-ciliary neurotrophic factor receptor alpha up-regulates connexin43 and intercellular coupling in astrocytes via the Janus tyrosine kinase/signal transducer and activator of transcription pathway. Molecular biology of the cell 15, 4761-4774.

Pagliaro, P., Penna, C., 2005. Rethinking the renin-angiotensin system and its role in cardiovascular regulation. Cardiovascular drugs and therapy / sponsored by the International Society of Cardiovascular Pharmacotherapy 19, 77-87.

Palacios-Prado, N., Sonntag, S., Skeberdis, V.A., Willecke, K., Bukauskas, F.F., 2009. Gating, permselectivity and pH-dependent modulation of channels formed by connexin57, a major connexin of horizontal cells in the mouse retina. The Journal of physiology 587, 3251-3269.

Palatinus, J.A., Rhett, J.M., Gourdie, R.G., 2012. The connexin43 carboxyl terminus and cardiac gap junction organization. Biochimica et biophysica acta 1818, 1831-1843.

Pan, J., Fukuda, K., Kodama, H., Makino, S., Takahashi, T., Sano, M., Hori, S., Ogawa, S., 1997. Role of angiotensin II in activation of the JAK/STAT pathway induced by acute pressure overload in the rat heart. Circulation research 81, 611-617.

Pan, J., Fukuda, K., Saito, M., Matsuzaki, J., Kodama, H., Sano, M., Takahashi, T., Kato, T., Ogawa, S., 1999. Mechanical stretch activates the JAK/STAT pathway in rat cardiomyocytes. Circ Res 84, 1127-1136.

Park, D.J., Wallick, C.J., Martyn, K.D., Lau, A.F., Jin, C., Warn-Cramer, B.J., 2007. Akt phosphorylates Connexin43 on Ser373, a "mode-1" binding site for 14-3-3. Cell communication & adhesion 14, 211-226.

Park, I., Lee, H.S., 2015. EphB/ephrinB signaling in cell adhesion and migration. Molecules and cells 38, 14-19.

Pasquale, E.B., 2008. Eph-ephrin bidirectional signaling in physiology and disease. Cell 133, 38-52.

Paulson, A.F., Lampe, P.D., Meyer, R.A., TenBroek, E., Atkinson, M.M., Walseth, T.F., Johnson, R.G., 2000. Cyclic AMP and LDL trigger a rapid enhancement in gap junction assembly through a stimulation of connexin trafficking. Journal of cell science 113 (Pt 17), 3037-3049.

Pelletier, R.M., Akpovi, C.D., Chen, L., Kumar, N.M., Vitale, M.L., 2015. Complementary expression and phosphorylation of Cx46 and Cx50 during development and following gene deletion in mouse and in normal and orchitic mink testes. American journal of physiology. Regulatory, integrative and comparative physiology 309, R255-276.

Peracchia, C., Bernardini, G., Peracchia, L.L., 1983. Is calmodulin involved in the regulation of gap junction permeability? Pflugers Archiv : European journal of physiology 399, 152-154.

Peracchia, C., Sotkis, A., Wang, X.G., Peracchia, L.L., Persechini, A., 2000. Calmodulin directly gates gap junction channels. The Journal of biological chemistry 275, 26220-26224.

Peracchia, C., Wang, X.C., 1997. Connexin domains relevant to the chemical gating of gap junction channels. Brazilian journal of medical and biological research = Revista brasileira de pesquisas medicas e biologicas / Sociedade Brasileira de Biofisica 30, 577-590.

Peracchia, C., Wang, X.G., Peracchia, L.L., 2000. Slow gating of gap junction channels and calmodulin. The Journal of membrane biology 178, 55-70.

Peracchia, C., Young, K.C., Wang, X.G., Peracchia, L.L., 2003. Is the voltage gate of connexins CO2-sensitive? Cx45 channels and inhibition of calmodulin expression. The Journal of membrane biology 195, 53-62.

Peters, G.H., Iversen, L.F., Branner, S., Andersen, H.S., Mortensen, S.B., Olsen, O.H., Moller, K.B., Moller, N.P., 2000. Residue 259 is a key determinant of substrate specificity of protein-tyrosine phosphatases 1B and alpha. The Journal of biological chemistry 275, 18201-18209.

Peterson-Roth, E., Brdlik, C.M., Glazer, P.M., 2009. Src-Induced cisplatin resistance mediated by cell-to-cell communication. Cancer research 69, 3619-3624.

Petrocelli, T., Lye, S.J., 1993. Regulation of transcripts encoding the myometrial gap junction protein, connexin-43, by estrogen and progesterone. Endocrinology 133, 284-290.

Pfeffer, M.A., Braunwald, E., Moye, L.A., Basta, L., Brown, E.J., Jr., Cuddy, T.E., Davis, B.R., Geltman, E.M., Goldman, S., Flaker, G.C., et al., 1992. Effect of captopril on mortality and morbidity in patients with left ventricular dysfunction after myocardial infarction. Results of the survival and ventricular enlargement trial. The SAVE Investigators. N Engl J Med 327, 669-677.

Pfeifer, I., Anderson, C., Werner, R., Oltra, E., 2004. Redefining the structure of the mouse connexin43 gene: selective promoter usage and alternative splicing mechanisms yield transcripts with different translational efficiencies. Nucleic acids research 32, 4550-4562.

Phelan, P., Bacon, J.P., Davies, J.A., Stebbings, L.A., Todman, M.G., Avery, L., Baines, R.A., Barnes, T.M., Ford, C., Hekimi, S., Lee, R., Shaw, J.E., Starich, T.A., Curtin, K.D., Sun, Y.A., Wyman, R.J., 1998. Innexins: a family of invertebrate gap-junction proteins. Trends in genetics : TIG 14, 348-349.

Piechocki, M.P., Burk, R.D., Ruch, R.J., 1999. Regulation of connexin32 and connexin43 gene expression by DNA methylation in rat liver cells. Carcinogenesis 20, 401-406.

Piechocki, M.P., Toti, R.M., Fernstrom, M.J., Burk, R.D., Ruch, R.J., 2000. Liver cell-specific transcriptional regulation of connexin32. Biochimica et biophysica acta 1491, 107-122.

Piehl, M., Lehmann, C., Gumpert, A., Denizot, J.P., Segretain, D., Falk, M.M., 2007. Internalization of large double-membrane intercellular vesicles by a clathrin-dependent endocytic process. Molecular biology of the cell 18, 337-347.

Pogoda, K., Kameritsch, P., Retamal, M.A., Vega, J.L., 2016. Regulation of gap junction channels and hemichannels by phosphorylation and redox changes: a revision. BMC cell biology 17 Suppl 1, 11.

Poliakov, A., Cotrina, M., Wilkinson, D.G., 2004. Diverse roles of eph receptors and ephrins in the regulation of cell migration and tissue assembly. Developmental cell 7, 465-480.

Presley, C.A., Lee, A.W., Kastl, B., Igbinosa, I., Yamada, Y., Fishman, G.I., Gutstein, D.E., Cancelas, J.A., 2005. Bone marrow connexin-43 expression is critical for hematopoietic regeneration after chemotherapy. Cell communication & adhesion 12, 307-317.

Purnick, P.E., Benjamin, D.C., Verselis, V.K., Bargiello, T.A., Dowd, T.L., 2000. Structure of the amino terminus of a gap junction protein. Archives of biochemistry and biophysics 381, 181-190.

Purnick, P.E., Oh, S., Abrams, C.K., Verselis, V.K., Bargiello, T.A., 2000. Reversal of the gating polarity of gap junctions by negative charge substitutions in the N-terminus of connexin 32. Biophysical journal 79, 2403-2415.

Qin, H., Shao, Q., Igdoura, S.A., Alaoui-Jamali, M.A., Laird, D.W., 2003. Lysosomal and proteasomal degradation play distinct roles in the life cycle of Cx43 in gap junctional intercellular communication-deficient and -competent breast tumor cells. The Journal of biological chemistry 278, 30005-30014.

Qu, C., Gardner, P., Schrijver, I., 2009. The role of the cytoskeleton in the formation of gap junctions by Connexin 30. Experimental cell research 315, 1683-1692.

Rabionet, R., Lopez-Bigas, N., Arbones, M.L., Estivill, X., 2002. Connexin mutations in hearing loss, dermatological and neurological disorders. Trends in molecular medicine 8, 205-212.

Rackauskas, M., Neverauskas, V., Skeberdis, V.A., 2010. Diversity and properties of connexin gap junction channels. Medicina 46, 1-12.

Rackauskas, M., Verselis, V.K., Bukauskas, F.F., 2007. Permeability of homotypic and heterotypic gap junction channels formed of cardiac connexins mCx30.2, Cx40, Cx43, and Cx45. American journal of physiology. Heart and circulatory physiology 293, H1729-1736.

Rash, J.E., Davidson, K.G., Kamasawa, N., Yasumura, T., Kamasawa, M., Zhang, C., Michaels, R., Restrepo, D., Ottersen, O.P., Olson, C.O., Nagy, J.I., 2005. Ultrastructural localization of connexins (Cx36, Cx43, Cx45), glutamate receptors and aquaporin-4 in rodent olfactory mucosa, olfactory nerve and olfactory bulb. Journal of neurocytology 34, 307-341.

Reaume, A.G., de Sousa, P.A., Kulkarni, S., Langille, B.L., Zhu, D., Davies, T.C., Juneja, S.C., Kidder, G.M., Rossant, J., 1995. Cardiac malformation in neonatal mice lacking connexin43. Science 267, 1831-1834.

Ren, L., Chen, X., Luechapanichkul, R., Selner, N.G., Meyer, T.M., Wavreille, A.S., Chan, R., Iorio, C., Zhou, X., Neel, B.G., Pei, D., 2011. Substrate specificity of protein tyrosine phosphatases 1B, RPTPalpha, SHP-1, and SHP-2. Biochemistry 50, 2339-2356.

Revilla, A., Bennett, M.V., Barrio, L.C., 2000. Molecular determinants of membrane potential dependence in vertebrate gap junction channels. Proceedings of the National Academy of Sciences of the United States of America 97, 14760-14765.

Revilla, A., Castro, C., Barrio, L.C., 1999. Molecular dissection of transjunctional voltage dependence in the connexin-32 and connexin-43 junctions. Biophysical journal 77, 1374-1383.

Rosenzweig, T., Aga-Mizrachi, S., Bak, A., Sampson, S.R., 2004. Src tyrosine kinase regulates insulin-induced activation of protein kinase C (PKC) delta in skeletal muscle. Cellular signalling 16, 1299-1308.

Rutledge, C.A., Ng, F.S., Sulkin, M.S., Greener, I.D., Sergeyenko, A.M., Liu, H., Gemel, J., Beyer, E.C., Sovari, A.A., Efimov, I.R., Dudley, S.C., 2014. c-Src kinase inhibition reduces arrhythmia inducibility and connexin43 dysregulation after myocardial infarction. Journal of the American College of Cardiology 63, 928-934.

Sadoshima, J., Izumo, S., 1993. Molecular characterization of angiotensin II--induced hypertrophy of cardiac myocytes and hyperplasia of cardiac fibroblasts. Critical role of the AT1 receptor subtype. Circulation research 73, 413-423.

Saez, J.C., Nairn, A.C., Czernik, A.J., Fishman, G.I., Spray, D.C., Hertzberg, E.L., 1997. Phosphorylation of connexin43 and the regulation of neonatal rat cardiac myocyte gap junctions. J Mol Cell Cardiol 29, 2131-2145.

Saez, J.C., Nairn, A.C., Czernik, A.J., Spray, D.C., Hertzberg, E.L., Greengard, P., Bennett, M.V., 1990. Phosphorylation of connexin 32, a hepatocyte gap-junction protein, by cAMP-dependent protein kinase, protein kinase C and Ca2+/calmodulin-dependent protein kinase II. European journal of biochemistry / FEBS 192, 263-273.

Saez, J.C., Spray, D.C., Nairn, A.C., Hertzberg, E., Greengard, P., Bennett, M.V., 1986. cAMP increases junctional conductance and stimulates phosphorylation of the 27-kDa principal gap junction polypeptide. Proceedings of the National Academy of Sciences of the United States of America 83, 2473-2477.

Saidi Brikci-Nigassa, A., Clement, M.J., Ha-Duong, T., Adjadj, E., Ziani, L., Pastre, D., Curmi, P.A., Savarin, P., 2012. Phosphorylation controls the interaction of the connexin43 C-terminal domain with tubulin and microtubules. Biochemistry 51, 4331-4342.

Sakurai, T., Tsuchida, M., Lampe, P.D., Murakami, M., 2013. Cardiomyocyte FGF signaling is required for Cx43 phosphorylation and cardiac gap junction maintenance. Experimental cell research 319, 2152-2165.

Sato, K., Shiota, M., Fukuda, S., Iwamoto, E., Machida, H., Inamine, T., Kondo, S., Yanagihara, K., Isomoto, H., Mizuta, Y., Kohno, S., Tsukamoto, K., 2009. Strong evidence of a combination polymorphism of the tyrosine kinase 2 gene and the signal transducer and activator of transcription 3 gene as a DNA-based biomarker for susceptibility to Crohn's disease in the Japanese population. J Clin Immunol 29, 815-825.

Savitski, M.M., Lemeer, S., Boesche, M., Lang, M., Mathieson, T., Bantscheff, M., Kuster, B., 2011. Confident phosphorylation site localization using the Mascot Delta Score. Molecular & cellular proteomics : MCP 10, M110 003830.

Saxon, M.L., Zhao, X., Black, J.D., 1994. Activation of protein kinase C isozymes is associated with post-mitotic

events in intestinal epithelial cells in situ. The Journal of cell biology 126, 747-763.

Scherer, S.S., Xu, Y.T., Nelles, E., Fischbeck, K., Willecke, K., Bone, L.J., 1998. Connexin32-null mice develop demyelinating peripheral neuropathy. Glia 24, 8-20.

Schneider, C.A., Rasband, W.S., Eliceiri, K.W., 2012. NIH Image to ImageJ: 25 years of image analysis. Nature methods 9, 671-675.

Schubert, A.L., Schubert, W., Spray, D.C., Lisanti, M.P., 2002. Connexin family members target to lipid raft domains and interact with caveolin-1. Biochemistry 41, 5754-5764.

Seki, A., Coombs, W., Taffet, S.M., Delmar, M., 2004. Loss of electrical communication, but not plaque formation, after mutations in the cytoplasmic loop of connexin43. Heart rhythm : the official journal of the Heart Rhythm Society 1, 227-233.

Severs, N.J., 1985. Intercellular junctions and the cardiac intercalated disk. Advances in myocardiology 5, 223-242.

Severs, N.J., 2001. Gap junction remodeling and cardiac arrhythmogenesis: cause or coincidence? Journal of cellular and molecular medicine 5, 355-366.

Severs, N.J., Dupont, E., Thomas, N., Kaba, R., Rothery, S., Jain, R., Sharpey, K., Fry, C.H., 2006. Alterations in cardiac connexin expression in cardiomyopathies. Advances in cardiology 42, 228-242.

Shah, M.M., Martinez, A.M., Fletcher, W.H., 2002. The connexin43 gap junction protein is phosphorylated by protein kinase A and protein kinase C: in vivo and in vitro studies. Molecular and cellular biochemistry 238, 57-68.

Shaw, R.M., Fay, A.J., Puthenveedu, M.A., von Zastrow, M., Jan, Y.N., Jan, L.Y., 2007. Microtubule plus-end-tracking proteins target gap junctions directly from the cell interior to adherens junctions. Cell 128, 547-560.

Shibayama, J., Paznekas, W., Seki, A., Taffet, S., Jabs, E.W., Delmar, M., Musa, H., 2005. Functional characterization of connexin43 mutations found in patients with oculodentodigital dysplasia. Circulation research 96, e83-91.

Shimizu, K., Shimoichi, Y., Hinotsume, D., Itsuzaki, Y., Fujii, H., Honoki, K., Tsujiuchi, T., 2006. Reduced expression of the Connexin26 gene and its aberrant DNA methylation in rat lung adenocarcinomas induced by N-nitrosobis(2-hydroxypropyl)amine. Molecular carcinogenesis 45, 710-714.

Simoncic, P.D., Lee-Loy, A., Barber, D.L., Tremblay, M.L., McGlade, C.J., 2002. The T cell protein tyrosine phosphatase is a negative regulator of janus family kinases 1 and 3. Current biology : CB 12, 446-453.

Singh, D., Lampe, P.D., 2003. Identification of connexin-43 interacting proteins. Cell communication & adhesion 10, 215-220.

Sirnes, S., Honne, H., Ahmed, D., Danielsen, S.A., Rognum, T.O., Meling, G.I., Leithe, E., Rivedal, E., Lothe, R.A., Lind, G.E., 2011. DNA methylation analyses of the connexin gene family reveal silencing of GJC1 (Connexin45) by promoter hypermethylation in colorectal cancer. Epigenetics 6, 602-609.

Sirnes, S., Leithe, E., Rivedal, E., 2008. The detergent resistance of Connexin43 is lost upon TPA or EGF treatment and is an early step in gap junction endocytosis. Biochem Biophys Res Commun 373, 597-601.

Sirnes, S., Lind, G.E., Bruun, J., Fykerud, T.A., Mesnil, M., Lothe, R.A., Rivedal, E., Kolberg, M., Leithe, E., 2015. Connexins in colorectal cancer pathogenesis. International journal of cancer 137, 1-11.

Smart, J.E., Oppermann, H., Czernilofsky, A.P., Purchio, A.F., Erikson, R.L., Bishop, J.M., 1981. Characterization of sites for tyrosine phosphorylation in the transforming protein of Rous sarcoma virus (pp60v-src) and its normal cellular homologue (pp60c-src). Proceedings of the National Academy of Sciences

of the United States of America 78, 6013-6017.

Smith, C.L., Debouck, C., Rosenberg, M., Culp, J.S., 1989. Phosphorylation of serine residue 89 of human adenovirus E1A proteins is responsible for their characteristic electrophoretic mobility shifts, and its mutation affects biological function. Journal of virology 63, 1569-1577.

Smyth, J.W., Hong, T.T., Gao, D., Vogan, J.M., Jensen, B.C., Fong, T.S., Simpson, P.C., Stainier, D.Y., Chi, N.C., Shaw, R.M., 2010. Limited forward trafficking of connexin 43 reduces cell-cell coupling in stressed human and mouse myocardium. J Clin Invest 120, 266-279.

Sohl, G., Willecke, K., 2004. Gap junctions and the connexin protein family. Cardiovascular research 62, 228-232.

Solan, J.L., Lampe, P.D., 2005. Connexin phosphorylation as a regulatory event linked to gap junction channel assembly. Biochimica et biophysica acta 1711, 154-163.

Solan, J.L., Lampe, P.D., 2007. Key connexin 43 phosphorylation events regulate the gap junction life cycle. The Journal of membrane biology 217, 35-41.

Solan, J.L., Lampe, P.D., 2008. Connexin 43 in LA-25 cells with active v-src is phosphorylated on Y247, Y265, S262, S279/282, and S368 via multiple signaling pathways. Cell communication & adhesion 15, 75-84.

Solan, J.L., Lampe, P.D., 2009. Connexin43 phosphorylation: structural changes and biological effects. The Biochemical journal 419, 261-272.

Solan, J.L., Lampe, P.D., 2014. Specific Cx43 phosphorylation events regulate gap junction turnover in vivo. FEBS letters 588, 1423-1429.

Solan, J.L., Lampe, P.D., 2016. Kinase programs spatiotemporally regulate gap junction assembly and disassembly: Effects on wound repair. Seminars in cell & developmental biology 50, 40-48.

Solan, J.L., Marquez-Rosado, L., Sorgen, P.L., Thornton, P.J., Gafken, P.R., Lampe, P.D., 2007. Phosphorylation at S365 is a gatekeeper event that changes the structure of Cx43 and prevents down-regulation by PKC. The Journal of cell biology 179, 1301-1309.

Sorgen, P.L., Duffy, H.S., Sahoo, P., Coombs, W., Delmar, M., Spray, D.C., 2004. Structural changes in the carboxyl terminus of the gap junction protein connexin43 indicates signaling between binding domains for c-Src and zonula occludens-1. The Journal of biological chemistry 279, 54695-54701.

Sosinsky, G.E., Solan, J.L., Gaietta, G.M., Ngan, L., Lee, G.J., Mackey, M.R., Lampe, P.D., 2007. The C-terminus of connexin43 adopts different conformations in the Golgi and gap junction as detected with structure-specific antibodies. The Biochemical journal 408, 375-385.

Sotkis, A., Wang, X.G., Yasumura, T., Peracchia, L.L., Persechini, A., Rash, J.E., Peracchia, C., 2001. Calmodulin colocalizes with connexins and plays a direct role in gap junction channel gating. Cell communication & adhesion 8, 277-281.

Sovari, A.A., Iravanian, S., Dolmatova, E., Jiao, Z., Liu, H., Zandieh, S., Kumar, V., Wang, K., Bernstein, K.E., Bonini, M.G., Duffy, H.S., Dudley, S.C., 2011. Inhibition of c-Src tyrosine kinase prevents angiotensin II-mediated connexin-43 remodeling and sudden cardiac death. Journal of the American College of Cardiology 58, 2332-2339.

Spagnol, G., Al-Mugotir, M., Kopanic, J.L., Zach, S., Li, H., Trease, A.J., Stauch, K.L., Grosely, R., Cervantes, M., Sorgen, P.L., 2016. Secondary structural analysis of the carboxyl-terminal domain from different connexin isoforms. Biopolymers 105, 143-162.

Spagnol, G., Kieken, F., Kopanic, J.L., Li, H., Zach, S., Stauch, K.L., Grosely, R., Sorgen, P.L., 2016. Structural

Studies of the Nedd4 WW Domains and their Selectivity for the Cx43 Carboxyl-terminus. The Journal of biological chemistry.

Spray, D.C., Hanstein, R., Lopez-Quintero, S.V., Stout, R.F., Jr., Suadicani, S.O., Thi, M.M., 2013. Gap junctions and Bystander Effects: Good Samaritans and executioners. Wiley interdisciplinary reviews. Membrane transport and signaling 2, 1-15.

Srisakuldee, W., Jeyaraman, M.M., Nickel, B.E., Tanguy, S., Jiang, Z.S., Kardami, E., 2009. Phosphorylation of connexin-43 at serine 262 promotes a cardiac injury-resistant state. Cardiovascular research 83, 672-681.

Stark, G.R., Darnell, J.E., Jr., 2012. The JAK-STAT pathway at twenty. Immunity 36, 503-514.

Stauch, K., Kieken, F., Sorgen, P., 2012. Characterization of the structure and intermolecular interactions between the connexin 32 carboxyl-terminal domain and the protein partners synapse-associated protein 97 and calmodulin. The Journal of biological chemistry 287, 27771-27788.

Stein, M., van Veen, T.A., Remme, C.A., Boulaksil, M., Noorman, M., van Stuijvenberg, L., van der Nagel, R., Bezzina, C.R., Hauer, R.N., de Bakker, J.M., van Rijen, H.V., 2009. Combined reduction of intercellular coupling and membrane excitability differentially affects transverse and longitudinal cardiac conduction. Cardiovascular research 83, 52-60.

Strobl, B., Stoiber, D., Sexl, V., Mueller, M., 2011. Tyrosine kinase 2 (TYK2) in cytokine signalling and host immunity. Frontiers in bioscience 16, 3214-3232.

Swenson, K.I., Piwnica-Worms, H., McNamee, H., Paul, D.L., 1990. Tyrosine phosphorylation of the gap junction protein connexin43 is required for the pp60v-src-induced inhibition of communication. Cell regulation 1, 989-1002.

Tan, L.L., Li, L., Liu, L.M., Zhao, H.L., 2013. Effect of RAAS antagonist on the expression of gap junction cx43 in myocardium of spontaneously hypertensive rat. Journal of Sichuan University. Medical science edition 44, 531-535, 549.

Tan, L.W., Bianco, T., Dobrovic, A., 2002. Variable promoter region CpG island methylation of the putative tumor suppressor gene Connexin 26 in breast cancer. Carcinogenesis 23, 231-236.

Temme, A., Buchmann, A., Gabriel, H.D., Nelles, E., Schwarz, M., Willecke, K., 1997. High incidence of spontaneous and chemically induced liver tumors in mice deficient for connexin32. Current biology : CB 7, 713-716.

Temme, A., Stumpel, F., Sohl, G., Rieber, E.P., Jungermann, K., Willecke, K., Ott, T., 2001. Dilated bile canaliculi and attenuated decrease of nerve-dependent bile secretion in connexin32-deficient mouse liver. Pflugers Archiv : European journal of physiology 442, 961-966.

ten Hoeve, J., de Jesus Ibarra-Sanchez, M., Fu, Y., Zhu, W., Tremblay, M., David, M., Shuai, K., 2002. Identification of a nuclear Stat1 protein tyrosine phosphatase. Molecular and cellular biology 22, 5662-5668.

Teunissen, B.E., Jongsma, H.J., Bierhuizen, M.F., 2004. Regulation of myocardial connexins during hypertrophic remodelling. Eur Heart J 25, 1979-1989.

Thevenin, A.F., Kowal, T.J., Fong, J.T., Kells, R.M., Fisher, C.G., Falk, M.M., 2013. Proteins and mechanisms regulating gap-junction assembly, internalization, and degradation. Physiology 28, 93-116.

Thomas, B.C., Minogue, P.J., Valiunas, V., Kanaporis, G., Brink, P.R., Berthoud, V.M., Beyer, E.C., 2008. Cataracts are caused by alterations of a critical N-terminal positive charge in connexin50. Investigative ophthalmology & visual science 49, 2549-2556.

Thomas, T., Jordan, K., Simek, J., Shao, Q., Jedeszko, C., Walton, P., Laird, D.W., 2005. Mechanisms of Cx43

and Cx26 transport to the plasma membrane and gap junction regeneration. Journal of cell science 118, 4451-4462.

Tiganis, T., Bennett, A.M., Ravichandran, K.S., Tonks, N.K., 1998. Epidermal growth factor receptor and the adaptor protein p52Shc are specific substrates of T-cell protein tyrosine phosphatase. Molecular and cellular biology 18, 1622-1634.

Torok, K., Stauffer, K., Evans, W.H., 1997. Connexin 32 of gap junctions contains two cytoplasmic calmodulin-binding domains. The Biochemical journal 326 (Pt 2), 479-483.

Touyz, R.M., Wu, X.H., He, G., Salomon, S., Schiffrin, E.L., 2002. Increased angiotensin II-mediated Src signaling via epidermal growth factor receptor transactivation is associated with decreased C-terminal Src kinase activity in vascular smooth muscle cells from spontaneously hypertensive rats. Hypertension 39, 479-485.

Toyofuku, T., Akamatsu, Y., Zhang, H., Kuzuya, T., Tada, M., Hori, M., 2001. c-Src regulates the interaction between connexin-43 and ZO-1 in cardiac myocytes. The Journal of biological chemistry 276, 1780-1788.

Toyofuku, T., Yabuki, M., Otsu, K., Kuzuya, T., Hori, M., Tada, M., 1998. Direct association of the gap junction protein connexin-43 with ZO-1 in cardiac myocytes. The Journal of biological chemistry 273, 12725-12731.

Toyofuku, T., Yabuki, M., Otsu, K., Kuzuya, T., Tada, M., Hori, M., 1999. Functional role of c-Src in gap junctions of the cardiomyopathic heart. Circulation research 85, 672-681.

Traub, O., Hertlein, B., Kasper, M., Eckert, R., Krisciukaitis, A., Hulser, D., Willecke, K., 1998. Characterization of the gap junction protein connexin37 in murine endothelium, respiratory epithelium, and after transfection in human HeLa cells. European journal of cell biology 77, 313-322.

Traub, O., Look, J., Dermietzel, R., Brummer, F., Hulser, D., Willecke, K., 1989. Comparative characterization of the 21-kD and 26-kD gap junction proteins in murine liver and cultured hepatocytes. The Journal of cell biology 108, 1039-1051.

Trexler, E.B., Bukauskas, F.F., Bennett, M.V., Bargiello, T.A., Verselis, V.K., 1999. Rapid and direct effects of pH on connexins revealed by the connexin46 hemichannel preparation. The Journal of general physiology 113, 721-742.

Tsiropoulou S, M.A., Scott A, Burchmore RJ, Touyz RM, 2014. Abstract 280: Protein Tyrosine Phosphatase Oxidation and Redox Proteomics Hypertension. Hypertension 2014; 64: A280.

Tsujiuchi, T., Shimizu, K., Itsuzaki, Y., Onishi, M., Sugata, E., Fujii, H., Honoki, K., 2007. CpG site hypermethylation of E-cadherin and Connexin26 genes in hepatocellular carcinomas induced by a choline-deficient L-Amino Acid-defined diet in rats. Molecular carcinogenesis 46, 269-274.

Ubel, C., Graser, A., Koch, S., Rieker, R.J., Lehr, H.A., Muller, M., Finotto, S., 2014. Role of Tyk-2 in Th9 and Th17 cells in allergic asthma. Scientific reports 4, 5865.

Umhauer, S., Ruch, R.J., Fanning, J., 2000. Gap junctional intercellular communication and connexin 43 expression in ovarian carcinoma. American journal of obstetrics and gynecology 182, 999-1000.

van Veen, T.A., van Rijen, H.V., Jongsma, H.J., 2000. Electrical conductance of mouse connexin45 gap junction channels is modulated by phosphorylation. Cardiovascular research 46, 496-510.

van Vliet, C., Bukczynska, P.E., Puryer, M.A., Sadek, C.M., Shields, B.J., Tremblay, M.L., Tiganis, T., 2005. Selective regulation of tumor necrosis factor-induced Erk signaling by Src family kinases and the T cell protein tyrosine phosphatase. Nature immunology 6, 253-260.

VanSlyke, J.K., Musil, L.S., 2002. Dislocation and degradation from the ER are regulated by cytosolic stress.

The Journal of cell biology 157, 381-394.

Verma, V., Larsen, B.D., Coombs, W., Lin, X., Spagnol, G., Sorgen, P.L., Taffet, S.M., Delmar, M., 2009. Novel pharmacophores of connexin43 based on the "RXP" series of Cx43-binding peptides. Circulation research 105, 176-184.

Verselis, V.K., Ginter, C.S., Bargiello, T.A., 1994. Opposite voltage gating polarities of two closely related connexins. Nature 368, 348-351.

Vinken, M., De Kock, J., Oliveira, A.G., Menezes, G.B., Cogliati, B., Dagli, M.L., Vanhaecke, T., Rogiers, V., 2012. Modifications in connexin expression in liver development and cancer. Cell communication & adhesion 19, 55-62.

Vinken, M., Henkens, T., Vanhaecke, T., Papeleu, P., Geerts, A., Van Rossen, E., Chipman, J.K., Meda, P., Rogiers, V., 2006. Trichostatin a enhances gap junctional intercellular communication in primary cultures of adult rat hepatocytes. Toxicological sciences : an official journal of the Society of Toxicology 91, 484-492.

Wallweber, H.J., Tam, C., Franke, Y., Starovasnik, M.A., Lupardus, P.J., 2014. Structural basis of recognition of interferon-alpha receptor by tyrosine kinase 2. Nature structural & molecular biology 21, 443-448.

Wan, J., Fu, A.K., Ip, F.C., Ng, H.K., Hugon, J., Page, G., Wang, J.H., Lai, K.O., Wu, Z., Ip, N.Y., 2010. Tyk2/STAT3 signaling mediates beta-amyloid-induced neuronal cell death: implications in Alzheimer's disease. J Neurosci 30, 6873-6881.

Wang, H., Wen, J., Wang, H., Guo, Q., Shi, S., Shi, Q., Zhou, X., Liu, Q., Lu, G., Wang, J., 2014. Loss of expression of EphB1 protein in serous carcinoma of ovary associated with metastasis and poor survival. International journal of clinical and experimental pathology 7, 313-321.

Wang, J.D., Dong, Y.C., Sheng, Z., Ma, H.H., Li, G.L., Wang, X.L., Lu, G.M., Sugimura, H., Jin, J., Zhou, X.J., 2007. Loss of expression of EphB1 protein in gastric carcinoma associated with invasion and metastasis. Oncology 73, 238-245.

Wang, R., Wang, Y., Lin, W.K., Zhang, Y., Liu, W., Huang, K., Terrar, D.A., Solaro, R.J., Wang, X., Ke, Y., Lei, M., 2014. Inhibition of angiotensin II-induced cardiac hypertrophy and associated ventricular arrhythmias by a p21 activated kinase 1 bioactive peptide. PLoS One 9, e101974.

Wang, X.G., Peracchia, C., 1996. Connexin 32/38 chimeras suggest a role for the second half of inner loop in gap junction gating by low pH. The American journal of physiology 271, C1743-1749.

Wang, Z., Schey, K.L., 2009. Phosphorylation and truncation sites of bovine lens connexin 46 and connexin 50. Experimental eye research 89, 898-904.

Warn-Cramer, B.J., Lampe, P.D., Kurata, W.E., Kanemitsu, M.Y., Loo, L.W., Eckhart, W., Lau, A.F., 1996. Characterization of the mitogen-activated protein kinase phosphorylation sites on the connexin-43 gap junction protein. The Journal of biological chemistry 271, 3779-3786.

Warn-Cramer, B.J., Lau, A.F., 2004. Regulation of gap junctions by tyrosine protein kinases. Biochimica et biophysica acta 1662, 81-95.

Werner, R., Levine, E., Rabadan-Diehl, C., Dahl, G., 1991. Gating properties of connexin32 cell-cell channels and their mutants expressed in Xenopus oocytes. Proceedings. Biological sciences / The Royal Society 243, 5-11.

White, T.W., 2002. Unique and redundant connexin contributions to lens development. Science 295, 319-320.

Wilgenbus, K.K., Kirkpatrick, C.J., Knuechel, R., Willecke, K., Traub, O., 1992. Expression of Cx26, Cx32 and

Cx43 gap junction proteins in normal and neoplastic human tissues. International journal of cancer 51, 522-529.

Xie, X., Lan, T., Chang, X., Huang, K., Huang, J., Wang, S., Chen, C., Shen, X., Liu, P., Huang, H., 2013. Connexin43 mediates NF-kappaB signalling activation induced by high glucose in GMCs: involvement of c-Src. Cell communication and signaling : CCS 11, 38.

Xiong, H., Hong, J., Du, W., Lin, Y.W., Ren, L.L., Wang, Y.C., Su, W.Y., Wang, J.L., Cui, Y., Wang, Z.H., Fang, J.Y., 2012. Roles of STAT3 and ZEB1 proteins in E-cadherin down-regulation and human colorectal cancer epithelial-mesenchymal transition. The Journal of biological chemistry 287, 5819-5832.

Xu, Q., Lin, X., Andrews, L., Patel, D., Lampe, P.D., Veenstra, R.D., 2013. Histone deacetylase inhibition reduces cardiac connexin43 expression and gap junction communication. Frontiers in pharmacology 4, 44.

Xue, Y., Ren, J., Gao, X., Jin, C., Wen, L., Yao, X., 2008. GPS 2.0, a tool to predict kinase-specific phosphorylation sites in hierarchy. Molecular & cellular proteomics : MCP 7, 1598-1608.

Yamasaki, H., Omori, Y., Krutovskikh, V., Zhu, W., Mironov, N., Yamakage, K., Mesnil, M., 1999. Connexins in tumour suppression and cancer therapy. Novartis Foundation symposium 219, 241-254; discussion 254-260.

Yang, K., Trepanier, C., Sidhu, B., Xie, Y.F., Li, H., Lei, G., Salter, M.W., Orser, B.A., Nakazawa, T., Yamamoto, T., Jackson, M.F., Macdonald, J.F., 2012. Metaplasticity gated through differential regulation of GluN2A versus GluN2B receptors by Src family kinases. EMBO J 31, 805-816.

Yang, K.C., Rutledge, C.A., Mao, M., Bakhshi, F.R., Xie, A., Liu, H., Bonini, M.G., Patel, H.H., Minshall, R.D., Dudley, S.C., Jr., 2014. Caveolin-1 modulates cardiac gap junction homeostasis and arrhythmogenecity by regulating cSrc tyrosine kinase. Circulation. Arrhythmia and electrophysiology 7, 701-710.

Yi, Z.C., Wang, H., Zhang, G.Y., Xia, B., 2007. Downregulation of connexin 43 in nasopharyngeal carcinoma cells is related to promoter methylation. Oral oncology 43, 898-904.

Yogo, K., Ogawa, T., Akiyama, M., Ishida, N., Takeya, T., 2002. Identification and functional analysis of novel phosphorylation sites in Cx43 in rat primary granulosa cells. FEBS letters 531, 132-136.

Yoon, N., Cho, J.G., Kim, K.H., Park, K.H., Sim, D.S., Yoon, H.J., Hong, Y.J., Park, H.W., Kim, J.H., Ahn, Y., Jeong, M.H., Park, J.C., 2013. Beneficial effects of an angiotensin-II receptor blocker on structural atrial reverse-remodeling in a rat model of ischemic heart failure. Experimental and therapeutic medicine 5, 1009-1016.

You-Ten, K.E., Muise, E.S., Itie, A., Michaliszyn, E., Wagner, J., Jothy, S., Lapp, W.S., Tremblay, M.L., 1997. Impaired bone marrow microenvironment and immune function in T cell protein tyrosine phosphatase-deficient mice. J Exp Med 186, 683-693.

Zang, Q., Frankel, P., Foster, D.A., 1995. Selective activation of protein kinase C isoforms by v-Src. Cell growth & differentiation : the molecular biology journal of the American Association for Cancer Research 6, 1367-1373.

Zhang, J.T., Chen, M., Foote, C.I., Nicholson, B.J., 1996. Membrane integration of in vitro-translated gap junctional proteins: co- and post-translational mechanisms. Molecular biology of the cell 7, 471-482.

Zhang, X., Meng, J., Wang, Z.Y., 2012. A switch role of Src in the biphasic EGF signaling of ER-negative breast cancer cells. PloS one 7, e41613.

Zhang, Z.Q., Hu, Y., Wang, B.J., Lin, Z.X., Naus, C.C., Nicholson, B.J., 2004. Effective asymmetry in gap junctional intercellular communication between populations of human normal lung fibroblasts and lung carcinoma cells. Carcinogenesis 25, 473-482.

Zhang, Z.Y., 1998. Protein-tyrosine phosphatases: biological function, structural characteristics, and

mechanism of catalysis. Critical reviews in biochemistry and molecular biology 33, 1-52.

Zhou, L., Kasperek, E.M., Nicholson, B.J., 1999. Dissection of the molecular basis of pp60(v-src) induced gating of connexin 43 gap junction channels. The Journal of cell biology 144, 1033-1045.

Zhou, S., Wang, L., Li, G., Zhang, Z., Wang, J., 2014. Decreased expression of receptor tyrosine kinase of EphB1 protein in renal cell carcinomas. International journal of clinical and experimental pathology 7, 4254-4260.

Zhou, Y., Yang, W., Lurtz, M.M., Chen, Y., Jiang, J., Huang, Y., Louis, C.F., Yang, J.J., 2009. Calmodulin mediates the Ca2+-dependent regulation of Cx44 gap junctions. Biophysical journal 96, 2832-2848.

Zhou, Y., Yang, W., Lurtz, M.M., Ye, Y., Huang, Y., Lee, H.W., Chen, Y., Louis, C.F., Yang, J.J., 2007. Identification of the calmodulin binding domain of connexin 43. The Journal of biological chemistry 282, 35005-35017.

Zhuang, S., Schnellmann, R.G., 2004. H2O2-induced transactivation of EGF receptor requires Src and mediates ERK1/2, but not Akt, activation in renal cells. American journal of physiology. Renal physiology 286, F858-865.

Zou, J., Salarian, M., Chen, Y., Veenstra, R., Louis, C.F., Yang, J.J., 2014. Gap junction regulation by calmodulin. FEBS letters 588, 1430-1438.

Girao, H., Catarino, S., Pereira, P., 2009. Eps15 interacts with ubiquitinated Cx43 and mediates its internalization. Experimental cell research 315, 3587-3597.

Lin, R., Martyn, K.D., Guyette, C.V., Lau, A.F., Warn-Cramer, B.J., 2006. v-Src tyrosine phosphorylation of connexin43: regulation of gap junction communication and effects on cell transformation. Cell communication & adhesion 13, 199-216.

Lum, H., Podolski, J.L., Gurnack, M.E., Schulz, I.T., Huang, F., Holian, O., 2001. Protein phosphatase 2B inhibitor potentiates endothelial PKC activity and barrier dysfunction. American journal of physiology. Lung cellular and molecular physiology 281, L546-555.